



Evaluation and optimisation of nucleoside triphosphate analogues as antiviral prodrugs

Dissertation

to obtain the Scientific Doctoral Degree

by

Stefan Weber

presented to

the Department of Chemistry of the Faculty of Sciences at the
University of Hamburg

Hamburg 2024

1st Reviewer: Prof. Dr. Chris Meier

2nd Reviewer: Prof. Dr. Ralph Holl

Date of defence: 14.04.2024

This thesis was conducted at the Institute of Organic Chemistry from June 2018 to December 2023

'The true delight is in the finding out rather than in the knowing.'

-Isaac Asimov, 1920-1992

Meinem Großvater Gerhard Weber, Erfinder

List of Publications

2022 Weising, S., Weber, S., Schols, D., Meier, C. *Triphosphate Prodrugs of the Anti-HIV Active Compound 3'-Deoxy-3'-fluoro-Thymidine (FLT)*, *J. Med. Chem.* 2022, 65, 112163-12175.

2020 Zhao, C., Weber, S., Schols, D., Balzarini, J., Meier, C. *Prodrugs of γ -Alkyl-modified Nucleoside Triphosphates - Improved Inhibition of HIV Reverse Transcriptase*, *Angew. Chem. Int. Ed.* 2020, 59, 22063-22071.

Jia, X., Weber, S., Schols, D., Meier, C. *Membrane Permeable, Bioreversibly Modified Prodrugs of Nucleoside Diphosphate-g-Phosphonates*, *J. Med. Chem.* 2020, 63, 11990-12007.

Nack, T., de Oliveira, T. D., Weber, S., Schols, D., Balzarini, J., Meier, C. *γ -Ketobenzyl-Modified Nucleoside Triphosphate Prodrugs as Potential Antivirals*, *J. Med. Chem.* 2020, 63, 13745-13761.

2017 Ploog, J., Pongs, J., Weber, S., Maison, W. *A Domino Aza-Prins/Friedel-Crafts Reaction for the Synthesis of Benzomorphans*, *Synthesis* **2017**, 49(03), 693-703.

Contents

.....	i
List of Publications	x
Abstract.....	iv
Zusammenfassung	v
List of Abbreviations	vi
1. Introduction	1
2. Literature Review	4
2.1. HIV and AIDS	4
2.1.1. Heritage and Spread of HIV.....	4
2.1.2. The HI Virus.....	5
2.1.3. Lifecycle of HIV	6
2.2. cART.....	9
2.2.1. Viral Targets and Drug Development.....	9
2.2.2. Drug Toxicity and NRTI Resistances	12
2.3. NRTI Prodrugs	14
2.3.1. Prodrug Development.....	14
2.3.2. Nucleoside Monophosphate Prodrugs	16
2.3.3. Nucleoside Diphosphate Prodrugs.....	19
2.3.4. Nucleoside Triphosphate Prodrugs.....	21
2.4. Viral and Human Polymerases	24
2.4.1. Nuclear Polymerases α , ϵ , and δ	24
2.4.2. Human Polymerase β	24
2.4.3. Human Mitochondrial Polymerase γ	25
2.4.4. Primer Extension Assay	25
3. Objectives.....	26
4. Results and Discussion	29
4.1. Preliminary Primer Extension Assay Evaluation.....	29

List of Publications

4.2.	Masking Group Optimisation	36
4.3.	Synthesis of Masking Units	38
4.3.1.	Synthesis of γ -Alkyl (AB) Pyrophosphates	38
4.3.2.	Synthesis of γ -Alkyl Cyanoethyl Pyrophosphates.....	41
4.4.	Synthesis of Nucleosides.....	42
4.4.1.	Synthesis of 3'-Fluoro-2',3'-dideoxythymidine (FLT).....	42
4.4.2.	Synthesis of (-)-2'-Deoxy-3'-oxa-4'-thiocytidine (dOTC)	43
4.4.3.	Synthesis of 2',3'-Didehydro-3'-deoxy-4'-ethynylthymidine (4'-Ed4T)	45
4.5.	Triphosphate Prodrugs, γ -Alkyl Triphosphates and Triphosphates	52
4.5.1.	FLT Triphosphate Prodrugs and γ -Alkyl Triphosphates.....	53
4.5.2.	dOTC Triphosphate Prodrug, γ -Alkyl Triphosphate and Triphosphate	57
4.5.3.	3TC Triphosphate Prodrug, γ -Alkyl Triphosphate and Triphosphate	63
4.5.4.	4'-Ed4T Triphosphate Prodrug, γ -Alkyl Triphosphate and Triphosphate.....	67
4.6.	Synthesis of the 2',3'-Dideoxy-3'-Fluorouridine Phosphonate Analogue	71
5.	Summary and Conclusions	78
6.	Experimental Procedure	83
6.1.	General.....	83
6.1.1.	Solvents, chromatography, and devices	83
6.1.2.	Preparation of buffer-solutions	86
6.1.3.	Primer extension assay	87
6.2.	Synthesis	88
6.2.1.	General Procedures.....	88
6.2.2.	Synthesis of AB masking unit pyrophosphates	91
6.2.3.	Synthesis Cyanoethyl Pyrophosphates	96
6.2.4.	Synthesis of Nucleosides	99
6.2.5.	Synthesis of Triphosphate Prodrugs	114
7.	References.....	142
8.	Appendix	163

List of Publications

8.1.	Hazard and Precaution Statements	163
8.2.	Acknowledgements.....	177
8.3.	Eidesstattliche Erklärung.....	178

Abstract

Over the past 40 years, human immunodeficiency virus (HIV) research has evolved from a quest to understand the virus to a multifaceted endeavour aimed at developing effective treatments and prevention strategies. This thesis highlights key milestones in this journey and focuses on recent developments concerning nucleoside reverse transcriptase inhibitors (NRTIs). One such approach lies in the development of robust and flexible prodrug systems that can target not only HIV but also other diseases, like SARS-CoV-2 or Alzheimer's disease. The prodrug strategy was pioneered by MEIER *et al.*, culminating in the development of triphosphate prodrugs (TriPPPPro) and γ -alkyl triphosphate prodrugs. These prodrugs offer a versatile platform for drug delivery, enabling the adaptation of existing NRTIs to multiple pathological targets. This work established methods to evaluate the efficacy and safety of these prodrugs through a responsive workflow that used data acquired from primer extension assays and testing in HIV-infected cell lines to infer new designs for prodrug delivery to yield better overall pharmacological profiles. As a result of the acquired data, four highly active NRTIs were transformed into their prodrugs, γ -alkyl triphosphates and triphosphates. It was found that adjustments according to the biological data led to significant improvements in the pharmacological profiles of thymidine derivatives.

Zusammenfassung

In den letzten 40 Jahren hat sich die Forschung zum humanen Immundefizienzvirus (HIV) von einem schlichten Bestreben, das Virus zu verstehen, zu einer vielschichtigen Aufgabe entwickelt. Dabei liegt der Fokus auf der Entwicklung wirksamer Behandlungen und Präventionsstrategien. Diese Arbeit beleuchtet wichtige Meilensteine dieses Weges und konzentriert sich auf die jüngsten Entwicklungen im Bereich Nucleosid Reverse Transkriptase Inhibitoren (NRTIs). Ein solcher Ansatz liegt in der Entwicklung robuster und flexibler Prodrug-Systeme, die nicht nur gegen HIV, sondern auch gegen andere Krankheiten wie SARS-CoV-2 oder Alzheimer wirksam sein können. Dieser Ansatz wurde von MEIER *et al.* entwickelt und fand seinen Höhepunkt in der Entwicklung von Triphosphat-Prodrugs (TriPPPro) und γ -Alkyltriphosphat-Prodrugs, welche eine vielseitige Plattform für die Wirkstofffreisetzung bieten und die Anpassung vorhandener NRTIs an verschiedene pathologische Ziele ermöglichen. Diese Arbeit zielt darauf ab, Methoden zur Bewertung der Wirksamkeit und Sicherheit dieser Prodrugs zu erforschen und durch einen reaktionsfähigen Arbeitsablauf die gewonnenen Informationen zu nutzen, um neue Ansätze für die Prodrug-Freisetzung abzuleiten und so insgesamt bessere pharmakologische Profile zu erzielen. Die Kombination hochaktiver NRTIs mit dem anpassungsfähigen Nucleotid-Prodrug-System könnte das Interesse an neuartigen NRTI-Prodrugs gegen HIV erneuern. Im Rahmen dieser Arbeit wurden Methoden zur Bewertung der Wirksamkeit und Sicherheit dieser Prodrugs durch einen anpassungsfähigen Arbeitsablauf entwickelt, bei dem Daten aus Primer-Verlängerungsstudien und Tests in HIV-infizierten Zelllinien verwendet wurden. Daraus folgend sollten neue Designs für Prodrug-Verabreichung abgeleitet werden, die ein besseres pharmakologisches Gesamtprofil zur Folge haben. Als Ergebnis der gewonnenen Daten wurden vier hochaktive NRTIs in ihre Prodrugs, γ -Alkyltriphosphate und Triphosphate, umgewandelt. Es zeigte sich, dass die Anpassung dieser Systeme auf Grund biologischer Daten zu erheblichen Verbesserungen der pharmakologischen Profile der Thymidin-Derivate führte.

List of Abbreviations

%ee	enantiomeric excess
3TC	lamivudine
A	ampere
AB	acyloxy benzyl
AIDS	acquired immunodeficiency syndrome
AZT	zidovudine
AP	apurinic/aprimidinic
APS	ammonium persulfate
ATP	adenosine triphosphate
BCNA	bicyclic nucleoside analogue
BSA	bovine serum albumin
BER	base excision repair
Bu	butyl
CA	capsid protein
cART	combined antiretroviral therapy
CC ₅₀	half-maximal cytotoxic concentration
CCR5	C-C chemokine receptor type 5
CD	cluster of differentiation
CSO	(1S)-(+)-(10-camphersulfonyl)-oxaziridine
CXCR4	C-X-C chemokine receptor type 4
Cy3	cyanine
d	doublet
DAST	(diethylamino)sulfur trifluoride
DBU	1,8-diazabicyclo[5.4.0]undec-7-ene

List of Abbreviations

DCI	4,5-dicyanoimidazole
DCSO	(1S(+)-(8,8-dichlorocamphorylsulfonyl)oxaziridine
DDQ	2,3-dichloro-5,6-dicyano-1,4-benzoquinone
DIPEA	<i>N,N</i> -diisopropylethylamine
DiPPro	diphosphat-Prodrugs
DMAP	4-(dimethylamino)-pyridine
DMF	dimethylformamide
DMSO	dimethyl sulfoxide
DMTr	4,4'-dimethoxytriphenylmethyl
DPP	diphenyl phosphite
DRC	Democratic Republic of Kongo
DMTr	4,4'-dimethoxytrityl
DYKAT	dynamic kinetic asymmetric transformation
EC ₅₀	half-maximal effective concentration
EDTA	ethylenediaminetetraacetic acid
eq.	equivalents
ESI	electron spray ionization
FDA	food and drug administration
FITC	fluorescein isothiocyanate
FLT	3'-deoxy-3'-fluorothymidine
FTC	emtricitabine
<i>Gag</i>	group specific antigen
gp	glycoprotein
HAART	highly active antiretroviral therapy
HIV	human immunodeficiency virus

List of Abbreviations

HMDS	hexamethyldisilazane
HPLC	high-performance liquid chromatography
HRMS	high-resolution mass spectrometry
IC ₅₀	half-maximal inhibitory concentration
IR	infrared
<i>J</i>	scalar spin-spin coupling
kb	alkylketobenzyl
m	multiplet
MALDI	matrix-assisted laser desorption/ionisation
<i>m</i> CPBA	<i>meta</i> -chloroperbenzoic acid
mRNA	messenger ribonucleic acid
MS	mass spectrometry
ms	mesyl
MVC	maraviroc
NC	nucleocapsid protein
NCS	<i>N</i> -chlorosuccinimide
NDP	nucleoside diphosphate
Nef	negative regulatory factor
NMP	nucleoside monophosphate
NMR	nuclear magnetic resonance
NNRTI	non nucleoside reverse transcriptase inhibitor
NRTI	nucleoside reverse transcriptase inhibitor
NTP	nucleoside triphosphate
NtRTI	nucleotide reverse transcriptase inhibitor
OXPHOS	oxidative phosphorylation

List of Abbreviations

PAA	polyacrylamide
PAGE	polyacrylamide gel electrophoresis
PBS	phosphate buffer saline
PDB	protein data bank
Ph	phenyl
pH	inverse logarithmic concentration of hydrogen ions
pol $\alpha/ \beta/ \delta/ \varepsilon/ \gamma/ \zeta/ \theta$	human DNA polymerase $\alpha/ \beta/ \delta/ \varepsilon/ \gamma/ \zeta/ \theta$
POLG	gene encoding pol γ
PPi	pyrophosphate ($P_2O_7^{4-}$)
ppm	parts per million
ProTide	pronucleotide
q	quartet
qu	quintet
rac	racemic
R_f	retention factor
RNase H	ribonuclease H
rp	reversed-phase
rt	room temperature
RT	reverse transcriptase
RTC	reverse transcription complex
s	singlet
sept	septet
sext	sextet
SIVcpzPtt	simian immunodeficiency virus chimpanzee pan troglodytes troglodytes
SIVsmm	simian immunodeficiency virus sooty mangabey

List of Abbreviations

SQV	saquinavir
t	triplet
TAE	tris-acetate-EDTA-buffer
TAF	tenofovir alafenamide
TBA	tetrabutylammonium
TBAI	tetrabutylammonium iodide
TDF	tenofovir disoproxil fumarate
TEA	triethylamine
TEAA	triethylammonium acetate
TEMED	<i>N,N,N',N'</i> -tetramethyl ethylenediamine
TFAA	trifluoroacetic anhydride
TFV	tenofovir
THF	tetrahydrofuran
TK ⁻	thymidine kinase deficient
TLC	thin layer chromatography
TMP	trimethyl phosphate
TMS	trimethylsilyl
TMSI	iodotrimethylsilane
TMSOTf	trimethylsilyl trifluoromethanesulfonate
TOF	time of flight
TPP	triphenylphosphine
<i>TriPPPPro</i>	Triphosphate-Prodrug
Tris	tris(hydroxymethyl)aminomethane
Ts	tosyl
U	units

List of Abbreviations

UV/vis	ultraviolet and visible light
V	volt
v/v	volume/volume
W	watt
WHO	World Health Organisation

1. Introduction

More than 40 years have passed since Michael S. Gottlieb was able to connect five cases of pneumocystis pneumonia to an underlying, unknown viral infection.¹ This kickstarted the discovery of the human immunodeficiency virus and the resulting disease of acquired immunodeficiency syndrome (AIDS). This discovery resulted in yet unseen efforts to come up with a cure.² The virus was first isolated in 1983³ by French clinicians and sequenced in 1985⁴, and only two years later 3'-azido-3'-deoxythymidin (AZT, zidovudine) was approved⁵ by the Food and Drug Administration (FDA) as an antiviral agent against HIV. Despite these immense efforts, HIV is still one of the most common infectious diseases worldwide. The newest estimates of people living with HIV today range from 34 to 43 million, according to the World Health Organisation (WHO).^{6,7}

Even though AZT started as a promising treatment against the new virus, several shortcomings became apparent. The long-term monotherapy with AZT led to severe mitochondrial myopathy⁸ and the development of AZT-resistant strains of HIV-1.^{9,10} Protease, integrase and reverse transcriptase (RT) were discovered as viable targets for novel antiviral drugs.^{4,11} The prior discovery of RT in 1970 and the similarity to human T cell leukaemia viruses¹² made RT the prime target for antiviral research.¹³ Consequently this resulted in the development and approval of seven NRTIs until 2003, of which five are still used in HIV treatment.⁵

In the mid-90s, efforts to target other enzymatic targets were successful.¹⁴ The first protease inhibitor Saquinavir, developed by ROCHE, was approved in 1995¹⁵, and after resolving the crystal structure of HIV-RT¹⁶, nevirapine was approved as a non nucleoside reverse transcriptase inhibitor (NNRTI).^{5,17} Although the first integrase strand transfer inhibitor was developed in 1993 by FESEN *et al.*¹⁸ it took an additional 14 years for raltegravir to be approved.^{5,19}

Despite the fast development of new antiviral drugs like stavudine (d4T), zalcitabine or didanosine, limitations to monotherapy were apparent.²⁰ High toxicity and the tendency of the virus to develop drug-resistant strains²¹ led to the investigation of multi-drug therapies developed by several groups.²² Through collective contributions, the first so-called fixed dose combination was approved.⁵

Introduction

This highly active antiretroviral therapy (HAART), later termed combination antiretroviral therapy (cART), consisted of at least two antiviral drugs. The introduction of HAART represented a turning point in the fight against HIV/AIDS (**Figure 1** orange) and led to a substantial decline in new infections from 1997 onward, and a steady decline of HIV/AIDS related deaths from 2004 onward (**Figure 1**, grey), which coincided with the deployment of widely available cART in sub-Saharan Africa.^{6,21,23,24} Yet, due to the problematic characteristic of the HIV infection to build dormant reservoirs in non-active CD4⁺ T cells, stored in host DNA, eradication of HIV remains challenging.^{25,26} Nevertheless, cART increased the life expectancy of HIV infected individuals by a significant margin²⁷ and is the primary tool to combat HIV to this day.

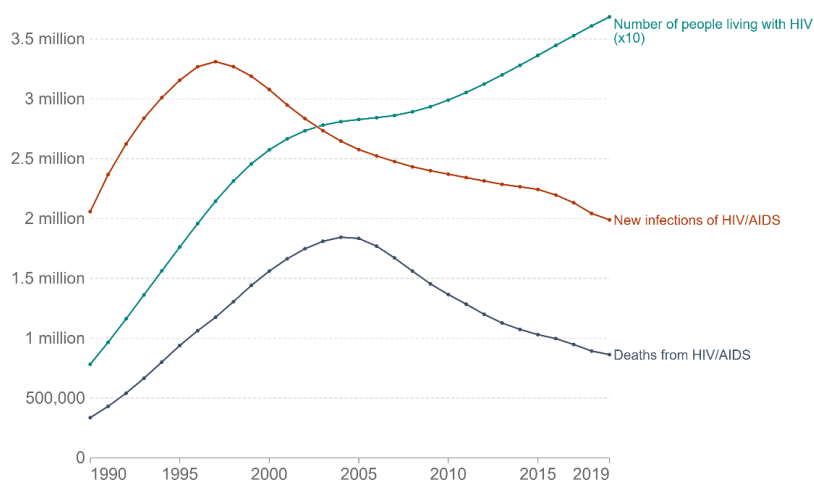


Figure 1: Statistical data of prevalence, new cases and deaths from HIV/AIDS between 1990 and 2019.²⁸

Several attempts were made to develop vaccines²⁹ or activate dormant HIV reservoirs inside the cells to fully eradicate the virus³⁰, though promising, no attempt bore success in delivering a broadly applicable cure for HIV. This is due to the virus intrinsic adaptability, resulting from constant mutations.^{31,32} Therefore, cART and consequently NRTIs as its backbone remain a focal point of antiviral research.^{33,34}

Since 2014 only five new drugs were approved by the FDA.⁵ For NRTIs in particular, several conditions must be met until regulatory approval is viable. New NRTIs necessarily would have to exhibit better long-term safety and tolerability³⁵ as well as more favourable metabolic profiles, than existing NRTIs.³⁴ To overcome the latter, intracellular phosphorylation for different nucleoside analogues was investigated.^{36,37} For NRTIs to be converted into their active forms, three phosphorylation steps are necessary, limiting the bioavailability of the drug.^{38,39} As a result, several prodrug concepts, delivering monophosphates, like the ProTide concept by McGUIGAN *et al.*^{40,41} or the *cycloSal* concept by MEIER *et al.*⁴², were developed. In 2001, tenofovir disoproxil fumarate (TDF)⁴³ was the first prodrug approved by the FDA to be used against HIV, followed in 2015 by tenofovir alafenamide (TAF)⁴⁴, which uses the aforementioned ProTide concept.

Introduction

Following the success of monophosphate prodrugs, the group of MEIER *et al.* developed prodrug systems for di- and triphosphates, circumventing two or all three intracellular phosphorylation steps. The diphosphate prodrug (DiPPro)⁴⁵⁻⁴⁷ and triphosphate prodrug (TriPPro)^{48,49} compounds bear two cleavable bis(acyloxybenzyl)phosphate (AB) esters, at the β - or γ -phosphate group, respectively, to mask the negative charge of the terminal phosphate and enable passive membrane permeability.⁴⁹ This concept was further improved by introducing non-cleavable protecting groups to modify substrate properties favouring the viral polymerase.⁵⁰⁻⁵²

A different approach, to achieve discrimination between human and viral polymerases, was the introduction of 'non-natural' nucleosides. A prominent example is the 1995 approved lamivudine (3TC), a L-configured nucleoside, which exhibited remarkable activity against HIV-RT while having a more favourable toxicological profile and better metabolic stability compared to its D-counterpart.⁵³ Contrary to common belief at the time, L-nucleosides could be phosphorylated to their active triphosphates by their corresponding kinases.⁵⁴ While L-nucleosides were also phosphorylated, the chirality turned out to be an advantage, as it resulted in lower toxicity of L-nucleosides due to the intrinsic D-stereospecificity of human DNA polymerases.⁵⁵

2. Literature Review

2.1. HIV and AIDS

2.1.1. Heritage and Spread of HIV

After the recognition of HIV as an independent virus in the 1980s³, molecular cloning⁵⁶, nucleotide sequencing⁴ and phylogenetic clustering⁵⁷, HIV-1 was grouped to the family of lentiviruses⁵⁸ prevalent across many mammalian species (**Figure 2**).⁵⁹ HIV-1 can be subdivided into four groups (M, N, O and P), of which only group M exhibits pandemic spread, while HIV-variants of the other groups are mostly confined to West Africa.⁶⁰ HIV-1, group M is most closely related to the simian immunodeficiency virus (SIV) found in the Cameroonian chimpanzees subspecies *Pan troglodytes troglodytes*, abbreviated as SIVcpzPtt.⁵⁷ Data analysis suggests that the earliest cross-species transmission can be traced back to the 1900s around the area of Kinshasa in the Democratic Republic of Kongo (DRC).⁶⁰

In 1986, when a different virus was found to cause AIDS, it was termed HIV-2, even though they were only distantly related. Phylogenetic analysis indicated, that the two morphologically similar but antigenetically distinct viruses resulted from two different cross-species transmission events.^{61,62} The origin of HIV-2 was traced back to sooty mangabeys and their specific strain of SIVsmm.⁶³

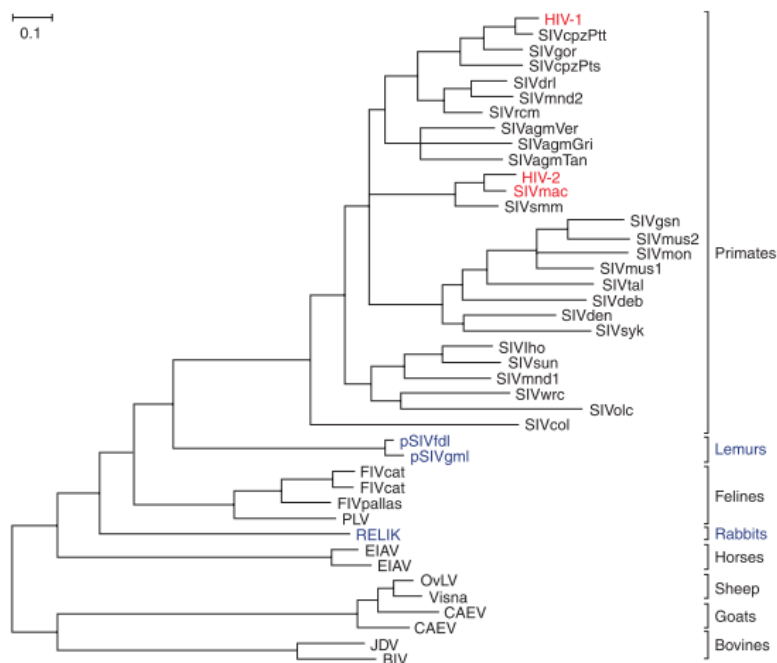


Figure 2: Phylogeny of lentiviruses, showing the evolutionary relationship between different lentivirus species pol sequences.⁶¹

2.1.2. The HI Virus

The HI virus is a type of lentivirus originating from different zoonotic events in West Africa.⁶⁰ It has varying particle sizes, ranging from diameters between 90 and 260 nm, with a spherical shape.⁶⁴ HIV-1 encodes 15 distinct proteins and contains two RNA strands (**Figure 3**).¹¹ The viral enzymes (**Figure 3**, pink) consist of the RT, transcribing the viral genome into a DNA copy⁶⁵, the integrase, splicing the DNA copy into the host genome⁶⁶ and the protease, which cleaves the group specific antigen (*Gag*) to produce a mature virus particle.²⁵ The structural proteins (**Figure 3**, blue) are integral in the viral delivery mechanism. The two envelope proteins, surface protein glycoprotein 120 (gp120) and transmembrane protein gp41, facilitate the binding of the virus to the cluster of differentiation 4 (CD4) receptor, the C-C chemokine receptor type 5 (CCR5) or the C-X-C chemokine receptor type 4 (CXCR4) of the host cells.⁶⁵ The matrix protein is crucial for host cell entry, viral assembly and exit⁶⁷, and the capsid protein (CA) is responsible to deliver the transcription machinery to the nucleus.⁶⁸ The task of the nucleocapsid proteins is the delivery of viral RNA to the assembling virion.¹¹ The last group is called accessory proteins (**Figure 3**, green). These serve various functions, such as the assistance of transcription or transport in the cell as well as the mediation of nuclear import and export.⁶⁹

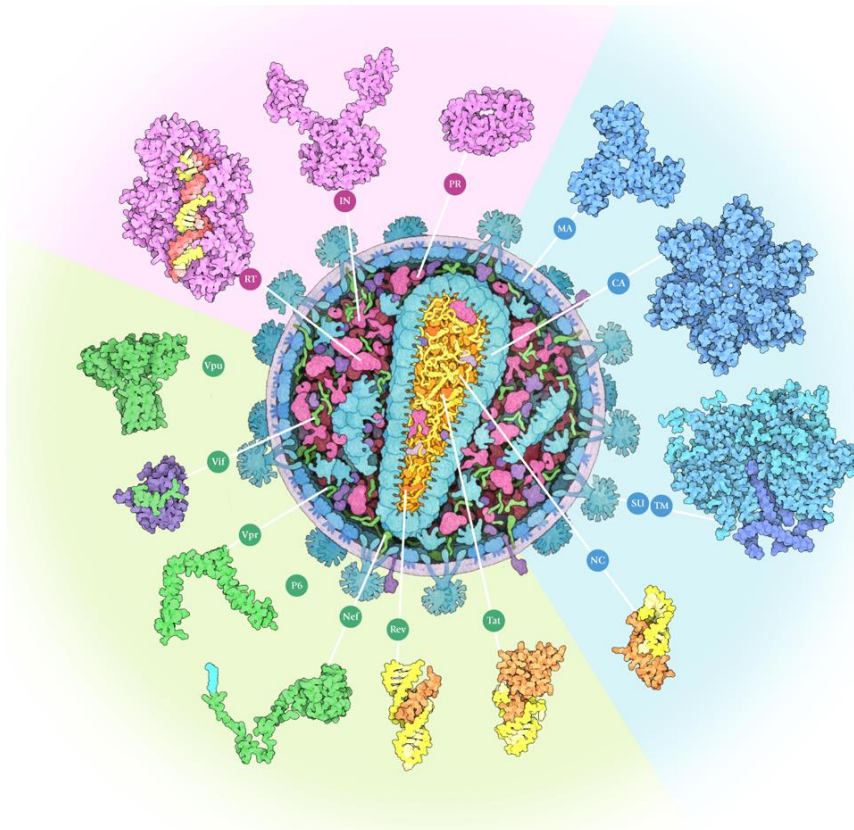


Figure 3: Artist rendition of an HIV particle and its corresponding viral proteins and genome. Protein data bank (PDB) codes are listed in the appendix.^{70,71}

HIV-1 transmission occurs mostly by genital or rectal mucosal surfaces and is therefore mostly attributed to sexual transmission.⁷² Population groups that are the most affected, are men that have sex with men, intravenous drug users, prisoners and sexworkers. Another group posed with a high risk of infection were infants of HIV-positive mothers, but cART almost eradicated this mode of transmission.⁷³

After infection, the virus is disseminated in the body and infects CD4⁺ T cells, which leads to their depletion.⁷⁴ Typical progression of the disease starts with the eclipitic phase, where the virus colonises in the mucosal tissue before infecting the lymphoid system.⁷³ During this phase, a latent reservoir of HIV is established in inactive CD4⁺ T cells.⁷⁵ After about three weeks, the acute phase starts, and the virus is detectable in the body. After four to six months, the chronic phase is reached, resulting in progressive loss of CD4⁺ T cells, chronic inflammation and finally the progressing to AIDS.⁷³

Viral progression reveals the major difference between HIV-1 and HIV-2. HIV-2 is characterized by lower CD4⁺ T cell loss and lower viral load. Since HIV transmission and progression is dependent on CD4⁺ T cells and viral load, HIV-2 is generally less infectious and has a lower chance of progression to AIDS.⁷⁶ If left untreated, HIV leads to a wide range of immunological dysfunctions and comorbidities.⁷³ These may range, from subsequent viral infections like hepatitis or herpes, neurological impairments like peripheral neuropathy, to oncological complications like Non-Hodgkin's lymphoma.⁷⁷ Other common comorbidities encompass cardiovascular diseases, bone disease as well as renal and hepatic dysfunctions.^{73,77}

2.1.3. Lifecycle of HIV

To eradicate the virus or to find suitable treatment methods, antiviral therapy is heavily reliant on the understanding of the virus, its replication and possible viral targets. Understanding the replication cycle of HIV has led to the discovery of the first NRTI¹³ and is to this day a crucial tool in the discovery of new viral targets or modes of interaction.⁷⁸

The replication cycle of HIV (**Figure 4**) starts after the viral glycoprotein envelop complex, consisting of gp120 and gp41, establishes contact with the CD4 receptor or other co-factors of the host cell. Through conformational changes and rearrangements a binding sheet between viral and host cell membrane is formed and through interaction with the chemokine co-receptors, fusion is initiated.^{68,79}

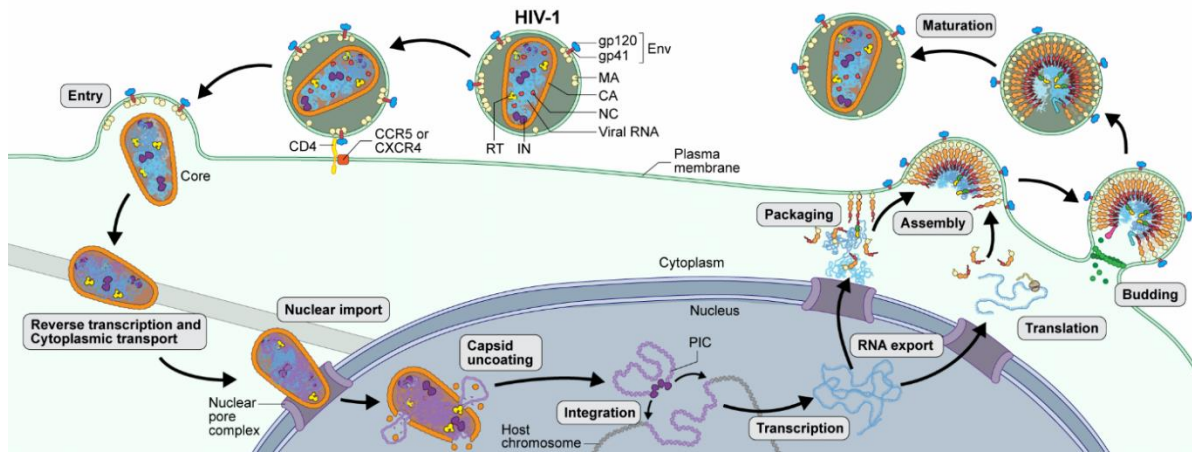


Figure 4: Depiction of the lifecycle of HIV.⁸⁰

After the successful merging, the capsid is released into the cytosol and is transported to the nucleus, hijacking cellular transport mechanisms.⁶⁵ The capsid protein plays an important role in this step, it consists of hexamers and pentamers of the capsid protein, which form a fullerene cone. This protective shell allows for the diffusion of nucleoside triphosphates (NTPs) into the core, while protecting the retroviral genome from the hostile cytosolic environment. Nucleases, host cell restriction factors or nucleic acid sensors, present in the cytosol, could trigger an innate immune response hampering successful infection.^{68,81} The capsid and its contents, which include two copies of the viral genome, integrase and reverse transcriptase, are referred to as the reverse transcription complex (RTC). There are several suggested mechanisms for the uncoating and trafficking of the RTC to the nucleus. Due to a lack of capsid protein associated to the RTC, isolated from cells shortly after, it was assumed, that uncoating occurs before transcription starts.⁶⁵ More recent studies present evidence for the uncoating process to start after docking of the RTC to the nuclear pore complex, which allows HIV-1 to infect non-dividing cells.⁸² Recent correlative light and electron microscopy studies published by MÜLLER *et al.* show that the uncoating event takes place inside the nucleus.⁸¹ Both models suggest that the uncoating process occurs well after transcription is completed.^{81,82}

Reverse transcription is a well-understood process. Following the import of the core into the cytosol, it starts with the pairing of the plus stranded viral RNAs 5'-primer binding site with host transport RNA as a primer.⁸³ According to its two functions, RT synthesizes the viral minus stranded DNA, while subsequently degrading the RNA plus strand through ribonuclease H activity. An exception to this are the polypurine areas, which are resistant to RNase H cleaving, priming the synthesis of the DNA plus

Literature Review

strand.^{83,84} The RT not only copies the minus strand, but also the first 18 nucleotides of the primer, leaving the genome with matching extensions on each side, which are substrate for integrase in the following process. Mistakes in viral RNA genome replication can lead to nicks, causing a transfer to the second RNA copy, during reverse transcription. This recombination can lead to virions of related viral genomes with different sequences. This elevated mutability can lead to highly resistant viral strains.³⁴

After delivery of the pre-integration complex into the nucleus, integrase cleaves a nucleotide dimer from both 3'-ends of the viral genome. The endonucleotide cleavage is subsequently followed by a strand transfer reaction to the host genome. In this step, integration takes place exactly five base pairs apart, connecting both 3'-viral ends with the corresponding 5'-DNA sequence simultaneously. Both 3'-processing and strand transfer reactions are catalysed by divalent metal ions like Mg^{2+} or Mn^{2+} .⁸⁵⁻⁸⁷

The integrated provirus is transcribed in the nucleus by RNA polymerase II, a process which is reported to be influenced by about 40 cellular factors. An especially crucial role is designated to the viral 'trans-activator of transcription' protein which binds to the trans-activation region of the RNA to promote transcription elongation, which was shown to stop after +45 to +50 nucleotides in the absence of transcription protein.^{69,88}

Eukaryotic cells have protective mechanisms, to stop the export of incompletely spliced RNA from the nucleus. This can hinder successful replication of the virus, as single- and unspliced viral RNA variants are necessary for complete translation in the cytoplasm. The transport of the incompletely spliced RNA is performed by the 'regulator of virion' protein, which can bind to the RNA, and through the formation of a complex with exportin-1, transports it through the nuclear pore^{69,89}

The translation of the differently spliced mRNAs leads to the formation of the *Gag* polyprotein precursor, the *GagPol* polyprotein precursor and the envelop glycoproteins. The different domains of the *Gag* are responsible for the targeting of the plasma membrane, the recruitment of the envelop glycoproteins, the incorporation of the viral genome and the catalysis of the final budding process. During the assembly process, several copies of the *GagPol* are incorporated in the *Gag* multimer.²⁵

After assembly, the viral particle is separated from the host cell, hijacking the 'endosomal sorting complex required for transport' apparatus and releasing an immature virion.⁹⁰ The final maturation step occurs after the dimerization of two *GagPol* polyproteins, activating the protease domain. The protease subsequently cleaves *Gag* and *GagPol* precursors, forming mature and infectious virions. In this step the CA fullerene lattice is formed.⁹¹

2.2. cART

2.2.1. Viral Targets and Drug Development

The discovery of different viral targets is the foundation for antiviral drug development. RT was the first known viral target. And the delivery of modified nucleosides, to infected cells, resulting in chain-termination events in viral DNA synthesis, was the earliest mode of action.¹² The nucleosides differed from natural nucleosides in either a lack in 3'-hydroxyl functionality, leading to immediate chain termination, or introduced structural stress to the growing DNA strand resulting in delayed chain termination.⁹² AZT was the first approved NRTI and is still used today. Nonetheless, AZT is subject to severe restrictions, due to its high cytotoxicity and the development of AZT-resistant strains after long-term monotherapy.^{9,93} Until 2003, seven additional NRTIs were developed (**Table 1**), of which three were discontinued due to their cytotoxicity, viral resistance, limited efficacy, unfavourable pharmacokinetics or inconvenient administration.^{21,94–96}

Table 1: FDA-approved drugs against HIV from 1987 to 2021.^{5,97}

Drug Types	Specific Drugs
NRTIs	abacavir; emtricitabine (FTC); lamivudine (3TC); tenofovir disoproxil fumarate (TDF); Tenofovir alafenamide (TAF); zidovudine (AZT); didanosine*; zalcitabine*; stavudine (d4T)*;
NNRTI	doravirine; efavirenz; etravirine; nevirapine; rilpivirine; delavirdine*;
Protease inhibitors	atazanavir; darunavir; fosamprenavir; ritonavir; tipranavir; indinavir*; nelfinavir*; amprenavir*;
Fusion inhibitors	enfuvirtide
CCR5 antagonist	maraviroc
Integrase strand transfer inhibitors	Cabotegravir; dolutegravir; raltegravir; elvitegravir*;
Attachment inhibitors	Fostemsavir
Post-attachment inhibitors	ibalizumab-uiyk
Pharmacokinetic enhancers	cobicistat

*: no longer available and/or recommended for use in the United States by the HHS HIV/AIDS medical practice guidelines.

Literature Review

Tenofovir, while technically being a nucleotide reverse transcriptase inhibitor (NtRTI), will be counted as a NRTI for simplicity. The sole development of new NRTIs for monotherapy did not improve the longevity of HIV therapy. A major breakthrough was the development of cART, in which a combination of two NRTIs is used. Combivir™ consists of a combination of AZT and 3TC and was the first FDA-approved co-formulation. It decreased the rate at which resistances developed and reduced the overall progression of the disease. The introduction of cART led to a drastic and steady decline in infections worldwide.^{28,98} The efficacy of cART was highly improved by combining NRTIs with newly developed non nucleosidic drugs, targeting different viral enzymes or active sites.⁹⁶

NNRTI were one of the first substance classes investigated for their antiviral activity. They are made up of a class of small (<600 Da) hydrophobic molecules, that can interact with a domain of HIV-1. Through allosteric binding, NNRTIs cause short- and long-range distortion in the catalytic site of HIV-RT, hampering viral reverse transcription. Unfortunately, NNRTIs can only be used in the treatment of HIV-1 and display no antiviral activity against HIV-2 strains.^{99,100}

As a result of a better understanding of the viral replication cycle, protease and integrase were logical targets for new antiviral drugs, thus targeting all enzymatic functions of HIV. In 1995 the first protease inhibitor was approved, and shortly after, clinical trials showed promising results of combination therapies with NRTIs resulting in significant reductions in short-term mortality.^{28,98} With the advent of protease inhibitors modern three-drug cART began and was able to suppress viral load to clinically undetectable levels, transforming HIV from a fatal disease to a manageable chronic infection, with a robust recovery of CD4⁺ cells.^{101,102} Due to several challenges (e.g. low barrier to resistance) the development of integral strand transfer inhibitors was by far more difficult. A milestone was the approval of raltegravir in 2007, which provided an additional drug in combating HIV and showed high activity against HIV strains that were resistant against other drug classes.¹⁰³

Three-drug combinations became the gold standard in HIV therapy, consisting of two NRTIs (AZT and 3TC) and either a protease inhibitor or NNRTI. Attempts to improve efficacy with four-drug regimens yielded inconclusive results, and often did not improve the outcome but resulted in more adverse effects. The improvement of co-formulations, and the switch of backbone NRTIs, from AZT and 3TC to either TAF/TDF and FTC/3TC, proved to be more beneficial. Most modern co-formulations use the 'new' backbone NRTIs with either a NNRTI, protease inhibitor or integrase strand transfer inhibitor (**Figure 5**) and have a reduced pill burden resulting in better patient adherence.^{96,102,104}

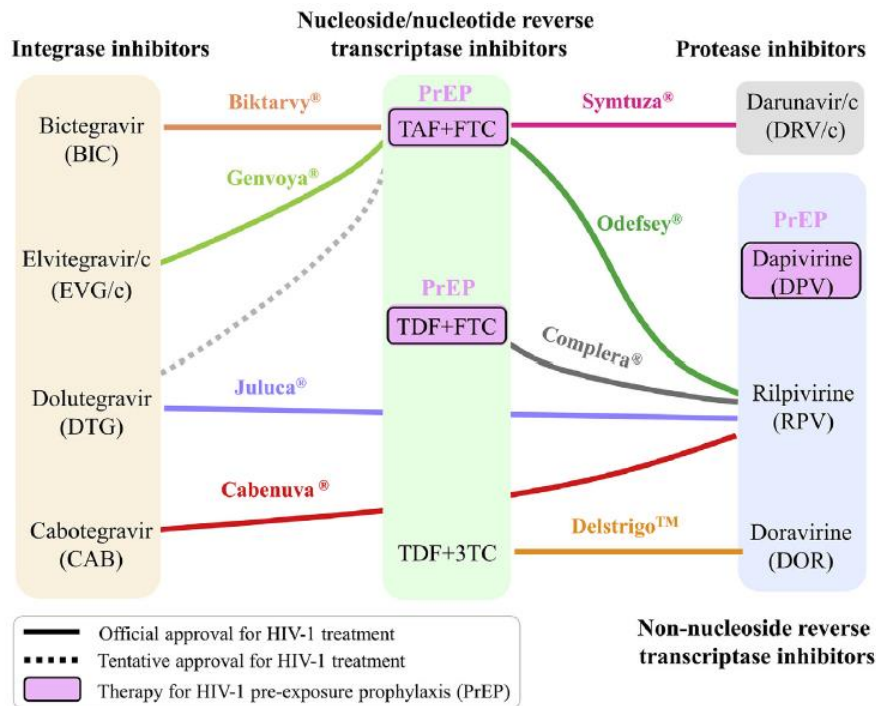


Figure 5: Co-formulations of (tentative) approved drugs for HIV-1 treatment. Most treatments involve the deployment of two NRTIs and one NNRTI, protease inhibitor or integrase strand inhibitor.^{96,105}

Due to the inevitability of emerging resistances, the final goal is the development of potent vaccines against all strains of HIV. Unfortunately, it has not yet been possible to develop a vaccine with sufficient efficacy, therefore the arsenal of different antiviral drugs needs constant expansion.^{106,107} Consequently, all viral and host proteins involved in the replication process are under investigation as potential targets. For example, each aspect of viral entry can be addressed and blocked through different kinds of drugs, targeting either viral proteins like gp120 or host factors like the CCR5 receptor.¹⁰⁸

2.2.2. Drug Toxicity and NRTI Resistances

Monotherapy with AZT has shown that the virus develops resistance to such approaches. Spontaneous mutations caused by the lack of a proofreading function of the HIV-RT can lead to resistance against all kinds of drugs.^{35,36} For the scope of this work, the focus will be on NRTIs and their pharmacological profiles.

Early NRTIs are associated with a variety of toxicities including cardiomyopathy, peripheral neuropathy, sensorineural deafness, diabetes type 2 and cytopenia (**Table 2**).^{95,109}

Table 2: Toxicity profiles of several NRTIs.^{95,109}

NRTI	Mitochondrial toxicity potential	Other predominant toxicities
Abacavir	+	Hypersensitivity reaction
Didanosine	++++	Pancreatitis, peripheral neuropathy, cardiomyopathy, lactic acidosis, diabetes type 2
FTC	+	Mild headache, rash, gastro intestinal upset
3TC	+	Constitutional symptoms
d4T	++++	Lipoatrophy, pancreatitis, peripheral neuropathy, lactic acidosis
TDF	+	Fanconi's syndrome, renal insufficiency, gastrointestinal upset
Zalcitabine	++++	Thrombocytopenia (5 %), anemia (10 %), pancreatitis, cardiomyopathy, peripheral neuropathy (35 %), lactic acidosis, sensorineural deafness
AZT	++	Myelosuppression, lipodystrophy, cardiomyopathy, lactic acidosis, cytopenia

++++ Strongest association with mitochondrial toxicity, + weakest association with mitochondrial toxicity,

Other NRTIs related toxic effects are lipodystrophy, which can cause an unnatural redistribution of fat and increased truncal fat, through hypertriglyceridaemia, hypercholesterolaemia and low high-density lipoprotein.^{95,97} Hypersensitivity, which is believed to be caused by a severe imbalance of CD4⁺ and CD8⁺ lymphocytes, is most commonly present in the form of erythematous, maculopapular, pruritic and confluent rash.⁹⁷ Dyslipidaemia, which can contribute to cardiovascular disease due to abnormal lipid levels and is likely a factor in insulin resistance.^{97,110}

One especially significant factor of NRTI toxicity is the inhibition of human mitochondrial polymerase γ (pol γ) or the mutation of the gene encoding pol γ , which in consequence leads to a depletion of mitochondrial DNA/RNA.¹¹¹ After intracellular phosphorylation, NRTI triphosphates are transported into the mitochondria via transport proteins competing with natural NTPs in mitochondrial DNA

synthesis. In contrast to cellular DNA, mitochondrial DNA is constantly replicated and encodes enzymes involved in oxidative phosphorylation (OXPHOS), which are essential for the production of adenosine triphosphate (ATP). The disruption of OXPHOS also leads to a disruption in the electron transport chain in the mitochondrial cell membrane. This can cause a proton gradient in the mitochondrial matrix, resulting in higher amounts of oxidative stress.^{111–114} Selective inhibition of HIV-RT over human polymerases will become an important parameter to improve the overall efficacy of NRTI based treatments.¹⁰⁹ Research also suggests that the persistence of phosphorylated NRTI analogues can disrupt exonucleolytic proofreading, resulting in mutated mitochondrial DNA species. The first manifestation of mitochondrial toxicity induced by NRTI therapy was reported in 2007 by YAMANAKA *et al.*¹¹⁵ Both the incorporation and the mutation are causing severe manifestations of mitochondrial toxicity like lactic acidaemia or neuropathy.^{10,111} Therefore, NRTIs with more favourable toxicological profiles, such as 3TC or FTC, have an advantage over their competitors.¹¹⁶

In addition to mutation-related toxicities, NRTI therapy can cause mutations in HIV-RT, resulting in emerging resistances. These resistances can be categorized into two types. The first type, e.g. M184V, results in spatial changes in the active site, excluding NRTIs through steric hindrance. The second type leads to the selective excision of the incorporated NRTIs. This mechanism is especially well understood for the excision of AZT (**Figure 6**), which is caused by mutations including M41L, D67N, K70R, L210W, T215F/Y, K219E/Q, collectively referred to as AZT resistant mutations.^{34,114,117–119}

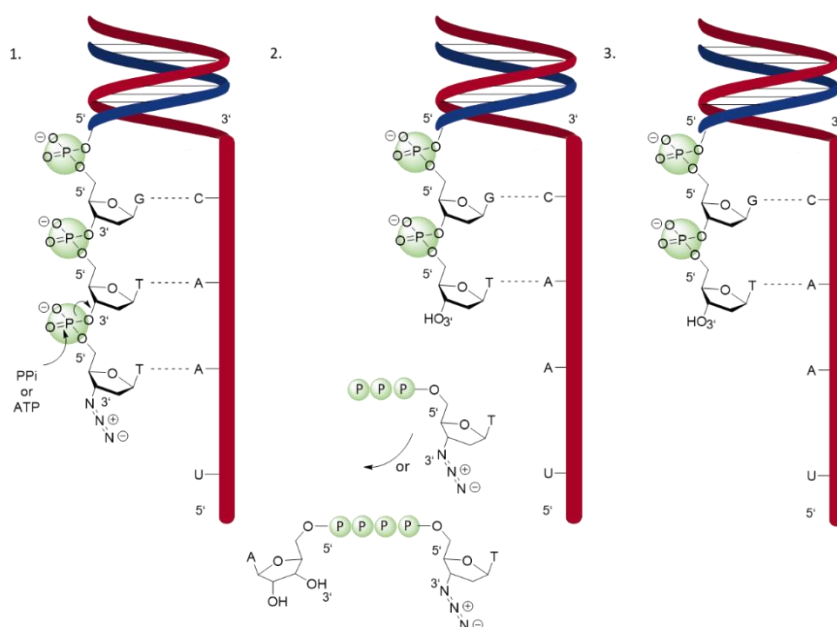


Figure 6: Depiction of HIV-RT catalysed NRTI excision, exemplified with AZT.¹²⁰

The AZT resistant mutations also lead to the excision of dNTPs, which is compensated by higher DNA synthesis activity. While mutations like Q151M are shown to cause multidrug resistances¹²⁰, studies have shown that some 3TC resistances prove detrimental to the overall fitness of the virus.²¹

2.3. NRTI Prodrugs

2.3.1. Prodrug Development

The pronounced cytotoxicity of several NRTIs, demands the development of new drugs or the improvement of existing drugs. Since the therapeutic window between efficacy and toxicity can be narrow for some NRTIs^{121,122}, enhancing the bioavailability of NRTIs can significantly improve the pharmacological profile of a drug. The active species of each NRTI is the triphosphate, which is formed by intracellular phosphorylation by corresponding host enzymes (**Figure 7**).¹²³ Each phosphorylation step can be a limiting factor to achieve the maximum availability of the active compound.¹²⁴ AZT for example is mostly phosphorylated to the monophosphate, therefore the triphosphate is not available in sufficient quantities.^{122,125} Direct delivery of NRTI-triphosphates as active compounds into the cell would yield best results. NRTIs, though hydrophilic, can mostly enter cells through passive diffusion or active carrier mediated transport.⁹ However, due to the high charge of mono-, di- and triphosphates, nucleotides have low cell membrane permeability and are susceptible to dephosphorylation.^{126,127}

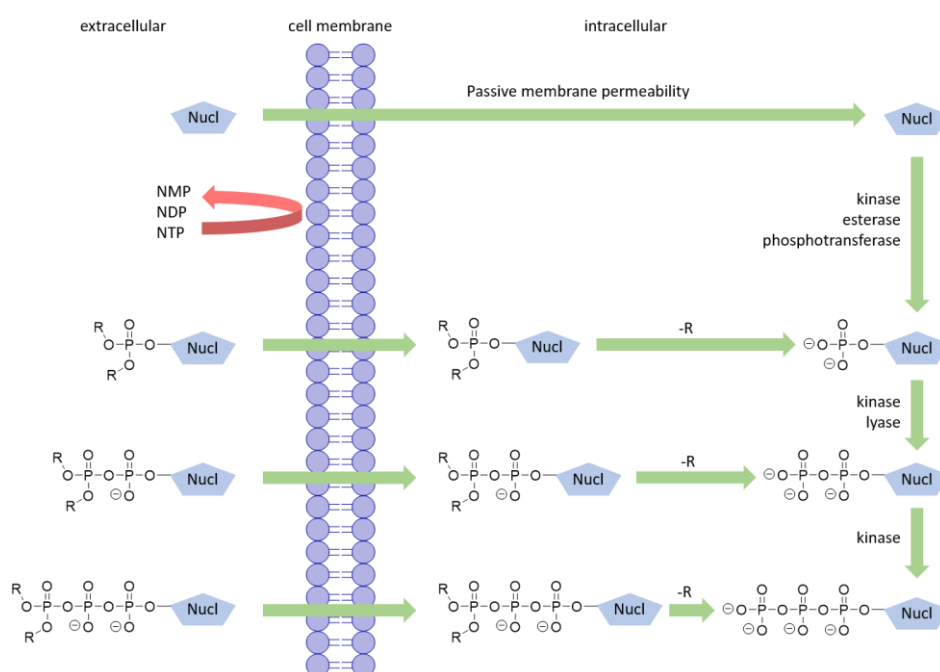


Figure 7: Delivery mechanism and metabolic pathway of NRTIs NMP-, NDP- and NTP-prodrugs into the cell.^{124,128–130}

Phosphorylation of different NRTIs is catalysed by different enzymes. For pyrimidine analogues, the metabolic pathways are similar. Monophosphates are generated by thymidine- and deoxycytidine kinase, respectively. The diphosphates are formed using either thymidine 5'-monophosphate kinase, cytidine monophosphate- or deoxycytidine monophosphate kinase. Both triphosphates are formed utilizing nucleoside diphosphate kinase. For purine-based NRTIs phosphorylation pathways are more varied. TAF and TDF (**Figure 8**) consists already of phosphonate group and thus only requiring phosphorylation to their monophosphate *via* adenylate kinase following formation of the diphosphate

via pyruvate- or creatine kinase. Dideoxyinosine is phosphorylated by 5'-nucleotidase, adenylate lyase and kinase, respectively. Abacavir monophosphate is formed using adenosine phosphotransferase, followed by the transformation to carbovir monophosphate through deaminase, before the di- and triphosphate are formed using guanylate kinase.^{124,128}

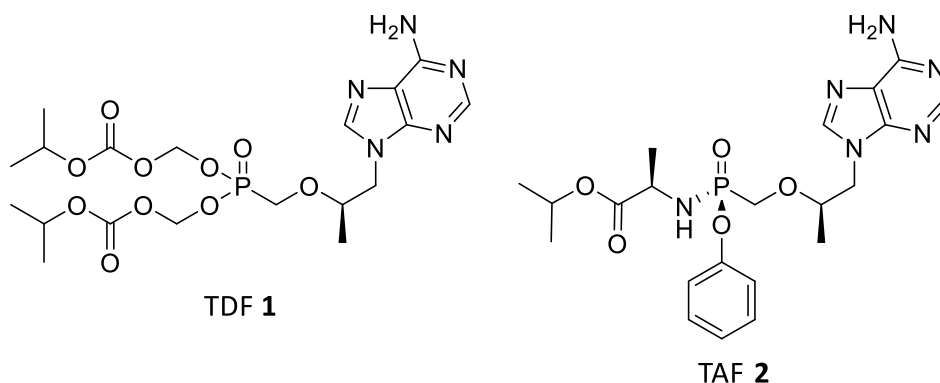


Figure 8: Nucleotide reverse transcriptase inhibitors TAF and TDF.

For many NRTIs the phosphorylation to the monophosphate is the rate-limiting step. The drug d4T, for example, has a 600-fold lower affinity to thymidine kinase than thymidine.¹³¹ To overcome this barrier, MONTGOMERY¹³² proposed the development of nucleotide prodrugs that can pass the cell membrane and are rapidly converted into their corresponding nucleotides.¹³³ The first approved drug, against HIV, employing this concept was TDF providing high levels of intracellular monophosphate analogue (**Figure 8**).¹³⁰ Providing prodrugs can also have the additional benefit of renewed activity for NRTIs. For example, aryl protected AZT prodrug showed activity against AZT resistant strains of HIV-1 *in vitro*.¹³⁴

2.3.2. Nucleoside Monophosphate Prodrugs

In order to overcome hurdles during the development of promising nucleosides, such as poor bioavailability, low absorption, instability, poor specificity, formulation difficulties or other adverse effects or toxicity, prodrugs have become the go-to method.^{135–137} A plethora of prodrugs were developed in the last four decades (**Figure 9**) to mask functional groups like phosphates and phosphonates. Each prodrug must find a delicate balance between facilitating efficient absorption and cleavage of the masking units, while also overcoming the challenges posed by a high negative charge. This includes addressing issues such as poor bioavailability and the potential generation of toxic by-products.¹³⁸

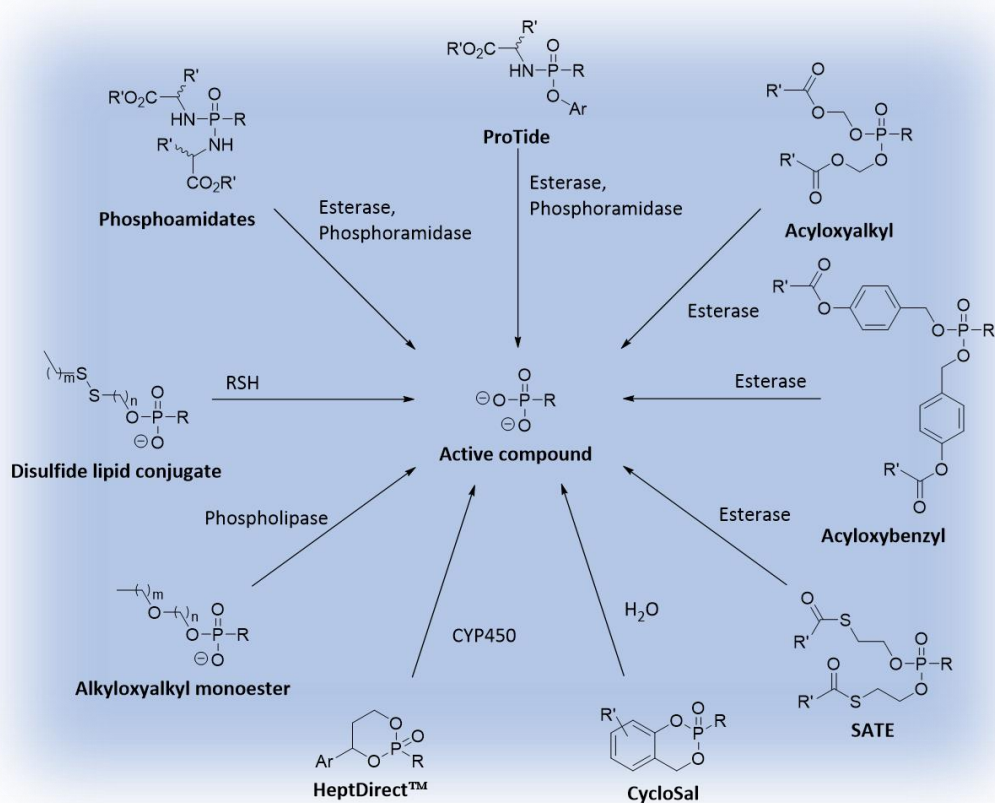


Figure 9: NRTI prodrug systems and corresponding modes of activation. Adapted from HEIDEL *et al.*^{136,139,140}

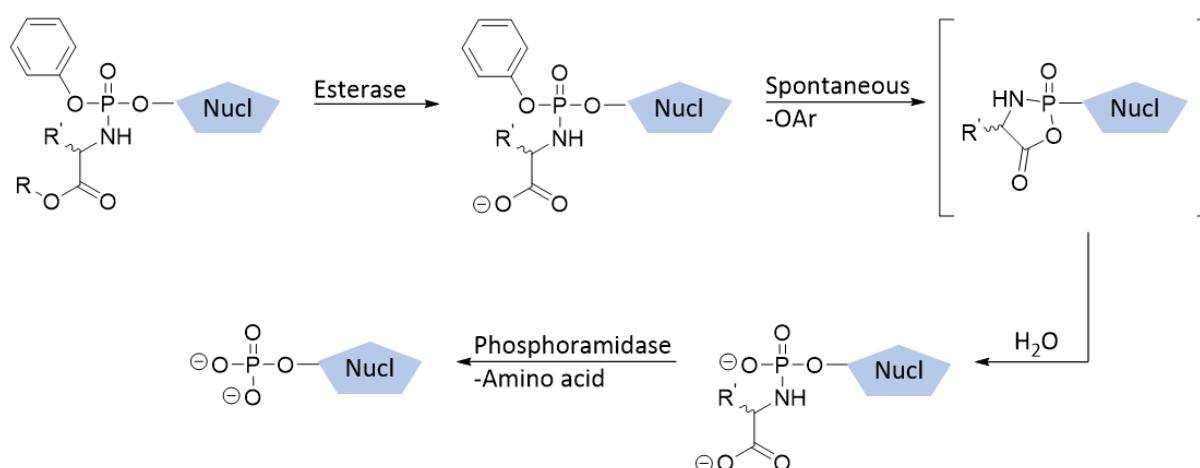
Stearyl-bearing masking units were the first to be employed in nucleotide-based prodrugs. They were proposed by ROSOWSKY *et al.* in 1982. They were conceived to overcome the short half-life of cytarabine, an anti-cancer drug. The mask can be cleaved via oxidation in liposomes. The successful implementation led to the approval of 1- β -D-arabino-furanosylcytosine-5'-stearylphosphate against leukaemia in 1992.^{138,141,142}

In 1984, FARQUHAR *et al.* proposed bis[(acyloxy)methyl] organophosphates to overcome the therapeutic failures of previous alky or aryl triesters to deliver their parent nucleotides. The acyloxyalkyl group is cleaved by unspecific carboxy esterase after passive diffusion into the cell. After dissociation of formaldehyde, a diester is formed. This process is repeated, though the second cleavage is much slower. One drawback of these compounds is the release of pivalic acid which can result in impaired ketone-body production, therefore newer compounds substitute pivalic esters with more suitable analogues.¹⁴³ The acyloxyalkyl delivery system is used in various drugs, adefovir dipivoxil for hepatitis B and the above-mentioned TDF against HIV are prominent examples for FDA approved drugs.^{144,145}

As an improvement on carboxy esters, DEVINE *et al.* proposed phosphoramidate triesters as masking groups. In contrast to their counterparts, esterified amino acids can be used, which are cleaved without formation of toxic by-products. In 2015, phosphonodiamidates have received attention as a measure to target *Bordetella pertussis* adenylate cyclase toxin with acyclic nucleosides.^{126,146,147}

The bis(phosphoramidate) approach was further improved by MCGUIGAN *et al.* by replacing one amidate with an aryl group.¹³⁴ In an effort to evaluate modified phosphoramidates, it was found that an **pronucleotide** (ProTide) containing alanine and an aryl moiety as substituents yielded the best results.¹⁴⁸ Through a multistep cleaving mechanism, catalysed by two different enzymes and the spontaneous release of phenol (

Scheme 1), the potency of several drugs were >1000-fold higher compared to their parent nucleosides and retained activity even in thymidine kinase deficient (TK⁻) cells.

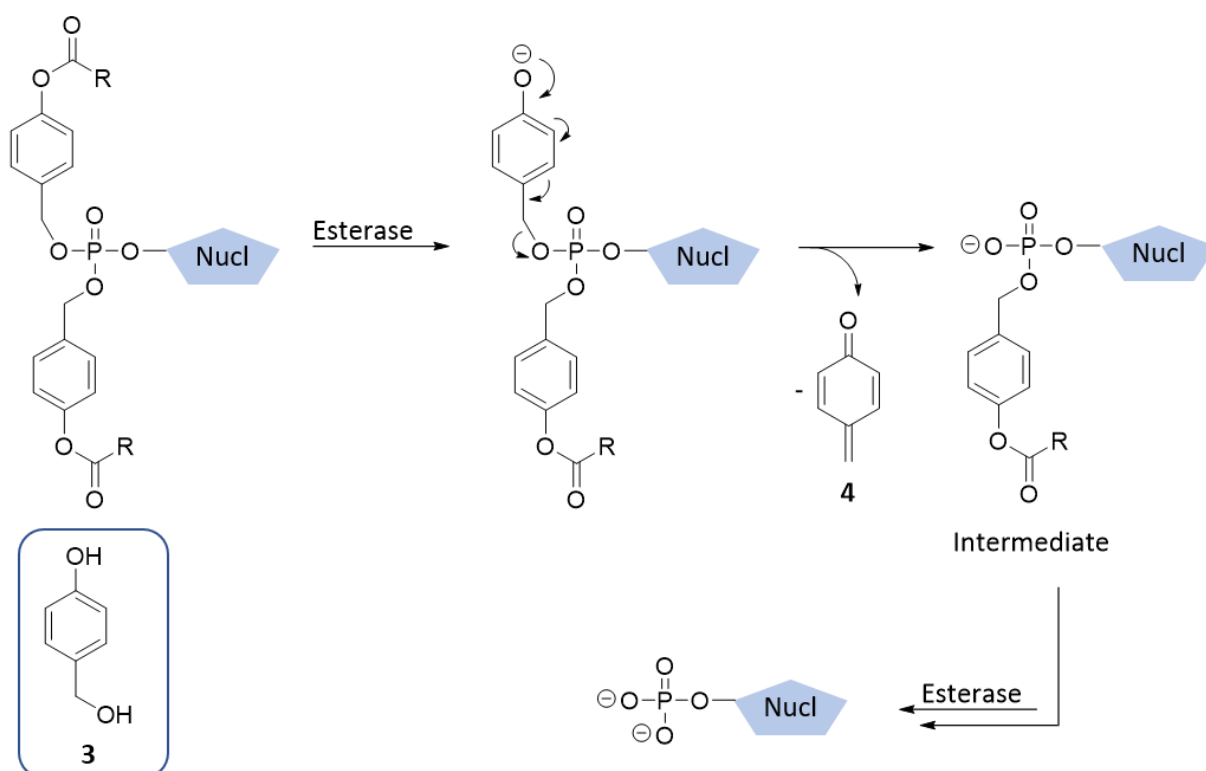


Scheme 1: Intracellular pathway for ProTide monophosphate release.¹⁴⁹

TAF is the most prominent application of the ProTide system and one of the most prescribed drugs, as part of several co-formulations, against HIV.¹⁵⁰ The ProTide system is further investigated for treatment against other diseases like malaria¹⁵¹, hepatitis C¹⁵² or SARS-CoV 2.¹⁵³

Both the S-acetylthioethanol and dithiodiethanol prodrugs, which were presented by PÉRIGAUD *et al.* in 1993, have a higher reducing potential within the cytosol. Cleavage either by carboxy esterase or reductase releases the monophosphate after an identical, spontaneous second degradation step. The formation of toxic episulfides was reported as an undesirable by-product.^{145,154,155}

In the same year, THOMPSON *et al.* developed the AB prodrug. In this concept, the benzene moiety of 4-hydroxybenzylalcohol **3** is placed between the phosphate and the enzyme cleavable acetyl function to separate the resulting negative charge and the cleavage site of the second masking unit. This minimizes the interference of the anionic charge with the carboxyl ester and the rate of removal of the second acetyl group is highly improved compared to their acetyloxyalkyl counterparts. After cleavage of the acyl group, the polarity of the benzyl moiety is inverted, from an electron acceptor to an electron donor, which leads to a spontaneous decomposition (1,6-elimination), forming *p*-quinonemethide **4** and the monosubstituted NMP (**Scheme 2**).^{138,156,157}



Scheme 2: Intracellular cleavage mechanism for acyloxy benzyl (AB) prodrugs.¹⁵⁷

Another prominent prodrug system was developed by MEIER *et al.* in 1996.¹⁵⁸ It was the first system that did not use enzyme-cleavable substituents and instead utilized the release of the monophosphate by chemically induced hydrolysis ($\text{pH} > 7$).¹⁵⁹ The **cyclosaligenyl** (*cycloSal*) masking group is cleaved in a concerted two-step process, with the phenolate bond being cleaved first due to the slightly higher cytosolic pH value. Subsequently, the benzylic group is cleaved due to an inversion of the polarity, comparable to the AB prodrugs, which leads to the spontaneous cleavage of the diester and the release of the monophosphate.¹⁶⁰ Due to the lipophilic nature of *cycloSal* prodrugs, these compounds were able to pass the cell membrane in both directions, so that a second-generation of so-called “lock-in”-prodrugs was developed. These “lock-in”-prodrugs have an additional with enzyme-cleavable substituent at the aromatic ring, so that the prodrug remains in a charged state after cleavage and the molecule is trapped in the cell.⁴² The third-generation of *cycloSal*-prodrugs was equipped with a lipophilic electron-donating substituent (e.g. 5-diacetoxymethyl group) to prevent extracellular hydrolysis.¹⁶¹ In some cases, *cycloSal* approach led to an up to 600-fold increase in activity compared to the parent nucleosides.¹⁶⁰

In 1997, HOSTETLER *et al.* synthesized alkyloxyalkyl prodrugs. These prodrugs did not only show high potency against HIV-1 and other viral targets like hepatitis C virus or the *Epstein-Barr* virus. A >10000-fold increased activity against HIV-1 was reported for their hexadecyloxypropyl prodrug compared to the parent nucleoside. These compounds also showed that lipid-like substituents can sufficiently mask negative charges eliminating the requirement of further masking groups.^{136,162,163}

ERION *et al.* tackled the problem of site-specific release of prodrugs. Cyclic 1,3-propanyl esters with aryl functions were used to increase local drug levels in specific organs without the use of antibodies or similar targeting vectors. The so-called *HepDirect*[™] prodrugs were sensitive to an oxidative cleavage reaction catalysed by cytochrome P450, which is predominantly present in the liver. With this concept, a 12-fold improvement in PMEAs-levels in the liver compared to adefovir dipivoxil was achieved.^{136,137,164}

2.3.3. Nucleoside Diphosphate Prodrugs

Like the first phosphorylation step for NRTIs such as d4T, the second phosphorylation step is the bottleneck for NRTIs such as AZT.¹⁶⁵ In the case of AZT, this not only led to lower concentrations of the active triphosphate, and thus to lower antiviral activity, but high concentrations of AZT-monophosphate led to severe side effects.^{166,167} HOSTETLER *et al.* proposed diacylglycerol NDP prodrugs to bypass this phosphorylation step (**Figure 10**, left). However, these prodrugs only yielded positive results for 2',3'-dideoxythymidine, while yielding weaker results for AZT and zalcitabine compared to their parent nucleosides.¹⁶⁸ A similar approach was published in 1995 by BONNAFFÉ *et al.* with an acylated NDP at the β -phosphate (**Figure 10**, right).¹⁶⁵ Studies showed that these prodrugs were hydrolysed to the corresponding NDP and NTP in triethylammonium acetate buffer at physiological pH

as well as in RPMI medium. In the latter case, however, hydrolysis was too fast ($t_{1/2} < 2$ h) for sufficient membrane permeability. This led to half-maximal effective concentration (EC_{50}) values for AZT analogues in the same range as their parent nucleosides.¹⁶⁹

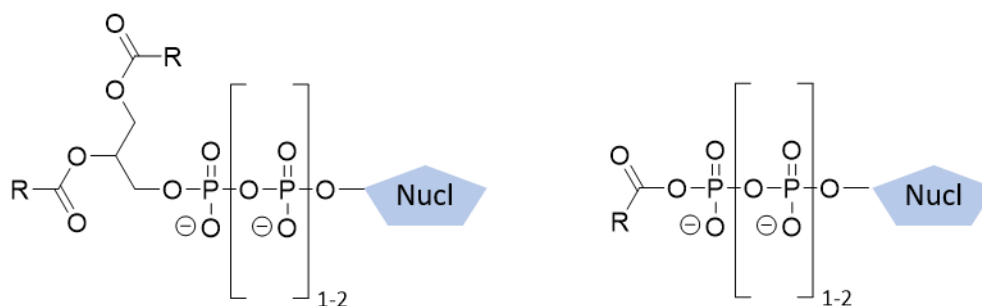
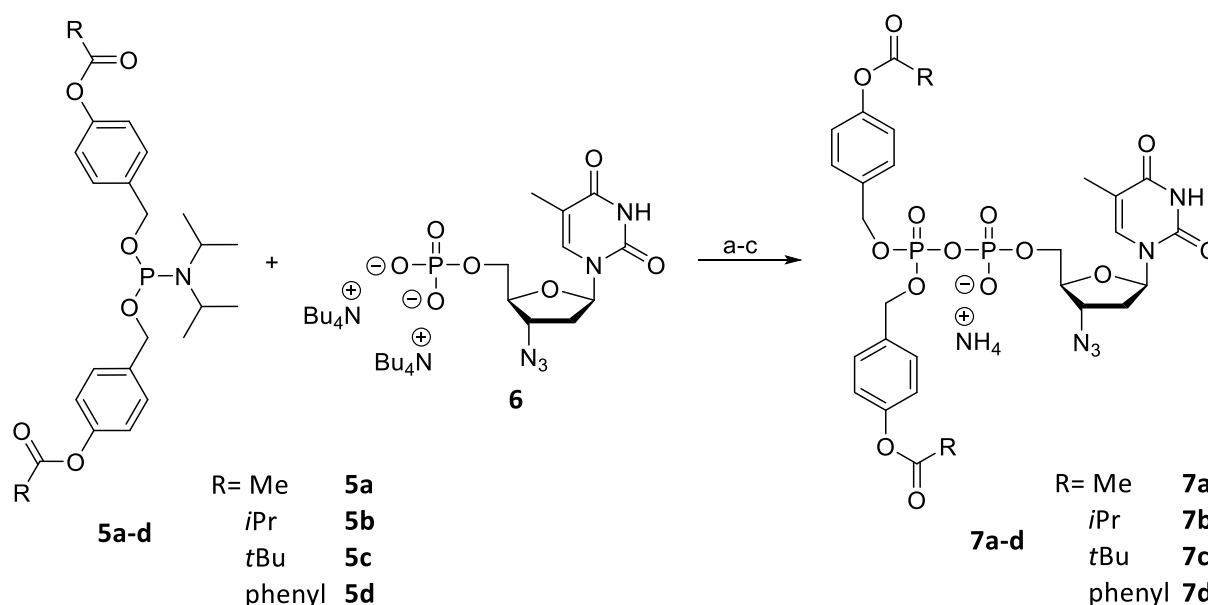


Figure 10: Schematic depiction of nucleoside di- and triphosphate diacylglycerol^{168,170} and acyl prodrugs.^{165,169}

Since the promising results of their *cycloSal* NMP prodrugs set a precedent for a successful delivery mechanism, MEIER *et al.* investigated *cycloSal* NDPs for their usefulness. Unfortunately, the hydrolysis of these *cycloSal* NDPs mainly yielded NMP as a product instead of the desired NDP.^{157,171} In an effort to develop chemically stable NDP prodrugs, the group investigated the concept of enzymatically cleavable AB prodrugs published by THOMPSON *et al.* and applied this to diphosphates.

In 2008, this effort resulted in the establishing of the first chemically stable NDP prodrugs with selective enzymatic cleavage in a cell extract by JESSEN *et al.*¹⁵⁷ The **diphosphate prodrugs (DiPPro)** were synthesized by coupling different phosphoramidates with NMPs using 4,5-dicyanoimidazole (DCI) (**Scheme 3**).

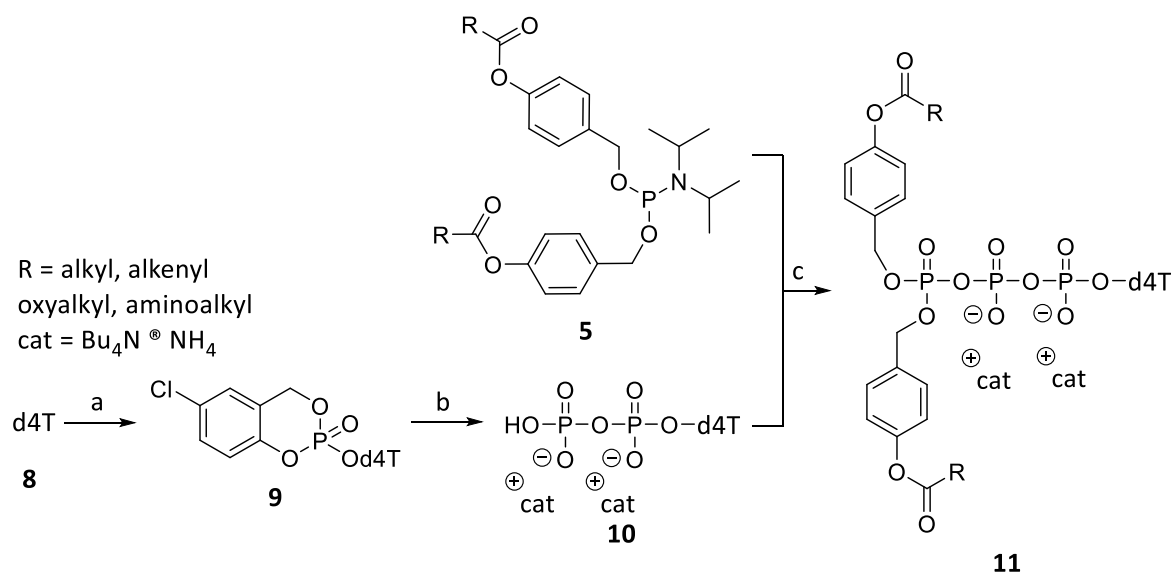


Scheme 3: Synthesis of AZT DiPPro prodrugs **7a-d**: Reagents and conditions: **a)** DCI, CH₃CN, rt, 1 h; **b)** *t*BuOOH, -20 °C → rt, 15 min; **c)** RP-18 flash chromatography, ion exchange: 1. DOWEX 50WX8 (NH₄⁺), RP-18 flash chromatography.¹⁵⁷

This synthetic pathway opened up access to a wide variety of antiviral compounds, enabling high adjustability of the chemical properties. Hydrolysis studies in plasma showed half-lives up to 30 min, enabling the formation of large amounts of NDPs and NMPs. The ratio of NDP to NMP was even improved by using non-symmetric masking units.^{46,157} DiPPro compounds with alkyl residues $R \geq C_6H_{13}$ were reported to be the most effective bioreversibly protected compounds tested *in vitro* against CEM/TK⁻ cells.⁴⁵

2.3.4. Nucleoside Triphosphate Prodrugs

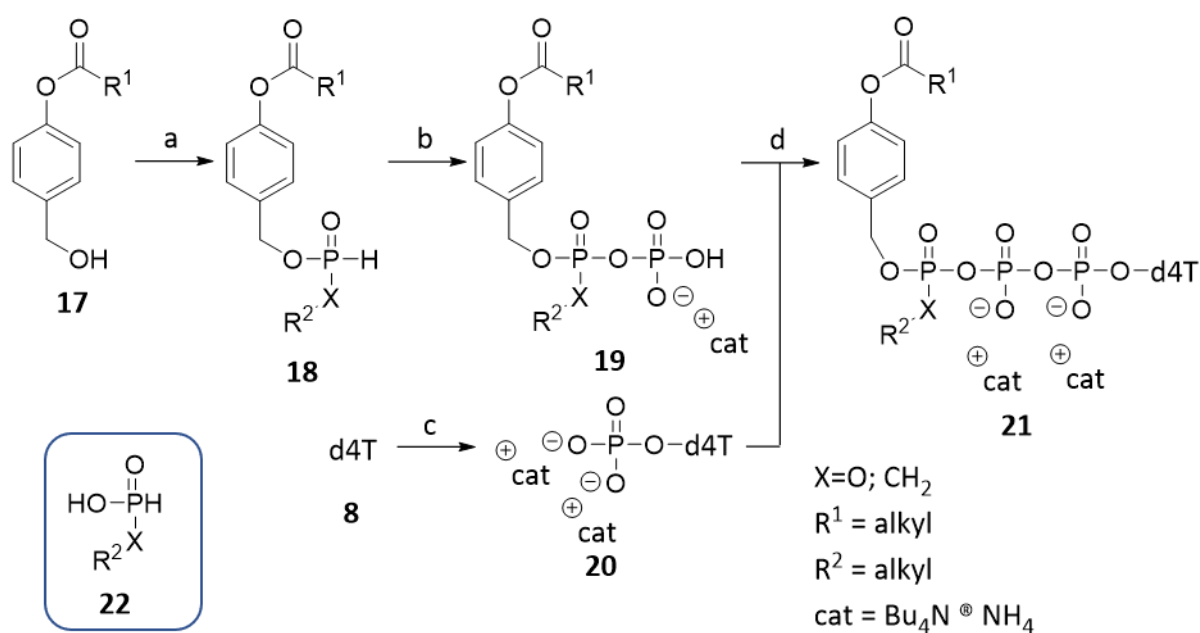
Since the delivery of diphosphate prodrugs did not significantly improve the antiviral activity of several DiPPro prodrugs compared to their parent nucleosides¹⁷², circumvention of the final phosphorylation step and thus maximizing the concentration of the active NTP was the declared goal of the group of MEIER *et al.* The first successful synthesis of a TriPPro was achieved by GOLLNEST *et al.* by a combination of the prior lessons learned in the pursuit of diphosphate prodrugs. The bis(AB) masked TriPPro-compounds were synthesized analogously to their DiPPro counterparts using DCI as coupling reagent. Here, instead of monophosphates, the respective diphosphates obtained by *cycloSal* chemistry were used (**Scheme 4**).^{48,173} Contrary to the assumption that triphosphate prodrugs are not feasible due to their chemical instability,¹⁷⁴ this approach reaffirmed the findings, that modifications at the γ -phosphate group lead to a marked increase of enzymatic stability of the triphosphate unit.^{175,176}



Scheme 4: Reagents and conditions. a) **1**. 5-Chlorosaligenylchlorophosphite **12**, *N,N*-diisopropylethylamine, CH₃CN, 20 °C→rt, 3 h, **2**. *t*BuOOH in *n*-decane, 0 °C→rt, 30 min; b) (H₂PO₄)Bu₄N, DMF, rt, 20 h; c) **1**. DCI, CH₃CN, rt, 1 min, **2**. *t*BuOOH in *n*-decane, 0 °C, 20 min.^{48,173}

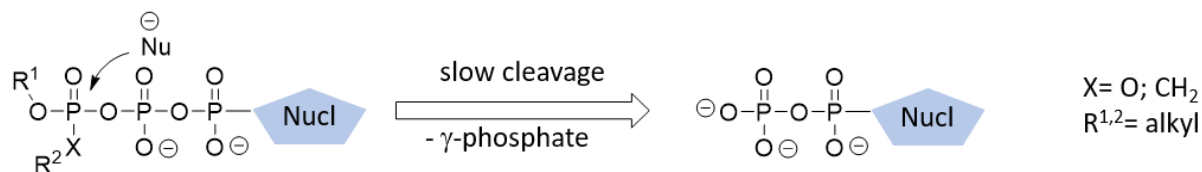
NACK *et al.* successfully developed γ -alkylketobenzyl (kb) protected d4T prodrugs (**Scheme 5**, red), which lacked the ester function, necessary for esterase-mediated cleavage. Both γ -(AB,kb)-d4TTP and single masked (kb)-d4TTP prodrugs were synthesized and the latter tested against HIV-RT, pol β , human polymerase α (pol α) and pol γ . These studies revealed, that (kb) prodrugs retained substrate properties regarding HIV-RT, while not being active in human polymerases for both d4TTP and dTTP single-masked analogues.⁵⁰ One requirement for antiviral prodrugs should be their selectivity to their respective target. The lack of substrate properties for human polymerases, especially for pol γ , could significantly reduce toxic side effects of these compounds. In addition to their enhanced selectivity, second-generation TriPPPPro-compounds also provide further advantages compared to their bis(AB) counterparts. The implementation of non-cleavable groups led to plasma hydrolysis half-lives >24 h, which results in increased availability of bioactive metabolite inside the cell.⁵⁰ It is suggested that the non-cleavable group may also impede transport into the mitochondria.¹¹¹

Further simplification of the second-generation was achieved by ZHAO *et al.* and JIA *et al.* by replacing the kb masking unit with an alkyl phosphate or alky phosphonate group respectively (**Scheme 6**). The overall hydrolytic and antiviral properties were comparable to the kb prodrugs, but the synthesis was shortened and allowed for easier adjustment of lipophilicity and substrate properties.^{51,52,179}



Scheme 6: Reagents and conditions: a) (DPP, alkyl alcohol)/ **22**, pyridine, 0 °C→38 °C, 3.5 h; b) i) NCS, CH₃CN, rt, 2 h ii) (H₂PO₄)Bu₄N, CH₃CN, rt, 1 h; c) POCl₃, pyridine, H₂O, CH₃CN, 0 °C→rt, 5 h; d) i) TFAA, Et₃N, CH₃CN, 0 °C, 10 min, ii) 1-methylimidazole, Et₃N, CH₃CN, 0 °C→rt, 10 min, iii) d4T-MP **20**, rt, 2-3 h.^{51,52}

Following the conformation of nucleotide diphosphates as substrates for HIV-RT, a third generation of triphosphate prodrugs were introduced by JIA *et al.*¹⁸⁰ In exchange for a cleavable mask a second non-cleavable group was introduced, utilizing nucleophile mediated intracellular cleaving of the γ -phosphate group to deliver nucleoside diphosphate to the target (**Scheme 7**).



Scheme 7: Release mechanism of triphosphate prodrugs with two non-cleavable masks.¹⁷⁹

2.4. Viral and Human Polymerases

As mentioned in 2.1.2 (p.5) HIV-RT is the viral enzyme responsible for the reverse transcription of the viral RNA to DNA. RT is a 51 kDa heterodimer containing a 560 amino acid residue subunit (p66) and a 440-residue subunit (p51) encoded at the gene encoding pol γ (POLG). The subunit p66 contains the polymerase and RNase H function.^{11,120} Inhibiting HIV-RT through NRTIs is the backbone in HIV therapy. Despite having lower affinity towards NRTIs human polymerases can also incorporate NRTIs, leading to severe side effects.¹⁰⁵

2.4.1. Nuclear Polymerases α , ϵ , and δ

Most human polymerases have several safety mechanisms to prevent the incorporation of wrong NTPs. High fidelity polymerases serially select against non-cognate pairings, while additionally exhibiting proofreading functionality to excise incorrectly incorporated nucleotides.¹⁸¹ The low affinity towards NRTIs (HIV-RT \gg pol γ > pol β > pol α = pol ϵ ¹⁰) and the fact, that nuclear polymerases are only active during mitosis, makes them a lower priority in consideration of NRTI design. Pol α consists of a catalytic subunit (p180; 166 kDa) and an ancillary subunit (p70; 66 kDa) and is involved in eukaryotic replication, which is enabled by a complex of multi-subunit polymerases (pol α , human polymerase ϵ (pol ϵ), human polymerase δ (pol δ) and primase).¹⁸² The synthesis of chromosomal DNA is divided into different parts. Pol ϵ is responsible for the synthesis of most of the leading strand, pol δ creates the lagging strand, and pol α together with primase synthesizes the DNA primers. Pol α exhibits the lowest fidelity among nuclear polymerases and has no proofreading function, making it an undesirable candidate for the incorporation of NRTIs.^{183,184}

2.4.2. Human Polymerase β

Pol β is the smallest human DNA polymerase (335 residues; 39 kDa), it lacks 3' \rightarrow 5' proofreading function, and it was believed that pol β mainly functions as a repair polymerase during DNA synthesis and during the repair of apurinic/aprimidinic (AP) sites. AP sites are formed by spontaneous

depurinations or lesion-specific hydrolysis of the *N*-glycosyl bond.^{185–187} In 2017, two groups independently presented evidence that pol β is significantly involved in base excision repair (BER) within the mitochondria and thus plays a vital role in mitochondrial DNA integrity and mitochondrial function.^{186,188}

2.4.3. Human Mitochondrial Polymerase γ

NRTI induced mitochondrial toxicity is mostly caused by the disruption of structural integrity of mitochondrial DNA, as mentioned in 2.2.2. (p.6). In contrast to nuclear DNA, mitochondrial DNA is continuously recycled,¹⁸⁹ leaving more opportunity for polymerase disruption. Mitochondrial DNA codes for 13 essential polypeptides involved in the respiratory chain, and its depletion therefore leads to significant cellular dysfunction or cell death.¹⁰ Although pol γ exhibits proofreading and exonuclease functionality, and is also considered a high fidelity polymerase ($<2 \times 10^{-6}$ errors per nucleoside), it is particularly susceptible to NRTI incorporation, compared to other polymerases.¹¹⁴ *In vitro* experiments with various NRTIs showed that some nucleotides were not removed by its proofreading function after 12 h incubation (Zalcitabine).^{186,190} On the other hand pol γ showed significant discrimination against some NRTIs, e.g. FTC and 3TC, which could be a stereochemically dependent mechanism. FTC and 3TC either are not incorporated or are efficiently removed after ~ 1 min.¹⁹¹

The exact involvement of NRTIs in mitochondrial DNA depletion and mitochondrial toxicity is not yet fully understood. Unfortunately, three (pol γ , pol β and PrimPol) out of five DNA polymerases localized in the mitochondria (pol γ , pol β , PrimPol, pol θ and pol ζ) are potential targets for NRTI incorporation. The design of future antiviral prodrugs based on results of structure function studies could contribute to a higher specificity for viral polymerases and limit the toxic effects of these compounds.¹⁸⁶

2.4.4. Primer Extension Assay

Primer extension assays commonly serve two purposes, to either measure the amount of a given RNA or to map the 5' end of that RNA, but can also be utilised to analyse substrate properties of nucleoside-based drugs.^{192,193} The RNA templates are annealed with a complementary primer, labelled with radioactive or fluorescent markers. Through incubation with different reverse transcriptases, like HIV-RT, pol γ or RNA-dependent DNA polymerase, the 5' end of the RNA is synthesised. The analysis through denaturing polyacrylamide gel electrophoresis (PAGE) can detect a single incorporation difference. Experiments are preferably designed with extended small strands (<100 nt).¹⁹⁴ In the context of antiviral drug development, these assays are instrumental in elucidating the ability of a compound to inhibit viral polymerases, such as HIV-RT.¹⁹³

3. Objectives

As HIV remains a heavy burden on our society today and vaccines^{106,107} are still unattainable, the development of potent antivirals remains the cornerstone in combating this disease. The group of MEIER *et al.* progressed on this path, starting with the development of highly active monophosphate prodrugs⁴² ending with the development of the TriPPPPro concept, which delivers triphosphates into the cell.⁴⁸ This delivery mechanism allows for triphosphates to cross the cell membrane and circumvent rate-limiting phosphorylation steps.⁴⁸

The stated goal of this work was to evaluate existing prodrugs using biological tests. Primer extension assays should be used as a tool to examine substrate properties, and this information could be used to adjust different prodrug parameters. These assays should incorporate findings received from antiviral data from external partners, who have tested prodrugs against HIV-infected CEM cells. Additionally, the design of future masking units should be based on the results of cell uptake studies, which were performed in our group. The TriPPPPro technology (**Figure 11**) provides several moieties, which offer room for modification.

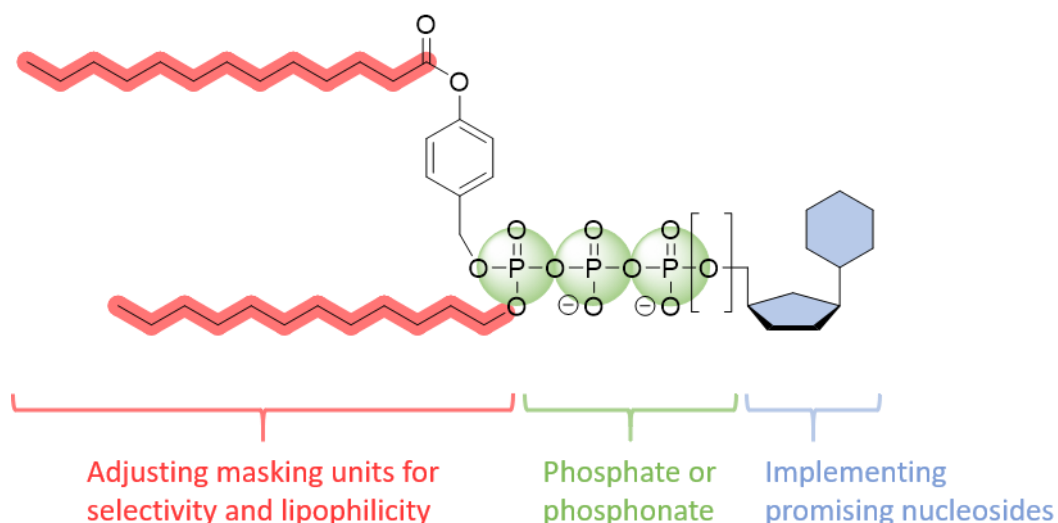


Figure 11: Schematic depiction of a γ -modified alkyl(AB) prodrug, and potential modification sites (red, green and blue).

The first part of this thesis addresses the modification and optimization of the alkyl chains, which were suggested to be essential to achieve two main objectives. First, this should change the substrate properties of the triphosphates so that only viral enzymes can utilize them for DNA synthesis, and secondly, it should improve bioavailability through better cell permeability. Studying the results of existing prodrugs is essential to alter the design of innovative antiviral nucleotides.

Objectives

After establishing suitable masking units, the second part of this thesis should focus on incorporating established, naturally selective, and exceptionally active nucleosides into this workflow. Several nucleosides were chosen due to their specific properties (**Figure 12**). 3'-Fluoro-2',3'-dideoxythymidine **23** (FLT; Alovudin) was chosen for its high antiviral activity shown to be in the low nanomolar ranges by WEISING *et al.*¹⁹⁵ 2',3'-Didehydro-3'-deoxy-4'-ethynylthymidine **24** (4'-Ed4T, Censavudin) demonstrated intrinsic discrimination against pol γ , resulting in a good balance between antiviral activity and host toxicity.¹⁹⁶ While the development for FLT was stopped due to high toxicity⁹ and lack of enhanced efficacy compared to approved NRTIs¹⁹⁷, the development of 4'-Ed4T was discontinued primarily due to commercial reasons.¹⁹⁸ (-)-2'-Deoxy-3'-thiocytidine **25** (3TC, Lamivudin) was selected on the basis of the two previous considerations. 3TC is widely used in several different co-formulations and has been part of successful HIV treatment since its approval.⁹⁶ In addition, the *L*-configuration leads to intrinsic discrimination against human polymerases due to their *D*-stereospecificity.^{53,55} Lastly, (-)-2'-deoxy-3'-oxa-4'-thiocytidine **26** (dOTC, Apricitabin), a 3TC/FTC replacement drug, was chosen due to its beneficial properties. It has been shown that dOTC remains active against viral strains that are resistant to 3TC and shows no interaction with pol γ .¹⁹⁹

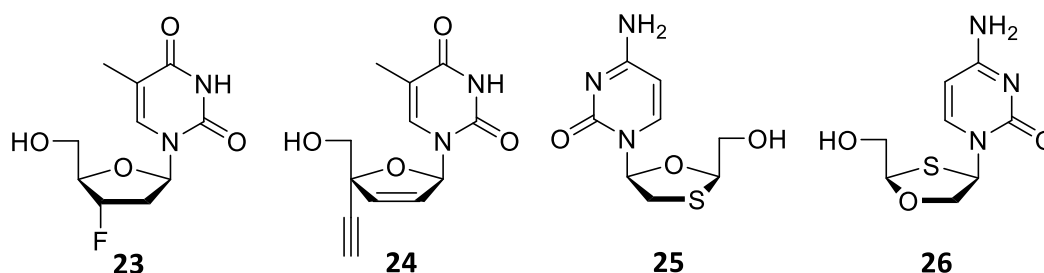
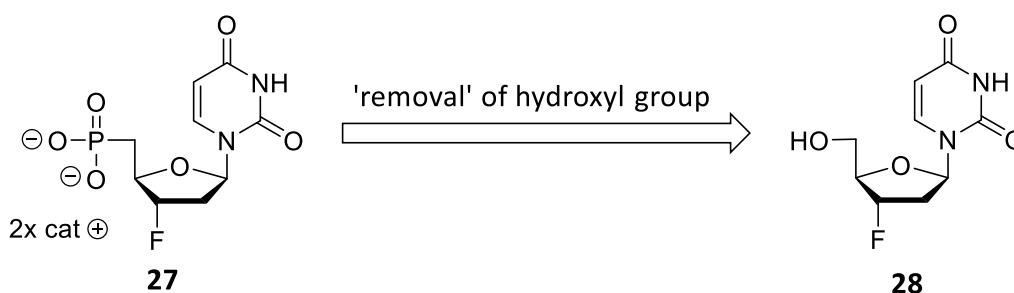


Figure 12: Selected NRTIs for the application in γ -modified alkyl(AB) prodrugs.

Starting from the selected nucleosides, their triphosphate prodrugs should be synthesized to both increase their bioavailability and potency, as well as in some cases decrease their toxicity, thereby potentially overcoming the obstacles that lead to the failure in their approval processes.

Objectives

The third part of the thesis was inspired by the success of phosphonate prodrugs like TAF and TDF, which led to more effective treatment of HIV. Since their inception, efforts have been made to transfer this motive to other nucleosides in order to achieve a similar pharmacological profile.²⁰⁰ Therefore, a synthesis route for nucleoside phosphonates (**Scheme 8**) should be established. Subsequently, these phosphonates should be used in place of regular NMPs in the triphosphate prodrug synthesis to provide versatile access to phosphonate analogues of already existing TriPPPro-compounds.



Scheme 8: Synthesis of nucleoside phosphonates by MICHAELIS-ARBUZOV type reactions.²⁰¹

After the successful synthesis of prodrugs, γ -alkyl triphosphates and triphosphates using previously established methods, these compounds should be tested using the same biological methods as other nucleoside triphosphate compounds to evaluate the suitability of the applied changes.

4. Results and Discussion

4.1. Preliminary Primer Extension Assay Evaluation

The group led by MEIER *et al.* has made significant progress in the development of various delivery systems for antiviral nucleosides.^{48–52,195,202} These investigations have confirmed the practical application and deployment of γ -modified triphosphate prodrugs as suitable candidates for antiviral therapeutics. While GOLLNEST demonstrated the applicability of double-masked TriPPPPro-derivatives through comprehensive evaluations involving HIV-infected cell lines and hydrolytic stability testing,^{48,49} NACK,⁵⁰ ZHAO⁵² and JIA⁵¹ explored non-symmetrically masked triphosphates, yielding comparable or even enhanced outcomes in biological settings. As described in Chapter 2.3.4. non-cleavable groups were introduced to enhance the pharmacological properties of the prodrugs. Notably, these compounds showed exceptional stability over long periods of time in both biological and chemical hydrolysis studies.^{50–52}

It has also been suggested that non-cleavable aliphatic masking units could alter the substrate properties of the prodrugs, resulting in less toxic drugs. Human polymerases have a much higher selectivity towards potential substrates compared to HIV-RT, therefore long aliphatic masking units should inhibit incorporation into human DNA polymerases.¹⁰⁹ As a stated goal of this work, evaluation of these different modifications in regard to their substrate properties was a crucial step to further advance the γ -modified nucleoside triphosphate prodrugs. Therefore, these prodrugs were compared to their triphosphate and NTP counterparts by using a previously established primer extension assay⁵² as well as an expanded version to test the relevant substances against pol α and pol γ . The assay conditions for HIV-RT and pol β were established by OLIVEIRA *et al.*²⁰³ and modified to employ fluorescent instead of radiolabelled primers. For the human polymerases, modified assay conditions derived from the work of DE WIT *et al.* were used.¹⁹³ A small collection of substances provided by NACK, ZHAO and WEISING (**Figure 13**) initially served as a valuable resource for elucidating the substrate-enzyme interactions and provided important insights for subsequent synthesis efforts.

Results and Discussion

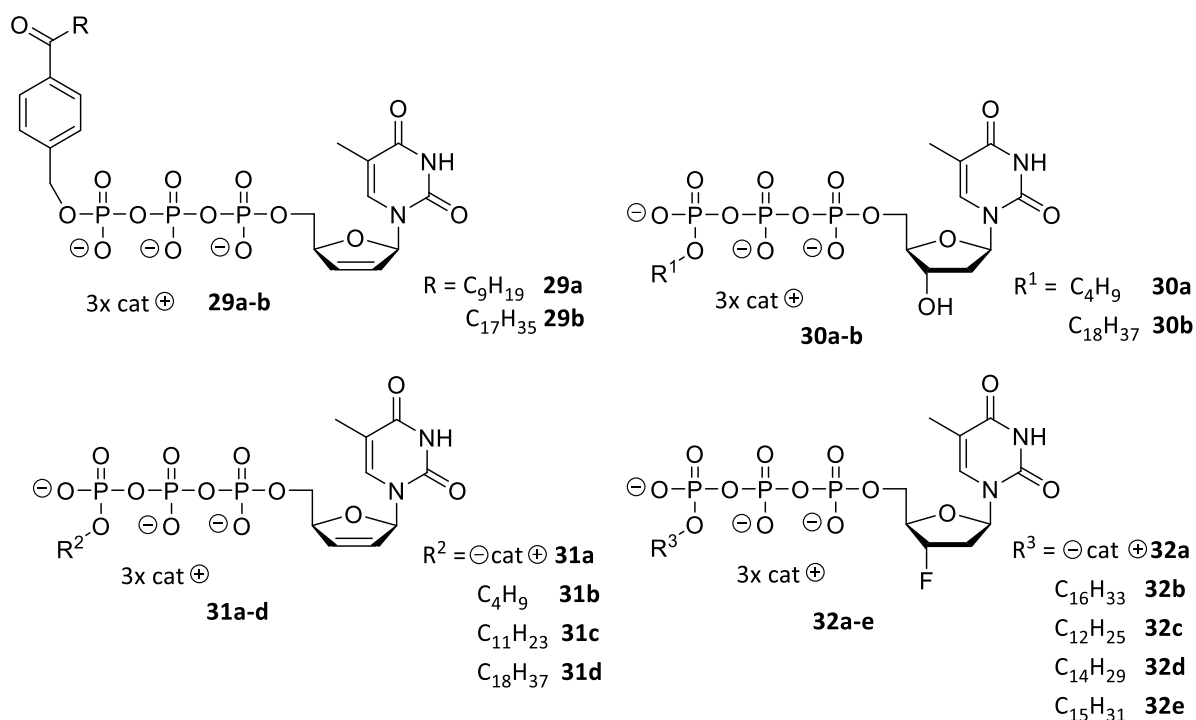


Figure 13: Substances provided by NACK, ZHAO and WEISING as well as additional triphosphates, which were synthesized in the course of this work.

The primer extension assays were performed on polyacrylamide gels with 30-base (30nt) long templates and 25-base (25nt) fluorescent labelled primers. The 5'- five base sequence was adjusted to the tested nucleoside (see Experimental Procedure 6.1.3, p. 89). The previously used 5'-fluorescein isothiocyanate labelled primers (**Figure 15** green) were replaced by Cy3 labelled primers (**Figure 14**, red), to provide better signal to background ratio, which significantly simplifies image analysis. After primer and template annealing, the substrates were incubated with four different polymerases according to the corresponding protocols (see Experimental Procedure 6.1.3, p. 89). Assays involving pol α and γ presented a major challenge, as their activity was several orders of magnitude lower than HIV-RT and pol β . Strict adherence to the cooling requirements and fast handling were key to successful experiments. Furthermore, it was found that better results for the pol γ assay were achieved when pol α buffer conditions were used with the pol γ enzyme instead of the buffers provided by the manufacturer. Ketobenzyl-modified d4T analogues were used as a starting point due to their similarity to bis(AB) TriPPP compounds. The single-masked triphosphates **29a** and **29b** and the d4T triphosphate **31a** were incubated with all four polymerases and developed with denaturing polyacrylamide gel electrophoresis. Each experiment was performed with a positive (+ : polymerase; with dATP, dCTP, dGTP and dTTP) and a negative (- : no polymerase; with dATP, dCTP, dGTP and dTTP) control (**Figure 14**), to determine if the tested compounds are substrate for the tested polymerases.

Results and Discussion

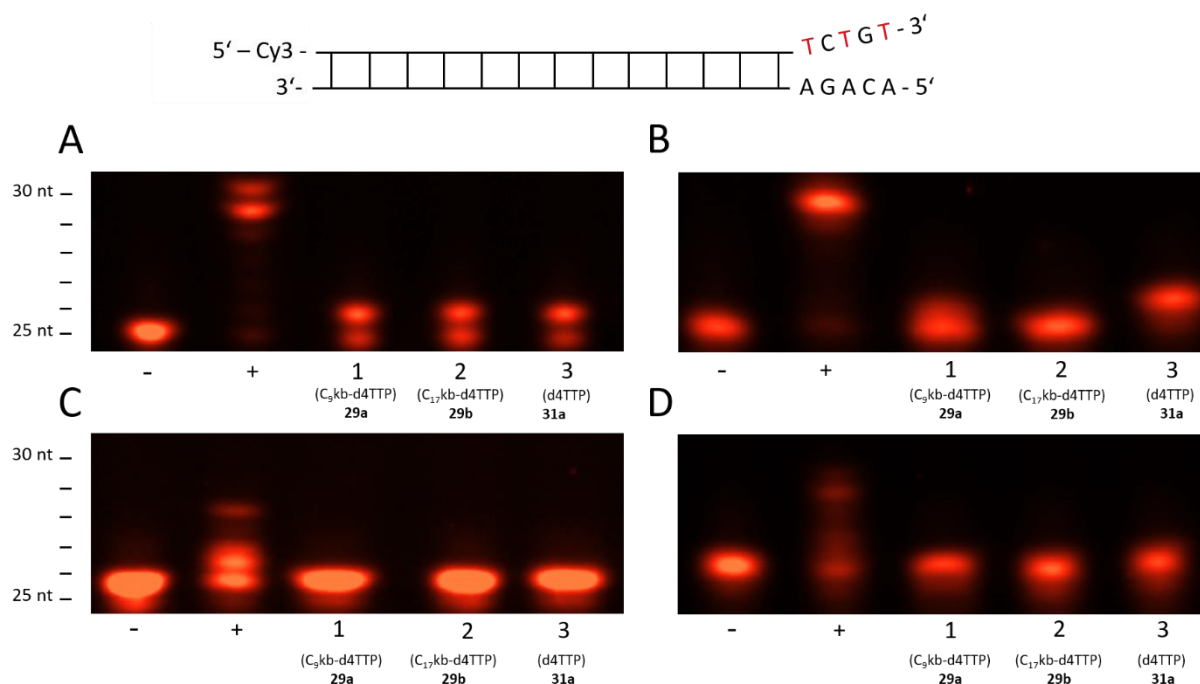


Figure 14: Primer extension assay using γ -ketobenzyl modified d4T triphosphates **29a** and **29b** and d4TTP **31a**. **A)** HIV-RT; negative control; positive control; lane 1: C₉kb-d4TTP **29a**; lane 2: C₁₇kb-d4TTP **29b**; lane 3: d4TTP **31a**. **B)** Pol β ; negative control; positive control; lane 1: C₉kb-d4TTP **29a**; lane 2: C₁₇kb-d4TTP **29b**; lane 3: d4TTP **31a**. **C)** Pol α ; negative control; positive control; lane 1: C₉kb-d4TTP **29a**; lane 2: C₁₇kb-d4TTP **29b**; lane 3: d4TTP **31a**. **D)** Pol γ ; negative control; positive control; lane 1: C₉kb-d4TTP **29a**; lane 2: C₁₇kb-d4TTP **29b**; lane 3: d4TTP **31a**. Assay conditions are summarized in the Experimental Procedure 6.1.3.

As expected for all four polymerases, no elongation was found for the negative while full elongation (n+5) occurred in the positive control for HIV-RT (**Figure 14, A**) and pol β (**Figure 14, B**). The positive control for pol α (**Figure 14, C**) and pol γ (**Figure 14, D**) was less pronounced compared to pol β and HIV-RT due to their relatively low activity, which was consistent across all experiments using pol α and γ . Nevertheless, the activity of both polymerases was observable, validating the corresponding experiments. As expected, the n+1 band was detected in HIV-RT in all cases, with slightly decreasing substrate properties with increasing chain length. These results align with findings from similar single-masked TriPPPPro compounds published by GOLLNEST *et al.*⁴⁹ Conversely, the experiments with human polymerases showed significant substrate selectivity. While pol α and pol γ did not accept non-natural NTPs as substrate (no elongation in **C** and **D** for lane 1-3, **Figure 14**), for pol β (**Figure 14, B**), the substrate properties declined with increasing chain lengths, similar to HIV-RT, although in this case the increasing chain length had a more pronounced effect. While lane 3 showed a n+1 band, demonstrating that d4TTP **31a** was a substrate for pol β , almost no n+1 could be observed for the longer γ -C₁₇kb-d4TTP **29b**. This shows a clear difference in substrate properties and an enhanced selectivity towards the target polymerase.

Results and Discussion

For γ -alkylated d4T derivatives and TTP derivatives, similar studies were performed by ZHAO *et al.*⁵² with HIV-RT (**Figure 15**) and pol β (**Figure 16**). The HIV-RT assay conditions demonstrated enhanced substrate properties for chain lengths around C₁₁. These experiments revealed a high tolerance of HIV-RT regarding single-modified triphosphates.

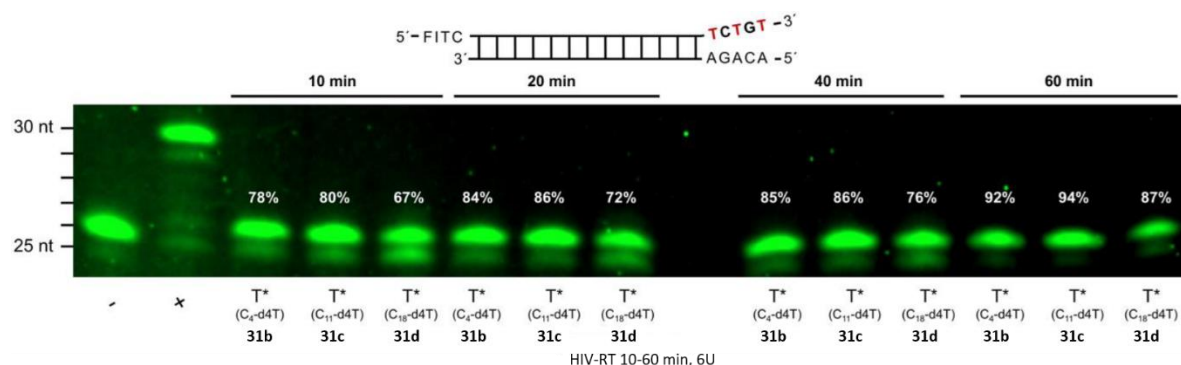


Figure 15: Primer extension assay for HIV-RT using γ -alkyl d4TTP **31b-d** with different incubation times. Lane 1: negative control; lane 2: positive control; lane 3: γ -C₄-d4TTP **31b**; lane 4: γ -C₁₁-d4TTP **31c**; lane 5: γ -C₁₈-d4TTP **31d**; the pattern of lane 3-5 was repeated for 10, 20, 40 and 60 min. Assay conditions are summarized in the Experimental Procedure 6.1.3.¹²⁹

In the pol β assay the influence of short, medium and long alkyl chains regarding their incorporation properties were explored. Therefore, d4TTPs **31a-d**, and for comparison γ -alkylated TTPs **30a-b**, were incubated with pol β (**Figure 16**). This experiment showed equal incorporation for NTPs with short and no alkyl chains, resulting in an n+1 band >50 % (**Figure 16**, lane 3, 5 and 8). The rate of incorporation was visibly reduced for d4TTP **31c** (<50 %), while no incorporation can be found for the long alkyl chains (**30b** and **31d**). These results suggest that pol β exhibits a range of tolerance for modifications on the phosphate moiety, which can be used to adjust substrate properties of potential NRTI prodrugs towards the viral polymerases.

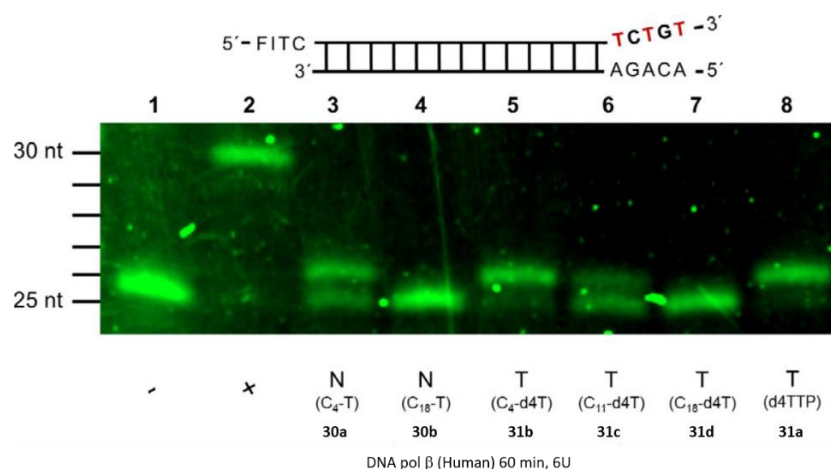


Figure 16: Primer extension assay for pol β using γ -alkyl- and d4TTP derivatives **31b-d**, d4TTP **31a** and γ -alkyl TTP derivatives **30a-b**. Lane 1: negative control; lane 2: positive control; lane 3: γ -C₄-TTP **30a**; lane 4: γ -C₁₈-TTP **30b**; lane 5: γ -C₄-d4TTP **31b**; lane 6: γ -C₁₁-d4TTP **31c**; lane 7: γ -C₁₈-d4TTP **31d**; lane 8: d4TTP **31a**. Assay conditions are summarized in the Experimental Procedure 6.1.3.

Results and Discussion

Early on, FLT was identified as a potential antiviral drug against HIV.²⁰⁴ Since fluorine is commonly used as an isosteric replacement to the hydroxyl group found in ribose nucleosides, it was considered a suitable substrate substitute for thymidine.¹²⁷ In collaboration with WEISING *et al.*, γ -alkyl triphosphate prodrugs and TriPPP-FLTTPs were examined for their substrate properties regarding the incorporation by HIV-RT.¹⁹⁵ Building on previous findings with d4T, chain lengths in between C₁₁ and C₁₈ were investigated in order to optimise the substrate properties.

The initial primer extension assays aimed to figure out the general differences in substrate properties between modified and unmodified FLT (**Figure 18**). The assay included positive and negative control, to validate the assay conditions, the unmodified FLTTP **32a**, the γ -C₁₆-alkyl FLTTP **32b** and for the human polymerases TTP as an additional control for the n+1 band.

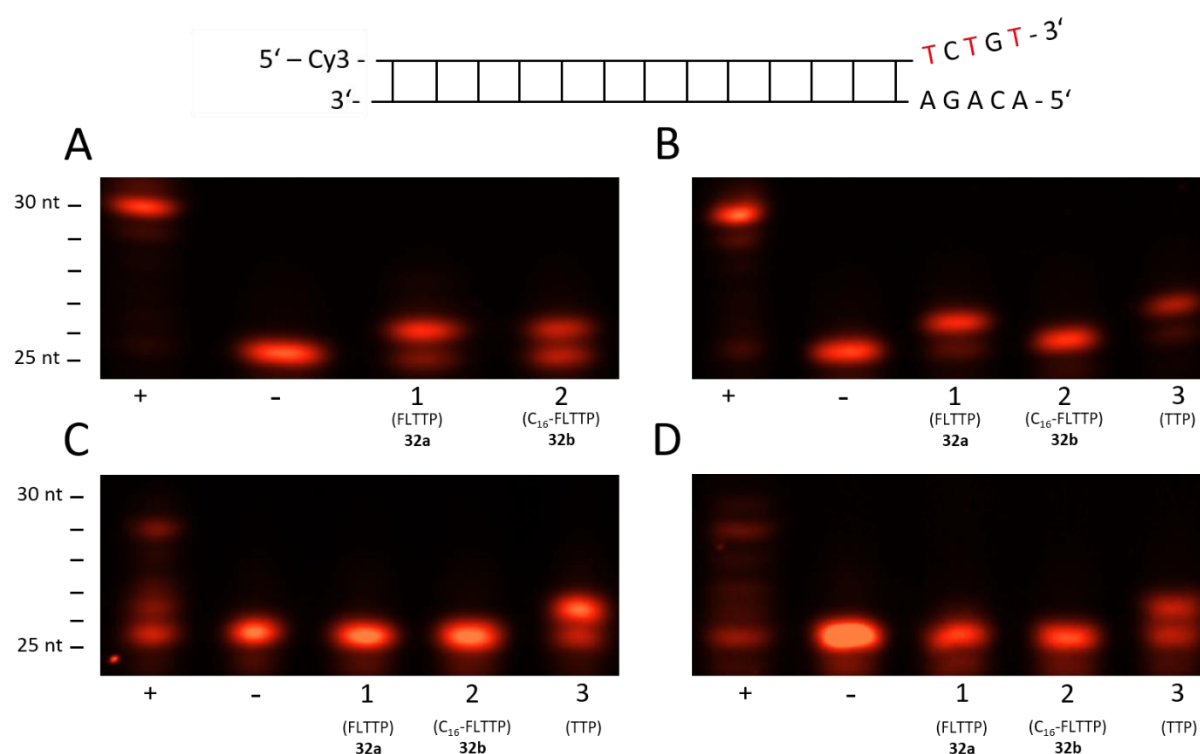


Figure 18: Primer extension assay using γ -C₁₆-FLTTP **32b** and FLTTP **32a** **A)** HIV-RT; positive control; negative control; lane 1: FLTTP **32a**; lane 2: γ -C₁₆-FLTTP **32b**. **B)** Pol β ; positive control; negative control; lane 1: FLTTP **32a**; lane 2: γ -C₁₆-FLTTP **32b**; lane 3: TTP. **C)** Pol α ; positive control; negative control; lane 1: FLTTP **32a**; lane 2: γ -C₁₆-FLTTP **32b**; lane 3: TTP. **D)** Pol γ ; positive control; negative control; lane 1: FLTTP **32a**; lane 2: γ -C₁₆-FLTTP **32b**; lane 3: TTP. Assay conditions are summarized in the Experimental Procedure 6.1.3.

Results and Discussion

The experiments confirmed the recurring trend for pol α and γ (**Figure 18, C and D**), wherein natural triphosphates are readily incorporated, while non-natural NTPs lacked substrate properties regardless of modification. Similar results were observed for pol β and HIV-RT, repeating the incorporation patterns as in the d4T assays. Both γ -C₁₆-FLTTP and FLTTP were substrates for the viral polymerase with slightly less incorporation of the alkylated derivative. The assay with pol β showed full elongation for the positive control and almost full incorporation for the TTP control (lane 3, **Figure 18, B**). FLTTP **32a** appears to be incorporated at a comparable level to its natural counterpart (lane 1, **Figure 18, B**). Whereas, for the γ -C₁₆-FLTTP **32b**, no incorporation was observed. Regardless of the influence of the nucleoside, chain lengths between C₁₁ and C₁₆ were assumed to be an acceptable range for pol β .

Exploring the limits of pol β , C₁₂-, C₁₄- and C₁₅-alkyl modified FLTTPs **32c-e** were synthesised and tested in the HIV-RT and pol β assay conditions (**Figure 19**). To obtain concise results the configuration included positive and negative control for both polymerases as well as TTP for pol β as an additional control for the n+1 band.

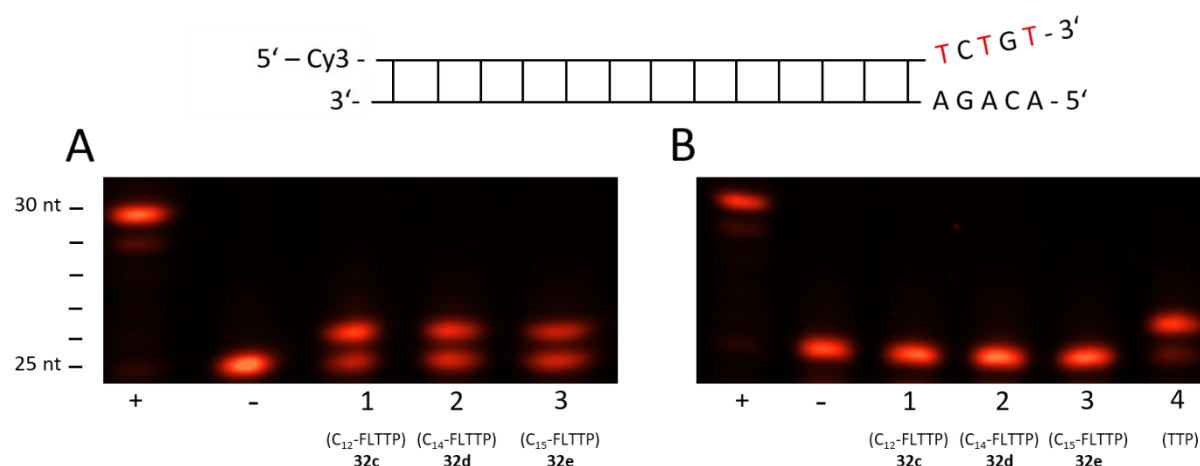


Figure 19: Primer extension assay using γ -alkyl modified FLT triphosphates **32c-e**. **A)** HIV-RT; positive control; negative control; lane 1: γ -C₁₂-FLTTP **32c**; lane 2: γ -C₁₄-FLTTP **32d**, lane 3: γ -C₁₅-FLTTP **32e**. **B)** Pol β ; positive control; negative control; lane 1: γ -C₁₂-**32c**; lane 2: γ -C₁₄-FLTTP **32d**, lane 3: γ -C₁₅-FLTTP **32e**, lane 4: TTP. Assay conditions are summarized in the Experimental Procedure 6.1.3.

As expected, all γ -alkyl modified FLTTPs were good substrates for HIV-RT with decreasing incorporation observed with longer chain lengths, suggesting a preference for short alkyl chains in the final prodrug design. Previous tests suggested preferred chain lengths between C₁₁- and C₁₆-, which are probably dependent on the nucleosides. Though available results appear consistent across similar thymine-based analogues. For pol β , modifications $\geq \gamma$ -C₁₂-alkyl resulted in no incorporation in the extension assay. These results were applied to thymidine- and cytidine-based triphosphate prodrugs in the subsequent experiments.

4.2. Masking Group Optimisation

To maximise the efficacy of prodrugs, the systemic delivery of the prodrug to the target must be considered. For antiviral drugs against HIV reverse transcription, mobility through cell membranes is crucial. Given the absence of known active transport mechanisms for alkylated triphosphates, passive diffusion is the most probable mode of cellular entry. A key property for cellular uptake is the lipophilicity of the prodrug.⁴⁸ In continuation of cellular uptake studies performed by GOLLNEST *et al.*²⁰⁵ with bicyclic nucleoside triphosphate analogues (BCNA), WITT *et al.*²⁰⁶ and ROßMEIER *et al.*²⁰⁷ synthesised and tested various differently masked TriPPPPro-compounds and triphosphates to assess their cell permeability.

The TriPPPPro compounds were incubated with several different types of cancer cell lines, and then the intra- and extracellular concentrations was determined by high-performance liquid chromatography (HPLC) elution experiments.²⁰⁶ The γ -alkyl(AB) triphosphates were evaluated with CEM-SS cells, which are relevant for HIV research, using a similar assay.²⁰⁷ The results indicated that TriPPPPro-BCNA **33** and γ -alkyl(AB) BCNA **34** have the most favourable properties for cellular uptake (**Figure 20**).

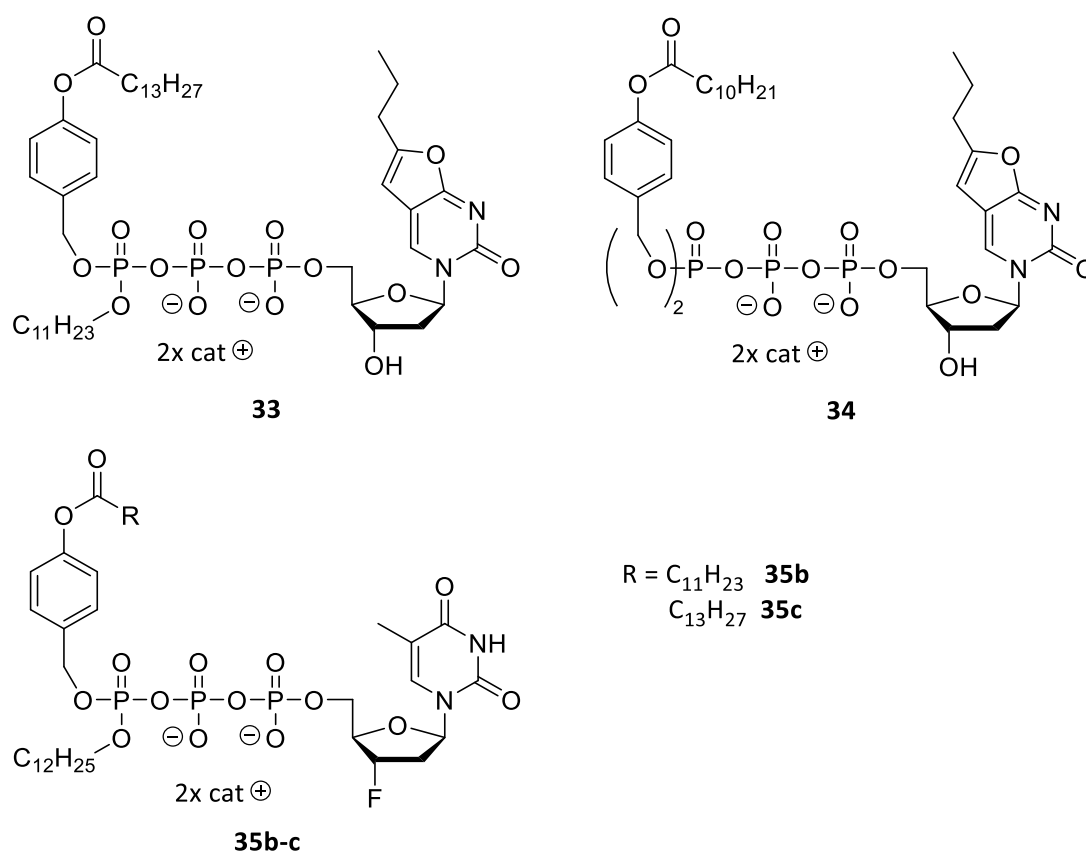


Figure 20: Substances provided to WITT and ROßMANN for lipophilic mask adjustments, TriPPPPro-BCNA **33** and γ -alkyl triphosphate BCNA **34**, and FLTTP prodrugs **35b-c** with optimised masking units.

Results and Discussion

CEM-cells were used to determine the cell permeability of triphosphate prodrugs. γ -C₁₂(C₁₁AB)-FLTTP **35b** (Figure 21, green) was synthesised in this work and compared to both BCNAs (Figure 21, red and grey). Dodecanoic acid was introduced as the lipophilic modification of the AB-unit to balance overall lipophilicity due to a longer γ -alkyl chain (C₁₁ vs. C₁₂). The lower retention time prompted the introduction of tetradecanoic acid (myristic acid) to further increase lipophilicity and reach a range similar to that of BCNA **33** and **34**. The synthesised γ -C₁₂(C₁₃AB)-FLTTP **35c** (Figure 21, blue, 17.86 min) matches well the retention time of BCNA **33** (17.91 min).

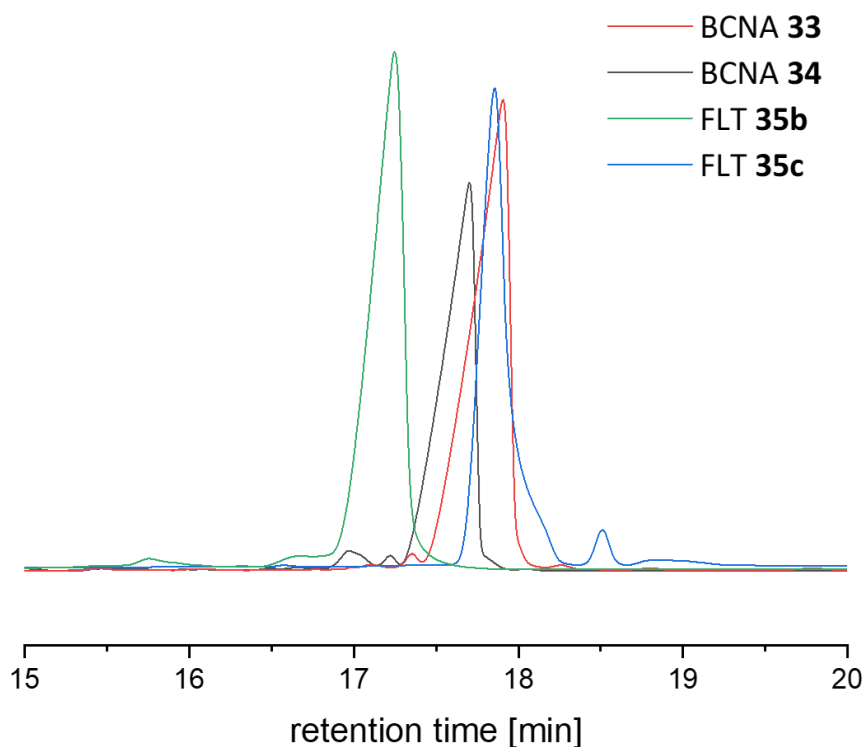


Figure 21: Retention time of BCNA **33** (17.91 min) and **34** (17.06 min) compared to γ -C₁₂(C₁₁AB)-FLTTP **35b** (17.25 min) and γ -C₁₂(C₁₃AB)-FLTTP **35c** (17.86 min). Substances were eluted using method A (Experimental procedure 6.1.1).

This ‘ideal’ configuration of masking unit and alkyl chain was adopted for all other nucleosides and for the FLU phosphonate. The synthesis of these compounds is described in chapter 4.5., while the results of the HPLC elution experiments are shown in Figure 22. All γ -alkyl triphosphate prodrugs exhibited very similar retention times, with γ -C₁₂(C₁₃AB)-FLTTP **35c** and γ -C₁₂(C₁₃AB)-4'-Ed4TTP **79** coming closest to the desired values at 17.86 min and 17.80 min, respectively. The retention time for the oxathiolane derivatives were shorter and could eventually be adjusted with longer alkyl chain modifications to the masking units. The FLU phosphonate **82a** displayed a longer retention time of 18.71 min, indicating higher lipophilicity compared to the FLT triphosphate counterpart.

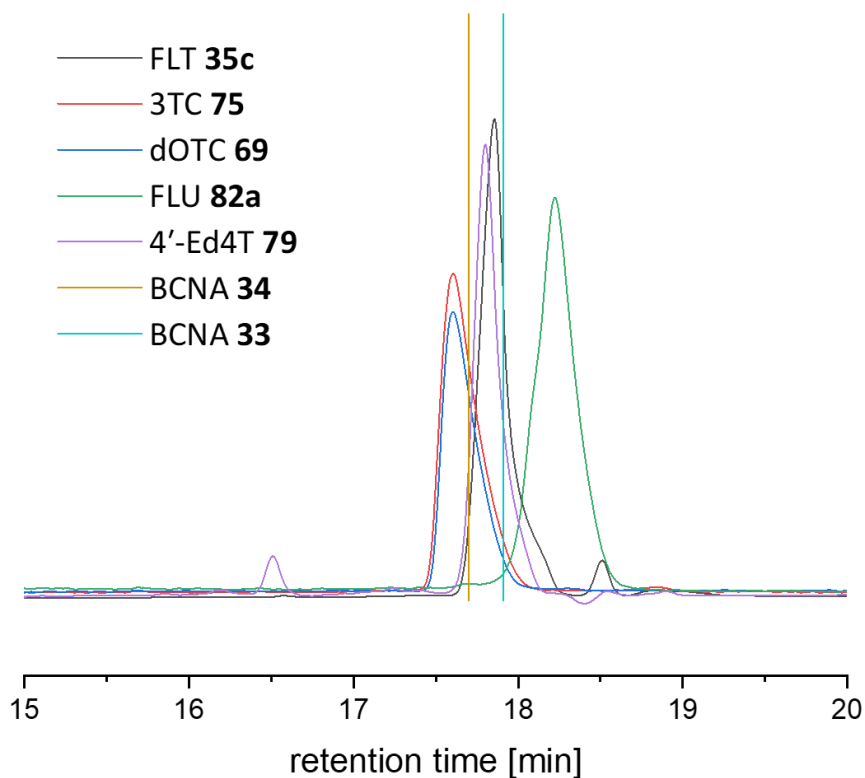
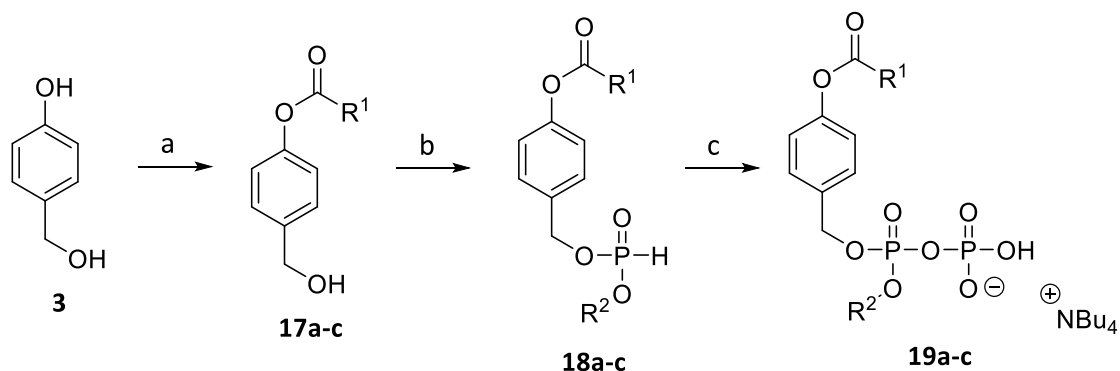


Figure 22: Retention time of TriPPPPro BCNA **32** (17.91 min) and γ -alkyl BCNA **33** (17.06 min) compared to γ -C₁₂(C₁₃AB)-FLTTP **34c** (17.86 min), γ -C₁₂(C₁₁AB)-dOTC **68** (17.60 min), γ -C₁₂(C₁₁AB)-3TC **74** (17.60 min), γ -C₁₂(C₁₁AB)-4'-Ed4T **78** (17.80 min) and γ -C₁₂(C₁₁AB)-FLU **81a** (18.71 min). Substances were eluted using method A (Experimental procedure 6.1.1).

4.3. Synthesis of Masking Units

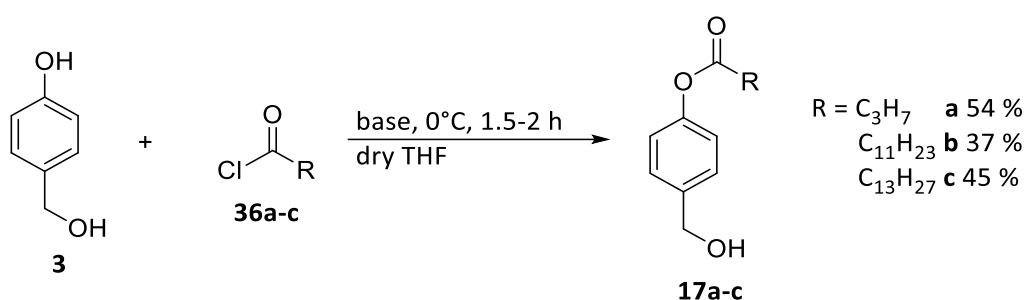
4.3.1. Synthesis of γ -Alkyl (AB) Pyrophosphates

The triphosphate prodrugs, which were used in chapter 4.1. and 4.2., were synthesized *via* their corresponding pyrophosphates. For this purpose, the well-established *H*-phosphonate route (**Scheme 9**) for non-symmetric pyrophosphates developed by ZHAO *et al.* was used.¹²⁹



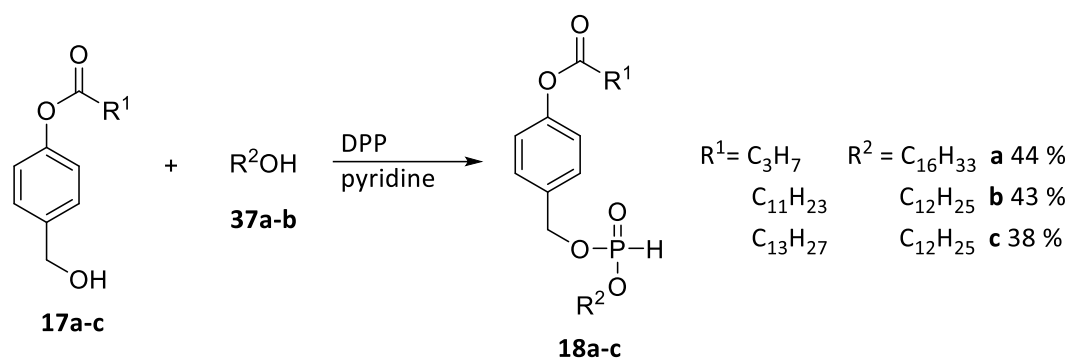
Scheme 9: Literature synthesis of pyrophosphates **19a-c**. **a)** acyl chloride, Et₃N, THF, 0 °C, 2 h; **b)** DPP, alkyl alcohol, pyridine, -10 °C to 40 °C, 6 h; **c)** NCS, TBA phosphate, CH₂CN, 50 °C, 1 h.

In the retrosynthetic scheme, 4-hydroxybenzyl alcohol **3** serves as the starting material for all masking units. These were transformed to the required ester using commercially available acyl chlorides (**Scheme 10**). The second esterification of benzyl alcohol function was prevented by using small excess (1.1 eq.) of 4-hydroxybenzyl alcohol **3** with the appropriate acyl chloride (1.0 eq.) and triethylamine (0.9-1.0 eq.) in dry tetrahydrofuran (THF) at 0°C. The moderate yields indicated that a further increase of the amount of benzyl alcohol **3** would be necessary. Furthermore, KULLIK *et al.* reported a 4-(dimethylamino)pyridine (DMAP) catalysed EINHORN-acylation²⁰⁸ in which the yield was increased up to 88%.^{209,210} This method was used in the synthesis of **17c**, but also this method did not improve the yield significantly.



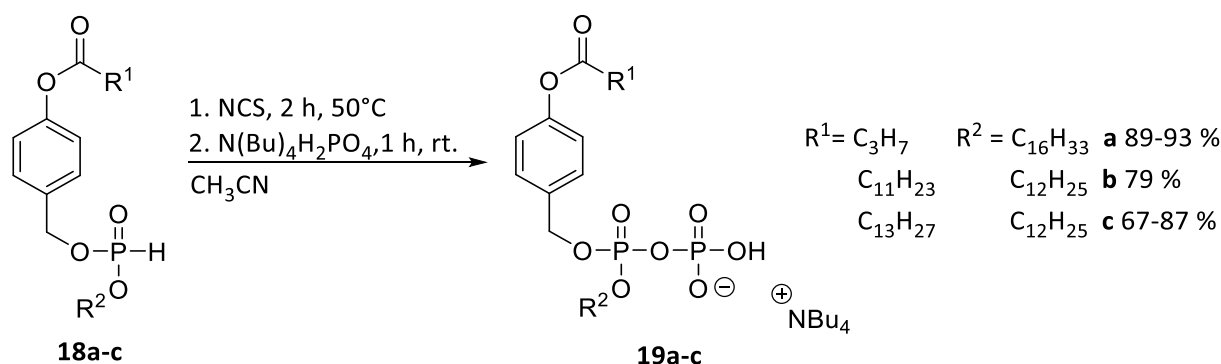
Scheme 10: Reaction scheme of AB masks: **17a/b**: Et₃N; **17c**: Et₃N; DMAP.

The synthesis of γ -modified triphosphates was achieved through several different strategies in the group of MEIER *et al.*²¹¹ The so-called *H*-phosphonate route proved to be a reliable and adjustable method for the synthesis of symmetrical and non-symmetrical building blocks in the convergent synthesis of triphosphate prodrugs.^{129,205} The building blocks are readily accessible through prior synthesis and commercial sources, and the final product is stable and can be stored long-term. For the synthesis of non-symmetrical *H*-phosphonates **18a-c** the protocol of ZHAO *et al.* was applied. Phenyl esters **17a-c** were stirred with 1.2 eq. diphenyl phosphite at -10 to 0 °C (**Scheme 11**). The formation of undesired side products was minimised by monitoring this step *via* TLC to ensure full conversion before adding the corresponding alcohol **37a-b**. Depending on the substituents, the products (**18b-c**) were obtained by crystallisation from isopropanol with yields up to 43 %, whereby a sufficient purity was achieved. For *H*-phosphonate **18a** crystallisation was not possible, but the difference in chain length of the two substituents allows for simple column chromatography, which meant that any by-products could be easily separated.



Scheme 11: Reaction scheme of non-symmetrical *H*-phosphonates **18a-c**.

The final step in the synthesis was the transformation of *H*-phosphonates to the corresponding pyrophosphates. This was achieved through oxidative chlorination of the *H*-phosphonate with *N*-chlorosuccinimide (NCS). The protocol was developed by GOLLNEST *et al.* using tetrabutylammonium (TBA) phosphate (monobasic) as a nucleophile to obtain the pyrophosphates in good to excellent yields (**Scheme 12**).^{205,212}



Scheme 12: Synthesis of pyrophosphates **19a-c** using non-symmetrical *H*-phosphonates.

Compared to the previously used phosphoramidite route, the development of this synthesis route enabled the use of nucleoside monophosphates instead of diphosphates, which were less accessible due to their time-consuming synthesis and their lower yields.²⁰⁵ The pyrophosphates were freshly prepared, and used after a thorough washing process with ammonium acetate and water, without further purification. Rapid washing cycles were crucial to maximise yields, and phase separation was achieved through centrifugal forces. The yields for this step were given for the crude product. The reaction time for the NCS activation was approximately 2 h, and the addition of $\text{N}(\text{Bu})_4\text{H}_2\text{PO}_4$ was started after full conversion was determined by NMR spectroscopy. A clear indicator was the vanishing of the H-P duplet with a distinct coupling constant of ~ 700 Hz (**Figure 23**).

Results and Discussion

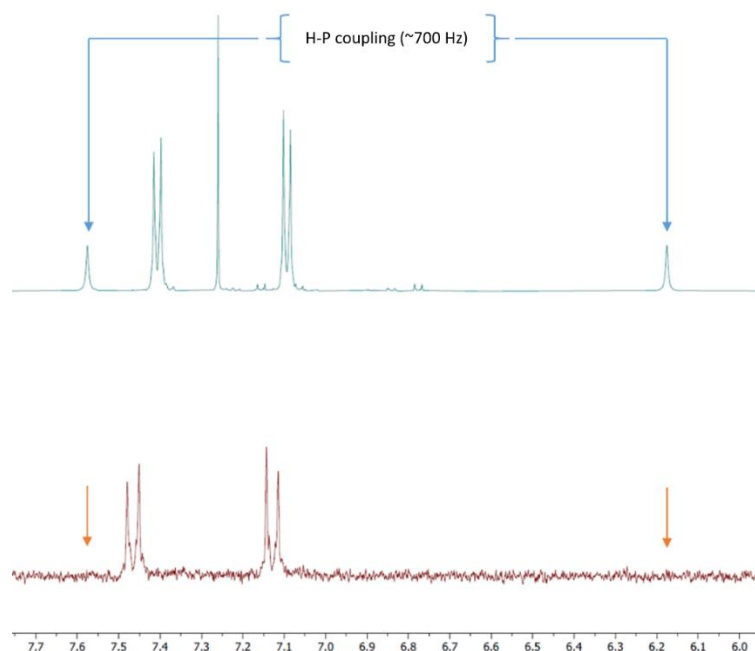
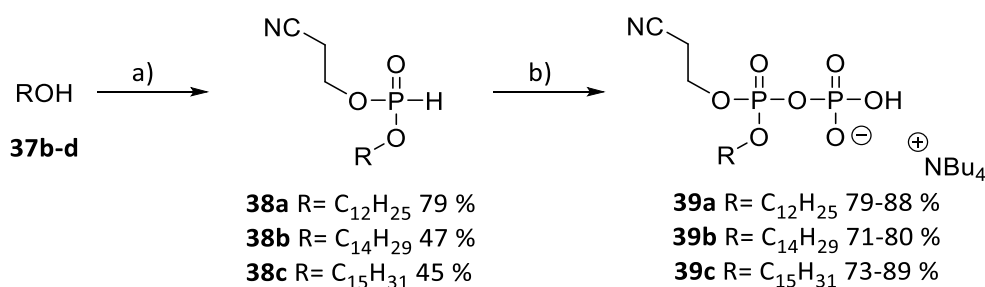


Figure 23: NMR signal for *H*-phosphonate P-H coupling (top) and after activation (bottom). Chemical shift is depicted in ppm.

4.3.2. Synthesis of γ -Alkyl Cyanoethyl Pyrophosphates

GOLLNEST and ZHAO *et al.* have demonstrated that (viral) polymerases generally do not readily accept double-masked nucleotides as substrates for DNA synthesis.^{129,205} This makes it necessary to synthesise the monosubstituted metabolites of the intended prodrugs for chemical and biological *in vitro* tests. Therefore, a synthetic route involving a 2-cyanoethyl protected *H*-phosphonate was developed. Historically, this protecting group has been employed in oligonucleotide synthesis due to its favourable cleaving properties.²¹³ 2-Cyanoethanol and the desired alcohol **36b-d** were stirred with diphenyl phosphine (DPP) at 0 °C for 3 h, whereby the reduced amount of DPP compared to the literature did not noticeably affect the yields of the reactions (**Scheme 13**). The second step was done analogous to the AB pyrophosphates with yields ranging from 59 to 89 %. As discussed above, the crude pyrophosphates were used without further purification for subsequent coupling reaction.



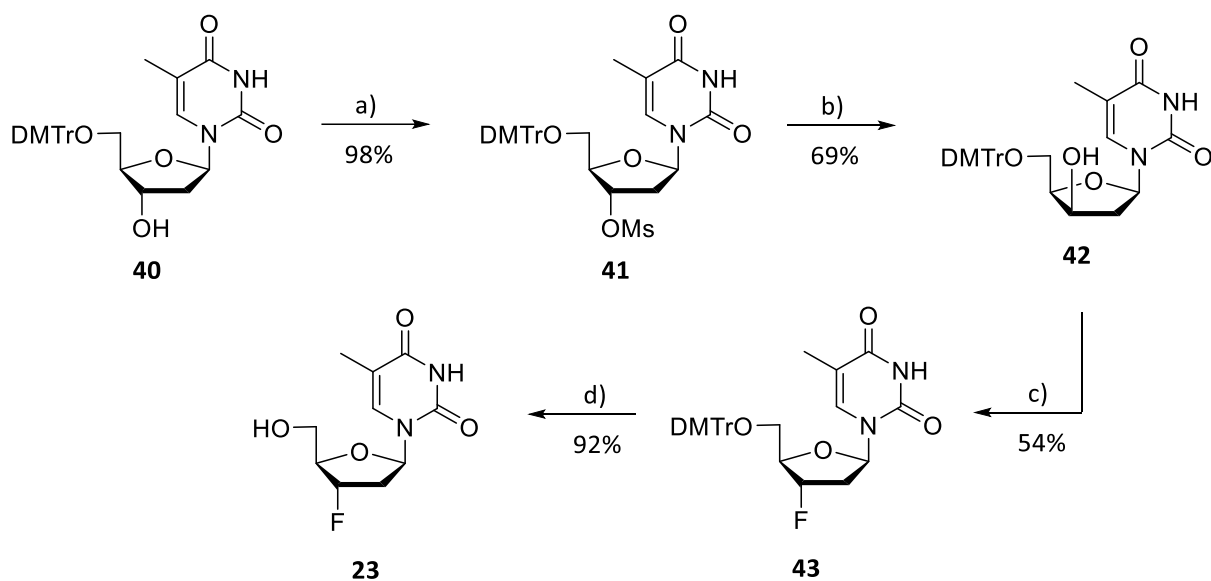
Scheme 13: Reaction scheme of different cyanoethyl pyrophosphates involving the corresponding *H*-phosphonates. **a)** DPP, pyridine, 0 °C, 3 h. Then 3-hydroxypropionitrile 40 °C, 3 h. **b)** NCS, 50 °C, 2 h. Then N(Bu₄) H₂PO₄, rt, 1 h.

4.4. Synthesis of Nucleosides

4.4.1. Synthesis of 3'-Fluoro-2',3'-dideoxythymidine (FLT)

Early on, FLT was considered a potential candidate in antiviral therapy against HIV due to its similarity to thymidine.⁹ One significant drawback of FLT was its high mitochondrial toxicity, which hindered potential FDA approval of the drug.²¹⁴ Even the efficacy at low doses did not lead to an improved pharmacological profile compared to drugs already on the market, therefore BOEINGER INGELHEIM discontinued the development of FLT.^{197,215} Furthermore, pre-steady state data by SOHL *et al.* showed that only a 8.3-fold difference in discrimination of FLTTP **32a** and TTP for wild type pol γ was achieved compared to HIV-RT. However, an additional ethynyl group at C4' resulted in a 12,000-fold discrimination of 4'-Ed4TTP **81** and TTP between pol γ and HIV-RT, leading to further investigation of this drug.¹⁹⁶ In 2022, a study on modified FLT derivatives with myristic acid revealed good antiviral activities and far reduced toxicity. These fatty acid FLT derivatives depend on intracellular hydrolysis of the ester followed by phosphorylation to the active FLTTP.²¹⁶ As previously mentioned lipophilic FLTTP derivatives were to be synthesised in this work. First of all, FLT **23** had to be synthesised, which was accomplished by a linear four step synthesis developed by SRIVASTAV *et al.* with good to quantitative yields (**Scheme 14**).^{217,218}

The pivotal step in FLT synthesis involves the introduction of a 3'-fluorine atom, which was accomplished by inversion of the 3'-hydroxyl group stereochemistry (**Scheme 14**). Therefore, 4,4'-dimethoxytriphenylmethyl (DMTr) protected thymidine **40** was converted into the corresponding 3'-mesylate using 1.5 eq. mesyl chloride and 2.5 eq. triethylamine. The inversion of configuration at C3' was then achieved by nucleophilic substitution with NaOH in ethanol and water. Due to the acid sensitivity of the DMTr protecting group, careful pH adjustment during work-up process was crucial for high yields in this step.²¹⁷



Scheme 14: Reaction scheme of FLT **23**. **a)** MsCl, Et₃N, THF, 0 °C to rt 3 h; **b)** NaOH, ethanol:water (90:10; v/v), reflux 2 h, adjust pH to 7 with acetic acid; **c)** DAST, pyridine, CH₂Cl₂, 0 °C to rt, 1.5 h; **d)** 1M HCl, CH₃CN, 45 °C, 0.5 h.

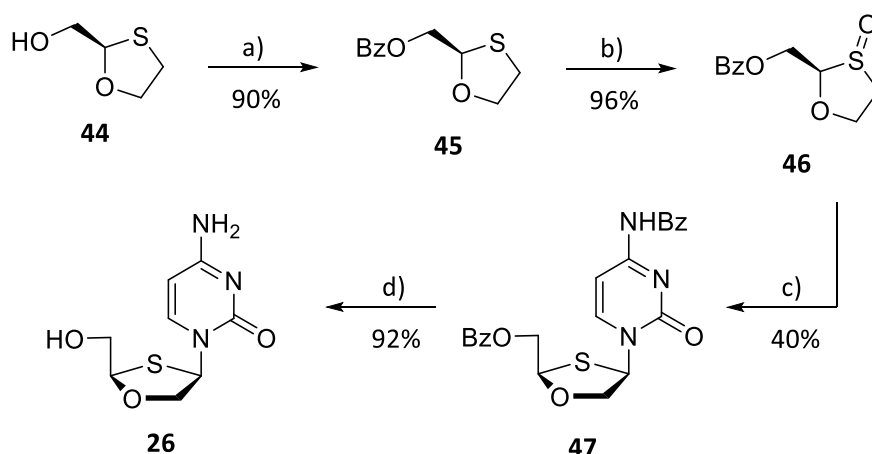
Subsequent fluorination was carried out with 2.3 eq. (diethylamino)sulfur trifluoride and 2.0 eq. pyridine in CH₂Cl₂ to give DMTr-FLT **43** in 54 % yield.²¹⁹ The cleavage of the DMTr group by hydrolysis with 1 M HCl yielded FLT **23** in quantitative amounts. The yields and analytical data were in accordance to previous publications.^{195,217–219}

4.4.2. Synthesis of (-)-2'-Deoxy-3'-oxa-4'-thiocytidine (dOTC)

The development of 3TC and FTC led to the emergence of numerous highly active combination drugs, to an increase in potency of antiviral drugs and to the replacement of many previously used NRTIs.⁹⁷ However, while advancing HIV therapy, the widespread use of 3TC and FTC has also led to the development against these drugs.²²⁰ Apricitabine (dOTC) was an *D*-isomer of 3TC that showed significant *in vitro* activity in viral strains with the prominent M184V mutation and other thymidine-associated mutations that causes 3TC and FTC resistance.^{199,220,221}

Additionally, studies with human liver cells (HepG2) performed by BAAR *et al.* suggested that dOTC does not interact with human γ pol and thus does not affect mitochondrial DNA, mitigating concerns about mitochondrial toxicity. However, it is noteworthy that these results were obtained using southern blots, which may be subject to cumulative errors due to separate amplification and hybridisation of mitochondrial DNA.²²¹

Despite showing promising result in phase III clinical studies and addressing an unmet clinical need, the development of dOTC **26** was dropped in 2016 due to a lack of improved efficacy and funding.^{220,222} JIA *et al.* showed the potential of sulphur based nucleosides by studying FTC TriPPP compounds that exhibited enhanced potency against HIV-2 compared to the parent nucleoside.²⁰² Therefore, dOTC was prepared by using the synthetic route developed by MARCUCCIO *et al.*, starting with the cheap and readily available (2*R*)-1,3-oxathiolane-2-methanol **44**.²²⁰ The initial step was the benzyl protection of the hydroxymethyl side-chain following the protocol of KRAUS *et al.* by using 1.5 eq. BzCl, 1.5 eq. pyridine and 0.05 eq. DMAP in CH₂Cl₂, which gave the desired Bz-oxathiolane **45** in 90% yield. This step was crucial to later introduce the nucleobase adjacent to the sulphur atom instead of the oxygen atom. Subsequent syntheses followed the protocol developed by MARCUCCIO *et al.* (**Scheme 15**). The oxidation to the S-oxide was carried out with 1.4 eq. H₂O₂ (30 % in water) and 1.5 eq. acetic acid as oxidising agent instead of *m*-chloroperbenzoic acid (*m*CPBA), which was used in previous attempts, as this considerably simplified the purification process. Afterwards, the nucleobase was introduced *via* sila-PUMMERER-VORBRÜGGEN coupling by using 2.2 eq. triethylamine, 3.0 eq. trimethylsilyl iodide and 0.2 eq. copper (II)-chloride as a catalyst. A mixture of both possible diastereomers was obtained in almost quantitative yield, but after crystallisation from methanol the desired Bz-dOTC **47** was isolated in 40 % yield. The benzyl groups were removed by stirring Bz-dOTC **47** in ammonia solution (2 M in methanol) overnight to give dOTC **26** in 92 % yield.



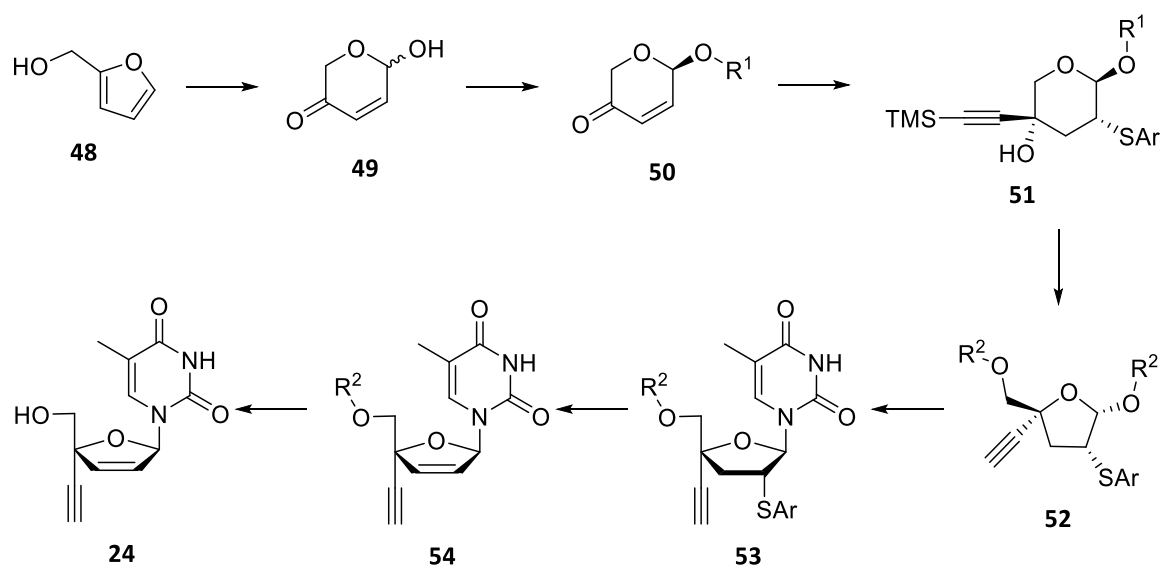
Scheme 15: Reaction scheme of dOTC **26**: **a)** BzCl, pyridine, DMAP, CH₂Cl₂, rt, 2 h; **b)** acetic acid, H₂O₂, 40 °C to rt, 3 h; **c)** *N*⁴-benzoyl cytidine, Et₃N, TMS-iodide, dry copper(II)-chloride, CH₂Cl₂, -50 °C to 0 °C, 1 h, 0 °C to rt, 18 h; **d)** 2 M NH₃ in MeOH, rt, 18 h.

4.4.3. Synthesis of 2',3'-Didehydro-3'-deoxy-4'-ethynylthymidine (4'-Ed4T)

In 2004, 4'-Ed4T (Censavudine) and other 4'-substituted d4T derivatives were investigated regarding their pharmacological profiles against HIV to reduce the high toxicity of d4T. In one of these studies, which was focusing on 4'-substituted thymidine derivatives, 4'-Ed4T was found to be most active in CEM and HepG2 cells.^{223,224} The high antiviral activity, the prior mentioned inherent selectivity against human polymerases (4.4.1), the significantly improved safety profile and the lack of interaction with the thymidine phosphorylase made 4'-Ed4T a promising candidate in HIV therapy.^{223,225,226} However, despite promising results in phase 2b clinical studies in 2014, further development of 4'-Ed4T as a NRTI was discontinued due to commercial reasons.¹⁹⁸ Moreover, the approval of Tenofovir alafenamide in 2015 led to a further decrease in interest of alternative NRTIs.²²⁷ Nevertheless, 4'-Ed4T has been re-investigated as a potential treatment for Alzheimer's disease since 2022.²²⁸

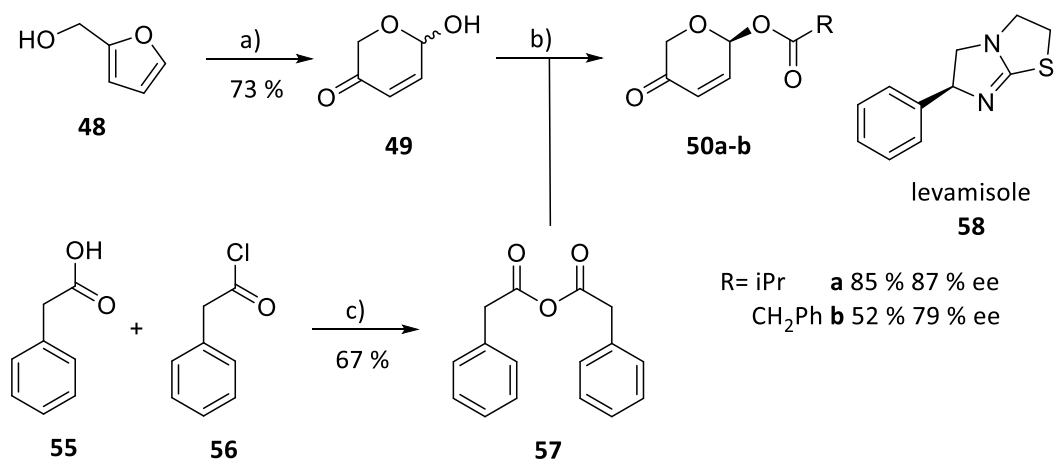
The synthesis of 1'- and 4'-substituted nucleoside poses a challenge due to the inert nature of these positions. In the case of 4'-Ed4T, several attempts resulted in difficult synthetic routes²²⁴, or relied on enzyme-mediated resolution to achieve high enantiomeric purity.^{229,230} In this study, a novel method developed by ORTIZ *et al.* was used (**Scheme 16**), which was leveraging dynamic kinetic asymmetric transformation (DYKAT) reactions to achieve highly enantioselective and scalable syntheses.²²⁵ 4'-Ed4T **24** was accessible by deprotection of nucleoside **54**, which should be obtained by successive oxidation of the thioether and thermolysis of the resulting sulfinimide. This step is crucial for the formation of the desired 2',3'-dehydrofuranose. The transformation of the pyranose sugar **51** to the furanose counterpart **52** was achieved through a ring tautomerization followed by an acylation and subsequent VORBRÜGGEN coupling. The pyranose **51** should be obtained from pyranone **50** through a diastereoselective 1,4-addition of the thioether and a subsequent 1,2-addition of the alkyne group. The key step of this synthetic approach should be the non-enzymatic enabled, stereoselective introduction of an ester protecting group via DYKAT.²²⁵ The pyranone **49** should be synthesised by an oxidation of the cheap and readily available furfuryl alcohol **48**.²³¹

Results and Discussion



Scheme 16: Literature synthesis of 4'-Ed4T **24**.^{225,231}

In this work, the starting pyranone **49** utilised by ORTIZ *et al.* was obtained by ACHMATOWICZ rearrangement of freshly distilled furfuryl alcohol **48** with 1.1 eq. *m*CPBA at 0 °C (**Scheme 17**). One of the main problems here was the removal of the chlorobenzoic acid. Therefore, the reaction mixture was cooled to -78 °C, whereby the chlorobenzoic acid was precipitated. After filtration and column chromatography, the racemic pyranone **49** was obtained in 67 % yield.^{231,232}



Scheme 17: Reaction scheme of pyranone ester **50a-b**: **a)** *m*CPBA, CH₂Cl₂, 0 °C, 3 h; **b)** appropriate anhydride, levamisole **58**, toluene/CH₂Cl₂, 0 °C, 12 h; **c)** NaOH, MeOH, reflux, 2 h.

The key step of this synthesis (**Scheme 17**) was developed by ORTIZ *et al.* to yield the acylated pyranone in high enantiomeric excess by DYKAT reactions with the commercially available organocatalyst levamisole **58**. There are two types of DYKAT reactions for the resolution of enantiomers (**Figure 24**). In a type I DYKAT reaction each enantiomeric substrate (**Figure 24, A and B**) forms a diastereomeric complex (**Figure 24, ACat and BCat**) with the chiral catalyst, with the interconversion of the two species leading to the formation of the kinetically favoured product (**Figure 24, P**). In the Type II case there is

no interconversion between diastereomeric intermediates. The complexation with the chiral catalyst leads to a loss of the chiral information (**Figure 24, YCat**), therefore the subsequent selectivity results from the nucleophilic attack.^{233,234} DYKAT reactions overcome the common restriction of kinetic resolution being capped at a yield of 50 %.²³⁵

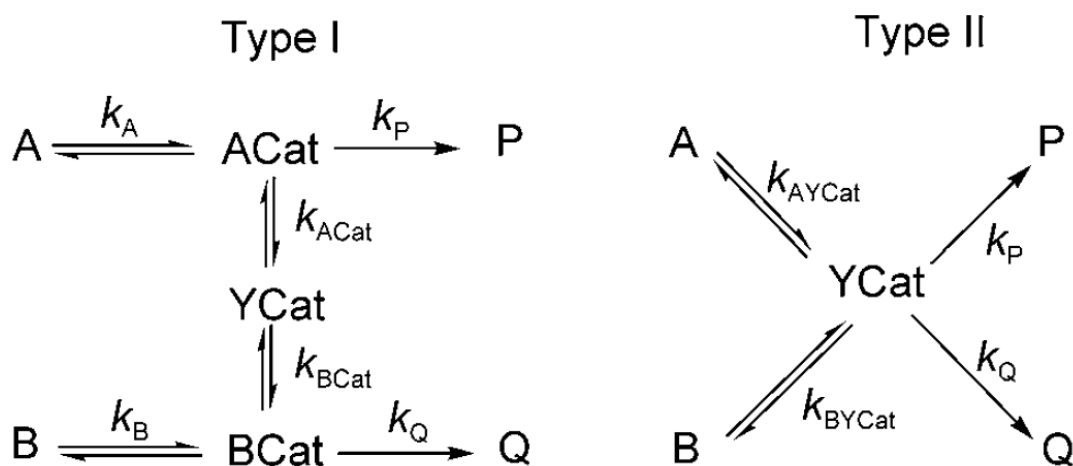


Figure 24: DYKAT mechanisms Type I and Type II.^{234,236}

Studies of ORTIZ *et al.* showed that the phenylacetic anhydride **57** and isobutyric anhydride gave the best results in the DYKAT reaction. Although the isobutyric anhydride gave a higher yield and a better enantiomeric excess, it was considered as the slightly inferior reagent, as no enantiomeric enrichment by crystallisation was possible. Since phenylacetic anhydride **57** was not commercially available it was synthesised from the corresponding acid **55** and acid chloride **56**.²³⁷ The phenylacetic acid **55** (1.0 eq.) and 1.0 eq. phenylacetic chloride **56** were stirred with 1.0 eq. NaOH in methanol and after full conversion the anhydride **57** was obtained by crystallisation from a mixture of petroleum ether and benzene (9:1; v/v) in a yield of 67 %. In the next step, levamisole base was used as a low molecular weight organocatalyst to obtain (*S*)-pyranones in high enantiomeric purity according to the DYKAT type II mechanism.²³⁸ The hydrochloride of levamisole is comparatively cheap and readily available as it is widely used in veterinary medicine. The free base of levamisole is obtained by stirring in aqueous NaOH followed by simple extraction process. The quality of the levamisole base isolated this way is sufficient for synthetic application and the solid can be stored for several years.²³⁶ Both the phenylacetic and the isobutyric anhydride were synthesised according to the protocol by ORTIZ *et al.* and yielded 52 % and 85 % of the respective product, respectively. Phenylacetic pyranone **50b** was synthesised with CH₂Cl₂ as a solvent and crystallised from isopropanol.

However, the crystallisation of **50b** and the yield over two steps (35 %, 79 %ee) were far below literature values in this case, which is why isobutyryl pyranone **50a** was chosen for further synthesis approaches. The synthesis was carried out in toluene and after column chromatography the isobutyryl derivative **50a** was obtained in 85 % yield (87 %ee, **Figure 25**), which was comparable to the literature. The enantiomeric excess was determined by chiral HPLC elution (method A) and the respective chromatogram for the isobutyric derivative **50a** is shown in **Figure 25**.

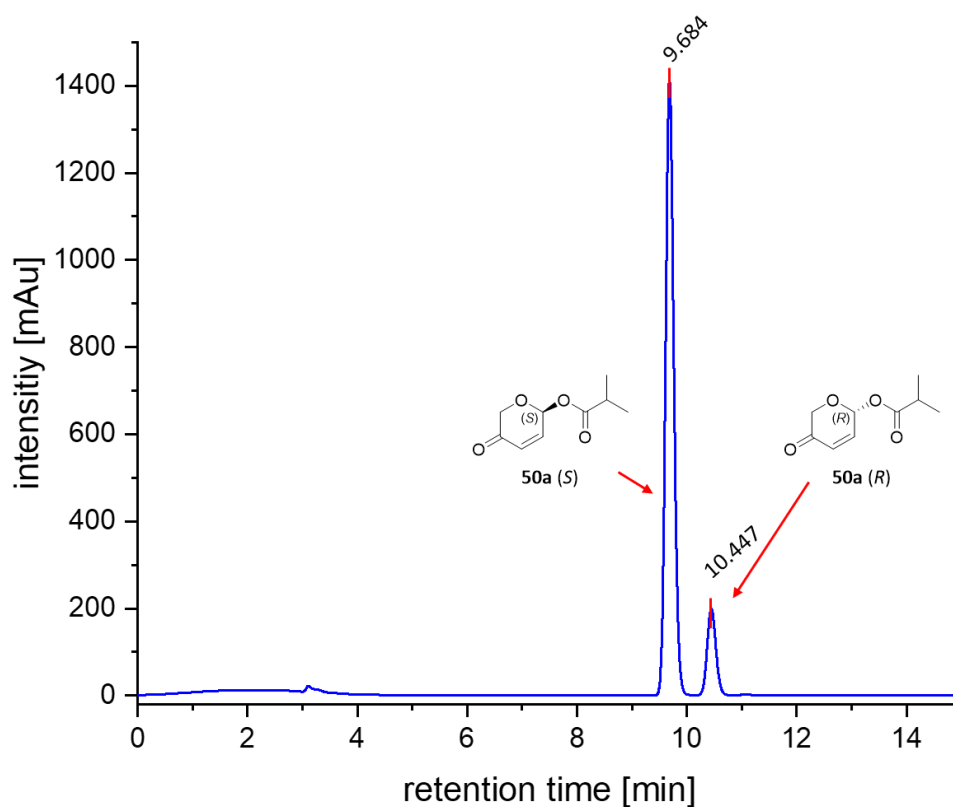
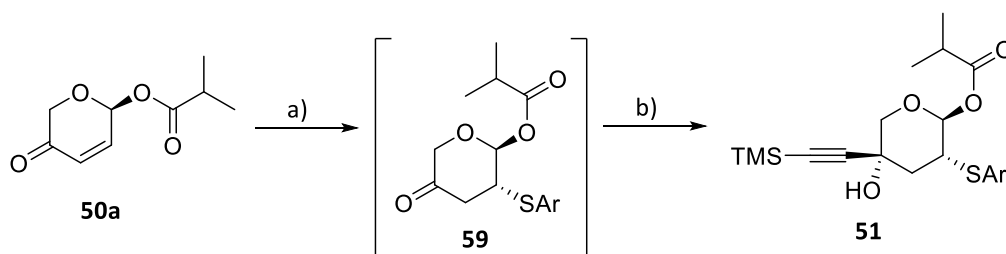


Figure 25: Determination of enantiomeric excess.

Afterwards, isobutyryl pyranone **50a** was converted to pyranone **51** by a one-pot procedure involving two reaction steps (**Scheme 18**). First, *p*-thiocresol reacts in a Thia-Michael-addition with pyranone **50a**, where the final configuration is *trans* (2*S*,3*R*) to the ester group. This configuration is important as it will direct the following substitution at the ketone group. Additionally, this thioether group preserves the double bond during the entire synthesis sequence. The Thia-MICHAEL-addition was accomplished with 1.1 eq. *p*-thiocresol and 0.05 eq. diisopropylethylamine (DIPEA) in toluene at rt. The nucleophilic substitution was done by using lithio-trimethylsilyl (TMS)-acetylene, which was prepared *in situ* by reacting 2.5 eq. *n*-butyllithium (2 M in THF) with 2.5 eq. TMS-acetylene in toluene. The fresh preparation of lithio-TMS-acetylene proved to be crucial, as the use of commercially available lithio-TMS-acetylene did not yield any pyranone **59** at all. In addition, it was necessary to slowly add the solution containing pyranone **59** to the lithio-TMS-acetylene solution. This procedure allowed the

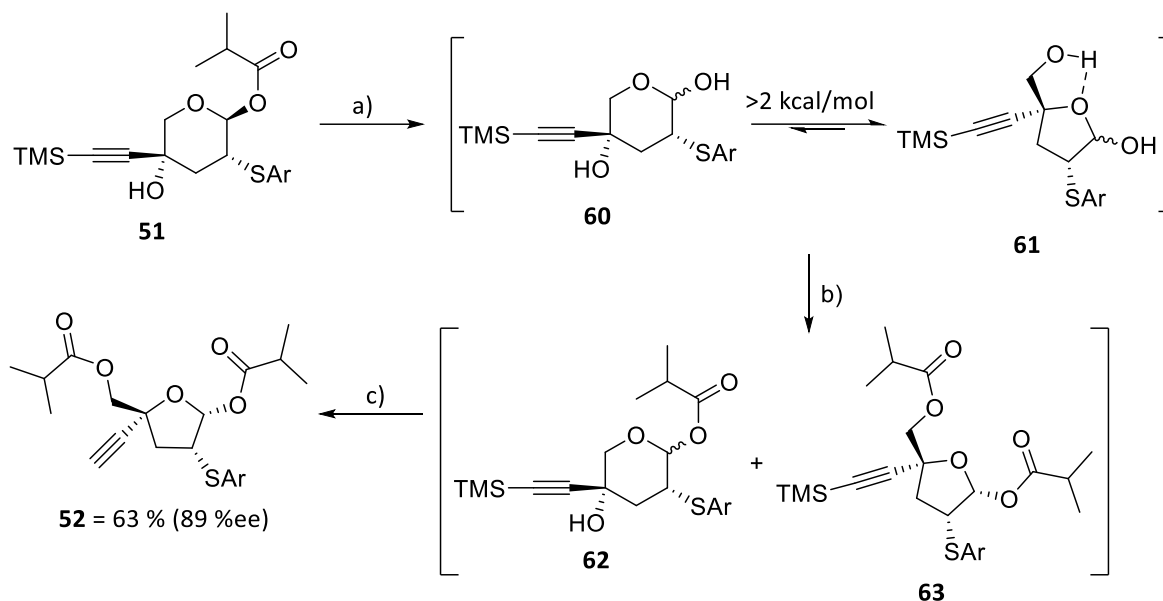
isolation of pyranone **51** in a yield of 58 % (87 %ee) after column chromatography, while crystallisation attempts were not successful. Transferring of stereochemical information is visible through the retention of enantiomeric ratios.²²⁵ The analysis of the enantiomeric excess showed that no epimerization occurred at the C2 carbon (ester substituent) during the two reactions.



Scheme 18: Reaction scheme of pyranone **51**. **a)** *p*-thiocresol, DIPEA, toluene, 45 min, rt; **b)** lithio-TMS-acetylene in THF, toluene, -78 °C, 1h, 58 % (87%ee).

Afterwards, ORTIZ *et al.* adjusted the substrate dependent tautomerization of carbohydrates (**Scheme 19**) by different variables (solvent, pH, temperature, pressure) to obtain furanone **63** in an excess of up to 98:2 compared to pyranone **62**. It was hypothesised that the hydrogen bond between the ring oxygen and the 5'-hydroxyl hydrogen results in a slight preference for the furanone form in the lactol mixture. This state can be trapped by benzoylation or, as in this case, by introducing the isobutyryl protecting group.²²⁵ The cleavage of the isobutyryl group was achieved by using 0.5 eq. 1 M aqueous HCl in acetonitrile over 10 h, whereby the reaction progress was monitored by TLC. After full conversion toluene was added and the mixture was washed with 5 % potassium phosphate solution followed by an exchange of the solvent from acetonitrile to toluene at 45 °C. The levamisole (0.05 eq.) catalysed introduction of the isobutyryl protecting group with 3.0 eq. isobutyric anhydride was accomplished over three days at room temperature. Excess anhydride was removed with MeOH and DMAP.

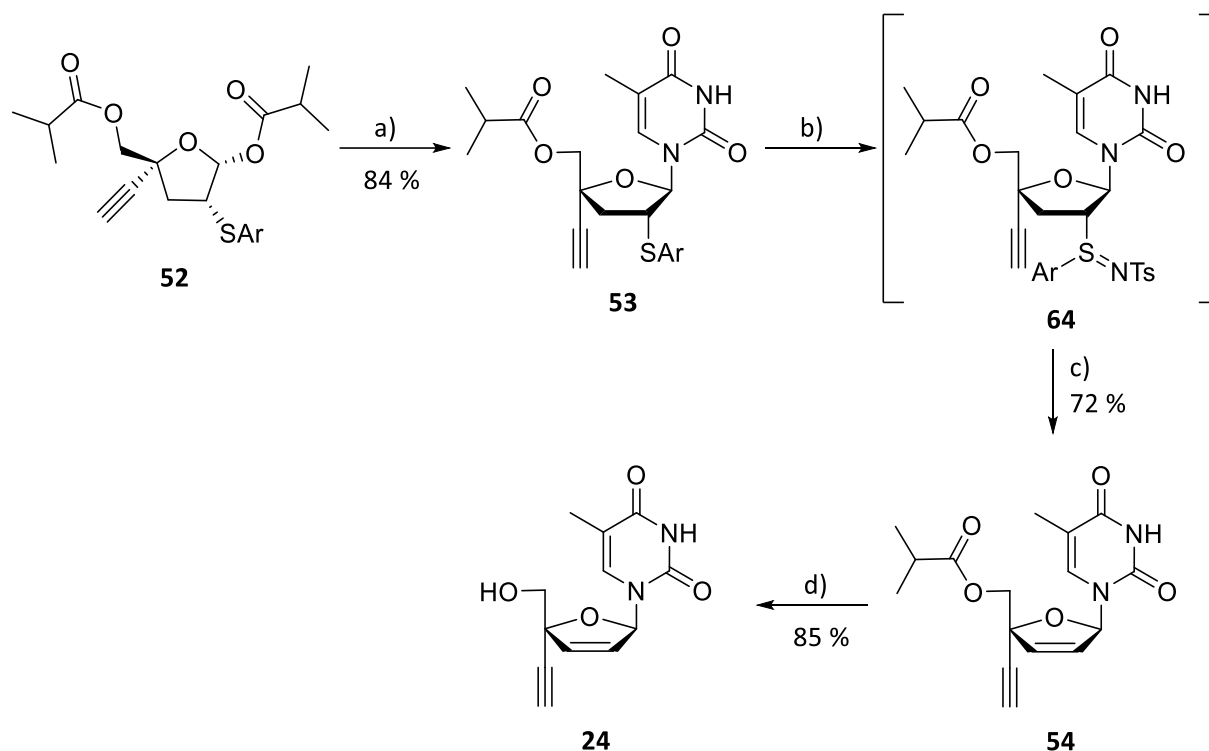
Results and Discussion



Scheme 19: Reaction scheme of furanone **52**. **a)** 1 M HCl, CH₃CN, 10 h, rt; **b)** isobutyric anhydride, levamisole, toluene, 72 h, rt; **c)** K₂PO₄, nBu₄HSO₄, H₂O, toluene, 0 °C, 1.5 h.

For the last step additional washing with 5 % potassium phosphate solution and drying over sodium sulphate was necessary to ensure appropriate amounts of water for the removal of the TMS group. This step was conducted with 0.2 eq. TBA sulphate, 3.0 eq. potassium phosphate and 3.0 eq. water in toluene at 0 °C. The furanone **52** was obtained in a yield of 63 % (89 %ee) *via* crystallisation by slow addition of hexane (100 mL) to a toluene solution (10 mL).

The conversion of furanone **52** to the desired nucleoside **24** was achieved by three consecutive steps (**Scheme 20**). In the first step, the trimethylsilyl trifluoromethanesulfonate (TMSOTf) protected nucleobase was introduced *via* a VORBRÜGGEN glycosylation.²³⁹ Therefore, 1.4 eq. thymine were suspended in acetonitrile and reacted with 2.2 eq. TMSOTf as well as 1.4 eq. hexamethyldisilazane (HMDS) under stirring at rt until the reaction was clear. Then, a solution of furanone **52** in acetonitrile was added dropwise and the mixture was stirred at rt until full conversion. After quenching 5 % potassium phosphate solution, water: acetonitrile and washing with heptane the nucleoside **53** was obtained by column chromatographic purification on RP₁₈-silica in 84 % (89 % ee) yield.



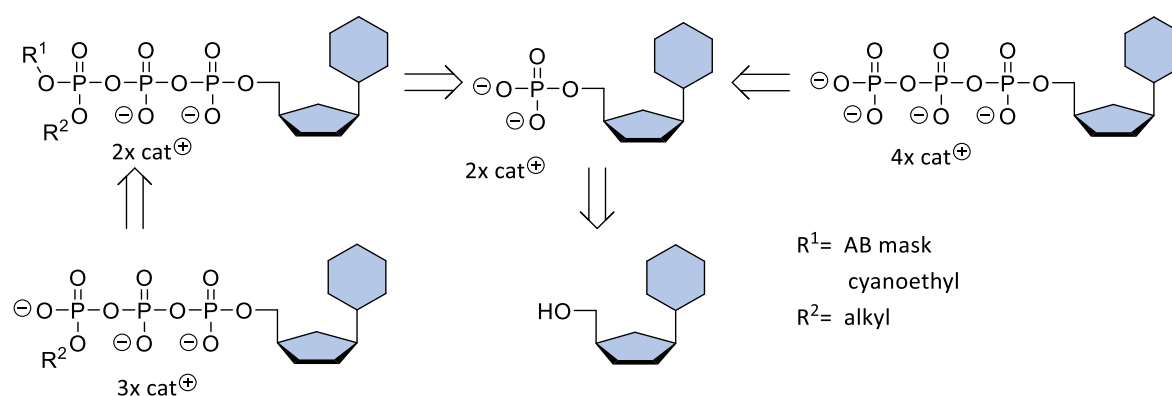
Scheme 20: Reaction scheme of 4'-Ed4T **24**. **a)** Thymidine, HMDS, TMSOTf, CH₃CN, 10 °C to rt, 6 h; **b)** Chloramine T, acetic acid, CH₃CN, rt., 2.5 h; **c)** *t*-BuOH, 95 °C, 1 h; **d)** DBU, MeOH, rt to 60 °C 15 h.

In the next step, the sulphur aryl residue was removed by Chloramine T (1.2 eq.) and acetic acid (0.1 eq.) mediated oxidation to the corresponding imine **64** followed by thermolytic cleavage.²⁴⁰ In this step the proficient design of the synthetic route became apparent with the reintroduction of the double bond. Finally the protecting group was removed via a catalysed transesterification with 0.05 eq. 1,8-diazabicyclo[5.4.0]undec-7-ene (DBU) in methanol.²²⁵ These steps were accomplished with yields of 72 % and 85 %, respectively. The nucleoside analogue 4'-Ed4T **24** was obtained in an overall yield of 12 % over seven steps.

The previously described nucleoside analogues **23**, **24** and **26** together with 3TC **25** will be used for the synthesis of different prodrugs, which will be discussed in the following chapter.

4.5. Triphosphate Prodrugs, γ -Alkyl Triphosphates and Triphosphates

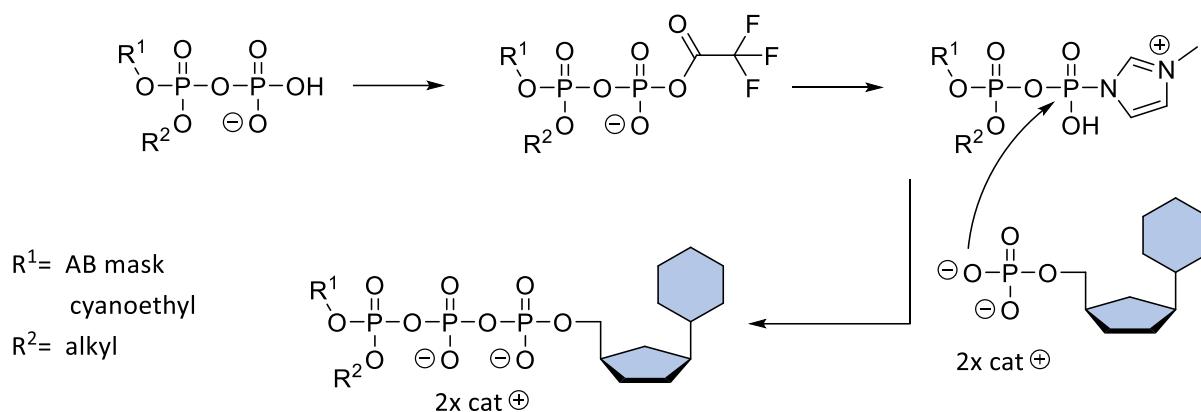
The syntheses of NTPs, NTP prodrugs and γ -alkyl NTPs were based on the synthetic approach, which was developed by GOLLNEST *et al.*⁴⁸ (**Scheme 21**) for the synthesis of TriPPPPro compounds. The corresponding monophosphates were obtained by different reactions depending on the respective nucleoside. Subsequently, the activation of NMP and reaction with pyrophosphate or other way around leads to the formation of the desired triphosphate. In order to obtain non-symmetrically masked prodrugs modified conditions developed by ZHAO *et al.* were applied.⁵²



Scheme 21: Representation of the synthesis of NTPs, NTP prodrugs and γ -alkyl NTPs starting from the corresponding nucleosides.

The TriPPPPro approach involves coupling conditions using a two-step process (**Scheme 22**) described by MOHAMADY *et al.*²⁴¹ In the first step, the masked pyrophosphate is treated with an excess of trifluoroacetic anhydride (TFAA), which activates the phosphate and can also remove any water present. In the second step, trifluoroacetic acid is substituted with 1-methylimidazole, thus leading to sufficient electrophilicity for nucleophilic displacement by NMP. These NMPs can be synthesised by the well-established routes of either SOWA and OUCHI¹⁷⁷ or YOSHIKAWA *et al.*¹⁷⁸ However, these highly acidic conditions are not applicable to sulphur containing nucleosides, thus the NMP synthesis for these compounds requires an initial conversion to the corresponding nucleoside-*H*-phosphonates.²⁴²

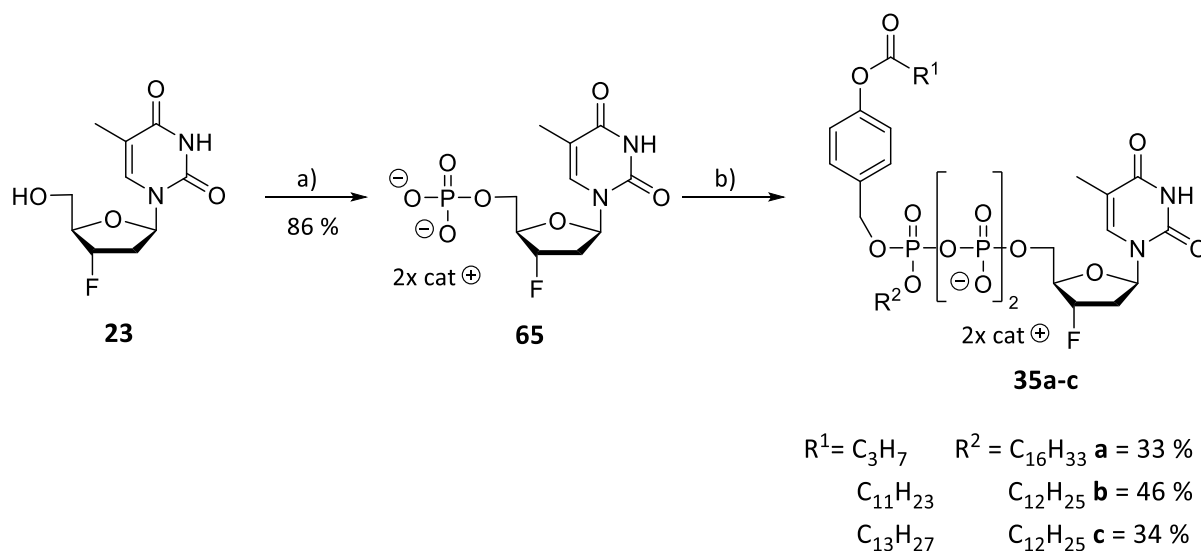
Results and Discussion



Scheme 22: Representation of the activation process and subsequent coupling of pyrophosphate with NMP.

4.5.1. FLT Triphosphate Prodrugs and γ -Alkyl Triphosphates

The syntheses of FLT derivatives shown here are based on results of WEISING *et al.*, who demonstrated high chemical stability for γ -modified FLT derivatives and an antiviral activity in the nano- to micromolar range against HIV-1 and 2.¹⁹⁵ The synthesis route for γ -modified NTP prodrugs (**Scheme 23**) followed established protocols.^{52,195} Monophosphate synthesis developed by SOWA and OUCHI was applied to FLT **23**, as it delivered higher yields for this nucleotide compared to the YOSHIKAWA method.²⁴³ The phosphorylation reaction with $POCl_3$ (4.4 eq.), pyridine (4.8 eq.) and water (2.8 eq.) in acetonitrile (18.1 eq.) at 0 °C gave FLTMP **65** in high yields up to 86 % after RP column chromatography.



Scheme 23: Reaction scheme of FLT triphosphate prodrugs **35a-c**. **a)** $POCl_3$, pyridine, H_2O , CH_3CN , 0 °C, 3.5 h; **b)** pyrophosphate **19a-c**, TFAA, 1-methylimidazole, Et_3N , 0 °C to rt, 3 h.

With FLTMP **65** in hand, the FLT triphosphate prodrugs were synthesised following the previously described protocol (Chapter 4.5). Due to the poor solubility of FLTMP (NH_4^+) **65** an ion exchange using 2.0 eq. 10 % aq. TBA hydroxyl solution was performed. Moreover, the TBA counter-ions ensure a better reactivity, thus leading to better conversion in the coupling reactions. Additionally, several drops of DMF were added to the reaction to ensure the solubility during the reaction.

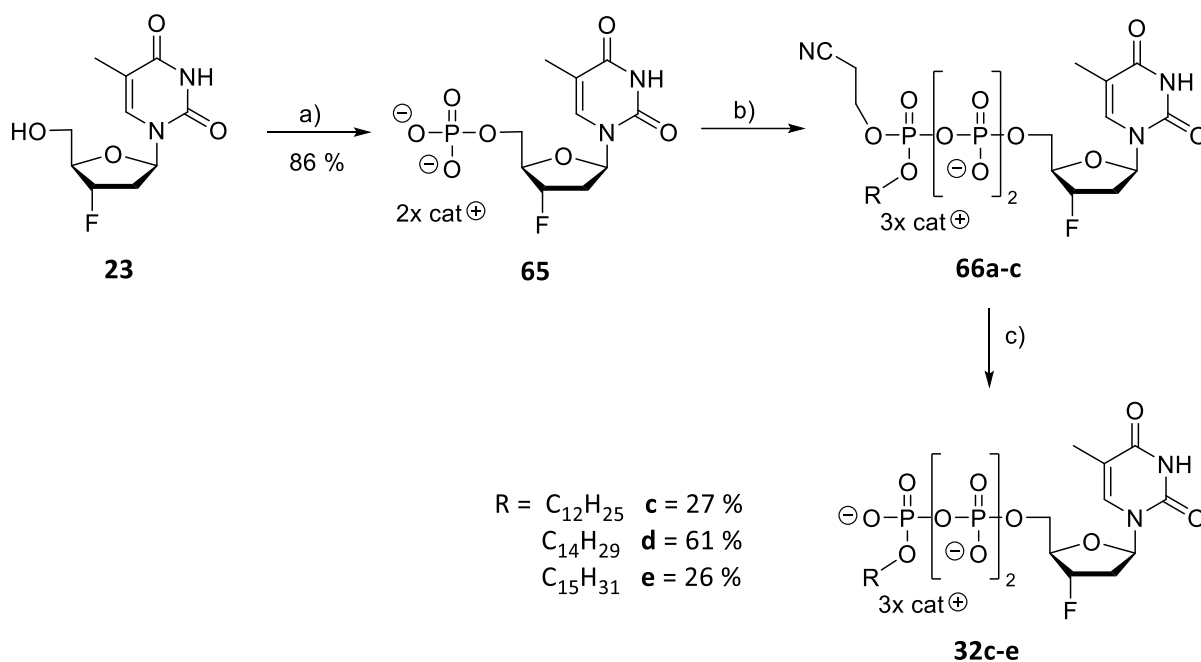
During this work, the reaction conditions for triphosphate synthesis were adjusted in relation to the monophosphate. In general, the pyrophosphate synthesis gave yields ranging from 67 % to 93 % and the coupling with the appropriate NMPs was usually performed 1.7 – 2.0 eq. of the masked pyrophosphate. There was no direct correlation of the yield and the used equivalents of pyrophosphate observed.

FLTMP **65** was converted to its FLT triphosphate prodrugs **35a-c** by using the corresponding pyrophosphates **19** (**a**, 2.0 eq.; **b**, 2.0 eq.; **c**, 1.8 eq.). These masked pyrophosphates were treated with 10.0 eq. TFAA and 16.0 eq. triethylamine in relation to NMP and afterwards all volatiles were removed in vacuo. Then, the second activation step was carried out with 10.0 eq. triethylamine and 5.0 eq. of 1-methylimidazole in DMF following the addition of NMP. The reaction progress was monitored by HPLC (method A) until no further conversion was observed. Full conversion could not be observed in most cases, but there was no direct link to one specific parameter of the reaction found.

The final triphosphate prodrugs were obtained by a purification sequence using RP₁₈ column chromatography followed by ion exchange chromatography (Dowex[®]) and an additional RP₁₈ column chromatography. The ion exchange from $n\text{Bu}_4\text{N}^+$ ions to ammonia leads to a different retention time during the second RP₁₈ column chromatography, which facilitates the removal of the remaining 1-methylimidazole. Using this process, FLT triphosphate prodrugs **35a-c** (NH_4^+) were obtained in 33 %, 46 % and 34 % yield, respectively.

Alkylated derivatives, which mimic the metabolite of the prodrug in biological experiments, were synthesised with the same *H*-phosphonate protocol, but included a final deprotection of the cyanoethyl protecting group at the γ -phosphate (**Scheme 24**). The γ -alkyl-FLTP **32c-e** were synthesised by using their corresponding cyanoethyl pyrophosphates **39** (**a**, 1.6 eq.; **b**, 2.5 eq.; **c**, 2.5 eq.). To address solubility and conversion issues, DMF was added during the first activation step until the reaction mixture was clear. The second step was carried out in DMF as a solvent. Removal of the protecting group was carried out in water by using 10.0 eq. TBA hydroxyl solution and the reaction was usually complete after stirring overnight at room temperature. The γ -alkyl FLTP **32c-e** were obtained in moderate to good yields of 27 %, 61 % and 26 %, respectively.

Results and Discussion



Scheme 24: Reaction scheme of γ -alkyl triphosphate FLT **32c-e**. **a)** POCl_3 , pyridine, H_2O , CH_3CN , $0\text{ }^\circ\text{C}$, 3.5 h; **b)** pyrophosphate **39a-c**, TFAA, 1-methylimidazole, Et_3N , $0\text{ }^\circ\text{C}$ to rt, 3 h; **c)** TBA hydroxide, CH_3CN , rt, 16 h.

The successful synthesis of prodrugs and alkylated triphosphates enabled the preliminary studies in pursuit of suitable chain lengths discussed in chapter 4.1. γ -Alkyl-FLTTP **31b-e** (**31b** WEISING *et al.*) and γ - $\text{C}_{16}(\text{C}_3\text{AB})$ -FLTTP **35a** were synthesised in a cooperation with WEISING *et al.* to evaluate and improve the substrate properties of FLT prodrugs as antiviral compounds against HIV.¹⁹⁵ These studies preceded the optimisation of the masking units. Therefore, γ - $\text{C}_{16}(\text{C}_3\text{AB})$ -FLTTP **35a** was equipped with a fast-cleaving masking unit, to obtain complementary data to the used TriPPPPro and γ -alkyl compounds. The result of the alkyl chain optimisation *via* primer extension assay is described in chapter 4.1. To verify the results of the primer extension assay, these compounds were tested against HIV in cooperation with SCHOLS *et al.* from the Rega institute in Leuven (**Table 3**).

Results and Discussion

Table 3: Antiviral data against HIV for FLT triphosphate prodrugs **34a-c**, γ -alkyl triphosphate FLT **31b-e** and FLT **22**.

Compound	Unit	CEM			CEM TK ^c	
		HIV-1 HE	HIV-2 ROD	cellular tox.	HIV-2 ROD	cellular tox.
		EC ₅₀ ^a	EC ₅₀ ^a	CC ₅₀ ^b	EC ₅₀ ^a	CC ₅₀ ^b
23*	μ M	0.0011 \pm 0.0044	0.011 \pm 0.079	>100	70 \pm 19	-
35a*	μ M	0.060 \pm 0.021	0.0028 \pm 0.0039	>100	1.16 \pm 0.45	>100
35b	μ M	0.0047 \pm 0.0042	0.013 \pm 0.006	63.70	2.83 \pm 0.72	>100
35c	μ M	0.0017 \pm 0.0016	0.0032 \pm 0.0030	>100	>20.00 \pm 0	20.00
32b*	μ M	0.015 \pm 0.0088	0.021 \pm 0.019	33 \pm 11	5.5 \pm 6.2	-
32d	μ M	0.014 \pm 0.0085	0.0019 \pm 0.0023	>100	>100 \pm 0	>100
32e	μ M	0.077 \pm 0.0092	0.0035 \pm 0.0051	>100	0.72 \pm 0.62	>100

*results obtained from previous work in cooperation with WEISING *et al.*¹⁹⁵

^a50% Effective concentration required to inhibit HIV induced cytopathogenic effect in cell culture

^b50% Cytotoxic concentration of the compound evaluated in this cell line

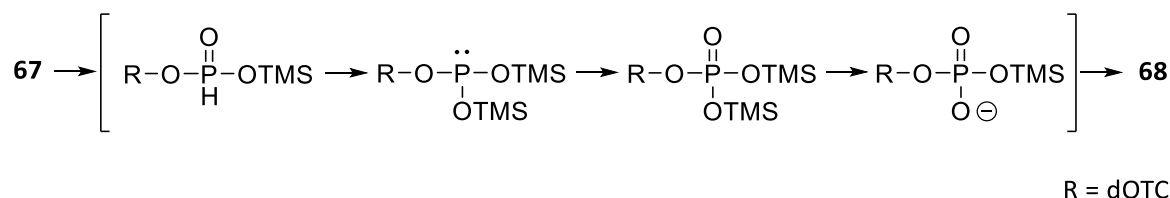
The γ -alkyl FLTTP **32b**, **32d** and **32e** exhibited antiviral activities against HIV-1 of 15.0 nM, 14.0 nM and 77.0 nM, respectively. These findings indicate a significant loss of activity, with γ -C₁₆-FLT **32b** exhibiting nearly a 14-fold decrease, γ -C₁₄-FLT **32d** a nearly 13-fold decrease, and γ -C₁₅-FLT **32e** a 70-fold decrease in activity compared to the parent nucleoside **23**. These results suggest an overall negative effect for γ -modified triphosphates against HIV-1, but they are still in the low nanomolar range. The addition of a short AB masking unit did not improve the overall activity against HIV-1 with similar antiviral activity of 60.0 nM. These results were significantly improved by using a C₁₁AB or C₁₃AB cleavable mask. Their EC₅₀ values against HIV-1 are 4.70 nM and 1.70 nM, respectively, which represents only a 4-fold and 1.5-fold decrease in activity compared to the parent nucleoside **23**. These results suggest that the γ -alkyl FLTTPs and the γ -C₁₆(C₃AB)-FLTTP **35a** cannot cross the cell membrane to the same degree, due to the lowered lipophilicity, or they may indicate that the long alkyl chains of the AB-masking units prevent intracellular degradation to the γ -alkyl NTPs, the latter would highly contrast findings of hydrolysis studies performed with similar compounds.^{244,245} Both scenarios would result in lower bioavailability of substrate and therefore in lower activity against HIV-1. The active carrier mediated cell uptake of the parent nucleoside could also lead to increased concentration of the parent nucleoside compared to the prodrugs.¹⁹⁵ The overall improved antiviral activity against HIV-2, except for the derivatives **35b** and **32b** (13 and 21 nM), suggest higher intracellular concentration of substrate compared to FLT **23**. In combination these results could point towards a lower acceptance of NRTIs of HIV-1-RT compared to HIV-2-RT. HIV-1-RT exhibits a greater ability for the excision of AZT, which could affect other NRTIs.²⁴⁶ Further testing with both wildtype HIV-RT variants in primer extension assays

could show the differences, either in activity or substrate acceptance. The testing in TK deficient cell lines showed overall good results, as both γ -alkyl(AB)-FLTTP and γ -alkyl-FLTTP derivatives showed retained activity against HIV-2. The unexpected loss of activity observed in γ -C₁₂(C₁₃AB)-FLTTP **35c** and γ -C₁₄-FLTTP **32d** cannot be explained and suggest repetition of the testing. Nevertheless, benefits of the γ -modifications can be observed in the TK⁻ cell lines. The toxicity of all tested compounds was above the measured threshold except for γ -alkyl modified compounds (**32b**, **35b** and **35c**). As the pharmacological properties of the prodrugs were nevertheless improved, the synthesis and extensive biological tests of several FLT prodrugs served as the basis for the further conversion of various nucleosides, which are described in the following chapters.

4.5.2. dOTC Triphosphate Prodrug, γ -Alkyl Triphosphate and Triphosphate

The synthesis of sulphur containing nucleoside is described in the literature as a complicated and time consuming process, as the acidic conditions in the most commonly used procedures lead to deglycosylation.²⁴² A modified YOSHIKAWA protocol developed by ROY *et al.* using 10.0 eq. POCl₃ was tested with moderate success.²⁴² The reaction was monitored by hplc (method A) and stopped after one hour after significant amounts of cytosine were detected. The targeted yields of 41 % to 52 % were not achieved and dOTCMP was only obtained in a yield of 33 %.

As a result, different synthetic approaches were considered. ROY *et al.* proposed the transformation to the corresponding *H*-phosphonate, followed by oxidation.^{242,247} This procedure was derived from a 5'-phosphorylation method introduced by WADA *et al.*, which produced 5'-protected monophosphates of several purine and pyrimidine based nucleosides in high yields over two steps.²⁴⁷ The reaction conditions for the first step were very similar to the well-established *H*-phosphonate route described in chapter 4.3. The following oxidation (**Scheme 25**) involved silylation with bis(trimethylsilyl)acetamide followed by DAVIS-oxidation²⁴⁸ using either (1S)-(+)-(10-camphersulfonyl)-oxaziridine **69a** (CSO) or (1S(+)-(8,8-dichlorocamphorylsulfonyl)oxaziridine **69b** (DCSO).



Scheme 25: Reaction scheme of dOTCMP **68** via silylation and subsequent DAVIES-oxidation.

As CSO and DCSO are quite expensive, alternative oxidation methods were investigated to further improve the process.²⁴⁹ The most promising approach involved iodine as an oxidizing agent. This method was developed by SUN *et al.* and led to NMPs with yields up to 94 %.²⁴⁹ This reaction follows

the same mechanistic pathway as described for the DAVIES-oxidation (**Scheme 25**). The silylation was carried out with 5.0 eq. bis(trimethylsilyl) acetamide in pyridine and after 1 h a solution of iodine (1.2 eq.) in DMF was added. Already after two minutes of stirring the mixture was hydrolysed in water. The purification process involved an ion exchange chromatography on Sephadex™ (NH₄⁺) with subsequent RP₁₈ column chromatography to afford dOTCMP **68** with 58 % yield. The unexpected low yield and comparatively complex purification process prompted the use of the method involving the DAVIES-oxidation. The synthesis of dOTCTP **71**, γ -C₁₂(C₁₃AB)-dOTCTP **69** and γ -C₁₂-dOTCTP **70** is shown (**Scheme 26**) and starts from dOTC **26**, which is converted to the *H*-phosphonate by using DPP in pyridine. After hydrolysis with water and purification on silica via column chromatography dOTC *H*-phosphonate **67** was isolated with an excellent yield of 98 %. Subsequently, dOTC *H*-phosphonate **67** was silylated with 5.0 eq. bis(trimethylsilyl) acetamide in DMF and converted to the corresponding monophosphate with 2.0 eq. CSO **72a** in combination with a mixture of methanol:DBU (97:3; v/v). After removal of the TMS-groups, excess of reagents and other impurities were removed by several washing cycles with CH₂Cl₂ followed by an ion exchange chromatography on Sephadex™ (NH₄⁺), yielding dOTCMP **68** in a very good yield (88 %). This led to a comparable overall yield of 86 % over two steps and far exceeds the single-step phosphorylation methods.

observed in prior work with other cytidine derivatives by WITT *et al.*²⁰⁶ It was hypothesised that either intra- or intermolecular interactions between the free amine function and the phosphate moieties lead to degradation of the triphosphate to the monophosphate.

The synthesis of unmodified triphosphate dOTCTP **71** was performed using the phosphate activation method developed by MOHAMADY *et al.*²⁴¹ In this case, the coupling was achieved by activating the monophosphate instead of the pyrophosphate. The activation sequence and reagent amounts were very similar to the previously described synthesis of masked pyrophosphate (see Chapter 4.3.1). After activation the monophosphate was added to a solution of 3.0 eq. pyrophosphate in acetonitrile. The slow addition and the high amount of pyrophosphate minimized potential side reactions (e.g. formation of dinucleoside tetraphosphate). The final product dOTCTP **71** was obtained after RP₁₈ column chromatography, ion exchange on Dowex® to ammonia and a second RP₁₈ column chromatography in 59 % yield. The ³¹P NMR of the final products is depicted in **Figure 26**.

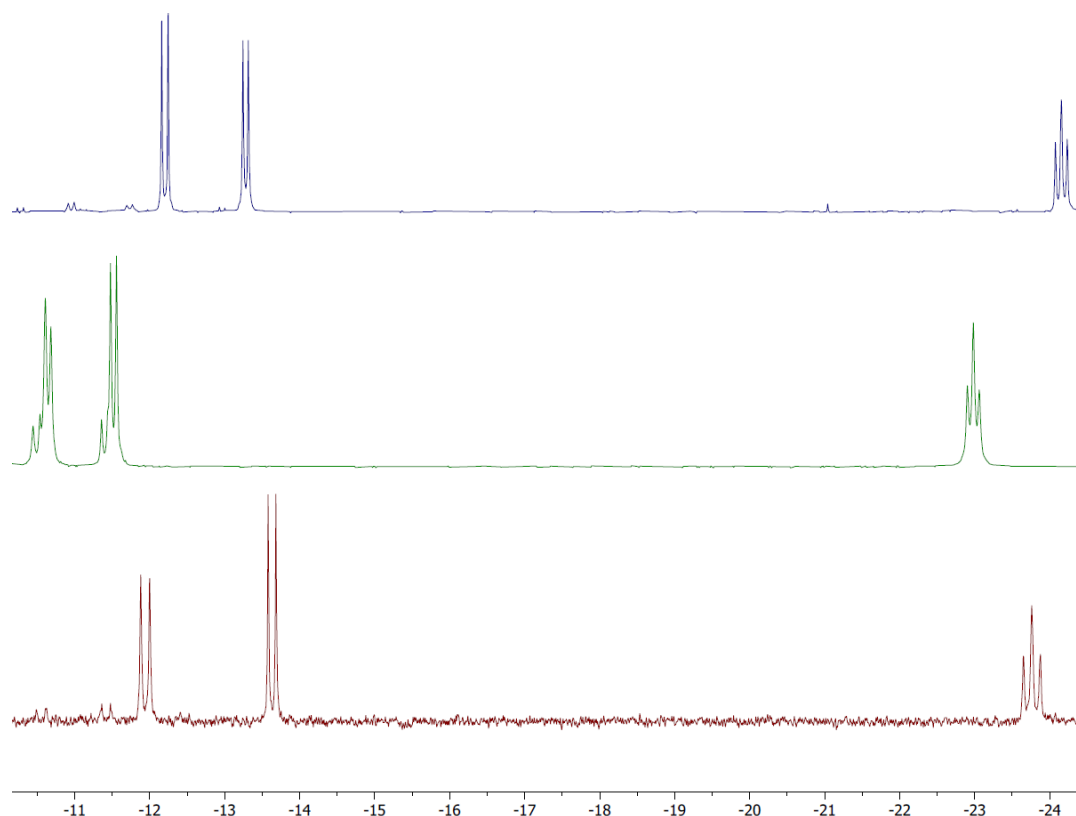


Figure 26: ³¹P NMR spectra of dOTCTP derivative **69** (top), **70** (bottom) and **71** (middle).

The evaluation of the dOTCTP derivative **69**, **70** and **71** was carried out according to the already established protocols (see Chapter 4.1). At first, γ -C₁₂(C₁₃AB)-dOTCTP **69**, the γ -C₁₂-dOTCTP **70** and the triphosphate **71** as well as CTP, if required for visualisation, were tested in primer extension assay using templates for cytidine. The dOTCTP derivatives **69**, **70** and **71** were tested against HIV-RT (**Figure 27**) using standard assay conditions (see Experimental Procedure 6.1.3).

Results and Discussion

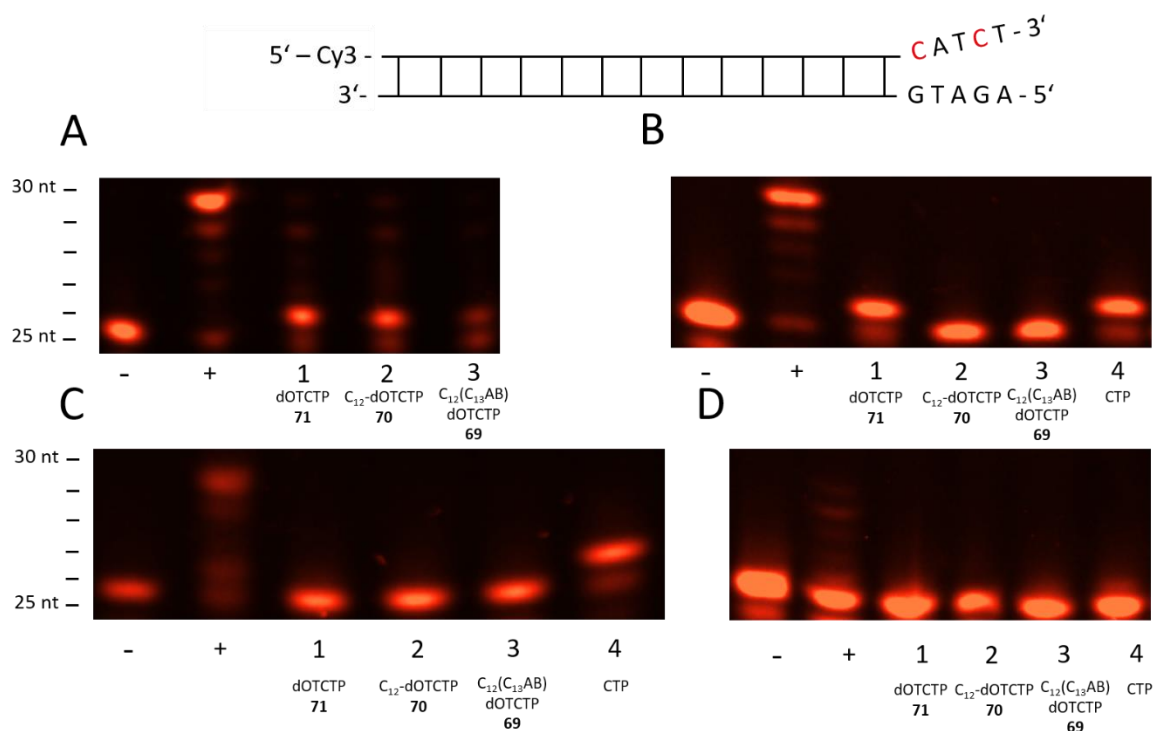


Figure 27: Primer extension assay using dOTC triphosphates **69**, **70** and **71** and CTP; **A**) HIV-RT; negative control; positive control; lane 1: dOTCTP **71**; lane 2: γ -C₁₂-dOTCTP **70**, lane 3: γ -C₁₂(C₁₃AB)-dOTCTP **69**. **B**) Pol β ; negative control; positive control; lane 1: dOTCTP **71**; lane 2: γ -C₁₂-dOTCTP **70**, lane 3: γ -C₁₂(C₁₃AB)-dOTCTP **69**, lane 4: CTP. **C**) Pol α ; negative control; positive control; lane 1: dOTCTP **71**; lane 2: γ -C₁₂-dOTCTP **70**, lane 3: γ -C₁₂(C₁₃AB)-dOTCTP **69**, lane 4: CTP. **D**) Pol γ ; negative control; positive control; lane 1: dOTCTP **71**; lane 2: γ -C₁₂-dOTCTP **70**, lane 3: γ -C₁₂(C₁₃AB)-dOTCTP **69**, lane 4: CTP. Assay conditions are summarized in the Experimental Procedure 6.1.3.

The results were as expected, with both dOTCTP **71** and γ -C₁₂-dOTCTP **70** exhibiting good substrate properties with a n+1 band tending towards full incorporation. The unexpected incorporation of the γ -C₁₂(C₁₃AB)-dOTCTP **69** was most likely a result of AB mask cleavage due to the basic conditions of the assay buffer. Therefore, an exemplary γ -alkyl(AB)-triphosphate was incubated for 1 h in HIV-RT assay buffer (**Figure 28**). Both intermediate and monophosphate were found, of which the prior could explain the positive n+1 band.⁵⁰

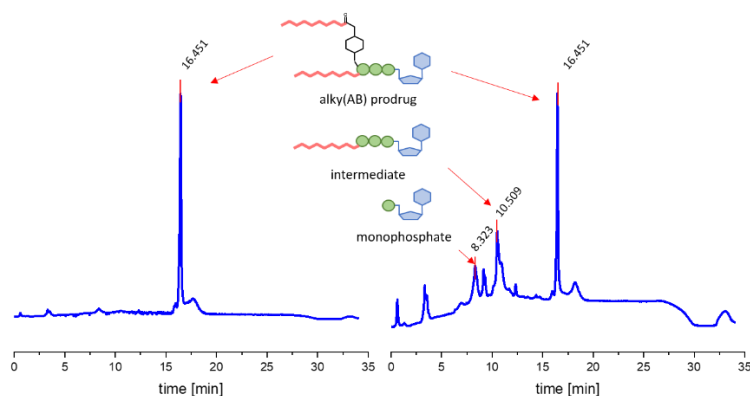


Figure 28: Hplc analysis (method A) of exemplary γ -alkyl(AB)-triphosphate incubated HIV-RT assay buffer. Left: aliquot after addition of buffer 0 min. Right: Aliquot taken after 60 min.

Results and Discussion

The same assay setup was used for pol β , with CTP added in lane 4 for a clear indication of a n+1 band (**Figure 27, B**). The accuracy of the assay was demonstrated with the full elongation (n+5) in the positive control. As expected, both modified dOTCTPs **69** (**Figure 27, B**) and **70** (**Figure 27, B**) were not incorporated into the growing strand and are therefore not substrates for pol β , while the dOTCTP **71** was incorporated in a manner comparable to CTP.

Similar results were obtained in the pol α assay (**Figure 27, C**) except for the dOTCTP **71**, which was either not incorporated at all or only in barely detectable amounts. Nevertheless, while not entirely negligible, the more plausible explanation, based on other pol α experiments, was diffusion of fluorescent material while preparing the gel for the imaging process.

The most difficult evaluation was posed by the pol γ assays, which yielded the lowest intensity among all primer extension assays. The gel depicted in **Figure 27 D** was adjusted to the other polymerases and does barely show visible bands for the positive control. The positive control is visible when increasing the contrast (**Figure 29**). While this shows the remaining activity of the polymerase not enough CTP was incorporated to generate a n+1 band (**Figure 29**). The positive control with CTP in lane 4 was barely visible and could be confused with the previously described diffusion. The overall weak activity of the polymerase necessitates repetition of this experiment with either 'newer' polymerase or a more sensitive method like radiolabeling.²⁵⁰

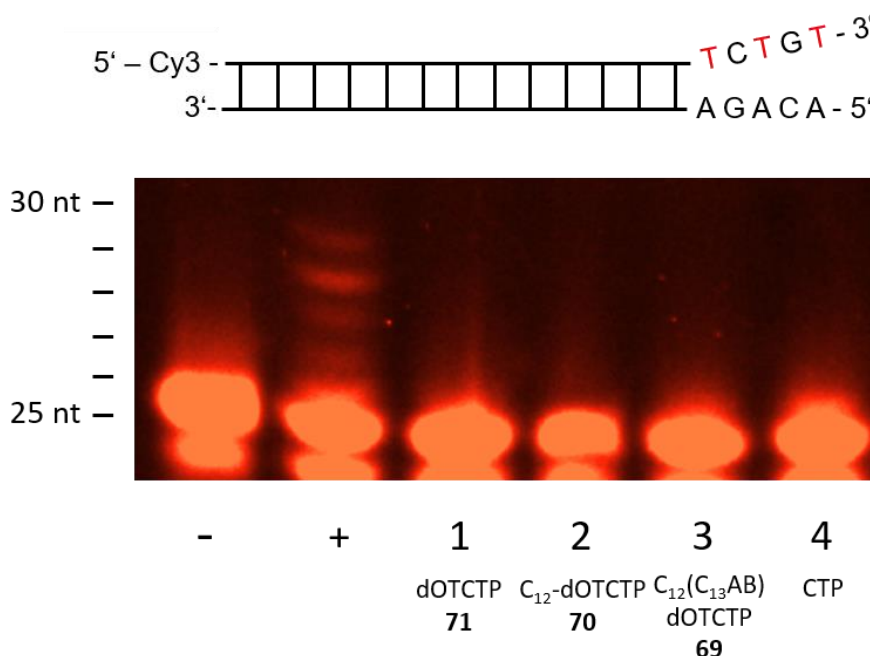


Figure 29: Primer extension assay using dOTC triphosphates **68**, **69**, **70** and CTP. Polymerase γ ; negative control; positive control; lane 1: dOTCTP **70**; lane 2: γ -C₁₂-dOTCTP **69**, lane 3: γ -C₁₂(C₁₃AB)-dOTCTP **68**, lane 4: CTP. Assay conditions are summarized in the Experimental Procedure 6.1.3.

The *in vitro* testing of nucleoside **26** and prodrug **69** against HIV-1 and HIV-2 (**Table 4**), while revealing favourable properties in the primer extension assays, did not show any benefit in antiviral activity by applying the prodrug approach. In tests with HIV-1 and HIV-2 infected CEM cells, a 1.1-fold increase and a 1.2-fold decrease in activity was observed. These results are consistent with previous studies of dOTC derivatives, which showed an average value of approximately $1.3 \pm 0.9 \mu\text{M}$ in HIV-1 infected PBMC cell lines.²⁵¹ Despite promising primer extension assay results, the γ -alkyl prodrug dOTC did not lead to a significant improvement in antiviral activity compared to the parent nucleoside.

Table 4: Antiviral data against HIV for γ -C₁₂(C₁₃AB)-dOTCTP **69** and dOTC **26**.

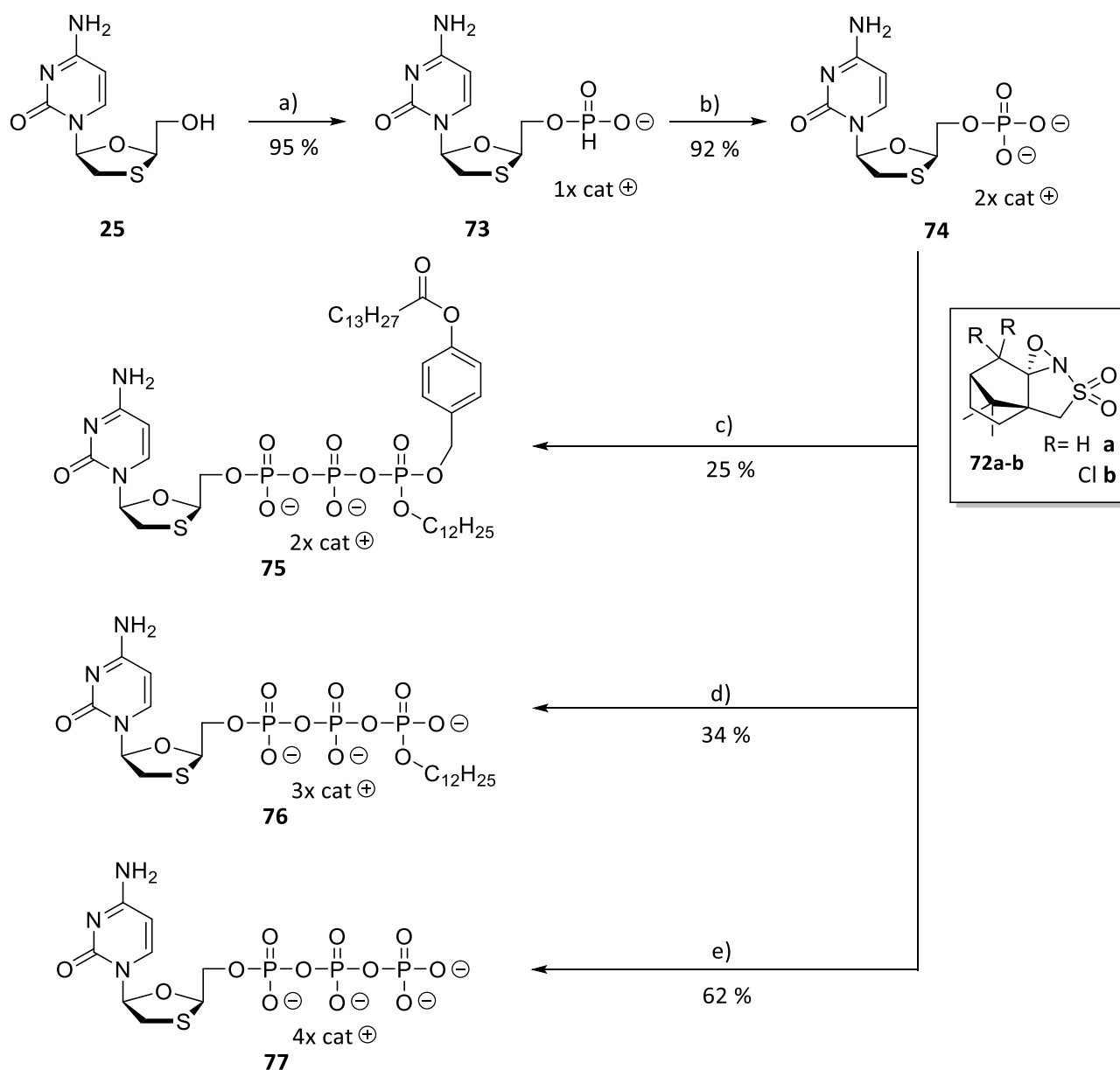
Compound	Unit	CEM		
		HIV-1 HE	HIV-2 ROD	cellular tox.
		EC ₅₀ ^a	EC ₅₀ ^a	CC ₅₀ ^b
26	μM	2.17±1.97	1.42±0.83	>100
69	μM	1.94±0.15	1.71±1.40	>100

^a50% Effective concentration required to inhibit HIV induced cytopathogenic effect in cell culture
^b50% Cytotoxic concentration of the compound evaluated in this cell line

4.5.3. 3TC Triphosphate Prodrug, γ -Alkyl Triphosphate and Triphosphate

For the synthesis (**Scheme 27**) of the 3TC triphosphate derivatives **75**, **76** and **77** an identical route like for the dOTCTP derivatives was used. First, the nucleoside **25** was converted into the corresponding *H*-phosphonate **73** with DPP in pyridine followed by a hydrolysis with water. In this case, 3TC *H*-phosphonate **74** was obtained in 95 % yield after purification on silicagel via column chromatography. The preparation of 3TCMP **74** was done in a similar way to the synthesis of dOTCMP **66**, but in this case CSO **72a** was replaced by the cheaper DCSO **72b**, resulting a comparable yield. After cleavage of the TMS-groups and purification *via* ion exchange chromatography with Sephadex™ 3TCMP **74** was obtained in 92 % yield, resulting in an overall yield of 87 % over two steps, again far exceeding traditional monophosphate syntheses for this type of nucleoside.

Results and Discussion



Scheme 27: Reaction scheme of 3TC triphosphate prodrug, γ -dodecyl triphosphate and triphosphate. **a)** DPP, pyridine, rt, 1 h; **b)** bis(trimethylsilyl) acetamide, DCSO **72b**, DMF, rt, 3 min; **c)** i) pyrophosphate **19c**, TFAA, Et₃N, CH₃CN, 0 °C, 10 min; ii) 1-methylimidazole, DMF, rt, 10 min; iii) NMP **74**, DMF, rt, 2 h; **d)** i) pyrophosphate **39a**, TFAA, Et₃N, CH₃CN, 0 °C, 10 min; ii) 1-methylimidazole, DMF, rt, 10 min; iii) NMP **74**, DMF, rt, 2 h; **e)** i) TBA hydroxide, CH₃CN, rt, 16 h **e)** i) NMP **74**, TFAA, Et₃N, CH₃CN, 0 °C, 10 min; ii) 1-methylimidazole, DMF, rt, 10 min; iii) pyrophosphate, CH₃CN, rt, 2 h.

The syntheses of 3TC triphosphates **75**, **76** and **77** were performed according to the established protocols described in the previous chapter (Chapter 4.5). The γ -C₁₂(C₁₃AB)-3TCTP **75** and the γ -C₁₂-3TCTP **75** were synthesised using the corresponding pyrophosphates **19c** and **39a**. The equivalents of activating reagents and the purification process were identical to the corresponding dOTC derivative syntheses. γ -C₁₂(C₁₃AB)-3TCTP **75** and γ -C₁₂-3TCTP **76** were obtained in yields of 25 % and 34 %, respectively. As mentioned before (see page 61, Chapter 4.5.2), traces of 3TCMP **74** could be detected after each purification step. By using the MOHAMADY protocol the unmodified 3TCTP **77** was obtained in good yield of 62 %.

Results and Discussion

Upon successful synthesis, the 3TC triphosphates **75**, **76** and **77** were incubated with viral and human polymerases to evaluate their substrate properties. For these primer extension assays identical conditions were used as described before. In the case of human polymerases, CTP was added for better visualisation. The primer extension assay using HIV-RT (**Figure 30, A**) showed incorporation of all 3TCTP derivatives. These results were identical to the dOTCTP derivatives. As mentioned in Chapter 4.5.2 the weak incorporation of γ -C₁₂(C₁₃AB)-3TCTP **75** is most likely attributed to the mask cleavage in assay conditions. In this setup, the first two lanes were used for the negative and positive control, which show no and full elongation of the primer, respectively. The results for the tested triphosphates were similar to those observed for the corresponding dOTC derivatives, showing exceptional incorporation of unmodified 3TCTP **77** close to complete conversion. Lane 2 deviated slightly from the dOTC results and showed less pronounced incorporation of γ -C₁₂-3TCTP **76** compared to its dOTC counterpart. While HIV-RT has less selective mechanisms compared to human polymerases, the combination of L-nucleosides with long alkyl chains may lead to an amplification of both selectivity-driving effects.

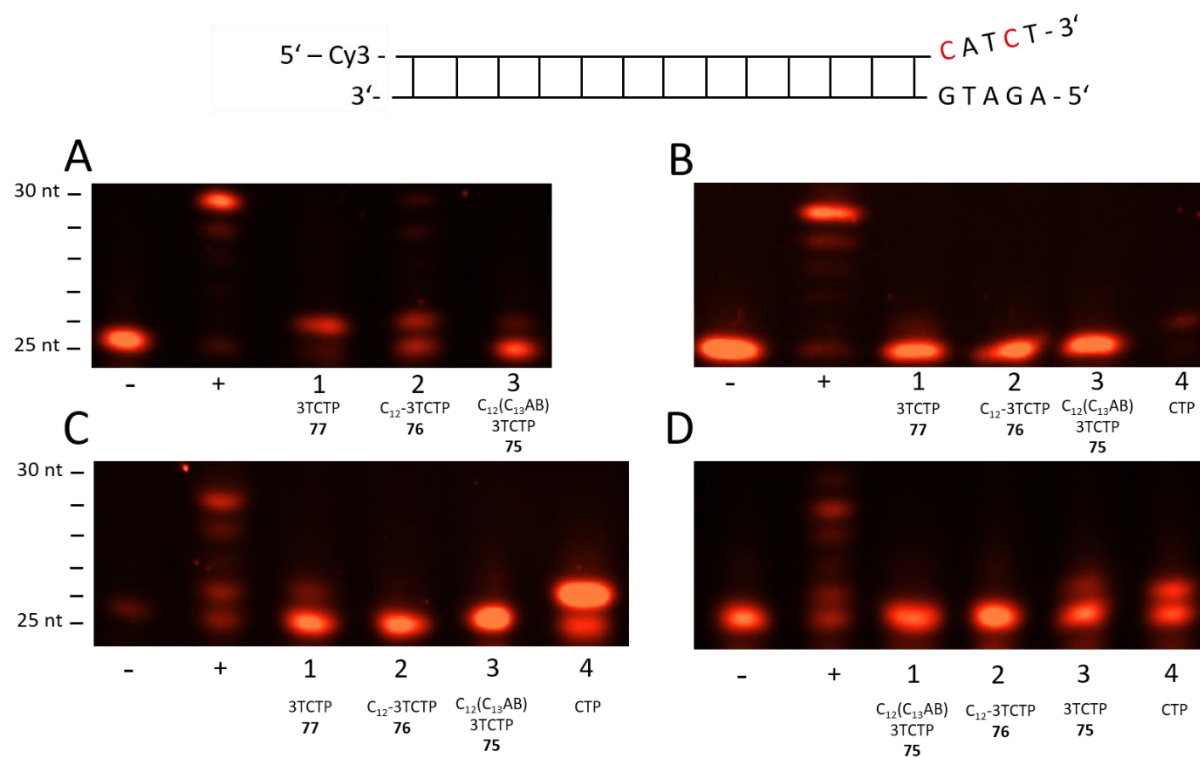


Figure 30: Primer extension assay using 3TC triphosphates **75**, **76**, **77** and CTP; **A)** HIV-RT; negative control; positive control; lane 1: 3TCTP **77**; lane 2: γ -C₁₂-3TCTP **76**, lane 3: γ -C₁₂(C₁₃AB)-3TCTP **75**. **B)** Pol β ; negative control; positive control; lane 1: 3TCTP **77**; lane 2: γ -C₁₂-3TCTP **76**, lane 3: γ -C₁₂(C₁₃AB)-3TCTP **75**, lane 4: CTP. **C)** Pol α ; negative control; positive control; lane 1: 3TCTP **77**; lane 2: γ -C₁₂-3TCTP **76**, lane 3: γ -C₁₂(C₁₃AB)-3TCTP **75**, lane 4: CTP. **D)** Pol γ ; negative control; positive control; lane 1: γ -C₁₂(C₁₃AB)-3TCTP **75**; lane 2: γ -C₁₂-3TCTP **76**, lane 3: 3TCTP **77**, lane 4: CTP. Assay conditions are summarized in the Experimental Procedure 6.1.3.

Results and Discussion

The selectivity effect was particularly evident in the pol β assay (**Figure 30, B**). While dOTCTP **71** (**Figure 27, B**) is incorporated by pol β in a similar way to CTP, 3TCTP **77** has almost no affinity for the polymerase (**Figure 30, B**). This is perfectly in line with the results of cell tests for 3TC, which has high antiviral activity but no toxic side effects.^{95,109}

The pol α assay showed a very similar result to the pol β assay. (**Figure 30, C**), with the positive and negative controls exhibiting reduced intensity. Lanes 1 to 3 again are identical to the corresponding lanes in the pol β assay. Masked triphosphates **75** and **76** show no signs of incorporation in the presence of pol α , while 3TCTP **77** was integrated to a certain degree. This assay showed a good comparison between CTP and 3TCTP **77**, with the stronger intensity indicating a significant difference in affinity for the polymerase.

The pattern of nucleotide incorporation was consistently repeated in the pol γ (**Figure 30, D**), as only the 3TCTP **77** and CTP were incorporated to form a n+1 band. The experiment demonstrated successful positive and negative control as well as no incorporation for the γ -C₁₂(C₁₃AB)-3TCTP **75** (**Figure 30, D**, lane 1) and γ -C₁₂-3TCTP **76**, while 3TCTP **77** and CTP are mediocre to good substrates for pol γ , respectively. The incorporation of 3TCTP reaffirmed findings of previous research, that showed no 3TC metabolites concentrate in the mitochondria.⁹⁵ However, as shown by these results, the combination of L-nucleosides with the prodrug system can significantly alter the substrate properties of 3TC.

In collaboration with SCHOLS *et al.*, 3TC **25**, γ -C₁₂(C₁₃AB)-3TCTP **75** and γ -C₁₂-3TCTP **76** were tested against HIV-1 and HIV-2 in CEM cell lines (**Table 5**). The data revealed antiviral activity in the nanomolar range for both nucleoside **25** and γ -C₁₂-3TCTP **76** against HIV-1 with 45 nM and 54 nM, respectively. These results are consistent with previous results in PBMCs, with 3TC having an EC₅₀ of 85 nM and exhibiting cytotoxicity at 41.9 μ M.²⁵² In this case, no cytotoxic effects were observed for either compound within the tested concentration range. However, for γ -C₁₂(C₁₃AB)-3TCTP **75** a strong decrease in activity was observed in both HIV-1 (0.80 μ M) and HIV-2 (0.97 μ M) infected cells. This corresponds to an almost 18-fold and almost 9-fold decrease in activity for the prodrug compared to parent nucleoside **25**, whereas only a 1.2-fold and 1.7-fold decrease was observed for the γ -C₁₂-3TCTP **76**, respectively. These results score below expectations for both γ -C₁₂(C₁₃AB)-3TC **75** γ -C₁₂-3TCTP **76**. The loss in activity of γ -C₁₂(C₁₃AB)-3TC **75** compared to the intermediate **76** suggest, that the prodrug is prone to further decomposition within the cell to the DP or MP, which would correlate with prior research.^{195,244} However, it should be noted that both active transport pathways and passive diffusion are available for the cellular uptake of 3TC.^{253,254} These pathways further increase the concentration of the parent nucleoside compared to the prodrug, and could therefore explain the reduced activity of γ -C₁₂(C₁₃AB)-3TCTP **75** and γ -C₁₂-3TCTP **76**.

Results and Discussion

Table 5: Antiviral data against HIV for γ -C₁₂(C₁₃AB)-3TCTP **75**, γ -C₁₂-3TCTP **75** and 3TC **25**.

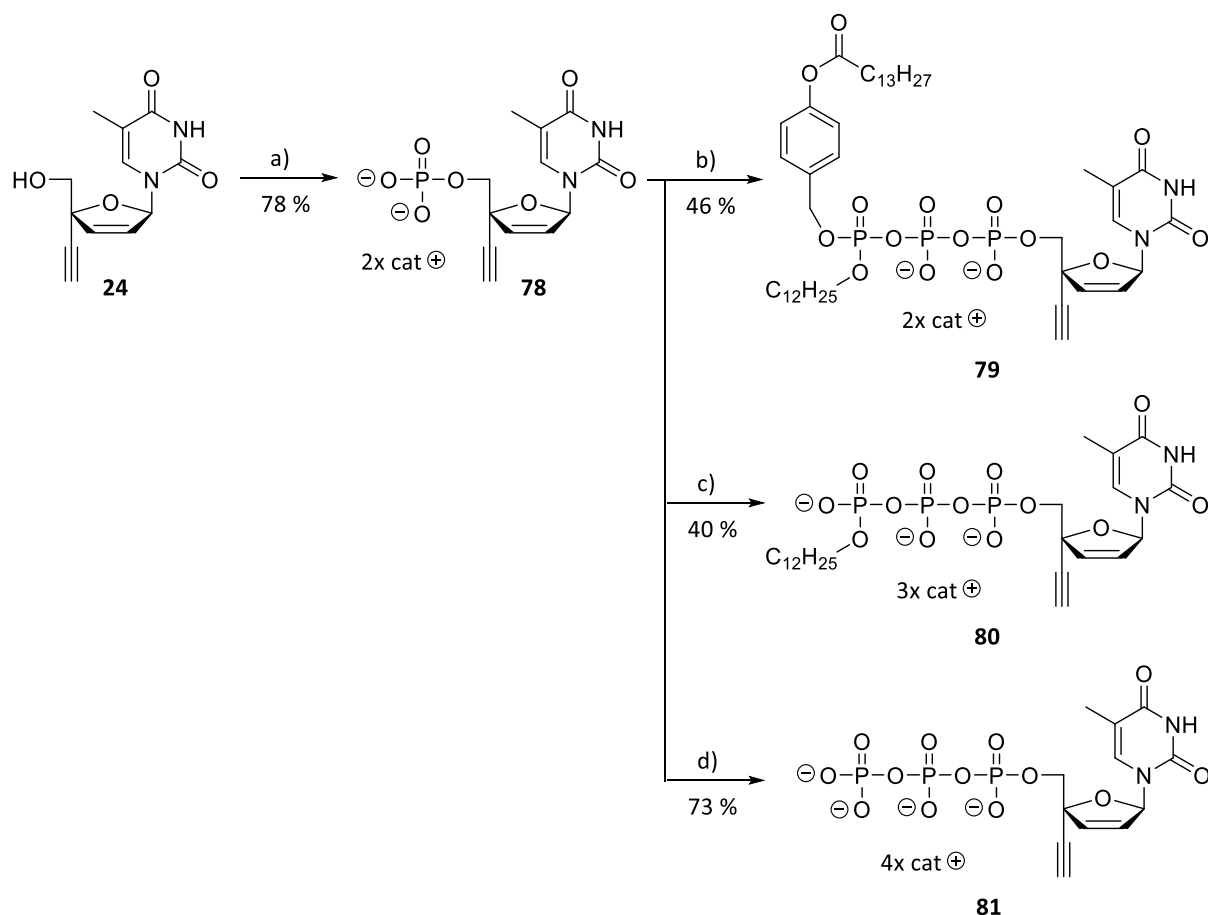
Compound	Unit	CEM		
		HIV-1 HE	HIV-2 ROD	cellular tox.
		EC ₅₀ ^a	EC ₅₀ ^a	CC ₅₀ ^b
25	μ M	0.045 \pm 0.011	0.11 \pm 0.04	>100
75	μ M	0.80 \pm 0.35	0.97 \pm 0.67	>100
76	μ M	0.054 \pm 0.042	0.19 \pm 0.19	>100

^a50% Effective concentration required to inhibit HIV induced cytopathogenic effect in cell culture

^b50% Cytotoxic concentration of the compound evaluated in this cell line

4.5.4. 4'-Ed4T Triphosphate Prodrug, γ -Alkyl Triphosphate and Triphosphate

4'-Ed4T **24**, known for its chemical properties comparable to the well-studied d4T **8**, was used in SOWA and OUCHI as well as YOSHIKAWA monophosphate synthesis.^{177,178} Following the SOWA and OUCHI protocol (**Scheme 28**), 4'-Ed4T **24** was dissolved in acetonitrile and converted into its corresponding monophosphate using POCl₃, pyridine and water. The 4'-Ed4TMP **78** was obtained in 63 % yield after RP₁₈ column chromatography, ion exchange using 2.0 eq. of TBA hydroxide and an additional RP₁₈ column chromatography. In another attempt using the YOSHIKAWA protocol, 4'-Ed4T **24** was converted into its monophosphate using POCl₃, and 1,8-bis(dimethylamino)naphthalene (proton sponge) in trimethyl phosphate. 4'-Ed4TMP **78** was obtained in 78 % yield after RP₁₈ column chromatography, ion exchange to Et₃N⁺ and additional RP₁₈ column chromatography. Therefore, the YOSHIKAWA protocol was considered to be the superior method for the synthesis of 4'-Ed4T monophosphate.



Scheme 28: Reaction scheme of γ -C₁₂(C₁₃AB)-4'-Ed4TTP **79**, γ -C₁₂-4'-Ed4TTP **80** and triphosphate **81**. a) POCl₃, proton sponge, trimethyl phosphate 0 °C, 3 h; b) i) pyrophosphate **19c**, TFAA, Et₃N, CH₃CN, 0 °C, 10 min; ii) 1-methylimidazole, DMF, rt, 10 min; iii) NMP **78**, CH₃CN, rt, 2 h; c) i) pyrophosphate **39a**, TFAA, Et₃N, CH₃CN, 0 °C, 10 min; ii) 1-methylimidazole, DMF, rt, 10 min; iii) NMP **78**, DMF, rt, 2 h; iv) TBA hydroxide, CH₃CN, rt, 16 h d) i) NMP **78**, TFAA, Et₃N, CH₃CN, 0 °C, 10 min; ii) 1-methylimidazole, DMF, rt, 10 min; iii) pyrophosphate, CH₃CN, rt, 2 h.

The synthesis of 4'-Ed4T triphosphate derivatives followed the previous approaches, although due to the higher solubility of 4'-Ed4T derivatives both DMF and acetonitrile were viable solvents for the reaction. γ -C₁₂(C₁₃AB)-4'-Ed4TTP **79** was obtained using pyrophosphate **19c**, TFAA, triethylamine and 1-methylimidazole. The equivalents were adjusted to the monophosphate and adopted from established protocols. After RP₁₈ column chromatography, ion exchange to NH₄⁺ and additional RP₁₈ chromatography, γ -C₁₂(C₁₃AB)-4'-Ed4TTP **79** was obtained in a good yield of 46 %. Using pyrophosphate **39a** and an additional deprotection step with 10.0 eq. TBA hydroxide gave γ -C₁₂-4'-Ed4TTP **80** in 40 % yield after purification. 4'-Ed4TTP **81** was obtained using the MOHAMADY protocol. Both the equivalents and the preparation remained unchanged, leading to 4'-Ed4TTP **81** in 73 % yield. It was assumed that the higher yield was due to the better solubility of 4'-Ed4TMP **78** in acetonitrile compared to previously used monophosphates.

Results and Discussion

In an effort to confirm the superior reported properties of 4'-Ed4T **24**, polymerase assays were conducted to gain better insight into its substrate properties. Particularly interesting was the discrimination for human polymerases, especially pol γ . The assay setup and conditions were adopted from the previous experiments. In the HIV-RT assay, a negative, a positive control, γ -C₁₂(C₁₃AB)-4'-Ed4TTP **79**, γ -C₁₂-4'-Ed4TTP **80** and 4'-Ed4TTP **81** were tested (**Figure 31, A**). The results are consistent with the results from previous experiments with other nucleotides. Lane 1 showed weak to moderate incorporation of γ -C₁₂(C₁₃AB)-4'-Ed4TTP **79**, which as reported in chapter 4.5.2 can most likely be attributed to the cleavage of the masking unit in assay buffer. The degree of incorporation decreased with the degree of substitution at the γ -phosphate, showing around 50 % conversion for the γ -C₁₂-4'-Ed4TTP **80** and almost full conversion for the unmodified triphosphate **81**.

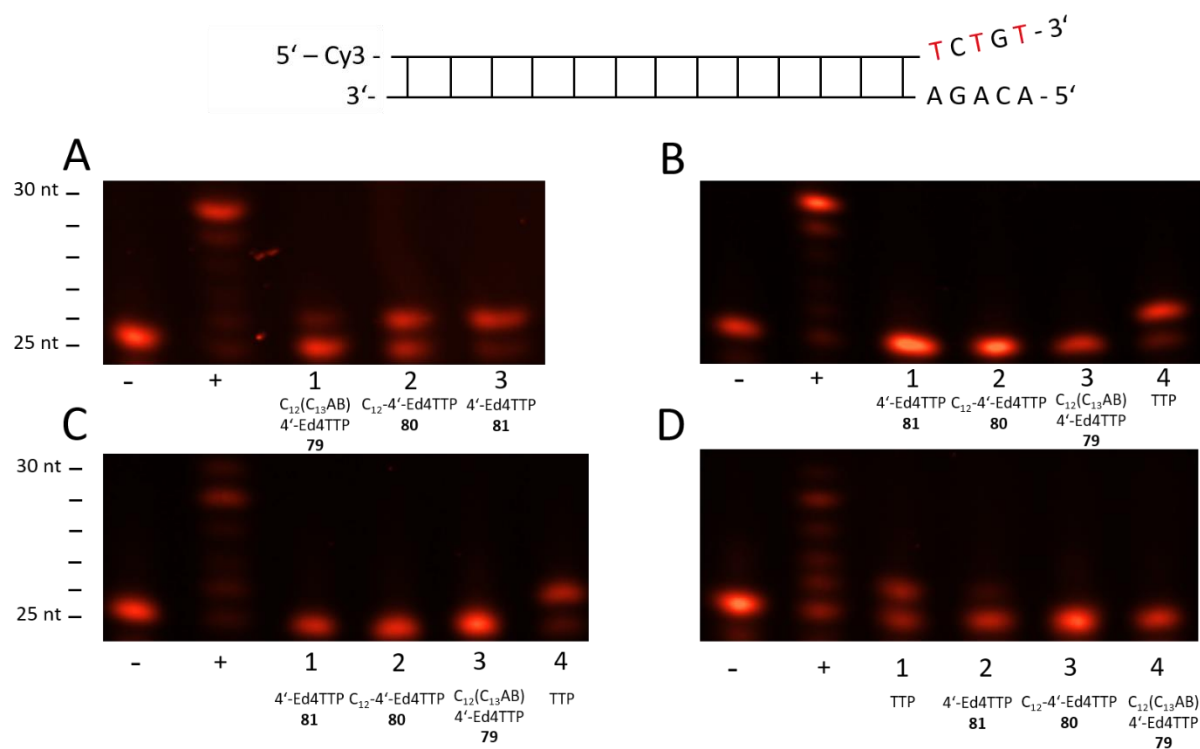


Figure 31: Primer extension assay using 4'-Ed4T triphosphates **79**, **80**, **81** and TTP. **A**) HIV-RT; negative control; positive control; lane 1: γ -C₁₂(C₁₃AB)-4'-Ed4TTP **79**; lane 2: γ -C₁₂-4'-Ed4TTP **80**, lane 3: 4'-Ed4TTP **81**. **B**) Pol β ; negative control; positive control; lane 1: 4'-Ed4TTP **81**; lane 2: γ -C₁₂-4'-Ed4TTP **80**, lane 3: γ -C₁₂(C₁₃AB)-4'-Ed4TTP produg **79**, lane 4: TTP. **C**) Pol α ; negative control; positive control; lane 1: 4'-Ed4TTP **81**; lane 2: γ -C₁₂-4'-Ed4TTP **80**, lane 3: γ -C₁₂(C₁₃AB)-4'-Ed4TTP **79**, lane 4: TTP. **D**) Pol γ ; negative control; positive control; lane 1: TTP, lane 2: 4'-Ed4TTP **81**; lane 3: γ -C₁₂-4'-Ed4TTP **80**, lane 4: γ -C₁₂(C₁₃AB)-4'-Ed4TTP **79**. Assay conditions are summarized in the Experimental Procedure 6.1.3.

For the primer extension assay with pol β , the experimental arrangement of the tested compounds included a lane for TTP (**Figure 31, B**, lane 4). In contrast to other nucleotides tested, 4'-Ed4TTP **81** was the only unsubstituted triphosphate with no substrate properties for pol β . As depicted, apart from both positive controls (+ and lane 4), no n+1 band was observed. This result suggests that the selectivity for 4'-substituted nucleosides may be equal to or greater than that of L-nucleosides. This could offer more flexibility in the choice of alkyl chains, potentially enhancing the substrate properties for HIV-RT even further.

As described in chapter 2.4.1. pol α exhibits the lowest affinity for non-natural nucleosides¹⁸², resulting in no incorporation observed for 4'-Ed4T derivatives (**Figure 31**), excluding pol α as a target for NRTI prodrugs. Although pol α lacks proofreading function, it is advisable to exclude the possibility of any incorporation.¹⁸³

SOHL *et al.* reported significant discrimination by wild type pol γ between 4'-Ed4TTP and TTP (up to 12000-fold), compared to an 8.3-fold difference in discrimination observed for FLTTP, suggesting weak to no substrate properties for the tested compounds.¹⁹⁶ The assay setup for pol γ is shown in **Figure 31 D**. The positive control with TTP was moved to lane 1 followed by 4'-Ed4TTP **81**, γ -C₁₂-4'-Ed4TTP **80** and γ -C₁₂(C₁₃AB)-4'-Ed4TTP **79**. Negative and positive control exhibited expected results, with the n+4 band most visible in the positive control, reflecting the lower activity of pol γ compared to polymerases like pol β or HIV-RT. The low activity was also reflected in the second n+1 positive control in lane 1, wherein TTP is an ideal substrate for pol γ while only showing around 50 % incorporation. Considering this, the slightly visible n+1 band in lane 2 corresponds with a significant incorporation of 4'-Ed4T **81** during DNA synthesis. No incorporation was observed for either the γ -C₁₂-4'-Ed4TTP **80** (**Figure 31, D**, lane 3) or γ -C₁₂(C₁₃AB)-4'-Ed4TTP **79** (**Figure 31, D**, lane 4). These findings suggest that a 4'-alkyl modification may be essential for final prodrug design.

Due to its high antiviral activity and low toxicity (EC₅₀: 0.25±0.14 μ M in MT-4 cells; CC₅₀: >100 μ M in CEM cells)²²³, enhanced discrimination against pol γ (12000-fold compared to TTP)¹⁹⁶ and the superior enzyme interactions (thymidine kinase and thymidine phosphorylase) compared to d4T²²⁴, 4'-Ed4T **24** was considered a potential therapeutic against HIV. However, the development was discontinued in 2015 due to the lack of advantages over the already approved TAF.⁹⁶ The antiviral data (**Table 6**) provided by SCHOLS *et al.* indicated improvement of the pharmacological profile of 4'-Ed4TTP derivatives. Antiviral activity against HIV-1 and HIV-2 improved by 1.3 and 1.4-fold, respectively, for γ -C₁₂(C₁₃AB)-4'-Ed4TTP **79** with 27 nM and 6.7 nM compared to 36 nM and 9.7 nM for the parent nucleoside **24**. The advantages of the prodrug were especially noticeable in thymidine kinase-deficient cell lines. While the parent nucleoside lost its antiviral activity in TK deficient cell lines, the prodrug **79**

retained most of its activity (21 nM), with only a small increase in cytotoxicity. The results for γ -C₁₂-4'-Ed4TTP **80** were further increased in CEM cells for both HIV-1 and HIV-2 with 11 nM and 1.4 nM respectively this could point to a higher availability of substrate due to less degradation of γ -alkyl TPs compared to their prodrugs.¹⁹⁵ The unexpected low antiviral activity (2.55 μ M) of γ -C₁₂-4'-Ed4TTP **80** in TK-deficient CEM cells does not fit the previous assumption. This data would suggest, that the masking unit appeared to prevent intracellular dephosphorylation and therefore retention of antiviral activity, which would contrast hydrolysis studies performed with similar compounds in several media.^{195,244} Other reasons could be extracellular decomposition during incubation or reduced diffusion into CEM-TK⁻ cells, which both cannot be deferred from the available data. Therefore, further investigation and repetition of the antiviral assays is necessary. Nonetheless, 4'-Ed4T prodrugs exhibit great potential as antiviral drugs, as they are good and selective substrates for HIV-RT and improve on the efficacy of the parent nucleoside.

Table 6: Antiviral data against HIV for 4'-Ed4T triphosphate prodrug **79**, γ -dodecyl triphosphate **80** and 4'-Ed4T **24**.

Compound	Unit	CEM			CEM TK ⁻	
		HIV-1 HE	HIV-2 ROD	cellular tox.	HIV-2 ROD	cellular tox.
		EC ₅₀ ^a	EC ₅₀ ^a	CC ₅₀ ^b	EC ₅₀ ^a	CC ₅₀ ^b
24	μ M	0.036 \pm 0.0090	0.0097 \pm 0.0023	>100	>10 \pm 0	>100
79	μ M	0.027 \pm 0.019	0.0067 \pm 0.0026	>100	0.021 \pm 0.010	45.5
80	μ M	0.011 \pm 0.014	0.0014 \pm 0.0016	>100	2.55 \pm 2.60	>100

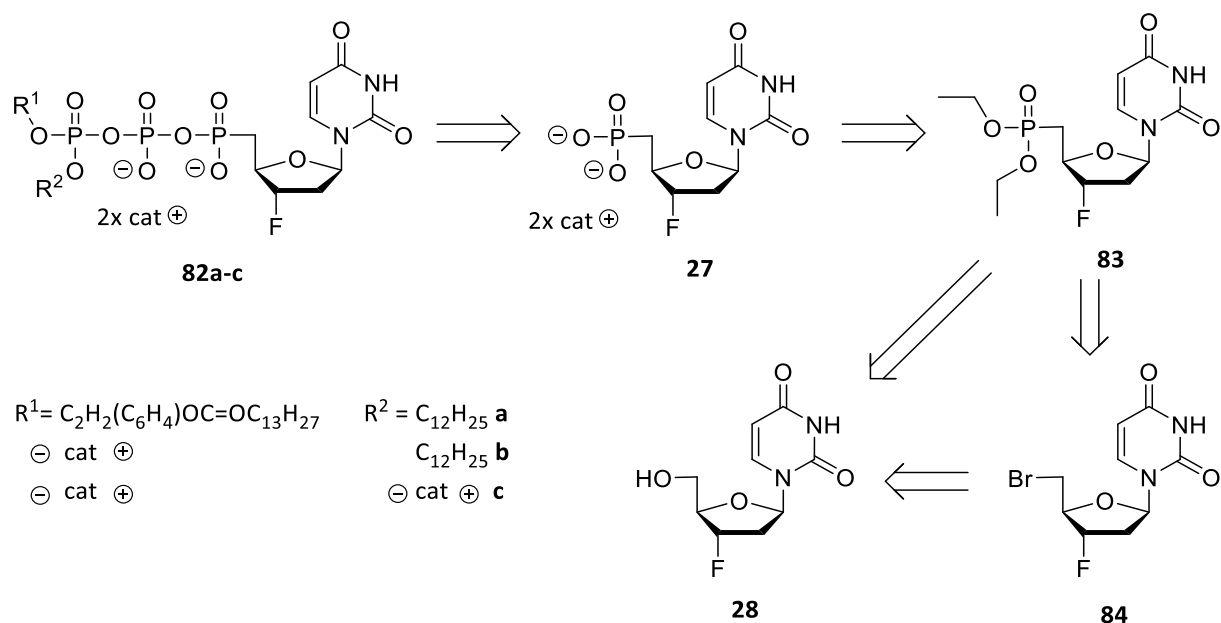
^a50% Effective concentration required to inhibit HIV induced cytopathogenic effect in cell culture

^b50% Cytotoxic concentration of the compound evaluated in this cell line

4.6. Synthesis of the 2',3'-Dideoxy-3'-Fluorouridine Phosphonate Analogue

The investigation of cyclic nucleoside phosphonates as substrates for HIV-RT was inspired by the success of their acyclic counterparts TAF and TDF.²⁵⁵ A similar approach was pursued by RAJWANSHI *et al.*²⁰⁰ to address high resistance issues associated with nucleosides like AZT. During this work a route to phosphonate prodrugs should be established, therefore 2',3'-dideoxy-3'-fluorouridine (FLU) was chosen as its chemical properties were comparable to FLT. Moreover, FLU is less expensive than FLT. It was assumed that once a synthesis to FLU phosphonate prodrugs was established, this could be also applied on FLT and other dideoxy nucleosides.

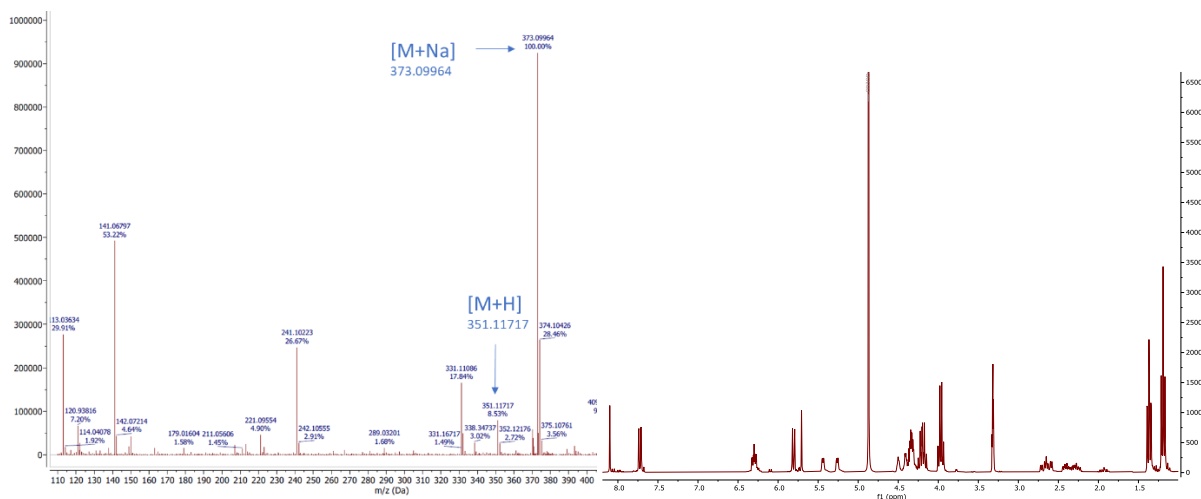
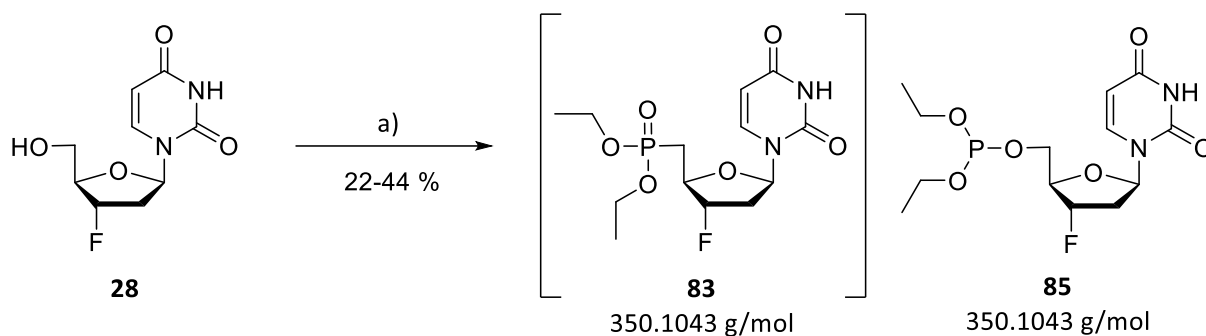
Two different routes were considered for the synthesis of the ethyl diester phosphonate **82** (**Scheme 29**). The first method was developed by HAKIMELAH *et al.* for the synthesis of AZT-5'-phosphonate.²⁰¹ In this case, the phosphonate **27** would be obtained by using the MICHAELIS-ARBUZOV reaction to transform alcohol to the corresponding phosphonate *via* halogenation. Recently, MA *et al.* discovered another approach involving the direct conversion of alcohols to phosphonates using a specific MICHAELIS-ARBUZOV reaction with a phosphite solvent and catalytic amounts of iodine at high temperatures.



Scheme 29: Retrosynthetic approach for the synthesis of FLU phosphonates **82a-c**.^{200,201,256}

Despite the demonstrated success of this reaction for the synthesis of various phosphonates starting from alcohols,^{256,257} its application using FLU proved unfeasible. NMR and mass analysis (**Scheme 30**) indicated the formation of the ethyl diester phosphonate **83**, but there was no conversion to phosphonate **27** observed, which led to the assumption that the structural isomer **85** was formed. These findings were further corroborated by the formation of FLU **28** in the following reaction with TMSBr.

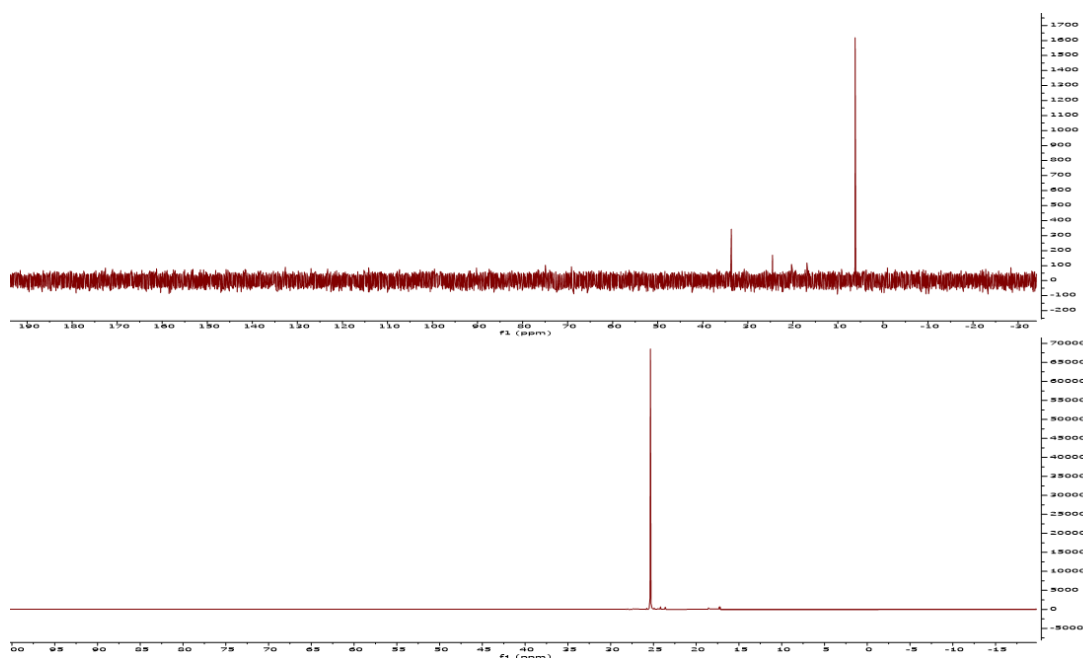
Results and Discussion



Scheme 30: Attempted synthesis and analytical data of FLU **83**. a) triethyl phosphite, TBAI, 125 °C, 24 h. Left: ESI-MS spectrum. Right: ¹H-NMR spectrum.

After switching to the traditional MICHAELIS-ARBUZOV reaction condition, as described in the following section, the phosphonate **83** was successfully obtained. This was confirmed through the ³¹P-NMR spectra, showing a singlet at 25.35 ppm (**Scheme 31**), which is the typical range for diethyl phosphonate shifts, the lack of which further indicated the formation of **85**.

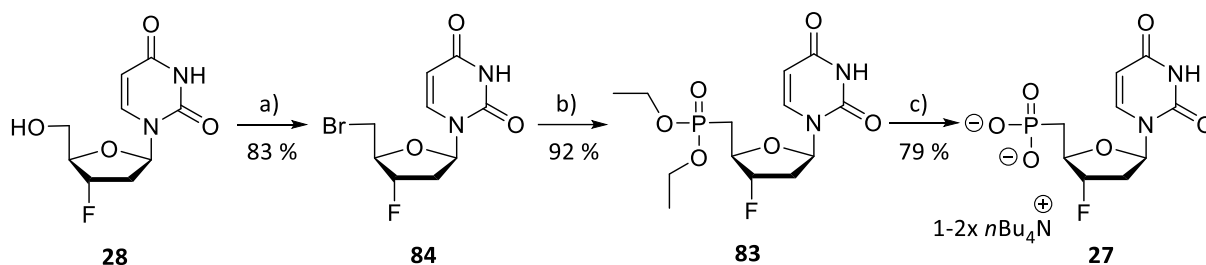
Results and Discussion



Scheme 31: ^{31}P -NMR spectrum of phosphite **85** (top; 6.16 ppm) and phosphonate **83** (bottom; 25.35 ppm).

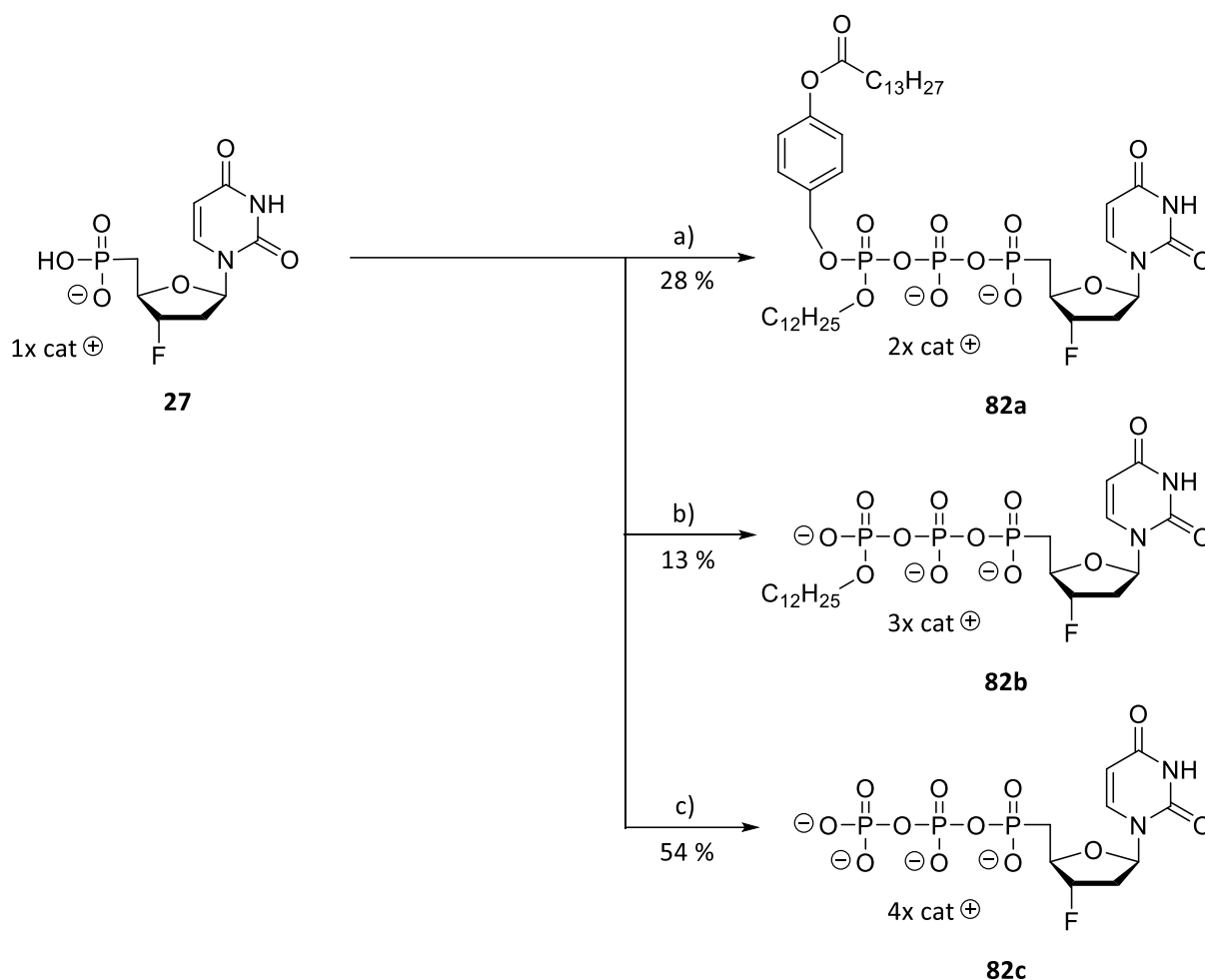
In this case, FLU phosphonate **27** was synthesized in accordance to the protocol published by HAKIMELAHI *et al.* This involves the traditional MICHAELIS-ARBUZOV reaction. Starting from FLU **28** (**Scheme 32**), the brominated derivative was obtained using 1.2 eq. CBr_4 and 1.5 eq. triphenyl phosphine in dichloromethane. The brominated FLU **84** was obtained in 83 % yield after purification. The non-quantitative yields were mostly due to triphenyl phosphine oxide formed in the reaction, which was difficult to separate. This issue was known in many organic syntheses and was addressed by using a protocol developed by BATESKY *et al.* in 2017.²⁵⁸ Phosphorylation with triethyl phosphine was performed at 120 °C overnight. Since almost no conversion was detected with 3.0 eq. triethyl phosphine additional 3.0 eq. were added. After heating the mixture for 16 h and subsequent purification on silica gel *via* column chromatography the phosphonate **83** was obtained in 92 % yield. The deprotection was carried out by using 3.5 eq. trimethylsilyl bromide in acetonitrile. The solvent was removed and the reaction was quenched with water and washed with dichloromethane to yield the corresponding phosphonate **27** in 79 %. The solubility and the reactivity of phosphonate **27** was increased by adding 2.0 eq. of TBA hydroxide, so that the final phosphonate contains $n\text{Bu}_4\text{N}^+$ ions. After purification on RP_{18} silica gel only 0.5 to 1.0 eq. of $n\text{Bu}_4\text{N}^+$ ions were detected. As the counterions play an important role in the GOLLNEST protocol,⁴⁸ an additional 1.0 eq. of TBA hydroxide was added before removing the solvent.

Results and Discussion



Scheme 32: Reaction scheme of FLU phosphonate **27**. a) CBr_4 , triphenyl phosphine, dichloromethane $0\text{ }^\circ\text{C}$, 3 h; b) triethyl phosphine, $120\text{ }^\circ\text{C}$, 32 h; c) trimethylsilyl bromide, acetonitrile, rt, 16 h.

The coupling reactions with the appropriate pyrophosphates to the respective (pro)nucleotides were carried out as described before for nucleoside monophosphates (**Scheme 33**). $\gamma\text{-C}_{12}(\text{C}_{13}\text{AB})\text{-FLUDP } \mathbf{82a}$ and $\gamma\text{-C}_{12}\text{-FLUDP } \mathbf{82b}$ syntheses started with the activation of the corresponding pyrophosphates **39a** and **19c** with TFAA and triethylamine, followed by the second activation step with 1-methylimidazole and triethylamine. After addition of the phosphonate **27**, the reaction was monitored *via* HPLC. Compared to previous syntheses conversion rates stayed below 50 % even after prolonged reaction times. This led to a moderate yield of 28 % for $\gamma\text{-C}_{12}(\text{C}_{13}\text{AB})\text{-FLUDP } \mathbf{82a}$ and a low yield of 13 % for the $\gamma\text{-C}_{12}\text{-FLUDP } \mathbf{82b}$. Following the standard protocol for the synthesis of FLUDP **82c** was obtained in a yield of 54 %. Although initial yields were not ideal, the successful synthesis of three phosphonate diphosphates proved, that the synthesis of phosphonate-based pronucleotides is feasible. To further evaluate the viability of cyclic nucleoside phosphonates as potential antiviral therapeutics, it would be necessary to use active nucleosides like FLT or 4'-Ed4T to gather more information in future experiments.



Scheme 33: Reaction scheme of FLU triphosphate prodrug **82a**, γ -dodecyl triphosphate **82b** and triphosphate **82c**. a) i) pyrophosphate **19c**, TFAA, triethylamine, CH₃CN, 0 °C, 10 min; ii) 1-methylimidazole, DMF, rt, 10 min; iii) phosphonate **27**, CH₃CN, rt, 2 h; b) i) pyrophosphate **39a**, TFAA, Et₃N, CH₃CN, 0 °C, 10 min; ii) 1-methylimidazole, DMF, rt, 10 min; iii) phosphonate **27**, DMF, rt, 2 h; iv) TBA hydroxide, CH₃CN, rt, 16 h c) i) phosphonate **27**, TFAA, Et₃N, CH₃CN, 0 °C, 10 min; ii) 1-methylimidazole, DMF, rt, 10 min; iii) pyrophosphate, CH₃CN, rt, 2 h.

Due to limited quantities of the final products, biological testing could only be performed once. The available data yielded ambiguous results, necessitating repetition to draw conclusive findings. Therefore, both antiviral and polymerase assay data are provided in the following for completion, but were not considered in the evaluation of the phosphonate compounds.

The FLUTPs **82a-c** were subjected to three of the four primer extension assays, described in prior chapters (**Figure 32**), with the exception of pol γ , due to insufficient material. Results for both pol α and pol β (**Figure 32, B and C**) were consistent with prior observations, demonstrating that none of the compounds exhibited substrate properties. However, the HIV-RT assay provided inconclusive data, with an incorporation (n+1) for both FLUTP **82c** as well as FLU prodrug **82a**. These findings are inconsistent with previous observations and explanations, particularly regarding the lack of substrate properties in the γ -alkyl derivative **82b**. Consequently, the validity of the results obtained for human polymerases cannot be conclusively affirmed.

Results and Discussion

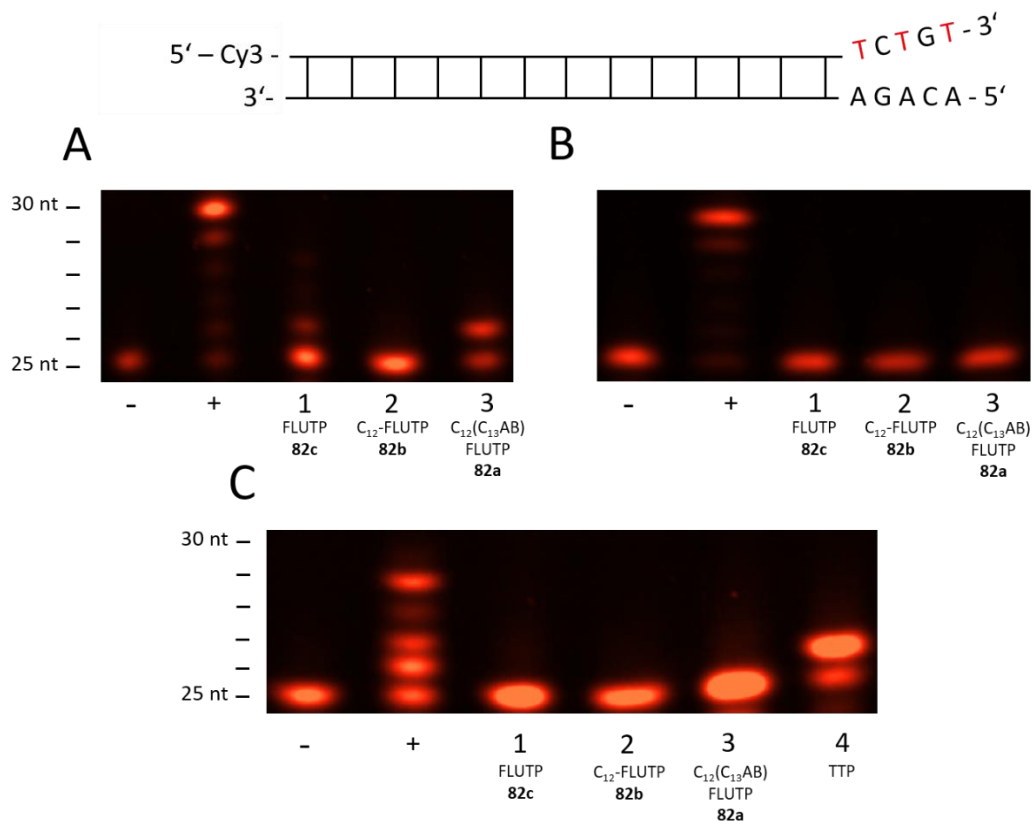


Figure 32: Primer extension assay using FLU triphosphates **82a-c** and TTP. **A)** HIV-RT; negative control; positive control; lane 1: FLUTP **82c**; lane 2: γ -C₁₂-FLUTP **82b**, lane 3: γ -C₁₂(C₁₃AB)-FLUTP **82a**. **B)** Pol β ; negative control; positive control; lane 1: FLUTP **82c**; lane 2: γ -C₁₂-FLUTP **82b**, lane 3: γ -C₁₂(C₁₃AB)-FLUTP **82a**. **C)** Pol α ; negative control; positive control; lane 1: FLUTP **82c**; lane 2: γ -C₁₂-FLUTP **82b**, lane 3: γ -C₁₂(C₁₃AB)-FLUTP **82a**, lane 4: TTP. Assay conditions are summarized in the Experimental Procedure 6.1.3.

Antiviral data was obtained for the FLU prodrug **82a** and γ -alkyl FLU **82b** (Table 7), no comparison with a parent nucleoside was possible, as FLU phosphonate **27** was suspected to be unable to cross the cell membrane. Both prodrug **82a** and γ -alkyl FLU **82b** produced low antiviral activity, with 4.67 and 6.42 μ M for HIV-1 and 6.81 and 2.75 μ M for HIV-2, respectively. These mediocre results compared to other NRTIs could be expected, since FLU acts as an uridine mimetic, and should therefore not be utilised in DNA synthesis. Nevertheless, these positive results further corroborate the potential of nucleoside phosphonates as therapeutic prodrugs for HIV.

Table 7: Antiviral data against HIV for FLU triphosphate prodrug **82a**, γ -dodecyl triphosphate **82b**.

Compound	Unit	CEM		
		HIV-1 HE	HIV-2 ROD	cellular tox.
		EC ₅₀ ^a	EC ₅₀ ^a	CC ₅₀ ^b
82a	μ M	4.67 \pm 0	6.81 \pm 0.31	>100
82b	μ M	6.42 \pm 0	2.75 \pm 0.49	>100

^a50% Effective concentration required to inhibit HIV induced cytopathogenic effect in cell culture

^b50% Cytotoxic concentration of the compound evaluated in this cell line

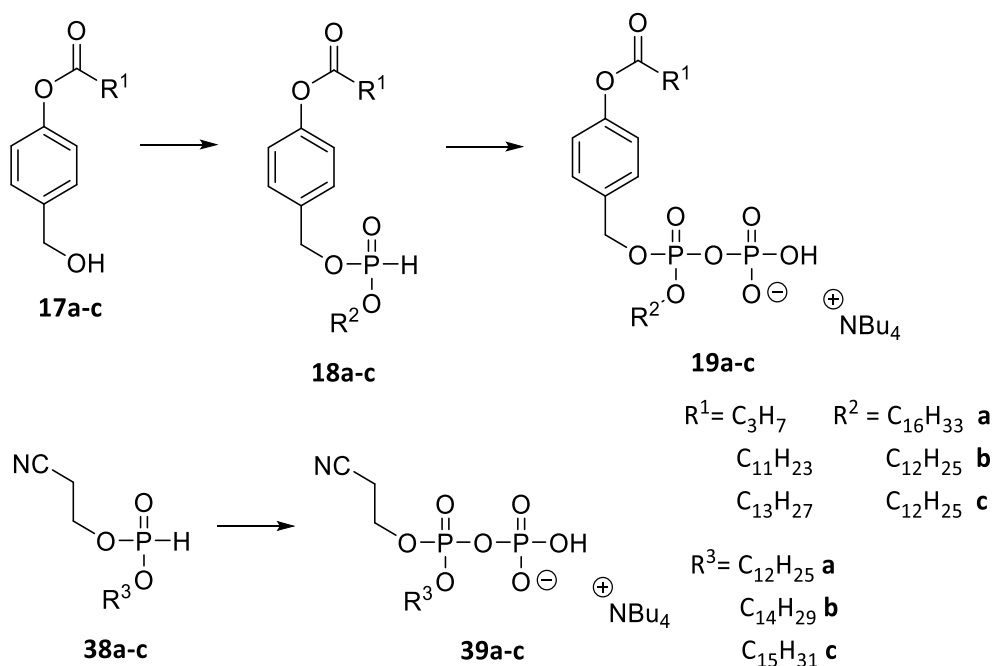
5. Summary and Conclusions

Aim of this work was the evaluation of different antivirally active triphosphate prodrugs, and development of a comprehensive workflow to iteratively design prodrugs tailored to increase discrimination between HIV-RT and human polymerases.

In the first part a collection of antiviral prodrugs with known antiviral properties^{50–52,195} were combined into a small substance library, to be tested in several primer extension assays, to determine their substrate properties. As both HIV-RT and pol β assays were established, this thesis aimed to replicate a similar workflow to incorporate pol α and γ , without the necessity of radiolabelled primers. Expanding on the work of ZHAO *et al.* attempts were made to correlate chain length with substrate properties to increase activity while simultaneously increase discrimination against human polymerases. Through this process a preferential design of the prodrug metabolite was identified, indicating that dodecyl triphosphates demonstrated good incorporation through the viral polymerase, while being rejected by human polymerases. These findings served as a base for the final design of prodrugs against HIV (Chapter 4.1).

In comparison to data received from studies by WITT and ROßMEIER *et al.* concerning the cellular uptake of TriPPP_{ro}- and γ -alkyl triphosphate prodrugs, dodecyl bearing compounds were synthesised and to match prior results. The closest match was produced by γ -(C₁₂C₁₃AB)-FLT **35c** and consequently adopted for other nucleosides (Chapter 4.2). γ -Alky(AB) pyrophosphates, as well as the corresponding cyanoethyl pyrophosphates, were produced following the protocol for the synthesis of pyrophosphates, established by GOLLNEST (Chapter 4.3).²⁰⁵ Alkyl(AB) pyrophosphates **19a-c** (a: 93 %; b: 79 %; c: 87 %) were obtained from their corresponding *H*-phosphonates **18a-c** (a: 44 %; b: 43 %; c: 38 %) after synthesising the corresponding AB alcohols **17a-c** (a: 54 %; b: 37 %; c: 45 %). The cyanoethyl pyrophosphates **39a-c** (a: 88 %; b: 80 %; c: 89 %) were obtained from their *H*-phosphonates **38a-c** (a: 79 %; b: 47 %; c: 45 %) (Scheme 34).

Summary and Conclusions



Scheme 34: Synthesis of pyrophosphates.

The second part of this work, integrated several nucleosides, chosen for their antiviral potential, into the established prodrug system (Chapter 4.4). Depending on the availability, nucleosides were either synthesised or purchased. The nucleosides chosen, were FLT **23**, 4'-Ed4T **24**, 3TC **25** and dOTC **26** (**Figure 33**). As part of a cooperation project with WEISING *et al.*, FLT **23** was successfully synthesised following a four-step synthesis by SRIVASTAV *et al.*²¹⁸ Starting from 4,4'-dimethoxytriphenylmethyl protected thymidine **40**, FLT **23** was obtained in 34 % yield over four steps. 4'-Ed4T **24** was chosen for the intrinsic selectivity for viral polymerases, as well as the synthetic accessibility, compared to other 4'-substituted nucleoside.^{229,230} In the scope of this work, 4'-Ed4T was realized through a novel seven-step DYKAT based synthesis developed by ORTIZ *et al.*²²⁵ Starting from furfuryl alcohol **48**, 4'-Ed4T **24** was obtained in 11 % (87%ee) yield over seven steps. Accordingly, 3TC **25** was chosen due to its intrinsic selectivity. As a commonly prescribed drug, 3TC was cheap and readily available. dOTC **26** was developed to combat emerging resistances of viral strains against 3TC and other L-nucleosides. It was obtained in 32 % yield over four steps.

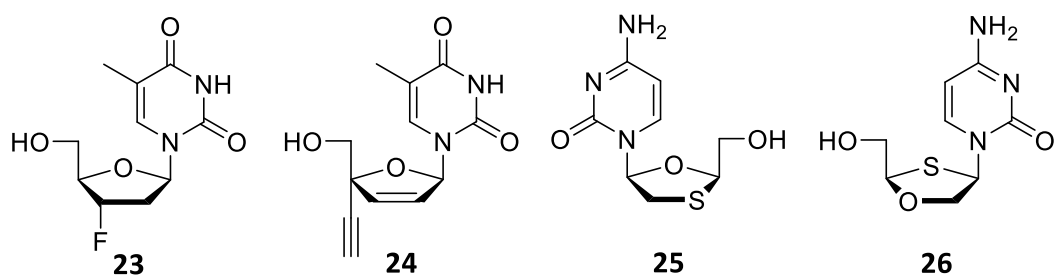


Figure 33: NRTIs for the application in γ -modified alkyl(AB) prodrugs.

Summary and Conclusions

In the same manner γ -C₁₂(C₁₃AB)-dOTCTP (**69**: 44 %), γ -C₁₂-dOTCTP (**70**: 31 %) and triphosphate (**71**: 59 %) were obtained. The collection of NRTI triphosphates was completed with the 3TC (**75**: 25 %; **76**: 34 %; **77**: 62 %) and 4'-Ed4T (**79**: 46 %; **80**: 40 %; **81**: 73 %) triphosphates (**Figure 35**).

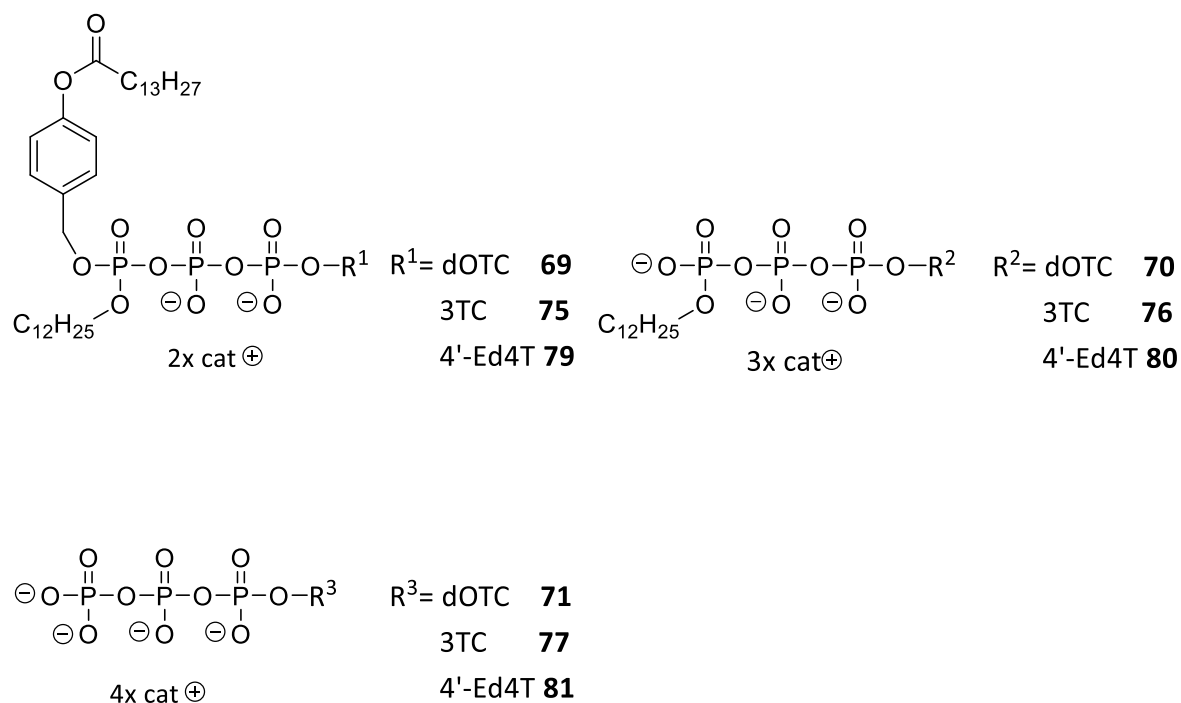


Figure 35: Triphosphates 69-81.

The validation of this prodrug library consisting of novel, promising triphosphates was conducted through primer extension assays, encompassing evaluation against the viral polymerase HIV-RT and the human polymerases α , β and γ (Chapter 4.5). The sulphur-based cytidine triphosphates exhibited intrinsic selectivity against human polymerases which resulted in low to no incorporation for dOTCTP **71** and 3TCTP **77** for all human polymerases. The strongest discrimination against human polymerases was exhibited by 4'-Ed4TTP **81**, suggesting high potential as an antiviral drug.

The prodrugs and γ -alkyl triphosphates were tested against HIV-1 and HIV-2, together with their parent nucleosides in cooperation with SCHOLS *et al.* at the Rega institute in Leuven. The results showed, an overall rise in efficacy for thymidine-based nucleosides, while cytidine-based nucleosides did not benefit from prodrug incorporation. For γ -C₁₆(C₃AB)-FLT **35a** an almost 4-fold increase in activity in HIV-2 was observed, compared to the parent nucleoside. The studies with thymidine kinase deficient cells showed sustained activity for prodrugs and metabolites and reduced cytotoxicity compared to previous studies.¹⁹⁵ The evaluation of the antiviral data of γ -C₁₂(C₁₃AB)-4'-Ed4TTP **79** and γ -C₁₂-Ed4TTP **80** showed improved activity in HIV-1 and HIV-2 compared the parent nucleoside. γ -C₁₂(C₁₃AB)-Ed4TTP **79** also retained low nanomolar activity in TK.deficient cells. These results corroborated the

Summary and Conclusions

advantageous pharmacological profile of 4'-Ed4T. The results obtained from both cytidine-based triphosphates showed slight increased activity for γ -C₁₂(C₁₃AB)-dOTCTP **69** and decreased activity for γ -C₁₂(C₁₃AB)-3TCTP **75** and γ -C₁₂-3TCTP **76**.

Nevertheless, in this work various triphosphate and triphosphate prodrugs, were successfully synthesised showcasing the feasibility of a flexible triphosphate prodrug system. Depending on the nucleoside, substantial benefits of the γ -alkyl triphosphate prodrug system were demonstrated, offering valuable insights applicable to future research, whether targeting viral diseases or expanding into other therapeutic areas, such as Alzheimer's disease.

The final section of this thesis focused on the synthesis of nucleoside phosphonate prodrugs (Chapter 4.6). Inspired by the success of tenofovir, efforts were made to produce nucleoside phosphonate prodrugs that could offer similar or superior antiviral effects while maintaining favourable pharmacological profiles. Protected FLU phosphonate **83** (92 %) was synthesised *via* its halide precursor **84** (83 %) by traditional MICHAEL-ARBUZOV reactions. After conversion to the phosphonate **27** (79 %), γ -C₁₂(C₁₃AB)-FLUDP **82a** (28 %), γ -C₁₂(C₁₃AB)-FLUDP **82b** (13 %) and FLUDP **82c** (54 %) were successfully obtained using established protocols by GOLLNEST and ZHAO successfully establishing the synthesis route for the synthesis of nucleoside γ -alkyl- and γ -alkyl(AB)-phosphonate diphosphates. While the available data for polymerase assays remained inconclusive, antiviral testing against HIV-1 and 2 did produce positive results, that warrant further investigation into cyclic nucleoside phosphonate prodrugs.

6. Experimental Procedure

6.1. General

6.1.1. Solvents, chromatography, and devices

Solvents

Acetonitrile	C_2H_3N ; bp.: 81 °C; Walter-CMP HOW34851 2500, HPLC-grade; Fisher Scientific 10660131, HPLC-grade; VWR Chemicals 83639.320, HPLC-grade.
Acetonitrile- <i>d</i> 3	C_2D_3N ; bp.: 81 °C; Euriso-Top D021B; for spectroscopic use.
Chloroform	$CHCl_3$; 61.2 °C; VWR 22711.324.
Chloroform- <i>d</i> 1	$CDCl_3$; bp.: 62 °C; Euriso-Top D007H, for spectroscopic use.
Dichloromethane	CH_2Cl_2 ; bp.: 40 °C; distilled before use.
Dimethyl sulfoxide- <i>d</i> 6	C_2D_6OS ; bp.: 190 °C; Euriso-Top D010ES, for spectroscopic use.
Ethyl acetate	$C_4H_8O_2$; bp.: 77 °C; distilled before use.
<i>n</i> -Hexane	C_6H_{14} ; bp.: 69 °C; Fisher Scientific 10783601, used without further purification.
<i>n</i> -Heptane	C_7H_{16} ; bp.: 97 °C; Grüssing 111442500, used without further purification.
Methanol	CH_4O ; bp.: 65 °C; distilled before use.
Methanol- <i>d</i> 4	CD_4O ; bp.: 65 °C; Euriso-Top D024ES; for spectroscopic use.
Petroleum ether (50-70)	bp.: 50-70 °C; distilled before use.
<i>iso</i> -Propanol	$C_3H_8O_1$; bp.: 82 °C; VWR Chemicals 20842.323, used without further purification.
Tetrahydrofuran	C_4H_8O ; bp.: 66 °C; VWR Chemicals 28559.320, HPLC-grade.

Experimental Procedure

(HPLC): Analytical HPLC data were obtained with the following system: Agilent 1260 Infinity II (Pump: G7111; Autosampler: G7129A; Detector: DAD-G7117C). All measurements (if not otherwise noted) were performed with an EC 125/3 NUCLEODUR 100-5 C₁₈ec (length: 125 mm, ID: 3.0 mm, particle size: 5 µm) from Macherey Nagel; Pre-column: EC 4/3 NUCLEODUR 100-5 C₁₈ec from Macherey Nagel. Method A: CH₃CN gradient in 2 mM TBA acetate buffer (pH 6); 5-80 %; 0-20 min; flow 1 mL/min. HPLC-DAD: 265 nm. Measurements for enantiomeric excess were obtained with the following system: Agilent 1260 Infinity II (Pump: G7111A; Autosampler: G7129A; Detector: VWD-G7114CA). All measurements (if not otherwise noted) were performed with a Chiralpak AD-H (length: 250 mm, ID: 4.6 mm, particle size: 5 µm) from Daicel; Method B: heptane: isopropanol, isocratic; 50:50; 0-15 min; flow 1 mL/min. HPLC-VWD: 250 nm.

Spectroscopy

Nuclear magnetic resonance spectroscopy (NMR): All NMR spectra were measured at the institute of organic chemistry or inorganic chemistry at the University of Hamburg. The spectra were recorded on a Bruker Fourier 300 (300 MHz), a Bruker AV 400 (400 MHz), a Bruker AMX 400 (400 MHz), a Bruker DRX 500 (500 MHz) or a Bruker AVIII 600 (600 MHz). Chemical shifts are quoted in ppm and calibrated accordingly: Chloroform-*d*1: 7.26 (¹H), 77.16 (¹³C); Dimethyl sulfoxide-*d*6: 2.50 (¹H), 39.52 (¹³C); Methanol-*d*4: 3.31 (¹H), 49.00 (¹³C); Water-*d*2: 4.79 (¹H). For further identification, two-dimensional experiments (*H,H*-COSY; HSQC; HMBC; NOESY) were performed.

Infrared spectroscopy (IR): Infrared spectra were recorded using ALPHA Platinum ATR-IR-spectrometer (Bruker) at room temperature.

Mass Spectrometry (MS): All mass spectra were measured at the institute of organic chemistry at the University of Hamburg or the UKE. ESI mass spectra were recorded on an Agilent 6224 ESI-TOF spectrometer for positive and negative measurements. MALDI mass spectrometry was performed on a MALDI TOF-TOF Bruker rapifleX spectrometer in negative and positive mode.

Further Devices

Centrifuge: Phase separation for pyrophosphates was performed on a Heraeus Biofuge primo R with 8000 rpm for 5 min at 4 °C. For volumes < 2 mL a Heraeus Biofuge Pico at 13000 u/min was used.

Freeze Dryer: Compounds purified over reversed phase chromatography were dried using a Christ ALPHA 2-4 LDplus. **Ultrapure water:** For HPLC, automated flash chromatography and reactions ultrapure water, purified with a Sartorius Arium® Pro DI Ultrapure water system (Sartopore 0.2 µm, UV), was used. **Microwave:** Microwave reactions were conducted in a CEM discover system in closed vessel

Experimental Procedure

mode. **pH meter:** pH measurements were performed with a ProLab 3000 from Schott. **Thermomixer:** Incubation of biological samples was performed with a Thermomixer TS from CellMedia. **Fluorescent Imager:** Results from PAGE experiments were visualized with a ChemiDoc™ MP Imaging System (170-8280) from Bio-Rad Co. **Electrophoresis:** PAGE experiment was conducted with a Thermo Fisher Owl™ S4S Aluminum-Backed Sequencer System, powered by a Consort EV2230 Gel Electrophoresis power supply (1500 V, 300 mA, 150 W). **Polarimeter:** The optical rotation was measured on an A. Krüss Optonic GmbH P8000 polarimeter, with a wavelength of 589 nm. The cuvette used had a length of 100 mm.

6.1.2. Preparation of buffer-solutions

Preparation of 2 mM TBA acetate (TBAA) buffer (pH 6.0) (HPLC): 2 L ultra-pure water, 12.6 mL TBA hydroxide, adjust pH value to 6 with 1 M acetic acid (~5 mL).

Preparation of 10 mM Triethylammonium acetate buffer (pH 6.2) (flash chromatography): 3 L ultra-pure water, 4.16 mL triethylamine; adjust pH value to 6.2 with 1 M acetic acid.

50x TAE buffer (pH 8.5) (PAGE experiments): 242 g Tris (tris(hydroxymethyl)aminomethane), 18.6 g EDTA (disodium salt), 600 mL Ultra-pure water, 57 mL glacial acetic acid, adjust pH to 8.5 with NaOH. Fill up to 1 L.

Preparation of the PBS buffer (pH 7.3): 1.55 g Potassium dihydrogen phosphate, 5.47 g disodium hydrogen phosphate, 1 L ultrapure water. Diluted phosphoric acid was added to adjust the pH to 7.3.

6.1.3. Primer extension assay

HIV-RT and human DNA polymerase β and γ were obtained from Roboklon, human DNA polymerase α was obtained from CHIMERx. The primers and templates were purchased from Life Technologies and Microsynth. The fluorescent-labelled primer was purchased from Metabion and Microsynth. The gels were prepared with the size of 450 mm×200 mm ×0.4 mm according to the electrophoresis apparatus.

25nt primer sequence: (Cy3-labelled): 5'-Cy3-CGTTG GTCCT GAAGG AGGAT AGGTT-3'

30nt Template-sequence: Template T: 3'-GCAAC CAGGA CTTCC TCCTA TCCAA **AGACA**-5'

Template C: 3'-GCAAC CAGGA CTTCC TCCTA TCCAA **GTAGA**-5'

Templates were used according to the substrate used. The primer extension assays were conducted under the following conditions:

Hybridization: Primer and template (P/T) were mixed (1:1.5) and incubated at 95 °C for 5 min. Annealing was achieved by cooling from 95 °C to 20 °C over 2 h. The mixture was kept at 20 °C for 20 min and then cooled to 4 °C over 30 min.

HIV-RT assay: The final assay solution (10 μ L) consists of 50 mM Tris-HCl (pH 8.6 at 22 °C), 10 mM MgCl₂, 40 mM KCl, dNTPs 250 μ M, HIV-RT 3 or 6 U, P/T Hybrid 0.2 μ M in a reaction volume of 10 μ L, incubated at 37 °C for 30 min, 80 °C for 3 min; 50 mA, 45 W for 3 h. The assays were separated using a denaturing PAGE collecting gel (5 %) and separating gel (15 %). The result was visualized by fluorescence imaging.

Human DNA pol β assay: The final assay solution (10 μ L) consists of 50 mM Tris-HCl (pH 8.7 at 22 °C), 10 mM MgCl₂, 100 mM KCl, 1.0 mM dithiothreitol, 0.3 mg/mL of bovine serum albumin (BSA), 15 % glycerol, dNTPs 250 μ M, DNA pol β 2 U, P/T Hybrid 0.2 μ M in a reaction volume of 10 μ L, incubated at 37 °C for 60 min, 80 °C for 3 min; 50 mA, 45 W for 3 h. The assays were separated using a denaturing PAGE collecting gel (5 %) and separating gel (15 %). The result was visualized by fluorescence imaging.

Human DNA pol α assay: The final assay solution (25/12.5 μ L) consists of 60 mM Tris-HCl (pH 8.0 at 22 °C), 5 mM Mg(OAc)₂, 1.0 mM dithiothreitol, 0.3 mg/mL BSA, 0.1 mM spermine, dNTPs 250 μ M, DNA pol α 2 U, P/T Hybrid 0.2 μ M in a reaction volume of 12.5 μ L, incubated at 37 °C for 5 min without dNTPs, then incubated 60 min at 37 °C, 80 °C for 3 min; 50 mA, 45 W for 3 h. The assays were separated using a denaturing PAGE collecting gel (5 %) and separating gel (15 %). The result was visualized by fluorescence imaging.

Experimental Procedure

Human DNA pol γ assay: The final assay solution (25 μ L) consists of 60 mM Tris-HCl (pH 8.0 at 22 $^{\circ}$ C), 5 mM Mg(OAc)₂, 1.0 mM dithiothreitol, 0.3 mg/mL of BSA, 0.1 mM spermine, dNTPs 250 μ M, DNA pol γ 2 or 4 U, P/T Hybrid 0.2 μ M in a reaction volume of 25 μ L, incubated at 37 $^{\circ}$ C for 5 min without dNTPs, then incubated 120 min at 37 $^{\circ}$ C, 80 $^{\circ}$ C for 3 min; 50 mA, 45 W for 3 h. The assays were separated using a denaturing PAGE collecting gel (5 %) and separating gel (15 %). The result was visualized by fluorescence imaging.

6.2. Synthesis

6.2.1. General Procedures

General Procedure 1: Acyloxy Benzyl (AB) Alcohols²⁰⁵

The reaction was performed under an inert atmosphere of N₂. 4-Hydroxybenzyl alcohol **3** and Et₃N (1.0 eq.) were dissolved in THF and cooled to 0 $^{\circ}$ C. The corresponding acid chloride (0.9 eq.) and DMAP (0.1 eq.) were dissolved in THF and added dropwise to the first solution. After approx. 2 h, the reaction mixture was filtered and the solvent was removed under reduced pressure. The residue was dissolved in CH₂Cl₂ and washed with sat. NaHCO₃ and water, respectively, and dried over Na₂SO₄. The solvent was evaporated and the crude product was purified on silica gel (petroleum ether: ethyl acetate).

General Procedure 2: Acyloxy Benzyl (AB) and Cyanoethyl Phosphonates⁵²

(AB) *H*-Phosphonates: The reaction was performed under an inert atmosphere of N₂. Diphenyl phosphite (1.2 eq.) was dissolved in pyridine and cooled to -10 $^{\circ}$ C. Afterwards, the appropriate AB alcohol (1.0 eq.) dissolved in pyridine was added dropwise to the solution. The reaction was warmed to rt over 3 h. The corresponding alkyl alcohol (1.0 eq.) dissolved in pyridine was added in one portion and stirred at 40 $^{\circ}$ C for 3 h. The solvent was removed *via* freeze drying and the crude product was purified on silica gel (petroleum ether: ethyl acetate).

Cyanoethyl *H*-phosphonates: The reaction was performed under an inert atmosphere of N₂. Diphenyl phosphite (1.5 eq.) was dissolved in pyridine and cooled to -10 $^{\circ}$ C. Afterwards, the corresponding alkyl alcohol (1.0 eq.) dissolved in pyridine was added dropwise to the solution. The reaction was warmed to rt over 3 h. 3-Hydroxypropionitrile (2.0 eq.) was added in one portion and stirred at 40 $^{\circ}$ C for 3 h. The solvent was removed *via* freeze drying and the crude product was purified on silica gel (pentane: ethyl acetate).

General procedure 3: Stereoselective synthesis of Hydroxy-2*H*-pyran-3(6*H*)-one esters²²⁵

The corresponding pyranone (1.0 eq.) and anhydride (1.2 eq.) were dissolved in toluene at 10 °C. Basic levamisole **58** (0.09 eq.) dissolved in toluene was added dropwise over 15 min. The reaction was stirred at rt until full conversion was achieved (TLC monitoring). All volatiles were evaporated and the residue was dissolved in CH₃OH and stirred at rt for 1 h. The solvent was exchanged for toluene and the organic phase was washed successively with sat. sodium bicarbonate solution and brine. The organic phase was dried over Na₂SO₄ the solvent was removed under reduced pressure and the crude product was purified on silica gel (hexane:ethyl acetate, 3:1, v/v).

General Procedure 4: Nucleoside γ -Modified Triphosphates²⁵⁹

Preparation of pyrophosphates: The reaction was performed under an inert atmosphere of N₂. The corresponding *H*-phosphonate (1.0 eq.) was dissolved in CH₃CN. *N*-chlorosuccinimide (2.5 eq.) was added and heated to 50 °C until full conversion was confirmed through ¹H-NMR spectroscopy. The reaction mixture was added dropwise to a solution of 0.4 M TBA phosphate monobasic (3.0 eq.) in CH₃CN. After 1 h at rt, all volatiles were evaporated and the residue was dissolved in CH₂Cl₂ (15 mL). The organic phase was sequentially washed with 1 M aqueous NH₄OAc (20 mL, 4 °C) and H₂O (20 mL, 4 °C) followed by drying over Na₂SO₄ (phase separation via centrifuge). The solvent was evaporated to afford the crude pyrophosphate, which was used in the following synthesis without further purification.

Preparation of γ -AB-triphosphates: The reaction was performed under an inert atmosphere of N₂. The corresponding pyrophosphate (1.0 eq.) was dissolved in CH₃CN and cooled to 0 °C. Then an ice-cold solution of Et₃N (8.0 eq.) and TFAA (5.0 eq.) in CH₃CN was added dropwise. After stirring the solution at rt for 10 min all volatiles were evaporated and the residue was dissolved in CH₃CN. Et₃N (5.0 eq.) and 1-methylimidazole (2.5 eq.) were added and stirred at rt for 15 min. The corresponding nucleoside MP TBA salt (0.3-0.5 eq.) dissolved in CH₃CN was added and stirred at rt until full conversion was achieved (RP₁₈ HPLC monitoring). All volatiles were evaporated and the crude product was purified on RP₁₈ silica gel with automated flash chromatography (H₂O:CH₃CN, 100:0 to 0:100, v/v). Afterwards, an ion exchange chromatography (NH₄⁺) and purification on RP₁₈ silica gel with automated flash chromatography (H₂O:CH₃CN, 100:0 to 0:100, v/v) followed.

Preparation of γ -alkyl-triphosphates: The reaction was performed under an inert atmosphere of N₂. The corresponding pyrophosphate (1.0 eq.) was dissolved in CH₃CN and cooled to 0 °C. Then an ice-cold solution of Et₃N (8.0 eq.) and TFAA (5.0 eq.) in CH₃CN was added dropwise. After stirring the solution at rt for 10 min all volatiles were evaporated and the residue was dissolved in CH₃CN. Et₃N

Experimental Procedure

(5.0 eq.) and 1-methylimidazole (2.5 eq.) were added and stirred at rt for 15 min. The corresponding nucleoside MP TBA salt (0.3-0.5 eq.) dissolved in CH₃CN was added and stirred at rt until full conversion was achieved (RP₁₈ HPLC monitoring). An aqueous 10 % TBA hydroxide solution (10.0 eq.) was added and stirred at rt for 16 h. All volatiles were evaporated and the crude product was purified on RP₁₈ silica gel with automated flash chromatography (H₂O:CH₃CN, 100:0 to 0:100, v/v). Afterwards, an ion exchange chromatography (NH₄⁺) and purification on RP₁₈ silica gel with automated flash chromatography (H₂O:CH₃CN, 100:0 to 0:100, v/v) followed.

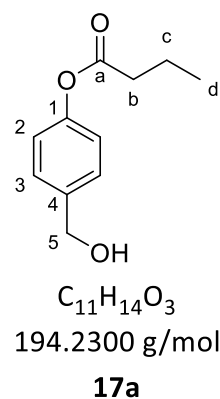
General procedure 5: Nucleoside Triphosphates²⁶⁰

The reaction was performed under an inert atmosphere of N₂. The corresponding nucleoside monophosphate (1.0 eq.) was dissolved in CH₃CN and cooled to 0 °C. A mixture of Et₃N (16.0 eq.) and TFAA (10.0 eq.) dissolved in CH₃CN. Was added. After 10 min at rt all volatiles were removed in vacuo and the residue was dissolved in CH₃CN. Et₃N (10.0 eq.) and 1-methylimidazole (6.0 eq.) were added and stirred for 15 min at rt. The solution was diluted with CH₃CN to a total volume of 8 mL. The reaction mixture was added dropwise (0.2 mL min⁻¹) to tris(TBA) hydrogen pyrophosphate in CH₃CN. The reaction progress was monitored by RP₁₈ HPLC. All volatiles were evaporated and the crude product was purified on RP₁₈ silica gel with automated flash chromatography (H₂O:CH₃CN, 100:0 to 0:100, v/v). Afterwards, an ion exchange chromatography (NH₄⁺) and purification on RP₁₈ silica gel with automated flash chromatography (H₂O:CH₃CN, 100:0 to 0:100, v/v) followed.

6.2.2. Synthesis of AB masking unit pyrophosphates

4-(Hydroxymethyl)phenyl butyrate **17a**

The reaction was performed according to general procedure 1: Acyloxy benzyl (AB) Alcohols: With 4-hydroxybenzyl alcohol **3** (1.00 g, 8.06 mmol), triethylamine (1.01 mL, 7.25 mmol) and butyryl chloride (750 μ L, 7.25 mmol) in THF (40 mL). The crude product was purified on silica gel (petroleum ether: ethyl acetate; 3:2; v/v) to afford **17a** (761 mg, 3.92 mmol, 54 %) as a colourless resin. **R_f-value:** 0.57 (petroleum ether: ethyl acetate; 3:2; v/v)



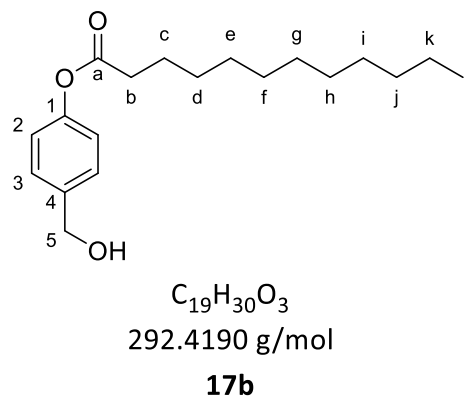
¹H-NMR (300 MHz, Chloroform-*d*1): δ [ppm] = 7.30 (d, ³J_{H,H} = 8.5 Hz, 2H, *H*-2), 6.99 (d, ³J_{H,H} = 8.5 Hz, 2H, *H*-3), 4.61 (s, 2H, *H*-5), 2.47 (t, ³J_{H,H} = 7.4 Hz, 2H, *H*-b), 1.72 (sext., ³J_{H,H} = 7.4 Hz, 2H, *H*-c), 1.64 (s, 1H, OH), 0.98 (t, ³J_{H,H} = 7.4 Hz, 3H, *H*-d).

¹³C-NMR (75 MHz, Chloroform-*d*1): δ [ppm] = 172.4 (C-a), 150.3 (C-1), 138.5 (C-4), 128.2 (C-2), 121.8 (C-3), 64.9 (C-5), 36.4 (C-b), 18.6 (C-c), 13.8 (C-d).

ESI⁺-MS (m/z): C₁₁H₁₄O₃K [M+K]⁺: theo.: 233.0574, found: 233.0499.

4-(Hydroxymethyl)phenyl dodecanoate **17b**

The reaction was performed according to general procedure 1: Acyloxy benzyl (AB) Alcohols: With 4-hydroxybenzyl alcohol **3** (2.00 g, 16.1 mmol), triethylamine (2.04 mL, 14.7 mmol) and dodecyl chloride (3.49 mL, 14.7 mmol) in THF (70 mL). The crude product was purified on silica gel (petroleum ether: ethyl acetate; 4:1; v/v) to afford **17b** (1.67 g, 5.45 mmol, 37 %) as a colourless resin. **R_f-value:** 0.43 (petroleum ether: ethyl acetate; 4:1; v/v)



¹H-NMR (500 MHz, Chloroform-*d*1): δ [ppm] = 7.43 – 7.33 (m, 2H, *H*-2), 7.11 – 7.03 (m, 2H, *H*-3), 4.69 (d, ³J_{H,H} = 5.6 Hz, 2H, *H*-5), 2.55 (t, ³J_{H,H} = 7.5 Hz, 2H, *H*-b), 1.74 (qu, ³J_{H,H} = 7.5 Hz, 2H, *H*-c), 1.67 (t, ³J_{H,H} = 5.9 Hz, 1H, OH), 1.48 – 1.36 (m, 2H, *H*-d), 1.36 – 1.19 (m, 14H, CH₂-alkyl), 0.88 (t, ³J_{H,H} = 6.7 Hz, 3H, *H*-l).

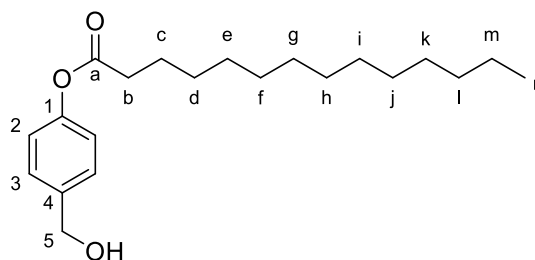
Experimental Procedure

¹³C-NMR (126 MHz, Chloroform-*d*1): δ [ppm] = 172.8 (*C*_q-a), 150.3 (*C*_q-1), 137.3 (*C*_q-4), 128.2 (*C*-2), 121.1 (*C*-3), 64.9 (*C*-5), 34.5 (*C*-b), 32.1 (*CH*₂-alkyl), 29.7 (*CH*₂-alkyl), 29.6 (*CH*₂-alkyl), 29.5 (*CH*₂-alkyl), 29.4 (*CH*₂-alkyl), 29.3 (*CH*₂-alkyl), 25.1 (*C*-c), 14.3 (*C*-l).

HRMS-ESI⁺ (*m/z*): C₁₈H₂₈O₃Na [M+Na]⁺: theo.: 315.1930, found: 315.1926.

4-(Hydroxymethyl)phenyl tetradecanoate **17c**

The reaction was performed according to general procedure 1: Acyloxy benzyl (AB) Alcohols: With 4-hydroxybenzyl alcohol **3** (3.00 g, 24.2 mmol), triethylamine (3.37 mL, 24.2 mmol), DMAP (295 mg, 2.24 mmol) and tetradecyl chloride (5.62 mL, 20.5 mmol) in THF (100 mL). The crude product was purified on silica gel (petroleum ether: ethyl acetate; 4:1; v/v) to afford **17c** (3.28 g, 9.80 mmol, 48 %) as a colourless resin. **R_f-value**: 0.52 (petroleum ether: ethyl acetate; 4:1; v/v)



C₂₁H₃₄O₃
334.5000 g/mol

17c

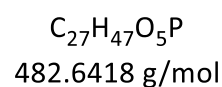
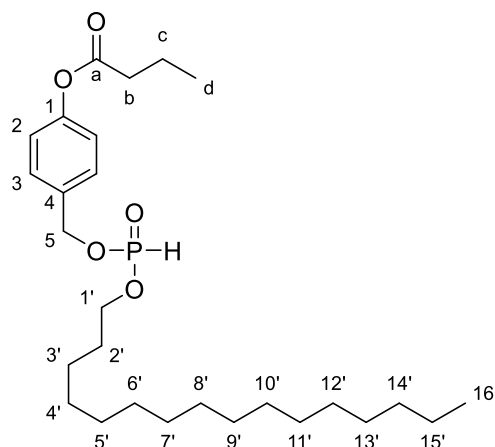
¹H-NMR (500 MHz, Chloroform-*d*1): δ [ppm] = 7.37 (d, ³*J*_{H,H} = 8.4 Hz, 2H, *H*-3), 7.09 – 7.04 (m, 2H, *H*-3), 4.68 (s, 2H, *H*-5), 2.55 (t, ³*J*_{H,H} = 7.5 Hz, 2H, *H*-b), 1.75 (qu, ³*J*_{H,H} = 7.5 Hz, 2H, *H*-c), 1.44 – 1.37 (m, 2H, *H*-d), 1.36 – 1.29 (m, 2H, *H*-e), 1.29 – 1.21 (m, 16H, *CH*₂-alkyl), 0.88 (t, ³*J*_{H,H} = 6.9 Hz, 3H, *H*-n).

¹³C-NMR (126 MHz, Chloroform-*d*1): δ [ppm] = 172.5 (*C*_q-a), 150.3 (*C*_q-1), 138.5 (*C*_q-4), 128.2 (*C*-2), 121.4 (*C*-3), 64.9 (*C*-5), 34.5 (*C*-b), 32.1 (*CH*₂-alkyl), 29.8 (*CH*₂-alkyl), 29.8 (*CH*₂-alkyl), 29.7 (*CH*₂-alkyl), 29.6 (*CH*₂-alkyl), 29.5 (*CH*₂-alkyl), 29.4 (*C*-d), 29.3 (*CH*₂-alkyl), 25.1 (*CH*₂-alkyl), 22.8 (*CH*₂-alkyl), 13.9 (*C*-n).

HRMS-ESI⁺ (*m/z*): C₂₁H₃₄O₃Na [M+Na]⁺: theo.: 357.2400, found: 357.2399.

(4-Butynoyloxybenzyl)-hexadecylphosphonate 18a

The reaction was performed according to general procedure 2: (AB) *H*-phosphonates: With AB alcohol **17a** (762 mg, 3.92 mmol), DPP (1.09 mL, 5.41 mmol) and hexadecanol (951 mg, 3.92 mmol) in pyridine (10 mL). The crude product was purified on silica gel (petroleum ether: ethyl acetate; 3:2; v/v) to afford **18a** (836 mg, 1.73 mmol, 44 %) as a colourless resin. **R_f-value**: 0.67 (petroleum ether: ethyl acetate; 3:2; v/v)

**18a**

¹H-NMR (500 MHz, Chloroform-*d*1): δ [ppm] = 7.57 – 6.17 (d, $^1J_{\text{H,P}} = 700 \text{ Hz}$, 1H, *PH*), 7.43 – 7.39 (m, 2H, *H*-2), 7.12 – 7.08 (m, 2H, *H*-3), 5.09 (d, $^3J_{\text{H,H}} = 9.5 \text{ Hz}$, 2H, *H*-5), 4.09 – 3.96 (m, 2H, *H*-1'), 2.54 (t, $^3J_{\text{H,H}} = 7.4 \text{ Hz}$, 2H, *H*-b), 1.79 (qu, $^3J_{\text{H,H}} = 7.4 \text{ Hz}$, 2H, *H*-c), 1.69 – 1.61 (m, 2H, *H*-2'), 1.39 – 1.19 (m, 26H, *CH*₂-alkyl), 1.04 (t, $^3J_{\text{H,H}} = 7.4 \text{ Hz}$, 3H, *H*-d), 0.87 (t, $^3J_{\text{H,H}} = 6.8 \text{ Hz}$, 3H, *H*-16').

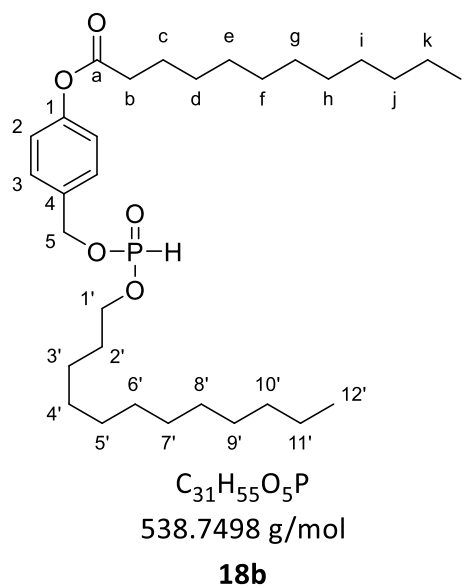
¹³C-NMR (126 MHz, Chloroform-*d*1): δ [ppm] = 172.4 (*C*_q-a), 151.1 (*C*_q-1), 133.3 (*C*_q-4), 129.3 (*C*-2), 122.1 (*C*-3), 66.7 (d, $^2J_{\text{C,P}} = 5.5 \text{ Hz}$, *C*-5), 66.2 (d, $^2J_{\text{C,P}} = 6.0 \text{ Hz}$, *CH*₂-alkyl), 36.3 (*C*-b), 29.8 (*CH*₂-alkyl), 29.8 (*CH*₂-alkyl), 29.7 (*CH*₂-alkyl), 29.6 (*CH*₂-alkyl), 29.5 (*CH*₂-alkyl), 29.2 (*CH*₂-alkyl), 25.6 (*CH*₂-alkyl), 22.8 (*CH*₂-alkyl), 18.6 (*C*-c), 14.3 (*C*-d), 13.8 (*CH*₃-alkyl).

³¹P-NMR (202 MHz, Chloroform-*d*1): δ [ppm] = 7.72 (s).

HRMS-ESI⁺ (m/z): C₂₇H₄₇O₅PNa [M+Na]⁺: theo.: 505.3053, found: 505.3063.

(4-Dodecanoyloxybenzyl)-dodecylphosphonate 18b

The reaction was performed according to general procedure 2: (AB) *H*-phosphonates: With AB alcohol **17b** (1.82 g, 5.94 mmol), DPP (1.43 mL, 7.13 mmol) and dodecanol (1.11 g, 5.94 mmol) in pyridine (10 mL). The crude product was purified on silica gel (petroleum ether: ethyl acetate; 4:1; v/v) to afford **18b** (1.40 g, 2.60 mmol, 44 %) as a colourless resin. **R_f-value**: 0.33 (petroleum ether: ethyl acetate; 4:1; v/v).



¹H-NMR (500 MHz, Chloroform-*d*1): δ [ppm] = 7.56 – 6.16 (d, $^1J_{H,P}$ = 700 Hz, 1H, *PH*), 7.41 (d, $^3J_{H,H}$ = 8.5 Hz, 2H, *H-2*), 7.14 – 7.05 (m, 2H, *H-3*), 5.09 (d, $^3J_{H,P}$ = 9.5 Hz, 2H, *H-5*), 4.09 – 3.95 (m, 2H, *H-1'*), 2.55 (t, $^3J_{H,H}$ = 7.5 Hz, 2H, *H-b*), 1.74 (qu, $^3J_{H,H}$ = 7.5 Hz, 2H, *H-c*), 1.69 – 1.59 (m, 2H, *H-2'*), 1.46 – 1.37 (m, 2H, *H-d*), 1.37 – 1.17 (m, 32H, *CH₂-alkyl*), 0.93 – 0.83 (m, *H-l*, *H-12'*).

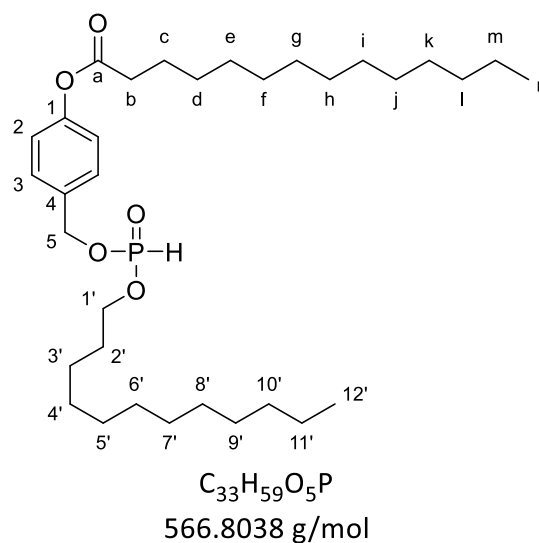
¹³C-NMR (126 MHz, Chloroform-*d*1): δ [ppm] = 172.1 (*C_q-a*), 151.1 (*C_q-1*), 133.4 (*C_q-4*), 129.3 (*C-2*), 122.1 (*C-3*), 66.7 (d, $^2J_{C,P}$ = 5.6 Hz, *C-5*), 66.2 (d, $^2J_{C,P}$ = 6.2 Hz, *C-1'*), 34.5 (*C-b*), 32.0 (*CH₂-alkyl*), 30.5 (*CH₂-alkyl*), 29.8 (*CH₂-alkyl*), 29.7 (*CH₂-alkyl*), 29.7 (*CH₂-alkyl*), 29.6 (*CH₂-alkyl*), 29.6 (*CH₂-alkyl*), 29.5 (*CH₂-alkyl*), 29.4 (*CH₂-alkyl*), 29.2 (*CH₂-alkyl*), 25.6 (*CH₂-alkyl*), 25.0 (*CH₂-alkyl*), 22.8 (*CH₂-alkyl*), 14.3 (*CH₃-alkyl*).

³¹P-NMR (202 MHz, Chloroform-*d*1): δ [ppm] = 8.97 (s).

HRMS-ESI⁺ (m/z): $C_{31}H_{55}O_5PNa$ [*M*+*Na*]⁺: theo.: 561.3679, found: 561.3661.

(4-Tetradecanoyloxybenzyl)-dodecylphosphonate 18c

The reaction was performed according to general procedure 2: (AB) *H*-phosphonates: With AB alcohol **17c** (321 mg, 961 μ mol), DPP (231 μ L, 1.15 mmol) and dodecanol (197 mg, 961 μ mol) in pyridine (10 mL). The crude product was purified on silica gel (petroleum ether: ethyl acetate; 4:1; v/v) to afford **18c** (208 mg, 368 μ mol, 38 %) as a colourless resin. **R_f**-value: 0.35 (petroleum ether: ethyl acetate; 5:1 +1% acetic acid; v/v).



¹H-NMR (500 MHz, Chloroform-*d*1): δ [ppm] = 7.57 –

6.17 (d, ¹J_{H,P} = 700 Hz, 1H, *PH*), 7.44 – 7.39 (m, 2H, *H*-2), 7.12 – 7.07 (m, 2H, *H*-3), 5.09 (d, ³J_{H,P} = 9.5 Hz, 2H, *H*-5), 4.09 – 3.95 (m, 2H, *H*-1'), 2.55 (t, ³J_{H,H} = 7.5 Hz, 2H, *H*-b), 1.75 (qu, ³J_{H,H} = 7.5 Hz, 2H, *H*-c), 1.70 – 1.62 (m, 2H, *H*-2'), 1.36 - 1.45 (m, 2H, *H*-d), 1.38 - 1.21 (m, 36H, *CH*₂-alkyl), 0.91 – 0.85 (m, 6H).

¹³C-NMR (126 MHz, Chloroform-*d*1): δ [ppm] = 172.1 (C_q-a), 151.1 (C_q-1), 133.4 (C_q-4), 129.3 (C-2), 122.1 (C-3), 66.7 (d, ²J_{C,P} = 5.3 Hz, C-5), 66.2 (d, ²J_{C,P} = 6.4 Hz, C-1'), 34.5 (C-b), 32.1 (*CH*₂-alkyl), 29.8 (*CH*₂-alkyl), 29.8 (*CH*₂-alkyl), 29.7 (*CH*₂-alkyl), 29.7 (*CH*₂-alkyl), 29.6 (*CH*₂-alkyl), 29.6 (*CH*₂-alkyl), 29.5 (*CH*₂-alkyl), 29.4 (*CH*₂-alkyl), 29.3 (*CH*₂-alkyl), 29.3 (*CH*₂-alkyl), 25.6 (*CH*₂-alkyl), 25.1 (*CH*₂-alkyl), 22.8 (*CH*₂-alkyl), 14.3 (*CH*₃-alkyl).

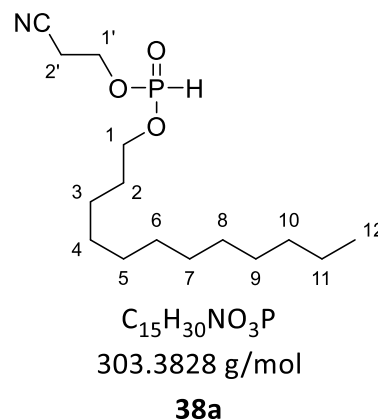
³¹P-NMR (202 MHz, Chloroform-*d*1): δ [ppm] = 8.93 (s).

HRMS-ESI⁺ (m/z): C₃₃H₅₉O₅PNa [M+Na]⁺: theo.: 589.3992, found: 589.4000.

6.2.3. Synthesis Cyanoethyl Pyrophosphates

2-Cyanoethyl dodecyl phosphonate **38a**

The reaction was performed according to general procedure 2: Cyanoethyl *H*-phosphonates: With dodecanol (1.50 g, 8.05 mmol), DPP (1.79 mL, 8.85 mmol) and 3-hydroxypropionitrile (647 μ L, 9.66 mmol) in pyridine (10 mL). The crude product was purified on silica gel (petroleum ether: ethyl acetate; 1:1; v/v) to afford **38a** (1.94 g, 6.39 mmol, 79 %) as a colourless resin. **R_f-value:** 0.25 (petroleum ether: ethyl acetate; 1:1; v/v).



¹H-NMR (400 MHz, Dimethyl sulfoxide-*d*6): δ [ppm] = 6.89 (d, $^1J_{H,P}$ = 706 Hz, 1H, *PH*), 4.17 (dt, $^3J_{H,P}$ = 8.4 Hz, $^3J_{H,H}$ = 5.8 Hz, 2H, *H-1'*), 4.07 – 3.99 (m, 2H, *H-1*), 2.92 (t, $^3J_{H,H}$ = 5.8 Hz, 2H, *H-2'*), 1.66 – 1.57 (m, 2H, *H-2*), 1.36 – 1.20 (m, 18H, *CH₂-alkyl*), 0.90 – 0.80 (m, 3H, *H-12*).

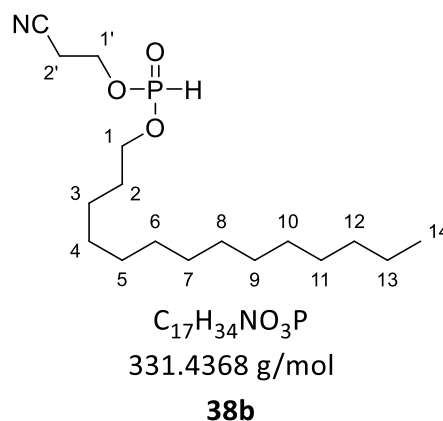
¹³C-NMR (101 MHz, Dimethyl sulfoxide-*d*6): δ [ppm] = 118.3 (CN), 65.3 (*CH₂-alkyl*), 60.2 (d, $^2J_{C,P}$ = 4.7 Hz, *C-1'*), 31.3 (*CH₂-alkyl*), 29.8 (*CH₂-alkyl*), 29.7 (*CH₂-alkyl*), 29.0 (*CH₂-alkyl*), 28.9 (*CH₂-alkyl*), 28.7 (*CH₂-alkyl*), 28.5 (*CH₂-alkyl*), 24.9 (*CH₂-alkyl*), 22.1 (*CH₂-alkyl*), 21.0 (*CH₂-alkyl*), 20.8 (*CH₂-alkyl*), 19.2 (*C-2'*), 14.0 (*CH₃-alkyl*).

³¹P-NMR (162 MHz, Chloroform-*d*1): δ [ppm] = 7.65 (s).

HRMS-ESI⁺ (m/z): $C_{15}H_{30}NO_3PNa$ [M+Na]⁺: theo.: 326.1856, found: 326.1860.

2-Cyanoethyl tetradecyl phosphonate 38b

The reaction was performed according to general procedure 2: Cyanoethyl *H*-phosphonates: With tetradecanol (1.07 g, 5.00 mmol), DPP (1.11 mL, 5.50 mmol) and 3-hydroxypropionitrile (402 μ L, 6.00 mmol) in pyridine (10 mL). The crude product was purified on silica gel (petroleum ether: ethyl acetate; 1:1; v/v) to afford **38b** (780 mg, 2.36 mmol, 47 %) as a colourless resin. **R_f-value**: 0.26 (petroleum ether: ethyl acetate; 1:1; v/v).



¹H-NMR (400 MHz, Dimethyl sulfoxide-*d*6): δ [ppm] = 6.89 (d, $^1J_{H,P}$ = 706 Hz, 1H, PH), 4.17 (dt, $^3J_{H,P}$ = 8.3 Hz, $^3J_{H,H}$ = 5.8 Hz, 2H, H-1'), 4.02 (dt, $^3J_{H,P}$ = 8.9 Hz, $^3J_{H,H}$ = 6.5 Hz, 2H, H-1), 2.92 (t, $^3J_{H,H}$ = 5.8 Hz, 2H, H-2'), 1.67 - 1.55 (m, 2H, H-2), 1.36 - 1.18 (m, 22H, CH₂-alkyl), 0.88 - 0.79 (m, 3H, H-14).

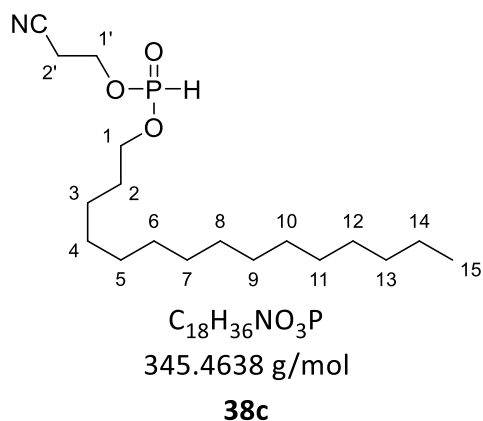
¹³C-NMR (101 MHz, Dimethyl sulfoxide-*d*6): δ [ppm] = 118.4 (CN), 65.4 (CH₂-alkyl), 60.2 (d, $^2J_{C,P}$ = 4.7 Hz, C-1'), 31.3 (CH₂-alkyl), 29.7 (CH₂-alkyl), 29.1 (CH₂-alkyl), 29.0 (CH₂-alkyl), 29.0 (CH₂-alkyl), 28.9 (CH₂-alkyl), 28.7 (CH₂-alkyl), 28.5 (CH₂-alkyl), 24.9 (CH₂-alkyl), 22.1 (CH₂-alkyl), 21.0 (CH₂-alkyl), 19.3 (CH₂-alkyl), 19.2 (C-2'), 14.0 (CH₃-alkyl).

³¹P-NMR (202 MHz, Chloroform-*d*1): δ [ppm] = 8.89 (s).

HRMS-ESI⁺ (m/z): C₁₇H₃₄NO₃PNa [M+Na]⁺: theo.: 354.2169, found: 354.2182.

2-Cyanoethyl pentadecyl phosphonate 38c

The reaction was performed according to general procedure 2: Cyanoethyl *H*-phosphonates: With pentadecanol (1.14 g, 5.00 mmol), DPP (1.11 mL, 5.50 mmol) and 3-hydroxypropionitrile (402 μ L, 6.00 mmol) in pyridine (10 mL). The crude product was purified on silica gel (petroleum ether: ethyl acetate; 1:1; v/v) to afford **38c** (777 mg, 2.25 mmol, 45 %) as a colourless resin. **R_f-value:** 0.19 (petroleum ether: ethyl acetate; 1:1; v/v).



¹H-NMR (500 MHz, Chloroform-*d*1): δ [ppm] = 6.89 (d, $^1J_{H,P}$ = 706 Hz, 1H, *PH*), 4.17 (dt, $^3J_{H,P}$ = 8.3 Hz, $^3J_{H,H}$ = 5.8 Hz, 2H, *H-1'*), 4.02 (dt, $^3J_{H,P}$ = 8.8 Hz, $^3J_{H,H}$ = 6.5 Hz, 2H, *H-1*), 2.92 (t, $^3J_{H,H}$ = 5.8 Hz, 2H, *H-2'*), 1.67 - 1.55 (m, 2H, *H-2*), 1.35 - 1.17 (m, 24H, *CH₂-alkyl*), 0.91 - 0.81 (m, 3H, *H-15*).

¹³C-NMR (101 MHz, Chloroform-*d*1): δ [ppm] = 118.2 (CN), 66.8 (*CH₂-alkyl*), 60.1 (d, $^2J_{C,P}$ = 5.6 Hz, *C-1'*), 29.8 (*CH₂-alkyl*), 29.8 (*CH₂-alkyl*), 29.7 (*CH₂-alkyl*), 29.6 (*CH₂-alkyl*), 29.6 (*CH₂-alkyl*), 29.5 (*CH₂-alkyl*), 29.2 (*CH₂-alkyl*), 29.2 (*CH₂-alkyl*), 25.6 (*CH₂-alkyl*), 25.5 (*CH₂-alkyl*), 22.8 (*CH₂-alkyl*), 21.6 (*CH₂-alkyl*), 20.1 (*C-2'*), 14.3 (*CH₃-alkyl*).

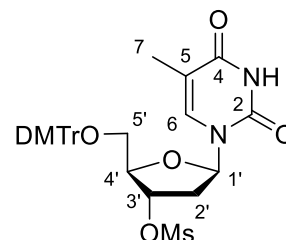
³¹P-NMR (202 MHz, Chloroform-*d*1): δ [ppm] = 8.91 (s).

HRMS-ESI⁺ (m/z): $C_{18}H_{36}NO_3PNa$ [*M*+*Na*]⁺: theo.: 368.2325, found: 368.2326.

6.2.4. Synthesis of Nucleosides

1-[3'-O-Mesy-5'-O-(4,4'-dimethoxytrityl)-2'-deoxy- β -D-furanosyl] thymidine **41**

The reaction was carried out according to the literature^{217,219,261} with modifications. The reaction was carried out under an inert atmosphere of N₂. Thymidine derivative **40** (15.0 g, 27.6 mmol) was dissolved in THF (80 mL) at 0 °C and treated with Et₃N (9.60 mL, 68.9 mmol) as well as methanesulfonyl chloride (3.20 mL, 41.3 mmol). The reaction was warmed to rt over 3 h. Ice-cold water (100 mL) was added and the organic solvent was removed under reduced pressure. The aqueous phase was extracted three times with ethyl acetate and the combined organic phases were dried over Na₂SO₄. The solvent was removed under reduced pressure. The crude product was purified on silica gel (CH₂Cl₂: methanol; 98:2; v/v) to afford **41** (16.8 g, 27.0 mmol, 98 %) as a colourless cotton. **R_f-value**: 0.45 (CH₂Cl₂: methanol; 98:2; v/v)



C₃₂H₃₄N₂O₉S
622.6890 g/mol

41

¹H-NMR (300 MHz, Dimethyl sulfoxide-*d*6): δ [ppm] = 11.40 (s, 1H, NH), 7.52 – 7.48 (m, 1H, H-6), 7.42 - 7.38 (m, 2H, H-DMTr), 7.36 – 7.30 (m, 2H, H-DMTr), 7.29 – 7.24 (m, 5H, H-DMTr), 6.91 - 6.88 (m, 4H, H-DMTr), 6.21 (t, ³J_{H,H} = 7.1 Hz, 1H, H-1'), 5.37 - 5.32(m, 1H, H-3'), 4.20 (q, ³J_{H,H} = 3.7 Hz, 1H, H-4'), 3.74 (s, 6H, DMTr-OCH₃), 3.33 - 3.28 (m, 2H, H-5'), 3.26 (s, 3H, H-Ms), 2.59 - 2.53 (m, 2H, H-2'), 1.47 (d, ⁴J_{H,H} = 1.2 Hz, 3H, H-7).

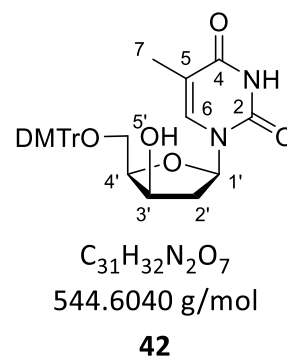
¹³C-NMR (75 MHz, Chloroform-*d*1): δ [ppm] = 163.6 (C_q-4), 158.2 (C_q-OCH₃), 158.2 (C_q-OCH₃), 150.3 (C_q-2), 144.5 (C_q-DMTr), 135.6 (C_q-5), 135.2 (C_q-DMTr), 135.1 (C_q-DMTr), 129.8 (4x C-DMTr), 127.9 (2x C-DMTr), 127.8 (2x C-DMTr), 126.9 (2x C-DMTr), 113.2 (4x C-DMTr), 109.9 (C-6), 86.2 (C_q-DMTr), 83.7 (C-1'), 82.7 (C-4'), 80.3 (C-3'), 62.9 (C-5'), 55.0 (2x OCH₃), 37.8 (SOCH₃), 11.7 (C-7).

HRMS-ESI⁺ (m/z): C₃₂H₃₄N₂O₉SNa [M+Na]⁺: theo.: 645.1877, found: 645.1874.

Experimental Procedure

1-[5'-O-(4,4'-Dimethoxytrityl)-2'-deoxy- β -D-furanosyl] thymidine **42**

The reaction was carried out according to the literature^{217,219,261} with modifications. The reaction was carried out under an inert atmosphere of N₂. Thymidine derivative **41** (5.04 g, 8.09 mmol) was dissolved in ethanol (100 mL, 90 %) and NaOH (3.24 g, 80.9 mmol) was added in portions. The reaction was heated to reflux for 18 h and then cooled to 0 °C. The pH-value was adjusted to 7 with glacial acetic acid (99 %). The solvent was removed *in vacuo* and the residue was dissolved in CH₂Cl₂/H₂O (1:1, 200 mL, v/v). The aqueous phase was extracted twice with CH₂Cl₂ and the combined organic phases were washed with brine. The organic phase was dried over Na₂SO₄ and the solvent was removed under reduced pressure. The crude product was purified on RP₁₈-silica gel with automated flash chromatography (H₂O: CH₃CN, 70:30 to 0:100, v/v) to afford **42** (3.04 g, 5.58 mmol, 69 %) as a colourless cotton. **R_f-value**: 0.37 (petroleum ether: ethyl acetate; 1:1; v/v).



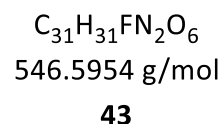
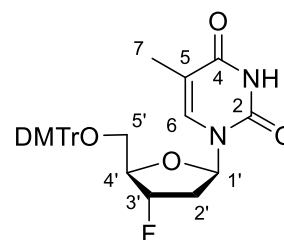
¹H-NMR (400 MHz, Dimethyl sulfoxide-*d*6): δ [ppm] = 11.27 (s, 1H, NH) 7.60 (d, ⁴J_{H,H} = 1.4 Hz, 1H, H-6), 7.46 - 7.41 (m, 2H, H-DMTr), 7.33 - 7.18 (m, 8H, H-DMTr), 6.91 - 6.84 (m, 3H, H-DMTr), 6.11 (dd, ³J_{H,H} = 8.1, 2.3 Hz, 1H, H-1'), 5.20 (d, ³J_{H,H} = 3.1 Hz, 1H, OH), 4.22 - 4.17 (m, 1H, H-3'), 4.08 (dt, ³J_{H,H} = 6.6, 3.1 Hz, 1H, H-4'), 3.75 - 3.73 (m, 6H, OCH₃), 3.41 - 3.37 (m, 1H, H-5'a), 3.18 (dd, ²J_{H,H} = 10.4 Hz, ³J_{H,H} = 2.9 Hz, 1H, H-5'b), 1.86 (dd, ³J_{H,H} = 14.4 Hz, ³J_{H,H} = 2.4 Hz, 2H, H-2'), 1.65 (d, ⁴J_{H,H} = 1.2 Hz, 3H, H-7).

¹³C-NMR (101 MHz, Dimethyl sulfoxide-*d*6): δ [ppm] = 163.8 (C_q-4), 158.0 (2x C_q-OCH₃), 150.5 (C_q-2), 144.9 (C_q-DMTr), 136.8 (C_q-5), 135.7 (C_q-DMTr), 135.5 (C_q-DMTr), 129.8 (2x C-DMTr), 129.7 (2x C-DMTr), 127.8 (2x C-DMTr), 127.7 (2x C-DMTr), 126.6 (C-DMTr), 113.1 (4x C-DMTr), 108.3 (C-6), 85.5 (C_q-DMTr), 84.2 (C-1'), 83.3 (C-4'), 69.0 (C-3'), 62.8 (C-5'), 55.0 (2x OCH₃), 40.8 (C-2'), 12.5 (C-7).

HRMS-ESI⁺ (m/z): C₃₁H₃₂N₂O₇Na [M+Na]⁺: theo.: 567.2102, found: 567.2102.

5'-O-(4,4'-Dimethoxytrityl)-3'-deoxy-3'-fluorothymidine 43

The reaction was carried out according to the literature^{217,219,261} with modifications. The reaction was carried out under an inert atmosphere N₂. Thymidine derivative **42** (1.48 g, 2.71 mmol) was dissolved in dry CH₂Cl₂ (50 mL) and cooled to 0 °C. Afterwards, pyridine (437 μL, 6.24 mmol) and DAST™ (90 % in CH₂Cl₂, 916 μL, 6.24 mmol) were added and after 15 min at 0 °C the reaction was warmed to rt. After 1.5 h at rt the reaction cooled to 0 °C and saturated NaHCO₃ solution was added. The aqueous phase was extracted two times with CH₂Cl₂ and the combined organic phases were washed sequentially with saturated NaHCO₃ solution and brine. The organic phase was dried over Na₂SO₄ and the solvent was removed under reduced pressure. The crude product was purified on silica gel (petroleum ether: ethyl acetate, 1:1, v/v) to afford **43** (797 mg, 1.46 mmol, 54 %) as a light-yellow cotton. **R_f-value**: 0.55 (petroleum ether: ethyl acetate; 1:1+ 1 % Et₃N)



¹H-NMR (400 MHz, Chloroform-*d*1): δ [ppm] = 8.19 (s, 1H, NH), 7.60 (q, ⁴J_{H,H} = 1.3 Hz, 1H, H-6), 7.37 - 7.35 (m, 2H, H-DMTr), 7.32 - 7.28 (m, 2H, H-DMTr), 7.27 - 7.23 (m, 6H, H-DMTr), 6.84 (d, ³J_{H,H} = 9.4 Hz, 3H, H-DMTr), 6.48 (dd, ³J_{H,H} = 9.4, 5.0 Hz, 1H, H-1'), 5.30 (dd, ³J_{H,H} = 5.3 Hz, ²J_{H,F} = 54.0 Hz, 1H, H-3'), 4.33 (td, ³J_{H,H} = 2.4 Hz, ³J_{H,F} = 28.3 Hz, 1H, H-4'), 3.80 (s, 6H, OCH₃), 3.53 (dd, ²J_{H,H} = 10.6 Hz, ³J_{H,H} = 2.9 Hz, 1H, H-5'a), 3.38 (dd, ²J_{H,H} = 10.7 Hz, ³J_{H,H} = 2.5 Hz, 1H, H-5'b), 2.66 (ddd, ³J_{H,F} = 20.3 Hz, ²J_{H,H} = 14.3 Hz, ³J_{H,H} = 5.4 Hz, 1H, H-2'a), 2.34 (dddd, ³J_{H,F} = 39.3 Hz, ³J_{H,H} = 14.4 Hz, ³J_{H,H} = 9.4 Hz, 5.0 Hz, 1H, H-2'b), 1.41 (d, ³J_{H,H} = 1.2 Hz, 3H, H-7).

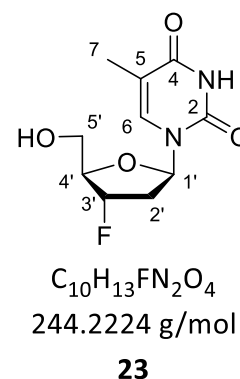
¹³C-NMR (101 MHz, Chloroform-*d*1): δ [ppm] = 163.4 (C_q-4), 159.0 (2x C_q-OCH₃), 150.2 (C_q-2), 144.2 (C_q-DMTr), 135.5 (C_q-5), 135.2 (C-6), 130.2 (C-DMTr), 130.2 (C-DMTr), 128.2 (4x C-DMTr), 128.2 (C-DMTr), 127.5 (C-DMTr), 113.5 (2x C-DMTr), 113.5 (C-DMTr), 113.8 (4x C-DMTr), 111.7 (C-2), 95.8 (d, ¹J_{C,F} = 177.6 Hz, C-3'), 87.4 (C_q-DMTr), 84.7 (C-1'), 84.4 (d, ²J_{C,F} = 25.6 Hz, C-4'), 63.5 (d, ³J_{C,F} = 10.9 Hz C-5'), 55.4 (2x OCH₃), 37.6 (d, ³J_{C,F} = 21.3 Hz, C-2'), 11.9 (C-7).

¹⁹F-NMR (565 MHz, Chloroform-*d*1): δ [ppm] = -172.78 (dddd, J_{F,H} = 54.2, 39.5, 28.5, 20.8 Hz).

HRMS-ESI⁺ (m/z): C₃₁H₃₁FN₂O₆Na [M+Na]⁺: theo.: 569.2058, found: 569.2050.

3'-Deoxy-3'-fluorothymidine (FLT) 23

The reaction was carried out according to the literature^{217,219,261} with modifications. Thymidine derivative **43** (892 mg, 1.63 mmol) was dissolved in CH₃CN (50 mL) heated to 45 °C. Afterwards, 1 M HCl (15 mL) was added and the mixture was stirred for 30 min. The solvent was removed under reduced pressure to about 10 % of the initial volume and the residual mixture was diluted with H₂O (20 mL). The solution was washed three times with ethyl acetate: hexane (3:2). The solvent of the aqueous phase was removed, and the crude product was purified on RP₁₈-silica gel with automated flash chromatography (H₂O: CH₃CN, 100:0 to 0:100, v/v) to afford **23** (368 mg, 1.51 mmol, 92 %) as a colourless cotton.



¹H-NMR (600 MHz, Dimethyl sulfoxide-*d*₆): δ [ppm] = 11.06 (s, 1H, NH), 7.70 (d, ⁴*J*_{H,H} = 1.3 Hz, 1H, H-6), 6.21 (dd, ³*J*_{H,H} = 9.4 Hz, 5.5 Hz, 1H, H-1'), 5.25 (dd, *J*_{H,F} = 54.0 Hz, ³*J*_{H,H} = 4.8 Hz, 1H, H-3'), 5.20 (t, ³*J*_{H,H} = 5.1 Hz, 1H, OH), 4.14 (dt, *J*_{H,F} = 27.8 Hz, ³*J*_{H,H} = 4.1 Hz, 1H, H-4'), 3.65 - 3.56 (m, 2H, H-5'), 2.45 - 2.22 (m, 2H, H-2'), 1.78 (d, ⁴*J*_{H,H} = 1.2 Hz, 3H, H-7).

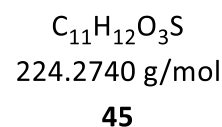
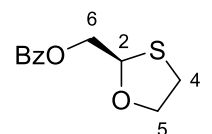
¹³C-NMR (151 MHz, Dimethyl sulfoxide-*d*₆): δ [ppm] = 163.6 (C_q-4), 150.5 (C_q-2), 135.8 (C-6), 109.8 (C_q-5), 94.8 (d, *J*_{C,F} = 174 Hz, C-3'), 84.8 (d, *J*_{C,F} = 22.7 Hz, C-4'), 83.7 (C-1'), 60.9 (d, *J*_{C,F} = 11.0 Hz, C-5'), 36.8 (d, *J*_{C,F} = 20.2 Hz, C-2'), 12.3 (C-7).

¹⁹F-NMR (565 MHz, Dimethyl sulfoxide-*d*₆): δ [ppm] = -174.00 (dddd, *J*_{F,H} = 53.7, 40.0, 27.8, 21.5 Hz).

HRMS-ESI⁺ (m/z): C₁₀H₁₃FN₂O₄Na [M+Na]⁺: theo.: 267.0751, found: 267.0746.

(R)-(1,3-oxathiolan-2-yl)methyl benzoate 45

The reaction was carried out according to the literature²⁶² with modifications. Oxathiolane **44** (970 mg, 8.07 mmol) and pyridine (0.975 mL, 12.1 mmol) were dissolved in CH₂Cl₂ (40 mL). Benzoyl chloride (1.41 mL, 12.1 mmol) was added dropwise and the mixture was stirred for 2 h at rt. The reaction mixture was washed with water. The organic phase was dried over Na₂SO₄ and the solvent was removed under reduced pressure. The crude product was purified twice on silica gel (CH₂Cl₂; 100 %; then toluene; 100 %) to afford oxathiolane **45** (1.63 g, 7.26 mmol, 90 %) as a colourless oil. **R_f-value**: 0.59 (CH₂Cl₂)



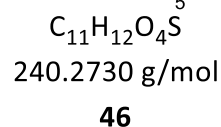
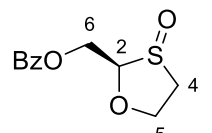
¹H-NMR (400 MHz, Chloroform-*d*1): δ [ppm] = 8.09-8.06 (m, 2H, *H*-Bz), 7.59-7.55 (m, 1H, *H*-Bz), 7.47-7.42 (m, 2H, *H*-Bz), 5.47 (dd, ³*J*_{H,H} = 7.3, 3.6 Hz, 1H, *H*-2), 4.50 (dd, ²*J*_{H,H} = 11.9 Hz, ³*J*_{H,H} = 7.3 Hz, 1H, *H*-6a), 4.41 (dd, ²*J*_{H,H} = 11.9 Hz, ³*J*_{H,H} = 3.6 Hz, 1H, *H*-6b), 4.29 (dt, ²*J*_{H,H} = 9.2 Hz, ³*J*_{H,H} = 5.4 Hz, 1H, *H*-5a), 4.02 (ddd, ²*J*_{H,H} = 9.2 Hz, ³*J*_{H,H} = 6.8, 5.9 Hz, 1H, *H*-5b), 3.10-3.01 (m, 2H, *H*-4).

¹³C-NMR (101 MHz, Chloroform-*d*1): δ [ppm] = 166.3 (C_q =O-Bz), 133.3 (C_q -Bz), 129.9 (C-Bz), 128.5 (C-Bz), 83.3 (C-2), 71.7 (C-5), 66.4 (C-6), 32.7 (C-4).

HRMS-ESI⁺ (m/z): C₁₁H₁₂O₃SNa [M+Na]⁺: theo.: 247.0399, found: 247.0430.

((2R)-3-oxido-1,3-oxathiolan-2-yl)methyl benzoate 46

The reaction was performed according to the literature²²⁰ with modifications. A mixture of oxathiolane **45** (1.97 mg, 8.77 mmol) and glacial acetic acid (0.753 mL, 13.2 mmol) was heated to 40 °C. Over a period of 40 min hydrogen peroxide (1.23 mL, 12.3 mmol, 30 % in water) was added in four portions. The reaction was stirred at 40 °C for an additional hour. The reaction was diluted with CH₂Cl₂ (10 mL) and sodium sulphite (10 mL, 10 % in water) was added in small portions. The aqueous phase was removed, and saturated NaHCO₃-solution was added until no further bubbling was observed. The aqueous phase was again removed, and the organic phase was washed with brine and dried over Na₂SO₄. The organic layer was filtered over Celite® and the solvent was removed under reduced pressure to afford oxathiolane **46** (2.02 g, 8.40 mmol, 96 %) as a colourless solid.



¹H-NMR (400 MHz, Chloroform-*d*1): δ [ppm] = 8.09-7.98 (m, 2H, *H*-Bz), 7.61-7.56 (m, 1H, *H*-Bz), 7.48-7.43 (m, 2H, *H*-Bz), 4.86-4.67 (m, 3H, *H*-2), 4.73-4.67 (m, 1H, *H*-6a), 4.46 (ddd, ²*J*_{H,H} = 9.8 Hz, ³*J*_{H,H} = 11.8, 4.0 Hz, 1H, *H*-6b), 4.13 (ddd, ²*J*_{H,H} = 9.7 Hz, ³*J*_{H,H} = 7.7, 5.6 Hz, 1H, *H*-5a), 3.29-3.09 (m, 1H, *H*-5b), 3.16 (dd, ²*J*_{H,H} = 13.3 Hz, ³*J*_{H,H} = 3.7 Hz, 1H, *H*-4a), 2.74 (ddd, ²*J*_{H,H} = 13.5 Hz, ³*J*_{H,H} = 11.8, 7.0 Hz, 1H, *H*-4b).

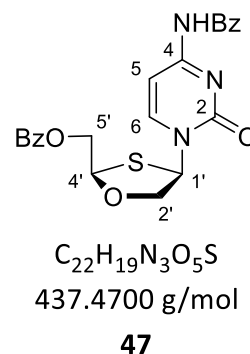
Experimental Procedure

¹³C-NMR (101 MHz, Chloroform-*d*1): δ [ppm] = 165.8 ($C_q=O-Bz$), 133.6 (C_q-Bz), 129.9 ($C-Bz$), 129.2 ($C-Bz$), 128.6 ($C-Bz$), 95.9 ($C-2$), 68.6 ($C-5$), 59.3 ($C-6$), 53.3 ($C-4$).

HRMS-ESI⁺ (m/z): $C_{11}H_{12}O_4SNa$ [M+Na]⁺: theo.: 263.0349, found: 263.0357.

5'-Benzoyl-2'-deoxy-3'-oxa-4'-thio-*N*⁴-benzoyl cytidine **47**

The reaction was performed according to the literature²²⁰ with modifications: Oxathiolane **46** (2.22 g; 9.23 mmol) and triethylamine (2.83 mL, 20.3 mmol) were dissolved in CH_2Cl_2 (25 mL) and cooled to -50 °C. Trimethylsilyl iodide (3.49 mL, 27.7 mmol) was added dropwise while keeping the temperature below -40 °C. After stirring for 45 min at -50 °C, dry copper(II) chloride (0.248 g, 1.85 mmol) was added. Then, *N*⁴-Benzoyl cytosine (1.87 g, 8.68 mmol) was added and the suspension was stirred another 15 min at -50 °C before



warming it to 0 °C overnight. After stirring for an additional hour at rt, the reaction was subsequently quenched with ice cold water (18.5 mL) and ammonia solution (18.5 mL, 5 % in water). Additional CH_2Cl_2 (10 mL) was added, the solution was filtered over Celite® and the organic layer was subsequently washed with a phosphorous acid solution (2 % in water) and ammonia solution (2.5 % in water). The organic layer was dried over Na_2SO_4 and the solvent was removed under reduced pressure to afford the crude cytidine **47** (3.75 g, 8.58 mmol, 99 %) as a light beige foam. Crystallisation with methanol aq. (14.5 vol./ %) afforded cytidine **47** (1.15 g, 3.35 mmol, 40 %) as a colourless solid.

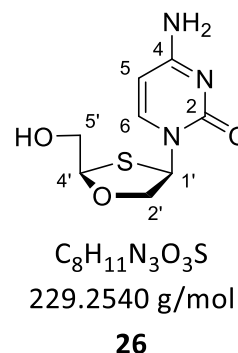
¹H-NMR (600 MHz, Chloroform-*d*1): δ [ppm] = 8.63 (bs, 1H, *NH*), 8.34 (d, $^3J_{H,H} = 7.1$ Hz, 1H, *H-6*), 8.09 (dd, $^3J_{H,H} = 8.2, 1.1$ Hz, 2H, *H-Bz*), 7.88 (d, $^3J_{H,H} = 7.4$ Hz, 2H, *H-Bz*), 7.70 – 7.59 (m, 2H, *H-Bz*), 7.55 – 7.49 (m, 4H, *H-Bz*), 7.39 (bs, 1H, *H-5*), 6.65 (d, $^3J_{H,H} = 4.2$ Hz, 1H, *H-1'*), 5.51 (dd, $^3J_{H,H} = 4.5, 3.2$ Hz, 1H, *H-4'*), 4.84 (dd, $^2J_{H,H} = 12.5$ Hz, $^3J_{H,H} = 3.0$ Hz, 1H, *H-5'a*), 4.78 (dd, $^2J_{H,H} = 12.5$ Hz, $^3J_{H,H} = 4.6$ Hz, 1H, *H-5'b*), 4.52 (d, $^3J_{H,H} = 10.8$ Hz, 1H, *H-2'a*), 4.07 (dd, $^2J_{H,H} = 10.9$ Hz, $^3J_{H,H} = 4.4$ Hz, 1H, *H-2'b*).

¹³C-NMR (151 MHz, Chloroform-*d*1): δ [ppm] = 166.1 ($C_q=O-Bz$), 162.2 (C_q-4), 155.6 (C_q-2), 146.1 ($C-6$), 133.9 (C_q-Bz), 133.4 (C_q-Bz), 133.1 ($C-Bz$), 129.9 ($C-Bz$), 129.4 ($C-Bz$), 129.2, 128.8 ($C-Bz$), 127.6 ($C-Bz$), 97.3 ($C-5$), 86.1 ($C-4'$), 78.5 ($C-2'$), 64.9 ($C-5'$), 63.9 ($C-1'$).

HRMS-ESI⁺ (m/z): $C_{22}H_{20}N_3O_5S$ [M+H]⁺: theo.: 438.1118, found: 438.1099.

(-)-2'-Deoxy-3'-oxa-4'-thiocytidine (dOTC) 26

The reaction was performed according to the literature²²⁰ with modifications: Cytidine **47** (840 g, 1.92 mmol) was suspended in an ammonia solution (2 M in methanol) and stirred at rt overnight. The solution was filtered over Celite® and the solvent was removed under reduced pressure. The crude product was purified on RP₁₈-silica gel with automated flash chromatography (H₂O: CH₃CN, 100:0 to 0:100, v/v) to afford **25** (413 mg, 1.80 mmol, 94 %) as a colourless cotton. **HPLC (Method A):** t_R = 2.21 min.



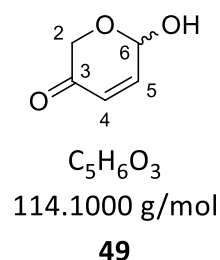
¹H-NMR (600 MHz, Water-d₂): δ [ppm] = 8.08 (d, ³J_{H,H} = 7.6 Hz, 1H, H-6), 6.36 (d, ³J_{H,H} = 4.5 Hz, 1H, H-1'), 6.04 (d, ³J_{H,H} = 7.6 Hz, 1H, H-5), 5.36 (dd, ³J_{H,H} = 4.4, 2.9 Hz, 1H, H-4'), 4.57 (d, ²J_{H,H} = 11.0 Hz, 1H, H-2'a), 4.08 (dd, ²J_{H,H} = 11.0 Hz, ³J_{H,H} = 4.6 Hz, 1H, H-2'b), 4.05 (dd, ³J_{H,H} = 12.9 Hz, ³J_{H,H} = 2.8 Hz, 1H, H-5'a), 3.89 (dd, ²J_{H,H} = 12.9 Hz, ³J_{H,H} = 4.4 Hz, 1H, H-5'b).

¹³C-NMR (151 MHz, Water-d₂): δ [ppm] = 165.9 (C_q-4), 157.8 (C_q-2), 142.8 (C-6), 96.4 (C-5), 87.7 (C-4'), 76.7 (C-2'), 64.0 (C-1'), 61.7 (C-5').

HRMS-ESI⁺ (m/z): C₈H₁₂N₃O₃S [M+H]⁺: theo.: 230.0594, found: 230.0598.

6-Hydroxy-2H-pyran-3(6H)-one 49

The synthesis was carried out according to the literature^{231,263} with modifications. The reaction was carried out under an inert atmosphere of N₂. Freshly distilled furfuryl alcohol **48** (7.08 mL, 81.6 mmol) and *m*CPBA (22.1 g, 89.7 mmol) were dissolved in CH₂Cl₂ (80 mL) and cooled to 0 °C. The reaction was stirred for 3 h at this temperature and then slowly warmed to rt. Then, *m*CPBA was precipitated by cooling the reaction to -78 °C. The reaction was filtrated and washed with CH₂Cl₂. All volatiles were evaporated, and the crude product was purified on silica gel (petroleum ether: ethyl acetate; 3:2 to 1:1; v/v) to afford **49** (6.80 g, 59.6 mmol, 73 %) as a colourless resin. **R_f-value:** 0.42 (CH₂Cl₂: methanol; 19:1; v/v)



¹H-NMR (500 MHz, Chloroform-d₁): δ [ppm] = 6.95 (dd, ³J_{H,H} = 10.4 Hz, ³J_{H,H} = 3.1 Hz, 1H, H-4), 6.17 (dd, ³J_{H,H} = 10.4 Hz, ⁴J_{H,H} = 0.9 Hz, 1H, H-5), 5.64 (dd, ³J_{H,H} = 3.0 Hz, ⁴J_{H,H} = 0.9 Hz, 1H, H-6), 4.51 (d, ²J_{H,H} = 16.9 Hz, 1H, H-2a), 4.07 (d, ²J_{H,H} = 16.9 Hz, 1H, H-2b), 3.13 (s br, 1H, OH).

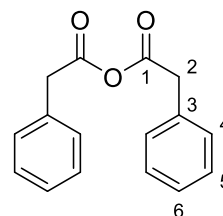
Experimental Procedure

¹³C-NMR (126 MHz, Chloroform-*d*1): δ [ppm] = 193.4 (*C*_q-3), 145.6 (*C*-4), 128.2 (*C*-5), 88.4 (*C*-6), 66.8(*C*-2).

ESI⁺-MS (m/z): C₅H₇O₃ [M+H]⁺: theo.: 115.0389, found: 115.0378.

2-Phenylacetic anhydride **57**

The synthesis was carried out according to the literature²³⁷ with modifications: Phenylacetic acid (11.38 g, 83.62 mmol) was added to a solution of NaOH (3.34 g, 83.62 mmol) in methanol (50 mL) and heated to reflux for 2 h. After cooling the reaction to rt, diethyl ether was added (100 mL), the solution was filtered, and the solvents were removed under reduced pressure to afford the corresponding sodium carboxylate in quantitative yields. The salt was suspended in toluene (100 mL) and phenylacetic chloride (11.14 mL, 83.62 mmol) dissolved in toluene (100 mL) was added dropwise. The solution was stirred for 3 h until the residue was fully dissolved. The solvent was removed under reduced pressure. After crystallisation in petroleum ether: benzene (9:1; v/v) phenylacetic anhydride **57** (14.62 g, 57.49 mmol, 69 %) was obtained as a colourless solid. **R_f-value:** 0.23 (petroleum ether: ethyl acetate; 3:1; v/v).



C₁₆H₁₄O₃
254.2850 g/mol

57

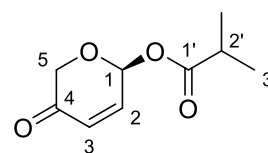
¹H-NMR (400 MHz, Chloroform-*d*1): δ [ppm] = 7.38 - 7.27 (m, 6H, *H*-5, *H*-6), 7.21 (dd, ³*J*_{H,H} = 7.6 Hz, ⁴*J*_{H,H} = 1.9 Hz, 4H, *H*-4), 3.72 (s, 4H, *H*-2).

¹³C-NMR (101 MHz, Chloroform-*d*1): δ [ppm] = 167.1 (*C*_q-1), 132.1 (*C*_q-3), 129.5 (*C*-4), 128.9 (*C*-6), 127.8 (*C*-5), 42.2 (*C*-2).

ESI⁺-MS (m/z): C₁₆H₁₄O₃Na [M+Na]⁺: theo.: 277.0835, found: 277.0852.

(*S*)-4-Oxo-4,5-dihydro-1*H*-pyran-1-yl isobutyrate **50a**

The synthesis was carried out according to general procedure 3: Stereoselective synthesis of Hydroxy-2*H*-pyran-3(6*H*)-one esters. With pyranone **49** (2.50 g, 21.9 mmol), isobutyric anhydride (4.70 mL, 27.4 mmol) and levamisole **58** (224 mg, 1.10 mmol) in toluene (50 mL). The crude product was purified on silica gel (hexane: ethyl acetate; 3:1, v/v) to afford isobutyric ester **50a** (3.43 g, 18.6 mmol, 85 %, 87 %ee) as a colourless resin. $[\alpha]_D^{24}$: +119.3° (*c* = 0.56, CH₂Cl₂) **R_f-value:** 0.55 (petroleum ether: ethyl acetate; 3:1; v/v).



C₉H₁₂O₄
184.1910 g/mol

50a

Experimental Procedure

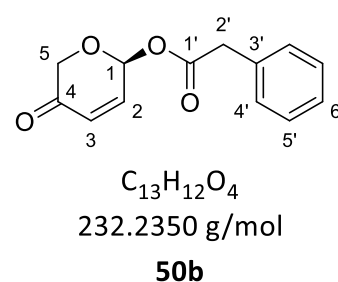
¹H-NMR (300 MHz, Chloroform-*d*1): δ [ppm] = 6.93 (dd, $^3J_{H,H} = 10.4, 3.6$ Hz, 1H, *H*-2), 6.49 (dd, $^3J_{H,H} = 3.6$ Hz, $^4J_{H,H} = 0.7$ Hz, 1H, *H*-1), 6.26 (d, $^3J_{H,H} = 10.4$ Hz, 1H, *H*-3), 4.49 (d, $^2J_{H,H} = 17.0$ Hz, 1H, *H*-5a), 4.22 (dd, $^2J_{H,H} = 17.0$ Hz, $^4J_{H,H} = 0.6$ Hz, 1H, *H*-5b), 2.61 (sept, $^3J_{H,H} = 7.0$ Hz, 1H, *H*-2'), 1.46 – 0.96 (m, 6H, *H*-3').

¹³C-NMR (75 MHz, Chloroform-*d*1): δ [ppm] = 193.6 (*C*_q-4), 175.7 (*C*_q-1'), 142.2 (*C*-2), 128.9 (*C*-1), 86.6 (*C*-3), 67.5 (*C*-5), 34.2 (*C*-2'), 19.0 (*C*-3'), 18.8 (*C*-3').

ESI⁺-MS (m/z): C₉H₁₂O₄K [M+K]⁺: theo.: 223.0367, found: 223.0275.

(*S*)-4-Oxo-4,5-dihydro-1*H*-pyran-1-yl 2-phenylacetate **50b**

The synthesis was carried out according to general procedure 3: Stereoselective synthesis of Hydroxy-2*H*-pyran-3(6*H*)-one esters. With pyranone **49** (5.25 g, 45.99 mmol), phenylacetic anhydride and levamisole **58** (939 mg, 4.40 mmol) in CH₂Cl₂ (90 mL). The crude product was purified on silica gel (hexane: ethyl acetate; 3:1, v/v) and crystallised (isopropyl alcohol) to afford phenylacetic ester **50b** (5.61 g,



24.17 mmol, 52 %, 79 %) as a colourless solid. $[\alpha]_D^{24}$: +152.3° (*c* = 0.0985, CH₂Cl₂). **R_f-value:** 0.50 (petroleum ether: ethyl acetate; 5:1; v/v).

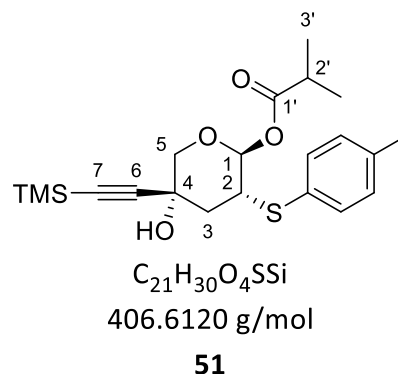
¹H-NMR (300 MHz, Chloroform-*d*1): δ [ppm] = 7.39 - 7.24 (m, 5H, *H*-4', *H*-5', *H*-6'), 6.91 (dd, $^3J_{H,H} = 10.4, 3.6$ Hz, 1H, *H*-2), 6.50 (dd, $^3J_{H,H} = 3.6$ Hz, $^4J_{H,H} = 0.7$ Hz, 1H, *H*-1), 6.30 - 6.22 (d, $^3J_{H,H} = 10.4$ Hz, 1H, *H*-3), 4.37 (d, $^2J_{H,H} = 17.0$ Hz, 1H, *H*-5a), 4.17 (d, $^3J_{H,H} = 17.0$ Hz, 1H, *H*-5b), 3.69 (s, 2H, *H*-2').

¹³C-NMR (75 MHz, Chloroform-*d*1): δ [ppm] = 193.4 (*C*-4), 170.3 (*C*-1), 142.2 (*C*-2), 133.2 (*C*-3'), 129.4 (*C*-4'), 129.0 (*C*-6'), 128.9 (*C*-3), 127.6 (*C*-5'), 87.1 (*C*-1), 67.5 (*C*-5), 41.4 (*C*-2').

ESI⁺-MS (m/z): C₁₃H₁₃O₄ [M+H]⁺: theo.: 233.0808, found: 233.0755.

(1*S*,2*R*,4*R*)-4-Hydroxy-2-(*p*-tolylthio)-4-((trimethylsilyl)ethynyl)tetrahydro-1*H*-pyran-1-yl isobutyrate 51

The synthesis was carried out according to the literature²²⁵ with modifications: Pyranone **50a** (2.00 g, 10.86 mmol) was dissolved in toluene (20 mL), 4-methylbenzenethiol (1.48 g, 11.94 mmol) and DIPEA (94.6 μ L, 542 μ mol) were added and the reaction was stirred at rt for 45 min. In a second flask THF (2.64 mL, 32.58 mmol) and *n*-butyl lithium (16.97 mL, 27.15 mmol, 1.6 M in THF) were dissolved in toluene (20 mL) at -78 °C followed by dropwise addition of trimethylsilyl acetylene (3.86 mL, 27.15 mmol).



After 45 min the first solution was slowly added to the second over a period of 30 min. After stirring for 90 min, glacial acetic acid (3.76 mL, 65.16 mmol) was added and the solution was warmed to 0 °C. Acetic acid solution (10 mL, 10 % in water) was added, the organic layer was separated, dried over Na_2SO_4 and purified on silica gel (hexane: *t*butyl methyl ether; 5:1; v/v) to afford pyranone **51** (2.54 g, 6.25 mmol, 58 %, 87 %ee) as a colourless resin. **R_f-value**: 0.28 (hexane: *t*butyl methyl ether; 5:1; v/v).

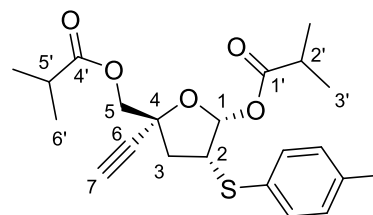
¹H-NMR (300 MHz, Chloroform-*d*1): δ [ppm] = 7.37 (d, $^3J_{H,H}$ = 8.0 Hz, 2H, *H*-Ph), 7.14 (d, $^3J_{H,H}$ = 8.0 Hz, 2H, *H*-Ph), 5.88 (d, $^3J_{H,H}$ = 4.3 Hz, 1H, *H*-1), 3.95 (dd, $^2J_{H,H}$ = 11.7 Hz, $^3J_{H,H}$ = 1.2 Hz, 1H, *H*-5a), 3.63 (dd, $^2J_{H,H}$ = 11.6 Hz, $^3J_{H,H}$ = 1.5 Hz, 1H, *H*-5b), 3.29 (dt, $^3J_{H,H}$ = 6.4, 4.6 Hz, 1H, *H*-2), 2.57 (hept., $^3J_{H,H}$ = 7.0 Hz, 1H, *H*-2'), 2.42 (ddd, $^2J_{H,H}$ = 14.2 Hz, $^3J_{H,H}$ = 4.8 Hz, $^4J_{H,H}$ = 1.1 Hz, 1H, *H*-3a), 2.34 (s, 3H, *H*-MePh), 2.06 (ddd, $^2J_{H,H}$ = 14.3 Hz, $^3J_{H,H}$ = 6.5 Hz, $^4J_{H,H}$ = 1.5 Hz, 1H, *H*-3b), 1.22 – 1.16 (m, 6H, *H*-3'), 0.18 (s, 9H, TMS).

¹³C-NMR (75 MHz, Chloroform-*d*1): δ [ppm] = 175.3 (C_q -1'), 138.7 (C_q -Ph), 133.8 (*C*-Ph), 130.2 (*C*-Ph), 128.6 (C_q -Ph), 105.2 (C_q -4), 93.1 (*C*-1), 90.5 (C_q -6), 70.6 (*C*-5), 65.6 (*C*-7), 44.5 (*C*-2), 37.9 (*C*-3), 34.1 (*C*-2'), 21.3 (*C*-MePh), 18.9 (*C*-3'), 0.0 (TMS).

HRMS-ESI⁺ (*m/z*): $C_{21}H_{30}O_4SSiNa$ [*M*+*Na*]⁺: theo.: 429.1526, found: 429.1540.

(1R,2R,4R)-4-ethynyl-4-((isobutyryloxy)methyl)-2-(p-tolylthio)tetrahydrofuran-1-yl isobutyrate 52

The synthesis was carried out according to the literature²²⁵ with modifications: Pyranone **51** (3.84 g, 9.46 mmol) was dissolved in CH₃CN (25 mL), then HCl (4.98 mL, 4.98 mmol, 1 M in water) was added and the mixture was stirred at rt for 10 h. the reaction process was monitored *via* TLC. After full conversion, toluene (50 mL) was added, the organic layer was washed with potassium phosphate solution (25 mL, 5 % in water) and dried over Na₂SO₄.



C₂₂H₂₈O₅S
404.5210 g/mol

52

The solvents were removed under reduced pressure and exchanged to toluene (50 mL). The mixture was heated to 45 °C and isobutyric anhydride (4.98 mL, 28.4 mmol) as well as levamisole **58** (193 mg, 945 μmol) were added followed by stirring for 72 h at rt. The reaction solution was washed with HCl solution (20 mL, 1 M in water). Remaining anhydride was hydrolysed by adding methanol (15 mL) and DMAP (50 mg). The mixture was washed three times with potassium phosphate solution (50 mL, 5 % in water) and dried over Na₂SO₄. Then, CH₃CN (15 mL), TBA sulphate (643 mg, 1.89 mmol) and water (511 μL, 28.4 mmol) were added to the dried organic phase and cooled to 0 °C. Afterwards, solid potassium phosphate (4.94 g, 28.4 mmol) was added, and the reaction was vigorously stirred for 90 min. The reaction was successively washed twice with ammonium acetate solution (25 mL, 20 % in water) and water (25 mL). The organic layer was dried over Na₂SO₄ and the solvent was exchanged to toluene (10 mL). This solution was added slowly to hexane (100 mL) to precipitate the furanone **52** (2.39 g, 5.92 mmol, 63 %, 89 %ee) as a colourless solid overnight. **R_f-value**: 0.42 (petroleum ether: ethyl acetate; 10:1; v/v).

¹H-NMR (600 MHz, Chloroform-*d*1): δ [ppm] = 7.37 (d, ³J_{H,H} = 8.2 Hz, 2H, *H*-Ph), 7.13 (d, ³J_{H,H} = 7.9 Hz, 2H, *H*-Ph), 6.33 (d, ³J_{H,H} = 1.4 Hz, 1H, *H*-1), 4.21 (d, ²J_{H,H} = 3.6 Hz, 2H, *H*-5), 3.75 (ddd, ³J_{H,H} = 7.7, 3.5, 1.5 Hz, 1H, *H*-2), 2.67 – 2.57 (m, 2H, *H*-3a, *H*-7, *H*-5'), 2.44 (hept., ³J_{H,H} = 7.0 Hz, 1H, *H*-2'), 2.40 (dd, ²J_{H,H} = 13.8 Hz, ³J_{H,H} = 3.5 Hz, 1H, *H*-3b), 2.33 (s, 3H, *H*-MePh), 1.21 – 1.18 (m, 6H, *H*-6'), 1.13 – 1.08 (m, 6H, *H*-3').

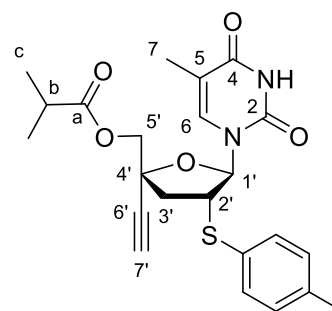
Experimental Procedure

¹³C-NMR (151 MHz, Chloroform-*d*1): δ [ppm] = 176.7 (C_q-4'), 175.3 (C_q-1'), 138.3 (C_q-Ph), 132.7 (C-Ph), 130.2 (C-Ph), 130.1 (C_q-Ph) 102.4 (C-1), 82.5 (C_q-6), 79.8 (C_q-4), 74.9 (C-7), 68.8 (C-5), 52.2 (C-2), 40.3 (C-3), 34.1 (C-5'), 34.0 (C-2'), 21.3 (C-MePh), 19.1 (C-6'), 19.1 (C-6'), 18.8 (C-3'), 18.7 (C-3').

HRMS-ESI⁺ (m/z): C₂₂H₂₈O₅Na [M+Na]⁺: theo.: 427.1550, found: 427.1542.

2'-*p*-Tolythio-5'-((isobutyryloxy)methyl)-3'-deoxy-4'-ethynylthymidine **53**

The synthesis was carried out according to the literature with modifications: Thymine (503 mg, 3.99 mmol) was suspended in CH₃CN (10 mL), then HMDS (825 mL, 3.99 mmol) and TMSOTf (1.19 mL, 6.27 mmol) were added while the temperature was kept below 25 °C. The reaction was stirred for approximately 45 min until all thymine was dissolved. Pyranone **52** (1.15 g, 2.85 mmol) was dissolved in CH₃CN (10 mL) and added dropwise to the reaction over a period of 1 h at 10 °C. The reaction was stirred for 1 h at 10 °C and 3.5 h at rt, until TLC monitoring showed full conversion. The reaction was quenched with



C₂₃H₂₆N₂O₅S
442.5300 g/mol

53

0.5 eq. tribasic potassium phosphate in water (8 mL/g). The resulting slurry was cooled to 0 °C, filtrated and the remaining solid was washed with CH₃CN: water (50:50; v/v; 3 mL/g) and water (20 mL) subsequently. The combined aqueous phases were washed with heptane (40 mL). The solvent of the aqueous phase was removed under reduced pressure and the crude product was purified on RP₁₈ silica gel with automated flash chromatography (H₂O:CH₃CN, 100:0 to 0:100, v/v) to afford **53** (1.05 g, 2.38 mmol, 84 %, 89 %ee) as a colourless solid. $[\alpha]_D^{24}$: +42.2° (c = 0.37, CH₂Cl₂). **R_f-value**: 0.33 (petroleum ether: ethyl acetate; 1:1; v/v)

¹H-NMR (600 MHz, Methanol-*d*4): δ [ppm] = 7.37 (d, ³J_{H,H} = 8.2 Hz, 2H, *H*-Ph), 7.10 (m, 3H, *H*-6, *H*-Ph), 6.16 (d, ³J_{H,H} = 8.6 Hz, 1H, *H*-1'), 4.39 (d, ²J_{H,H} = 11.4 Hz, 1H, *H*-5'a), 4.24 (d, ²J_{H,H} = 11.4 Hz, 1H, *H*-5'b), 3.87 (dt, ³J_{H,H} = 10.2, 8.7 Hz, 1H, *H*-2'), 2.85 (dd, ²J_{H,H} = 13.5 Hz, ³J_{H,H} = 8.9 Hz, 1H, *H*-3'a), 2.67 (hept., ³J_{H,H} = 6.9 Hz, 1H, *H*-b), 2.33 – 2.26 (m, 4H, *H*-3'b, *H*-7', *H*-MePh), 2.30 (s, 3H, *H*-MePh), 1.75 (d, ⁴J_{H,H} = 1.2 Hz, 3H, *H*-7), 1.25 – 1.18 (m, 6H, *H*-c).

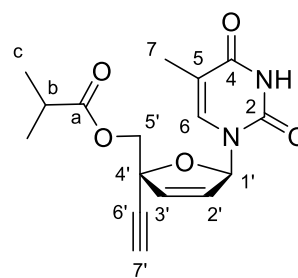
¹³C-NMR (126 MHz, Methanol-*d*4): δ [ppm] = 177.8 (C_q-a), 165.6 (C_q-4), 152.1 (C_q-2), 140.2 (C_q-Ph), 136.9 (C-Ph), 135.3 (C-6), 131.0 (C-Ph), 129.3 (C_q-Ph), 112.3 (C_q-5), 91.3 (C-1'), 83.6 (C-4'), 76.3 (C-7'), 76.3 (C_q-6'), 68.7 (C-5'), 48.6 (C-2'), 41.2 (C-3'), 35.1 (C-b), 21.1 (C-MePh), 19.4 (C-c), 19.4 (C-c), 12.3 (C-7).

HRMS-ESI⁺ (m/z): C₂₃H₂₆N₂O₅Na [M+Na]⁺: theo.: 465.1454, found: 465.1453.

Experimental Procedure

5'-((Isobutyryloxy)methyl)-2',3'-Didehydro-3'-deoxy-4'-ethynylthymidine **54**

To a slurry of thymidine **53** (825 mg, 1.93 mmol) in CH₃CN (10 mL), chloramine-T (525 mg, 2.31 mmol) and glacial acetic acid (11.01 mL, 192 μmol) were added at 20 °C. The reaction was stirred for 2.5 h at 20 °C and quenched with aq. NH₄OAc (5 mL, 10 wt %). Afterwards, CH₂Cl₂ was added and the organic layer was dried over Na₂SO₄, filtered and the solvent was removed under reduced pressure. The crude product was dissolved in *t*-butanol (10 mL) and heated to 95 °C for 1 h. The mixture was cooled to 20 °C to afford Thymidine **54** (445 mg, 1.40 mmol, 72 %, 99 % ee) as a colourless solid. $[\alpha]_D^{24}$: +48.8° (*c* = 0.635, CH₂Cl₂). **R_f-value**: 0.39 (petroleum ether: ethyl acetate; 1:1; v/v).



C₁₆H₁₈N₂O₅
318.3290 g/mol

54

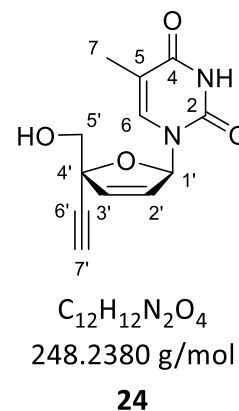
¹H-NMR (300 MHz, Chloroform-*d*1): δ [ppm] = 8.37 (s br, 1H, NH), 7.22 – 7.19 (m, 1H, H-6), 7.10 (dd, ³J_{H,H} = 2.0 Hz, ⁴J_{H,H} = 1.3 Hz, 1H, H-1'), 6.22 (dd, ³J_{H,H} = 5.8 Hz, ⁴J_{H,H} = 2.0 Hz, 1H, H-2'), 5.97 (dd, ³J_{H,H} = 5.8 Hz, ⁴J_{H,H} = 1.3 Hz, 1H, H-3'), 4.60 (d, ²J_{H,H} = 12.1 Hz, 1H, H-5'a), 4.21 (d, ²J_{H,H} = 12.1 Hz, 1H, H-5'b), 2.64 (s, 1H, H-7'), 2.55 (hept., ³J_{H,H} = 6.9 Hz, 1H, H-b), 1.91 (d, ³J_{H,H} = 1.3 Hz, 3H, H-7), 1.19 (s, 3H, H-c), 1.18 (s, 3H, H-c).

¹³C-NMR (75 MHz, Chloroform-*d*1): δ [ppm] = 176.3 (C_q-a), 163.4 (C_q-4), 150.5 (C_q-2), 135.3 (C-6), 134.5 (C-2'), 128.1 (C-3'), 111.5 (C_q-5), 89.7 (C-1'), 84.6 (C_q-4'), 79.2 (C_q-6'), 76.0 (C-7'), 66.8 (C-5'), 34.0 (C-b), 19.2 (C-c), 19.1 (C-c), 12.6 (C-7).

HRMS-ESI⁺ (m/z): C₁₆H₁₈N₂O₅Na [M+Na]⁺: theo.: 341.1108, found: 341.1110.

2',3'-Didehydro-3'-deoxy-4'-ethynylthymidine **24**

The reaction was carried out according to the literature²²⁵ with modifications: To a stirred solution of thymidine analogue **54** (433 mg, 1.36 mmol) in methanol (20 mL) was added DBU (10.2 μ L, 68.0 μ mol) at 20 °C. The reaction was heated to 60 °C and stirred for 15 h. The solvent was removed under reduced pressure and the crude product was purified on RP₁₈ silica gel with automated flash chromatography (H₂O:CH₃CN, 90:10 to 0:100, v/v) to afford thymidine derivative **24** (287 mg, 1.16 mmol, 85 %) as a colourless solid. **HPLC (Method A):** $t_R = 4.37$ min.



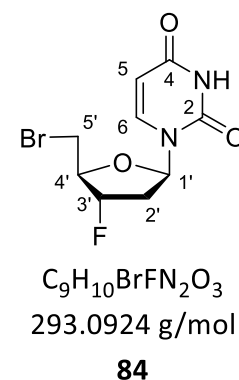
¹H-NMR (300 MHz, Dimethyl sulfoxide-*d*6): δ [ppm] = 11.34 (s, 1H, NH), 7.57 (d, ⁴ $J_{H,H} = 1.3$ Hz, 1H, H-6), 6.88 (dd, ³ $J_{H,H} = 2.0$ Hz, ⁴ $J_{H,H} = 1.4$ Hz, 1H, H-1'), 6.35 (dd, ³ $J_{H,H} = 5.8$, 2.0 Hz, 1H, H-2'), 6.05 (dd, ³ $J_{H,H} = 5.8$ Hz, ⁴ $J_{H,H} = 1.4$ Hz, 1H, H-3'), 5.47 (t, ³ $J_{H,H} = 5.8$ Hz, 1H, OH), 3.70 (dd, ² $J_{H,H} = 12.0$ Hz, ³ $J_{H,H} = 5.9$ Hz, 1H, H-5'a), 3.08 (s, 1H, H-7'), 3.59 (dd, ² $J_{H,H} = 12.0$ Hz, ³ $J_{H,H} = 5.9$ Hz, 1H, H-5'b), 1.71 (d, ⁴ $J_{H,H} = 1.2$ Hz, 1H, H-7).

¹³C-NMR (75 MHz, Dimethyl sulfoxide-*d*6): δ [ppm] = 163.9 (C_q-4), 150.8 (C_q-2), 141.8 (C-4'), 137.2 (C-6), 136.8 (C-2'), 135.5 (C-3'), 127.1 (C-6'), 109.3 (C_q-5), 88.9 (C-1'), 78.2 (C-7'), 65.8 (C-5'), 12.2 (C-7).

HRMS-ESI⁺ (m/z): C₁₂H₁₂N₂O₄Na [M+Na]⁺: theo.: 271.0689, found: 271.0682.

3'-Deoxy-3'-fluorouridine bromide **84**

The reaction was carried out according to the literature²⁶⁴ with modifications: The uridine derivative **28** (230 mg, 1.00 mmol) was dissolved in CH₂Cl₂ (5 mL) and cooled to 0 °C, then tetrabromomethane (398 mg, 1.20 mmol) and triphenylphosphine (393 mg, 1.50 mmol) were added and the reaction was warmed to rt. The reaction was stirred for 3 h and the resulting triphenylphosphine oxide was precipitated with a mixture of ethyl acetate and petroleum ether (3:1; v/v). The reaction was filtered over silica and the crude product was purified on silica gel (petroleum ether: ethyl acetate; 1:1, v/v) to afford crude uridine **84** (244 mg, 833 μ mol, 83 %) as a colourless solid. **R_f-Wert:** 0.55 (CH₂Cl₂: methanol; 95:5; v/v).



Experimental Procedure

¹H-NMR (400 MHz, Chloroform-*d*1): δ [ppm] = 8.55 (s, 1H, NH), 7.65 (d, $^3J_{H,H} = 8.2$ Hz, 1H, H-6), 6.33 (dd, $^3J_{H,H} = 9.3, 5.3$ Hz, 1H, H-1'), 5.80 (dd, $^3J_{H,H} = 8.1, 2.3$ Hz, 1H, H-5), 5.20 (ddd, $^3J_{H,H} = 5.7, 1.4$ Hz, $^2J_{H,F} = 53.8$ Hz, 1H, H-3'), 4.51 (tdd, $^3J_{H,H} = 3.8, 1.5$ Hz, $^3J_{H,F} = 27.1$ Hz, 1H, H-4'), 3.67 (dd, $^3J_{H,H} = 3.8, 1.3$ Hz, 2H, H-5'), 2.65 (dddd, $^3J_{H,F} = 21.5, ^2J_{H,H} = 14.6$ Hz, $^3J_{H,H} = 5.3, 1.1$ Hz, 1H, H-2'a), 2.36 - 2.15 (m, 1H, H-2'b).

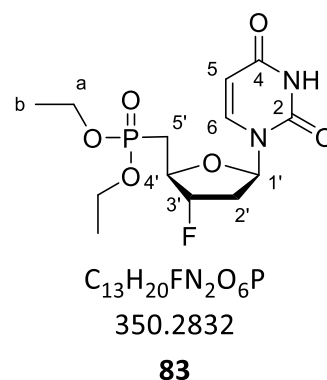
¹³C-NMR (101 MHz, Chloroform-*d*1): δ [ppm] = 162.6 (C_q-4), 150.0 (C_q-2), 139.6 (C-6), 103.3 (C-5), 94.8 (d, $^1J_{C,F} = 180.2$ Hz, C-3'), 85.4 (C-1'), 82.8 (d, $^2J_{C,F} = 28.4$ Hz, C-4'), 38.5 (d, $^2J_{C,F} = 21.5$ Hz, C-2'), 32.6 (d, $^1J_{C,Br} = 10.4$ Hz, C-5').

¹⁹F-NMR (565 MHz, Chloroform-*d*1): δ [ppm] = -174.20 (dddd, $J = 54.0, 36.4, 27.2, 22.1$ Hz).

ESI⁺-MS (m/z): C₉H₁₀BrFN₂O₃Na [M+Na]⁺: theo.: 314.9751, found: 314.9726.

3'-Deoxy-3'-fluorouridine diethylphosphonate **83**

The reaction was carried out according to the literature²⁶⁵ with modifications: The uridine derivative **84** (40 mg, 136 μ mol) was added to triethyl phosphite (124 μ L) in CH₃CN (2 mL) and stirred overnight at 120 °C. The solvent was removed under reduced pressure, the residue was dissolved in CH₂Cl₂ and washed successively with 1 M HCl (15 mL) and saturated NaHCO₃ solution (15 mL). The organic layer was dried over Na₂SO₄ and the solvent was removed under reduced pressure. The crude material was purified on RP₁₈ silica gel with automated flash chromatography (H₂O:CH₃CN, 100:0 to 0:100, v/v) to afford uridine **83** (44 mg, 126 μ mol, 92 %) as a colourless solid. **R_f-Wert:** 0.58 (CH₂Cl₂: methanol; 95:5; v/v).



¹H-NMR (400 MHz, Chloroform-*d*1): δ [ppm] = 9.89 (s, 1H, NH), 7.69 (d, $^3J_{H,H} = 8.1$ Hz, 1H, H-6), 6.21 (dd, $^3J_{H,H} = 8.9, 5.6$ Hz, 1H, H-1'), 5.74 (dd, $^3J_{H,H} = 8.2, 1.8$ Hz, 1H, H-5), 5.29 (ddt, $^3J_{H,F} = 54.1$ Hz, $^3J_{H,H} = 5.8, 1.6$ Hz, 1H, H-3'), 4.57 - 4.38 (m, 1H, H-4'), 4.22 - 4.01 (m, 4H, CH₂-ethyl), 2.68 - 2.53 (m, 1H, H-2'a), 2.41 - 2.28 (m, 1H, H-2'b), 2.25 - 2.13 (m, 2H, H-5'), 1.30 (q, $^3J_{H,H} = 6.8$ Hz, 6H, CH₃-ethyl).

Experimental Procedure

¹³C-NMR (101 MHz, Chloroform-*d*1): δ [ppm] = 163.6 (*C*_q-2), 150.4 (*C*_q-4), 140.4 (*C*-6), 103.0 (*C*-5), 95.3 (dd, ¹*J*_{C,F} = 170.0, 7.7 Hz, *C*-3'), 85.7 (*C*-1'), 80.0 (dd, ¹*J*_{C,F} = 28.7, 4.0 Hz, *C*-4'), 62.4 (d, ²*J*_{C,P} = 6.5 Hz, CH₂-ethyl), 62.1 (d, ²*J*_{C,P} = 6.6 Hz, CH₂-ethyl), 37.5 (d, ²*J*_{C,F} = 21.6 Hz, *C*-2'), 29.6 (dd, ¹*J*_{C,F} = 141.5, 7.7 Hz, *C*-5'), 16.44 (t, ³*J*_{C,P} = 5.3 Hz, CH₃-ethyl).

³¹P-NMR (162 MHz, Chloroform-*d*1): δ [ppm] = 25.35 (s).

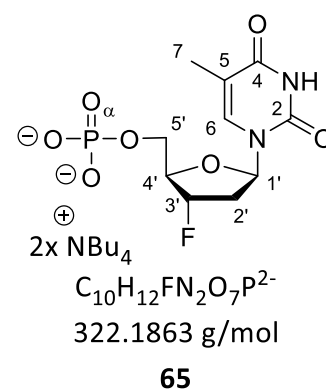
¹⁹F-NMR (565 MHz, Chloroform-*d*1): δ [ppm] = -173.07 (dddd, *J* = 55.4, 35.4, 26.5, 21.6 Hz).

HRMS-ESI⁺ (m/z): C₁₃H₂₁FN₂O₆P [M+H]⁺: theo.: 351.1116, found: 351.1124.

6.2.5. Synthesis of Triphosphate Prodrugs

3'-Deoxy-3'-fluorothymidine monophosphate **65**

The reaction was carried out according to the literature¹⁷⁷ with modifications: POCl₃ (604 μ L, 6.62 mmol) was dissolved in CH₃CN (1.43 mL, 27.2 mmol) and cooled to 0 °C. Pyridine (581 mL, 7.22 mmol) and H₂O (75.9 μ L, 4.21 mmol) were subsequently added drop-wise to the solution and stirred at 0 °C for 10 min. The appropriate nucleoside (367 mg, 1.50 mmol) was added and stirred for 2.5 h at 0 °C. The reaction was poured into ice-cold water and stirred for 30 min at 0 °C. The pH value was adjusted to 8 with solid NH₄HCO₃. The solvent was



removed by freeze drying and the crude product was purified on RP₁₈ silica gel with automated flash chromatography (H₂O:CH₃CN, 100:0 to 0:100, v/v) then 10 % aq. TBA hydroxide (2.0 eq.) was added and all volatiles were evaporated. The residue was purified on RP₁₈ silica gel with automated flash chromatography (H₂O: CH₃CN, 100:0 to 0:100, v/v) to afford **65** (1.19 g, 1.29 mmol, 86 %) as a colourless resin. **HPLC (Method A):** *t*_R = 7.49 min.

¹H-NMR (600 MHz, Water-*d*2): δ [ppm] = 7.84 (d, ⁴*J*_{H,H} = 1.4 Hz, 1H, *H*-6), 6.44 (dd, ³*J*_{H,H} = 9.5 Hz, 5.5 Hz, 1H, *H*-1'), 5.46 (dd, ²*J*_{H,F} = 52.9 Hz, ³*J*_{H,H} = 4.7 Hz, 1H, *H*-3'), 4.53 (dd, ³*J*_{H,F} = 27.5 Hz, ³*J*_{H,H} = 2.8 Hz, 1H, *H*-4'), 4.10 (ddd, ²*J*_{H,H} = 21.0 Hz, ³*J*_{H,P} = 5.0 Hz, ³*J*_{H,H} = 3.0 Hz, 1H, *H*-5'a), 4.06 - 4.01 (m, 1H, *H*-5'b), 3.27 - 3.15 (m, 16H, CH₂-NBu₄), 2.67 - 2.59 (m, 1H, *H*-2'a), 2.41 (dddd, ³*J*_{H,F} = 41.4 Hz, ²*J*_{H,H} = 14.9 Hz, ³*J*_{H,H} = 9.5, 4.8 Hz, *H*-2'b), 1.93 (d, ⁴*J*_{H,H} = 1.2 Hz, 3H, *H*-7), 1.67 (qu, ³*J*_{H,H} = 7.6 Hz, 16H, CH₂-NBu₄), 1.38 (sext., ³*J*_{H,H} = 7.4 Hz, 16H, CH₂-NBu₄), 0.97 (t, ³*J*_{H,H} = 7.4 Hz, 16H, CH₃-NBu₄).

¹³C-NMR (151 MHz, Water-*d*2): δ [ppm] = 166.5 (*C*_q-4), 151.8 (*C*_q-2), 137.3 (*C*-6), 112.0 (*C*-5), 95.1 (d, ¹*J*_{C,F} = 174 Hz, ⁴*J*_{C,P} = 12.4 Hz, *C*-3'), 84.9 (d, ³*J*_{C,F} = 4.9 Hz *C*-1'), 84.0 (td, ²*J*_{C,F} = 25.6 Hz, ³*J*_{C,P} = 7.8 Hz, *C*-4'), 64.3 (dd, ³*J*_{C,F} = 11.6 Hz, ²*J*_{C,P} = 4.8 Hz, *C*-5'), 37.3 (d, ²*J*_{C,F} = 20.6 Hz, *C*-2'), 11.6 (CH₃).

Experimental Procedure

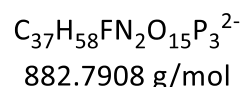
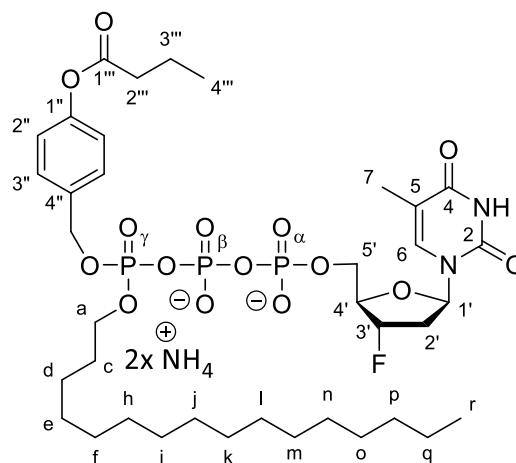
³¹P-NMR (162 MHz, Water-*d*2): δ [ppm] = 1.06 (s).

¹⁹F-NMR (565 MHz, Water-*d*2): δ [ppm] = -174.47 (dddd, $J_{F,H}$ = 53.5, 41.3, 28.0, 21.7 Hz).

ESI-MS (m/z): C₁₀H₁₃FN₂O₇P [M-H]⁻: theo.: 323.0459, found: 323.0406.

3'-Deoxy-3'-fluorothymidine (4-butynonylbenzyl)- γ -hexadecyl triphosphate **35a**

The synthesis of pyrophosphate was carried out according to general procedure 4: Synthesis of pyrophosphate. With *H*-phosphonate **18a** (248 mg, 500 μ mol), NCS (167 mg, 1.25 mmol) and 0.4 M TBA phosphate monobasic (3.75 mL, 1.50 mmol) in CH₃CN (3.0 mL). After purification the obtained pyrophosphate was used in the synthesis of triphosphate **35a** according to general procedure 4: Preparation of γ -AB-triphosphates. With pyrophosphate **19a** (231 mg, 400 μ mol, *n*Bu₄N⁺), TFAA (282 μ L, 2.00 mmol) and Et₃N (446 μ L, 3.20 mmol) in CH₃CN (3 mL). The second step was carried out with



35a

Et₃N (267 μ L, 2.00 mmol), 1-methylimidazole (79.8 μ L, 1.00 mmol), FLTMP **65** (186 mg, 200 μ mol, *n*Bu₄N⁺) and the activated pyrophosphate **19a** in CH₃CN (3 mL). After evaporation of all volatiles the crude product was purified on RP₁₈-silica gel with automated flash chromatography (H₂O:CH₃CN, 100:0 to 0:100, v/v) followed by ion exchange chromatography (NH₄⁺). Subsequent purification on RP₁₈-silica gel with automated flash chromatography (H₂O:CH₃CN, 100:0 to 0:100, v/v) afforded the γ -modified triphosphate **35a** (59.0 mg, 64.0 μ mol, 33 %) as a colourless solid. **HPLC (Method A):** t_R = 15.28 min.

¹H-NMR (600 MHz, Methanol-*d*4): δ [ppm] = 7.84 (q, $^4J_{H,H}$ = 1.4 Hz, 1H, *H*-6), 7.58 – 7.43 (m, 2H, *H*-3''), 7.10 – 7.04 (m, 2H, *H*-2''), 6.46 – 6.27 (m, 1H, *H*-1'), 5.50 (dq, $^2J_{H,F}$ = 52.8 Hz, $^3J_{H,H}$ = 2.8 Hz, 1H, *H*-3'), 5.22 – 5.18 (m, 2H, CH₂Ph), 4.35 (dq, $^3J_{H,F}$ = 27.5 Hz, $^3J_{H,H}$ = 2.9 Hz, 1H, *H*-4'), 4.31 – 4.27 (m, 1H, *H*-5'a), 4.20 – 4.16 (m, 1H, *H*-5'b), 2.56 (t, $^3J_{H,H}$ = 7.3 Hz, 2H, *H*-2'''), 2.50 – 2.30 (m, 2H, *H*-2'), 1.96 – 1.91 (m, 3H, CH₃), 1.76 (sext, $^3J_{H,H}$ = 7.6 Hz, 2H, *H*-3'''), 1.62 (quint, $^3J_{H,H}$ = 6.7 Hz, 2H, CH₂-alkyl), 1.35 – 1.27 (m, 28H, CH₂-alkyl), 1.04 (t, $^3J_{H,H}$ = 7.4 Hz, 3H, *H*-4'''), 0.90 (t, $^3J_{H,H}$ = 7.0 Hz, 3H, CH₃-alkyl).

¹³C-NMR (151 MHz, Methanol-*d*4): δ [ppm] = 173.5 (C_q-1'''), 166.4 (C_q-4), 152.5 (C_q-2), 152.4 (C_q-1''), 137.9 (C-6), 135.1 (d, $^3J_{C,P}$ = 7.6 Hz, C_q-4''), 130.4 (C-3''), 130.3 (C-3'), 122.9 (C-2''), 112.4 (C_q-5), 96.3 (d, $^1J_{C,F}$ = 174.7 Hz, C-3'), 85.9 (C-1'), 85.4 (dd, $^2J_{C,F}$ = 26.3 Hz, $^3J_{C,P}$ = 9.6 Hz, C-4'), 70.2 (dd, $^2J_{C,P}$ = 5.7, 3.3 Hz,

Experimental Procedure

CH₂Ph), 69.8 (d, ²J_{C,P} = 6.2 Hz, CH₂-alkyl), 66.7 (dd, ³J_{C,F} = 12.2 Hz, ²J_{C,P} = 5.7 Hz, C-5'), 38.8 (d, ²J_{C,F} = 20.5 Hz, C-2'), 36.9 (C-2'''), 33.1 - 23.7 (CH₂-alkyl), 19.4 (C-3'''); 14.4 (CH₃-alkyl), 13.9 (C-4'''), 12.6 (CH₃).

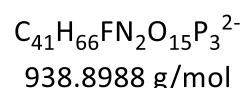
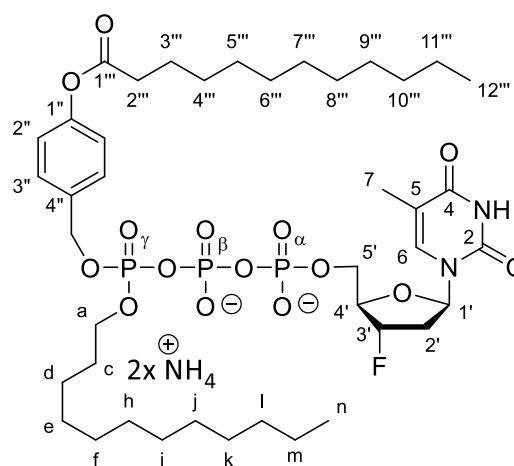
³¹P-NMR (243 MHz, Methanol-*d*4): δ [ppm] = -12.04 (d, ²J_{P,P} = 18.9 Hz, *P*-α), -12.62 – -13.38 (m, *P*-γ), -23.66 (t, ²J_{P,P} = 18.0 Hz, *P*-β).

¹⁹F-NMR (565 MHz, Methanol-*d*4): δ [ppm] = -175.4 - -175.7 (m)

HRMS-ESI⁺ (m/z): C₃₇H₆₁FN₂O₁₅P₃ [M+H]⁺: theo.: 885.3263, found: 885.3267.

3'-Deoxy-3'-fluorothymidine (4-dodecanoyloxybenzyl)-γ-dodecyl triphosphate **35b**

The synthesis of pyrophosphate was carried out according to general procedure 4: Synthesis of pyrophosphate. With *H*-phosphonate **18b** (269 mg, 500 μmol), NCS (167 mg, 1.25 mmol) and 0.4 M TBA phosphate monobasic (3.75 mL, 1.50 mmol) in CH₃CN (3.0 mL). After purification the obtained pyrophosphate was used in the synthesis of triphosphate **35b** according to general procedure 4: Preparation of γ-AB-triphosphates. With pyrophosphate **19b** (408 mg, 466 μmol, *n*Bu₄N⁺), TFAA (328 μL, 2.33 mmol) and Et₃N (519 μL, 3.73 mmol) in CH₃CN (3.0 mL). The second step was carried out with



35b

Et₃N (324 μL, 2.33 mmol), 1-methylimidazole (92.9 μL, 1.17 mmol), FLTMP **65** (170 mg, 233 μmol, *n*Bu₄N⁺) and the activated pyrophosphate **19b** in CH₃CN (3.0 mL). After evaporation of all volatiles the crude product was purified on RP₁₈-silica gel with automated flash chromatography (H₂O:CH₃CN, 100:0 to 0:100, v/v) followed by ion exchange chromatography (NH₄⁺). Subsequent purification on RP₁₈-silica gel with automated flash chromatography (H₂O:CH₃CN, 100:0 to 0:100, v/v) afforded the γ-modified triphosphate **35b** (103.0 mg, 107.2 μmol, 46 %) as a colourless solid. **HPLC (Method A):** t_R = 17.25 min.

Experimental Procedure

¹H-NMR (600 MHz, Methanol-*d*4): δ [ppm] = 7.89 – 7.82 (m, 1H, *H*-6), 7.53 - 7.45 (m, 2H, *H*-3''), 7.13 - 7.06 (m, 2H, *H*-2''), 6.43 - 6.34 (m, 1H, *H*-1'), 5.60 – 5.45 (m, 1H, *H*-3'), 5.26 - 5.19 (m, 2H, *CH*₂Ph), 4.39 – 4.28 (m, 2H, *H*-4', *H*-5'a), 4.23 – 4.17 (m, 1H, *H*-5'b), 4.15 – 4.07 (m, 2H, *CH*₂-alkyl), 2.58 (t, ³*J*_{H,H} = 7.4 Hz, 2H, *CH*₂-alkyl), 2.47 - 2.34 (m, 2H, *H*-2'), 1.96 – 1.92 (m, 3H, *H*-7), 1.74 (qu, ³*J*_{H,H} = 7.4 Hz, 2H, *CH*₂-alkyl), 1.62 (qu, ³*J*_{H,H} = 6.6 Hz, 2H, *CH*₂-alkyl), 1.47 – 1.40 (m, 2H, *CH*₂-alkyl), 1.40 – 1.25 (m, 32H, *CH*₂-alkyl), 0.96 – 0.84 (m, 6H, *CH*₃-alkyl).

¹³C-NMR (151 MHz, Methanol-*d*4): δ [ppm] = 173.7 (*C*_q-1'''), 166.4 (*C*_q-4), 152.5 (*C*_q-2), 152.4 (*C*_q-1''), 137.9 (*C*-6), 135.1 (*C*_q-4''), 130.4 (*C*-3''), 130.3 (*C*-3''), 122.9(*C*-2''), 112.4 (*C*_q-5), 96.4 (d, ¹*J*_{C,F} = 174.7 Hz, *C*-3'), 85.9 (*C*-1'), 85.3 (*C*-4'), 70.3 (d, ²*J*_{C,P} = 5.7 Hz, *CH*₂Ph), 69.8 (d, ²*J*_{C,P} = 6.2 Hz, *CH*₂-alkyl), 66.7 (dd, ³*J*_{C,F} = 12.2 Hz, ²*J*_{C,P} = 5.7 Hz, *C*-5'), 38.8 (d, ²*J*_{C,F} = 20.5 Hz, *C*-2'), 35.0 – 23.7 (*CH*₂-alkyl), 14.4 (*CH*₃-alkyl), 12.6 (*CH*₃).

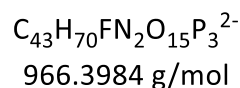
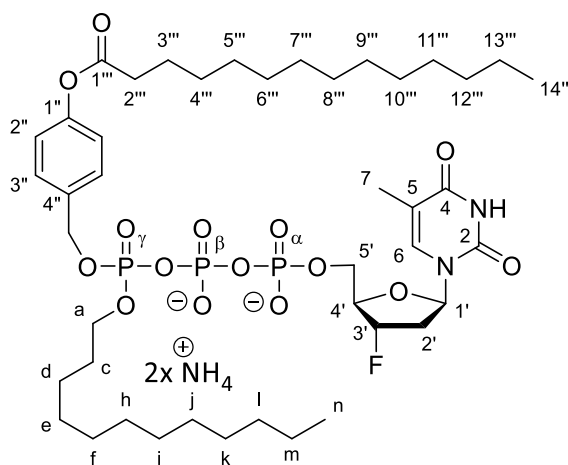
³¹P-NMR (243 MHz, Methanol-*d*4): δ [ppm] = -12.08 (d, ²*J*_{P,P} = 19.2 Hz, *P*- α), -12.50 – -13.31 (m, *P*- γ), -23.66 (t, ²*J*_{P,P} = 18.0 Hz, *P*- β).

¹⁹F-NMR (565 MHz, Methanol-*d*4): δ [ppm] = -175.56 (ddt, *J*_{F,H} = 52.8, 37.3, 27.1 Hz).

HRMS-ESI⁺ (m/z): C₄₁H₆₉FN₂O₁₅P₃ [M+H]⁺: theo.: 941.3890, found: 941.3852.

3'-Deoxy-3'-fluorothymidine (4-tetradecanoyloxybenzyl)- γ -dodecyl triphosphate 35c

The synthesis of pyrophosphate was carried out according to general procedure 4: Synthesis of pyrophosphate. With *H*-phosphonate **18c** (141.3 mg, 250 μ mol), NCS (86 mg, 630 μ mol) and 0.4 M TBA phosphate monobasic (1.88 mL, 750 μ mol) in CH₃CN (3.0 mL). After purification the obtained pyrophosphate was used in the synthesis of triphosphate **35c** according to general procedure 4: Preparation of γ -AB-triphosphates. With pyrophosphate **19c** (151 mg, 167 μ mol, *n*Bu₄N⁺), TFAA (139 μ L, 985 μ mol) and Et₃N (220 μ L, 1.58 mmol) in CH₃CN (3.0 mL). The second step was carried out with Et₃N (137 μ L, 985 μ mol), 1-methylimidazole (39.3 μ L, 492 μ mol), FLTMP **64** (133 mg, 98.5 μ mol, *n*Bu₄N⁺) and the activated pyrophosphate **19c** in CH₃CN (3.0 mL). After evaporation of all volatiles the crude product was purified on RP₁₈-silica gel with automated flash chromatography (H₂O:CH₃CN, 100:0 to 0:100, v/v) followed by ion exchange chromatography (NH₄⁺). Subsequent purification on RP₁₈-silica gel with automated flash chromatography (H₂O:CH₃CN, 100:0 to 0:100, v/v) afforded the γ -modified triphosphate **35c** (33.1 mg, 33.5 μ mol, 34 %) as a colourless solid. **HPLC (Method A):** *t*_R = 17.86 min.

**35c**

¹H-NMR (600 MHz, Water-*d*2): δ [ppm] = 7.82 – 7.80 (m, 1H, *H*-6), 7.31 – 7.28 (m, 2H, *H*-3''), 6.93 – 6.89 (m, 2H, *H*-2''), 6.43 (dd, ³*J*_{H,H} = 9.5, 5.5 Hz, 1H, *H*-1'), 5.53 (dd, ²*J*_{H,F} = 52.8 Hz, ³*J*_{H,H} = 4.6 Hz, 1H, *H*-3'), 4.57 – 4.54 (m, 2H, CH₂Ph), 4.33 – 4.16 (m, 3H, *H*-4', *H*-5'), 3.99 – 3.93 (m, 2H, CH₂-alkyl), 2.66 – 2.32 (m, 2H, *H*-2'), 2.50 – 2.40 (m, 2H, CH₂-alkyl), 1.94 (d, ⁴*J*_{H,H} = 1.2 Hz, 3H, *H*-7), 1.74 (qu, ³*J*_{H,H} = 7.4 Hz, 2H, CH₂-alkyl), 1.73 – 1.65 (m, 2H, CH₂-alkyl), 1.65 – 1.58 (m, 2H, CH₂-alkyl), 1.53 – 1.42 (m, 2H, CH₂-alkyl), 1.40 – 1.17 (m, 35H, CH₂-alkyl), 0.92 – 0.81 (m, 6H, CH₃-alkyl).

Experimental Procedure

^{13}C -NMR (151 MHz, Water-*d*2): δ [ppm] = 173.9 (C_q -1''), 166.5 (C_q -4), 155.1 (C_q -2), 151.2 (C_q -1'), 137.2 (C -6), 132.1 (C_q -4''), 129.5 (C -3''), 115.4 (C -2''), 112.1 (C_q -5), 95.0 (d, $^1J_{C,F}$ = 174.0 Hz, C -3'), 84.9 (C -1'), 83.7 (C -4'), 67.2 (CH_2Ph), 65.6 (CH_2 -alkyl), 63.5 (C -5'), 37.4 (C -2'), 35.0 - 23.7 (CH_2 -alkyl), 13.2 (CH_3 -alkyl), 11.7 (CH_3).

^{31}P -NMR (243 MHz, Water-*d*2): δ [ppm] = -10.44 – -11.57 (m, P - α), -12.08 (d, $^2J_{P,P}$ = 18.2 Hz, P - γ), -22.62 – -25.40 (m, P - β).

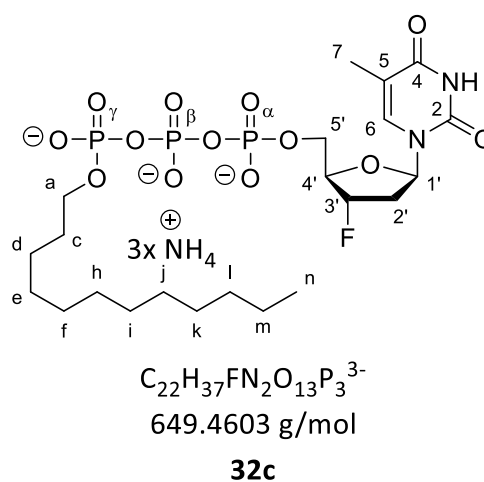
^{19}F -NMR (565 MHz, Water-*d*2): δ [ppm] = -173.99 - -174.55 (m).

MALDI-MS⁺ (m/z): $\text{C}_{43}\text{H}_{73}\text{FN}_2\text{O}_{15}\text{P}_3$ [$\text{M}+\text{H}$]⁺ theo: 969.420, found: 969.453.

3'-Deoxy-3'-fluorothymidine γ -dodecyl triphosphate **32c**

The synthesis of pyrophosphate was carried out according to general procedure 4: Synthesis of pyrophosphate. With *H*-phosphonate **38a** (166 mg, 500 μmol), NCS (167 mg, 1.25 mmol) and 0.4 M TBA phosphate monobasic (3.75 mL, 1.50 mmol) in CH_3CN (3.0 mL). After purification the obtained pyrophosphate was used in the synthesis of triphosphate **32c** according to general procedure 4: Preparation of γ -alkyl-triphosphates. With pyrophosphate **39a** (255 mg, 398 μmol , $n\text{Bu}_4\text{N}^+$), TFAA (281 μL , 1.99 mmol) and Et_3N (445 μL , 3.19 mmol) in CH_3CN (3 mL).

The second step was carried out with Et_3N (267 μL , 1.99 mmol), 1-methylimidazole (79.3 μL , 996 μmol), FLTMP **65** (185 mg, 199 μmol , $n\text{Bu}_4\text{N}^+$) and the activated pyrophosphate **39a** in CH_3CN (3mL). Removal of the cyanoethyl protecting group was performed with 10.0 eq. TBA hydroxide overnight. After evaporation of all volatiles the crude product was purified on RP_{18} -silica gel with automated flash chromatography ($\text{H}_2\text{O}:\text{CH}_3\text{CN}$, 100:0 to 0:100, v/v) followed by ion exchange chromatography (NH_4^+). Subsequent purification on RP_{18} -silica gel with automated flash chromatography ($\text{H}_2\text{O}:\text{CH}_3\text{CN}$, 100:0 to 0:100, v/v) afforded the γ -modified triphosphate **32c** (61.6 mg, 54.3 μmol , 27 %) as a colourless solid. **HPLC (Method A):** t_R = 12.19 min.



Experimental Procedure

¹H-NMR (600 MHz, Water-d₂): δ [ppm] = 7.81 – 7.78 (m, 1H, H-6), 6.44 (dd, ³J_{H,H} = 9.7, 5.5 Hz, 1H, H-1'), 5.54 (dd, ²J_{H,F} = 52.7 Hz, ³J_{H,H} = 4.6 Hz, 1H, H-3'), 4.57 - 4.50 (m, 1H, H-4'), 4.33 – 4.16 (m, 2H, H-5'), 3.94 (q, ³J_{H,H} = 6.9 Hz, 2H, CH₂-alkyl), 2.62 (ddd, ³J_{H,F} = 20.8 Hz, ²J_{H,H} = 14.9 Hz, ³J_{H,H} = 5.5 Hz, 1H, H-2'a), 2.41 (dddd, ³J_{H,F} = 42.0 Hz, ²J_{H,H} = 14.6 Hz, ³J_{H,H} = 9.7, 4.8 Hz, 1H, H-2'b), 1.95 (d, ⁴J_{H,H} = 1.2 Hz, 3H, H-7), 1.61 (qu, ³J_{H,H} = 6.9 Hz, 2H, CH₂-alkyl), 1.35 - 1.21 (m, 18H, CH₂-alkyl), 0.88 - 0.84 (m, 3H, CH₃-alkyl).

¹³C-NMR (151 MHz, Water-d₂): δ [ppm] = 167.3 (C_q-4), 152.1 (C_q-2), 137.2 (C-6), 112.1 (C_q-5), 95.1 (d, ¹J_{C,F} = 173.9 Hz, C-3'), 84.9 (C-1'), 84.0 - 83.6 (m, C-4'), 66.9 (d, ²J_{C,P} = 6.2 Hz, CH₂-alkyl), 65.4 (dd, ³J_{C,F} = 12.3 Hz, ²J_{C,P} = 5.8 Hz, C-5'), 37.3 (d, ³J_{C,F} = 20.5 Hz, C-2'), 31.2 - 22.1 (CH₂-alkyl), 13.4 (CH₃-alkyl), 11.8 (C-7).

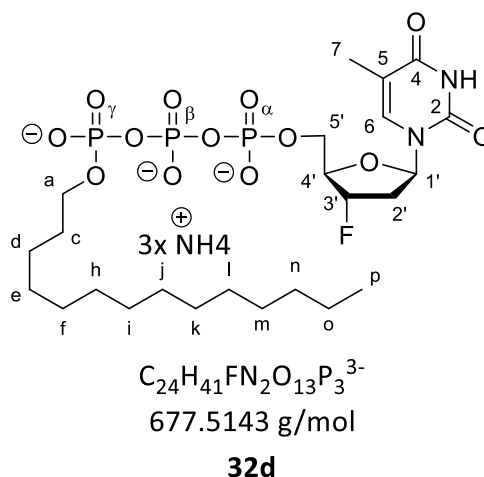
¹⁹F-NMR (565 MHz, Water-d₂): δ [ppm] = -174.15 (m).

³¹P-NMR (243 MHz, Water-d₂): δ [ppm] = -10.88 (d, ²J_{P,P} = 19.3 Hz, P- α), -11.87 (d, ²J_{P,P} = 18.5 Hz, P- γ), -23.12 (t, ²J_{P,P} = 18.8 Hz, P- β).

MALDI-MS⁺ (m/z): C₂₂H₄₁FN₂O₁₃P₃ [M+H]⁺ theo: 653.180, found: 653.054.

3'-Deoxy-3'-fluorothymidine γ -tetradecyl triphosphate **32d**

The synthesis of pyrophosphate was carried out according to general procedure 4: Synthesis of pyrophosphate. With *H*-phosphonate **38b** (374 mg, 1.13 mmol), NCS (376 mg, 2.81 mmol) and 0.4 M TBA phosphate monobasic (8.44 mL, 3.37 mmol) in CH₃CN (3.0 mL). After purification the obtained pyrophosphate was used in the synthesis of triphosphate **32d** according to general procedure 4: Preparation of γ -alkyl-triphosphates. With pyrophosphate



38b (601 mg, 900 μ mol, *n*Bu₄N⁺), TFAA (634 μ L, 4.50 mmol) and Et₃N (1.00 mL, 7.20 mmol) in CH₃CN (3 mL). The second step was carried out with Et₃N (625 μ L, 4.50 mmol), 1-methylimidazole (179 μ L, 2.25 μ mol), FLTMP **65** (417 mg, 450 μ mol, *n*Bu₄N⁺) and the activated pyrophosphate **39a** in CH₃CN (3 mL). Removal of the cyanoethyl protecting group was performed with 10.0 eq. TBA hydroxide overnight. After evaporation of all volatiles the crude product was purified on RP₁₈-silica gel with automated flash chromatography (H₂O:CH₃CN, 100:0 to 0:100, v/v) followed by ion exchange chromatography (NH₄⁺). Subsequent purification on RP₁₈-silica gel with automated flash chromatography (H₂O:CH₃CN, 100:0 to 0:100, v/v) afforded γ -modified triphosphate **32d** (203 mg, 277 μ mol, 61 % with 0.2 eq. *n*Bu₄N⁺) as a colourless solid. **HPLC (Method A)**: *t*_R = 13.41 min.

¹H-NMR (600 MHz, Water-*d*₂): δ [ppm] = 7.82 – 7.80 (m, 1H, *H*-6), 6.44 (dd, ³*J*_{H,H} = 9.7, 5.5 Hz, 1H, *H*-1'), 5.55 (dd, ²*J*_{H,F} = 52.7 Hz, ³*J*_{H,H} = 4.6 Hz, 1H, *H*-3'), 4.53 (dd, ²*J*_{H,F} = 27.6 Hz, ³*J*_{H,H} = 2.9 Hz, 1H, *H*-4'), 4.32 – 4.15 (m, *H*-5'), 3.94 (q, ³*J*_{H,H} = 6.9 Hz, 2H, CH₂-alkyl), 2.62 (ddd, ³*J*_{H,F} = 20.9 Hz, ²*J*_{H,H} = 14.9 Hz, ³*J*_{H,H} = 5.5 Hz, 1H, *H*-2'a), 2.41 (dddd, ³*J*_{H,F} = 42.1 Hz, ²*J*_{H,H} = 14.7 Hz, ³*J*_{H,H} = 9.7, 4.7 Hz, 1H, *H*-2'b), 1.95 (d, ⁴*J*_{H,H} = 1.2 Hz, 3H, *H*-7), 1.68 - 1.57 (m, CH₂-alkyl), 1.40 - 1.21 (m, 22H, CH₂-alkyl), 0.95 (t, ³*J*_{H,H} = 7.4 Hz, 2H, *n*Bu₄N), 0.90 – 0.84 (m, CH₃-alkyl).

Experimental Procedure

^{13}C -NMR (151 MHz, Water-*d*2): δ [ppm] = 167.2 (C_{q-4}), 151.1 (C_{q-2}), 137.1 ($C-6$), 112.1 (C_{q-5}), 95.1 ($C-3'$), 84.8 ($C-1'$), 83.9 ($C-4'$), 67.0 (CH_2 -alkyl), 65.5 ($C-5'$), 37.4 ($C-2'$), 31.2 - 22.1 (CH_2 -alkyl), 13.5 (CH_3 -alkyl), 11.7 ($C-7$).

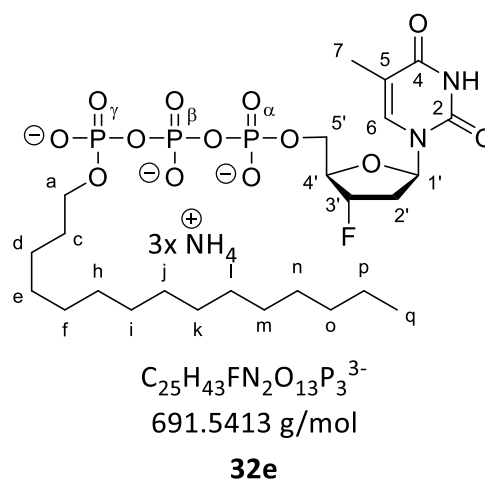
^{19}F -NMR (565 MHz, Water-*d*2): δ [ppm] = -174.02 - -174.32 (m).

^{31}P -NMR (243 MHz, Water-*d*2): δ [ppm] = -10.95 (d, $^2J_{P,P} = 18.9$ Hz, $P-\alpha$), -11.93 (d, $^2J_{P,P} = 18.3$ Hz, $P-\gamma$), -23.06 - -22.84 (m, $P-\beta$).

MALDI-MS⁺ (m/z): $\text{C}_{24}\text{H}_{45}\text{FN}_2\text{O}_{13}\text{P}_3$ [$\text{M}+\text{H}$]⁺ theo: 681.211, found: 681.220.

3'-Deoxy-3'-fluorothymidine γ -tetradecyl triphosphate **32e**

The synthesis of pyrophosphate was carried out according to general procedure 4: Synthesis of pyrophosphate. With *H*-phosphonate **38c** (116 mg, 335 μmol), NCS (112 mg, 836 μmol) and 0.4 M TBA phosphate monobasic (2.51 mL, 1.00 mmol) in CH_3CN (3.0 mL). After purification the obtained pyrophosphate was used in the synthesis of triphosphate **32e** according to general procedure 4: Preparation of γ -alkyl-triphosphates. With pyrophosphate **39c** (271 mg, 398 μmol , $n\text{Bu}_4\text{N}^+$), TFAA (280 μL , 1.99 mmol) and Et_3N (446 μL , 3.18 mmol) in CH_3CN (3 mL).



The second step was carried out with Et_3N (279 μL , 1.99 mmol), 1-methylimidazole (78 μL , 994 μmol), FLTMP **65** (256 mg, 199 μmol , $n\text{Bu}_4\text{N}^+$) and the activated pyrophosphate **39a** in CH_3CN (3 mL). Removal of the cyanoethyl protecting group was performed with 10.0 eq. TBA hydroxide overnight. After evaporation of all volatiles the crude product was purified on RP_{18} -silica gel with automated flash chromatography ($\text{H}_2\text{O}:\text{CH}_3\text{CN}$, 100:0 to 0:100, v/v) followed by ion exchange chromatography (NH_4^+). Subsequent purification on RP_{18} -silica gel with automated flash chromatography ($\text{H}_2\text{O}:\text{CH}_3\text{CN}$, 100:0 to 0:100, v/v) afforded the γ -modified triphosphate **32e** (39.6 mg, 53.1 μmol , 27 %) as a colourless solid.

HPLC (Method A): $t_R = 14.76$ min.

Experimental Procedure

¹H-NMR (600 MHz, Water-d₂): δ [ppm] = 7.81 – 7.78 (m, 1H, H-6), 6.36 (dd, ³J_{H,H} = 9.3, 5.6 Hz, 1H, H-1'), 5.58 – 5.46 (m, 1H, H-3'), 4.52 – 4.46 (m, 1H, H-4'), 4.30 – 4.15 (m, 2H, H-5'), 3.95 (q, ³J_{H,H} = 6.8 Hz, 2H, CH₂-alkyl), 2.61 (ddd, ³J_{H,F} = 20.8 Hz, ²J_{H,H} = 14.7 Hz, ³J_{H,H} = 5.5 Hz, 1H, H-2'a), 2.40 (dddd, ³J_{H,F} = 41.6 Hz, ²J_{H,H} = 14.7 Hz, ³J_{H,H} = 9.5, 4.8 Hz, 1H, H-2'b), 1.94 (d, ⁴J_{H,H} = 1.1 Hz, 3H, H-7), 1.62 (qu, ³J_{H,H} = 7.0 Hz, 2H, CH₂-alkyl), 1.33 - 1.22 (m, 24H, CH₂-alkyl), 0.85 (t, ³J_{H,H} = 6.9 Hz, 3H, CH₃-alkyl).

¹³C-NMR (151 MHz, Water-d₂): δ [ppm] = 166.7 (C_q-4), 151.8 (C_q-2), 137.6 (C-6), 112.0 (C_q-5), 96.0 (C-3'), 85.7 (C-1'), 84.5 (C-4'), 67.4 (CH₂-alkyl), 65.9 (C-5'), 38.1 (C-2') 30.5 - 22.8 (CH₂-alkyl), 14.1 (CH₃-alkyl), 12.2 (C-7).

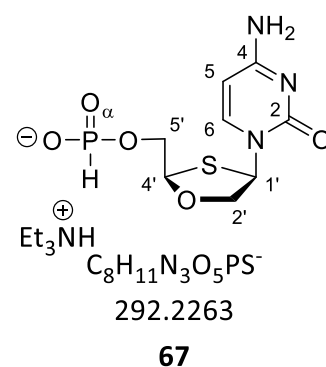
¹⁹F-NMR (565 MHz, Water-d₂): δ [ppm] = -173.94 - -174.27 (m).

³¹P-NMR (243 MHz, Water-d₂): δ [ppm] = -10.98 (d, ²J_{P,P} = 18.7 Hz, P- α), -11.93 (d, ²J_{P,P} = 18.7 Hz, P- γ), -22.98 (t, ²J_{P,P} = 18.8 Hz, P- β).

MALDI-MS⁺ (m/z): C₂₅H₄₆FN₂O₁₃P₃Na [M+Na]⁺ theo: 717.208, found: 717.257.

(-)-2'-Deoxy-3'-oxa-4'-thiocytidine-H-phosphonate **67**

The reaction was performed according to the literature²⁴² with modifications: Under stirring dOTC **26** (100 mg, 436 μ mol) in pyridine (2.20 mL) was added to DPP (249 μ L, 1.31 mmol) at rt. The reaction process was monitored by TLC. After 30 min a mixture of water and pyridine (0.90 mL; 1:1; v/v) was added and stirred for additional 15 min. The solvent was removed under reduced pressure and the crude product was purified on silica gel with automated flash chromatography (ethyl acetate:methanol; 1:0 to 7:3 +1 % triethylamine; 15 min; v/v) to afford dOTC phosphonate **67** (160 mg, 406 μ mol, 93 %) as a colourless foam.



Experimental Procedure

¹H-NMR (400 MHz, Water-d₂): δ [ppm] = 8.12 (d, $^3J_{H,H}$ = 7.6 Hz, 1H, H-6), 6.78 (d, $^1J_{H,P}$ = 643.8 Hz, 1H, PH), 6.37 (d, $^3J_{H,H}$ = 4.4 Hz, 1H, H-1'), 6.05 (d, $^3J_{H,H}$ = 7.6 Hz, 1H, H-5), 5.44 (dd, $^3J_{H,H}$ = 4.4, 2.7 Hz, 1H, H-4'), 4.55 (d, $^2J_{H,H}$ = 11.0 Hz, 1H, H-2'a), 4.33 (ddd, $^3J_{H,P}$ = 11.0 Hz, $^3J_{H,H}$ = 8.2, 2.5 Hz, 1H, H-5'a), 4.17 (ddd, $^3J_{H,P}$ = 12.3 Hz, $^3J_{H,H}$ = 8.6, 4.3 Hz, 1H, H-5'b), 4.09 (dd, $^2J_{H,H}$ = 11.0 Hz, $^3J_{H,H}$ = 4.5 Hz, 1H, H-2'b), 3.19 (q, $^3J_{H,H}$ = 7.3 Hz, Et₃N), 1.27 (t, $^3J_{H,H}$ = 7.3 Hz, Et₃N).

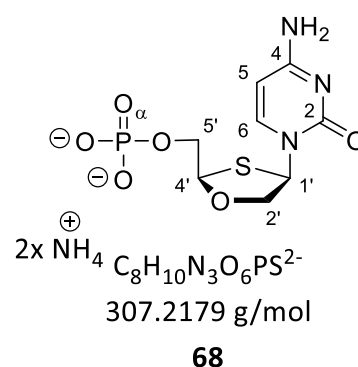
¹³C-NMR (101 MHz, Water-d₂): δ [ppm] = 165.9 (C_q-4), 158.0 (C_q-2), 143.0 (C-6), 96.5 (C-5), 86.0 (d, $^3J_{C,P}$ = 6.9 Hz, C-4'), 76.9 (C-2'), 64.1 (C-1'), 63.5 (d, $^2J_{C,P}$ = 4.4 Hz, C-5'), 46.6 (Et₃N), 8.2 (Et₃N).

³¹P-NMR (162 MHz, Water-d₂): δ [ppm] = 6.50 (s).

HRMS-ESI⁺ (m/z): C₈H₁₃N₃O₅PS [M+H]⁺: theo.: 294.0308, found: 294.0303.

(-)-2'-Deoxy-3'-oxa-4'-thiocytidine monophosphate **68**

Method A: (oxaziridine) The reaction was performed according to the literature²⁴⁷ with modifications: The phosphonate dOTC **67** (169 mg, 428 μ mol) was suspended in DMF (2.00 mL) and afterwards bis(trimethylsilyl)acetamide (524 μ L, 214 μ mol) was added followed by stirring for 10 min at rt. CSO **72a** (196 mg, 857 mmol) was added and the mixture was stirred for additional 10 min at rt. Then a mixture of methanol and DBU (2.20 mL, 97:3; v/v) was added and stirred for 10 min. The reaction mixture was poured into a mixture of water and pyridine (22.0 mL; 1:1; v/v) and washed with CH₂Cl₂ (3x 20 mL). The solvent of the aqueous phase was removed under reduced pressure and the crude product was purified with ion exchange chromatography on sephadex (water:5 M NH₄HCO₃; 100:0 to 0:100; v/v) to afford dOTC phosphate **68** (129 mg, 377 μ mol, 88 %) as a colourless solid.



Method B: (iodine) The reaction was performed according to the literature²⁴⁹ with modifications: The phosphonate dOTC **67** (70.0 mg, 187 μ mol) was suspended in pyridine (370 μ L) and afterwards bis(trimethylsilyl)acetamide (229 μ L, 935 μ mol) was added followed by stirring for 60 min at rt. Iodine (57.0 mg, 224 μ mol) in DMF (340 μ L) was added dropwise. After two minutes, the reaction was hydrolysed with water (340 μ L, 18.7 mmol) and the mixture was stirred for additional 5 min. All volatiles were removed under reduced pressure and the crude product was purified sequentially with ion exchange chromatography on sephadex (water:5 M NH₄HCO₃; 100:0 to 0:100; v/v) and automated flash chromatography on RP₁₈-silica gel (H₂O:CH₃CN, 100:0 to 0:100, v/v) to afford dOTC phosphate **68** (37.4 mg, 109 μ mol, 58 %) as a colourless solid.

Experimental Procedure

Method C: (YOSHIKAWA) The reaction was performed according to the literature²⁴² with modifications: To a suspension of dOTC **26** (92.2 mg, 402 μmol) in trimethyl phosphate (1.40 mL, 12.1 mmol) was added POCl_3 (376 μL , 4.02 mmol) and the mixture was stirred for 50 min at 0 °C. The reaction progress was monitored via HPLC (method A). After reaching maximum conversion, the reaction was poured onto 1 M triethylammonium bicarbonate buffer (15 mL) and stirred for 15 min. The solvent of the aqueous phase was removed under reduced pressure and the crude product was purified with ion exchange chromatography on sephadex (water:5 M NH_4HCO_3 ; 100:0 to 0:100; v/v) to afford dOTC phosphate **68** (39.0 mg, 132 μmol , 33 %) as a colourless solid. **HPLC (Method A):** $t_R = 7.85$ min.

$^1\text{H-NMR}$ (400 MHz, Water-*d*2): δ [ppm] = 8.21 (d, $^3J_{\text{H,H}} = 7.6$ Hz, 1H, *H*-6), 6.42 (d, $^3J_{\text{H,H}} = 4.3$ Hz, 1H, *H*-1'), 6.10 (d, $^3J_{\text{H,H}} = 7.6$ Hz, 1H, *H*-5), 5.48 (dd, $^3J_{\text{H,H}} = 4.6$, 3.1 Hz, 1H, *H*-4'), 4.57 (d, $^2J_{\text{H,H}} = 10.9$ Hz, 1H, *H*-2'a), 4.31 (ddd, $^3J_{\text{H,P}} = 11.7$ Hz, $^3J_{\text{H,H}} = 6.0$, 3.0 Hz, 1H, *H*-5'a), 4.19 (ddd, $^3J_{\text{H,P}} = 11.7$ Hz, $^3J_{\text{H,H}} = 6.5$, 5.0 Hz, 1H, *H*-5'b), 4.12 (d, $^2J_{\text{H,H}} = 10.9$ Hz, 1H, *H*-2'b).

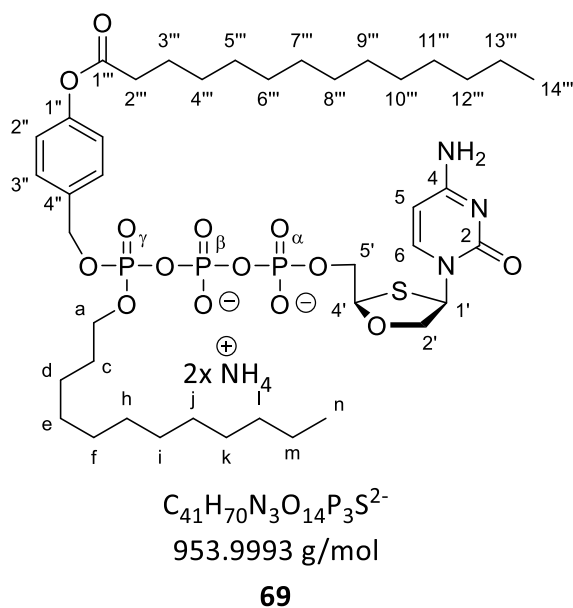
$^{13}\text{C-NMR}$ (101 MHz, Water-*d*2): δ [ppm] = 165.4 (*C*_q-4), 157.0 (*C*_q-2), 143.3 (*C*-6), 96.5 (*C*-5), 86.2 (d, $^3J_{\text{C,P}} = 8.5$ Hz, *C*-4'), 77.1 (*C*-2'), 65.0 (d, $^2J_{\text{C,P}} = 4.7$ Hz, *C*-5'), 64.0 (*C*-1').

$^{31}\text{P-NMR}$ (162 MHz, Water-*d*2): δ [ppm] = 0.68 (s).

HRMS-ESI⁺ (m/z): $\text{C}_8\text{H}_{13}\text{N}_3\text{O}_6\text{PS}$ [$\text{M}+\text{H}$]⁺: theo.: 310.0257, found: 310.0246.

(-)-2'-Deoxy-3'-oxa-4'-thiocytidine (4-tetradecanoyloxybenzyl)- γ -dodecyl triphosphate 69

The synthesis of pyrophosphate was carried out according to general procedure 2: Synthesis of pyrophosphate. With *H*-phosphonate **18c** (142 mg, 250 μ mol), NCS (69.0 mg, 0.50 mmol) and 0.4 M TBA phosphate monobasic (1.56 mL, 0.63 mmol) in CH₃CN (3.0 mL). After purification the obtained pyrophosphate was used in the synthesis for triphosphate **69** according to general procedure 7: Preparation of γ -AB-triphosphates. With pyrophosphate **19c** (170 mg, 195 μ mol, *n*Bu₄N⁺), TFAA (141 μ L, 1.00 mmol) and Et₃N (223 μ L, 1.60 mmol) in CH₃CN (3.0 mL). The second step was carried out with Et₃N (101 μ L, 1.00 μ mol), 1-methylimidazole (39.9 μ L, 500 μ mol), dOTCMP **67** (34.3 mg, 100 μ mol, H₄N⁺) and the activated pyrophosphate **19c** in CH₃CN (3.0 mL). After evaporation of all volatiles the crude product was purified on RP₁₈-silica gel with automated flash chromatography (H₂O:CH₃CN, 100:0 to 0:100, v/v) followed by ion exchange chromatography (NH₄⁺). Subsequent purification on RP₁₈-silica gel with automated flash chromatography (H₂O:CH₃CN, 100:0 to 0:100, v/v) afforded the γ -modified triphosphate **69** (43.2 mg, 44.4 μ mol, 44 %) as a colourless solid. **HPLC (Method A):** t_R = 17.60 min.



¹H-NMR (600 MHz, Methanol-*d*4): δ [ppm] = 8.31 (d, ³*J*_{H,H} = 7.7 Hz, 1H, *H*-6), 7.50 (d, ³*J*_{H,H} = 8.6 Hz, 2H, *H*-3''), 7.07 (d, ³*J*_{H,H} = 8.5 Hz, 2H, *H*-2''), 6.42 – 6.37 (m, 1H, *H*-1'), 6.04 (d, ³*J*_{H,H} = 7.7 Hz, 1H, *H*-5), 5.40 (t, ³*J*_{H,H} = 3.5 Hz, 1H, *H*-4'), 5.25 (dd, ²*J*_{H,H} = 8.1 Hz, 2H, CH₂Ph), 4.51 - 4.46 (m, 1H, *H*-5'a), 4.43 - 4.38 (m, 2H, *H*-5'b, *H*-2'a), 4.18 – 4.10 (m, 2H, CH₂-alkyl), 3.97 (ddd, ²*J*_{H,H} = 10.6 Hz, ³*J*_{H,H} = 4.4, 1.3 Hz, 1H, *H*-2'b), 3.26 - 3.19 (m, 15H, CH₂-NBu₄), 2.57 (t, ³*J*_{H,H} = 7.4 Hz, 2H, CH₂-alkyl), 1.73 (qu, ³*J*_{H,H} = 7.4 Hz, 2H, CH₂-alkyl), 1.69 - 1.57 (m, 18H, CH₂-alkyl, CH₂-NBu₄), 1.47 – 1.37 (m, 16H, CH₂-alkyl, CH₂-NBu₄), 1.36 - 1.22 (m, 47H, CH₂-alkyl), 1.02 (t, ³*J*_{H,H} = 7.4 Hz, 23H, CH₃-NBu₄), 0.94 – 0.85 (m, 6H, CH₃-alkyl).

Experimental Procedure

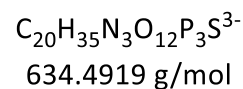
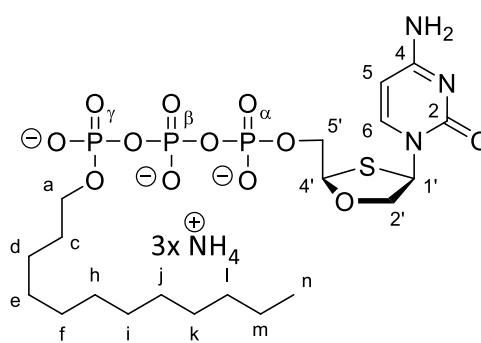
^{13}C -NMR (151 MHz, Methanol- d_4): δ [ppm] = 173.7 (C_q -1'''), 167.7 (C_q -4), 154.7 (C_q -4), 152.2 (C_q -1''), 145.8 (C -6), 135.5 (C_q -4''), 130.4 (C -2''), 122.8 (C -3''), 96.5 (C -5), 88.4 (d, $J_{C,P}$ = 8.5 Hz, C -4'), 78.9 (C -2'), 70.2 (d, $J_{C,P}$ = 5.5 Hz, CH_2Ph), 69.8 (d, $J_{C,P}$ = 6.4 Hz, OCH_2), 67.3 (C -5'), 65.2 (C -1'), 59.5 ($\text{CH}_2\text{-NBu}_4$), 35.1 ($\text{CH}_2\text{-alkyl}$), 33.1 ($\text{CH}_2\text{-alkyl}$), 30.8 - 26.0 ($\text{CH}_2\text{-alkyl}$), 24.8 ($\text{CH}_2\text{-NBu}_4$), 23.8 ($\text{CH}_2\text{-alkyl}$), 23.8 ($\text{CH}_2\text{-alkyl}$), 20.7 ($\text{CH}_2\text{-NBu}_4$), 14.5 ($\text{CH}_3\text{-alkyl}$), 14.5 ($\text{CH}_3\text{-alkyl}$), 14.0 ($\text{CH}_3\text{-NBu}_4$).

^{31}P -NMR (243 MHz, Methanol- d_4): δ [ppm] = -12.20 (d, $J_{P,P}$ = 20.8 Hz, P - α), -13.28 (d, $J_{P,P}$ = 20.8 Hz, P - γ), -24.15 (t, $J_{P,P}$ = 19.1 Hz, P - β).

HRMS-ESI $^+$ (m/z): $\text{C}_{41}\text{H}_{71}\text{N}_3\text{O}_{14}\text{P}_3\text{S}$ [$\text{M}+\text{H}$] $^+$: theo.: 954.3864, found: 954.3907.

(-)-2'-Deoxy-3'-oxa-4'-thiocytidine γ -decyl triphosphate **70**

The synthesis of pyrophosphate was carried out according to general procedure 4: Synthesis of pyrophosphate. With H-phosphonate **38a** (75.9 mg, 250 μmol), NCS (83.6 mg, 625 μmol) and 0.4 M TBA phosphate monobasic (1.87 mL, 750 μmol) in CH_3CN (3 mL). After purification the obtained pyrophosphate was used in the synthesis for triphosphate **70** according to general procedure 4: Preparation of γ -alkyl-triphosphates. With pyrophosphate **39a** (113 mg, 176 μmol , $n\text{Bu}_4\text{N}^+$), TFAA (141 μL , 1.00 mmol) and Et_3N (223 μL , 1.60 mmol) in DMF (3 mL). The second step was



70

carried out with Et_3N (101 μL , 1.00 mmol), 1-methylimidazole (40.0 μL , 500 μmol), dOTCMP **68** (81.0 mg, 100 μmol , $n\text{Bu}_4\text{N}^+$) and the activated pyrophosphate **39a** in CH_3CN (3 mL). Removal of the cyanoethyl protecting group was performed with 10.0 eq. TBA hydroxide overnight. After evaporation of all volatiles the crude product was purified on RP_{18} -silica gel with automated flash chromatography ($\text{H}_2\text{O}:\text{CH}_3\text{CN}$, 100:0 to 0:100, v/v) followed by ion exchange chromatography (NH_4^+). Subsequent purification on RP_{18} -silica gel with automated flash chromatography ($\text{H}_2\text{O}:\text{CH}_3\text{CN}$, 100:0 to 0:100, v/v) afforded γ -modified triphosphate **70** (21.3 mg, 30.9 μmol , 31 %) as a colourless solid. **HPLC (Method A):** t_R = 12.41 min.

^1H -NMR (600 MHz, Water- d_2): δ [ppm] = 8.56 – 8.49 (m, 1H, H -6), 6.44 - 6.39 (m, 1H, H -1'), 6.45 – 6.39 (m, 1H, 1H'), 5.53 - 5.46 (m, 1H, H -4'), 4.61 – 4.55 (m, 1H, H -2'a), 4.54 – 4.46 (m, 1H, H -5'a), 4.36 - 4.28 (m, 1H, H -5'b), 4.14 - 4.08 (m, 1H, H -2'b), 4.04 - 3.89 (m, 2H, H - $\text{CH}_2\text{-alkyl}$), 1.68 - 1.57 (m, 2H, $\text{CH}_2\text{-alkyl}$), 1.40 - 1.20 (m, 16H, $\text{CH}_2\text{-alkyl}$), 0.97 - 0.91 (m, 2H, $\text{CH}_2\text{-alkyl}$), 0.86 (t, $^3J_{H,H}$ = 6.8 Hz, 3H, $\text{CH}_3\text{-alkyl}$).

Experimental Procedure

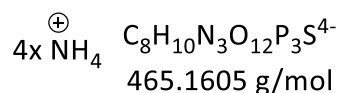
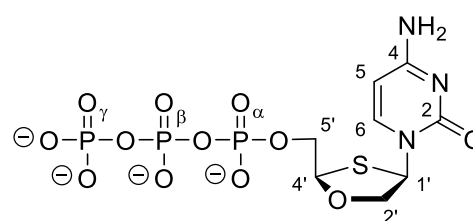
$^{13}\text{C-NMR}$ (151 MHz, Water-*d*2): δ [ppm] = 159.6 (*C*_q-4), 149.0 (*C*_q-2), 146.0 (*C*-6), 95.2 (*C*-5), 85.9 (*C*-4'), 77.3 (*C*-2'), 67.0 (*CH*₂-alkyl), 64.9 (*C*-5'), 63.9 (*C*-1'), 29.9 - 19.2 (*CH*₂-alkyl), 13.5 (*CH*₂-alkyl), 12.4 (*CH*₂-alkyl).

$^{31}\text{P-NMR}$ (162 MHz, Methanol-*d*4): δ [ppm] = -11.94 (d, $^2J_{\text{P,P}}$ = 19.2 Hz, *P*- α), -13.63 (d, $^2J_{\text{P,P}}$ = 16.8 Hz, *P*- γ), -23.76 (t, $^2J_{\text{P,P}}$ = 18.1 Hz, *P*- β).

MALDI-MS⁺ (m/z): C₂₀H₃₉N₃O₁₂P₃S [M+H]⁺ theo: 638.146, found: 638.113.

(-)-2'-Deoxy-3'-oxa-4'-thiocytidine triphosphate **71**

The reaction was performed according to general procedure 5: Nucleoside Triphosphates: With dOTCMP **68** (45.2 mg, 100 μmol , *n*Bu₄N⁺), TFAA (141 μL , 1.00 mmol) and Et₃N (223 μL , 1.60 mmol) in CH₃CN (3.00 mL). After the first activation step the triphosphate was synthesised with Et₃N (101 μL , 100 μmol), 1-methylimidazole (47.8 μL , 600 μmol) and pyrophosphate (271 mg, 300 μmol , *n*Bu₄N⁺) in CH₃CN (8.0 mL). The reaction was washed with CHCl₃ (3x



71

10 mL) the solvent was removed under reduced pressure and the crude product was purified on RP₁₈ silica gel with automated flash chromatography (H₂O:CH₃CN, 100:0 to 0:100, v/v). followed by an ion exchange chromatography (NH₄⁺) and purification on RP₁₈ silica gel with automated flash chromatography (H₂O:CH₃CN, 100:0 to 0:100, v/v) to afford triphosphate **71** (31.8 mg, 59.2 μmol , 59 %) as a colourless solid. **HPLC (Method A):** t_{R} = 9.87 min.

$^1\text{H-NMR}$ (600 MHz, Water-*d*2): δ [ppm] = 8.32 (d, $^3J_{\text{H,H}}$ = 7.8 Hz, 1H, *H*-6), 6.43 – 6.39 (m, 1H, *H*-1'), 6.20 (d, $^3J_{\text{H,H}}$ = 7.8 Hz, 1H, *H*-5), 5.51 - 5.47 (m, 1H, *H*-4'), 4.60 – 4.56 (m, 1H, *H*-2'a), 4.47 (ddd, $^2J_{\text{H,H}}$ = 12.1 Hz, $^3J_{\text{H,H}}$ = 6.5, 2.6 Hz, 1H, *H*-5'a), 4.30 (ddd, $^2J_{\text{H,H}}$ = 12.0 Hz, $^3J_{\text{H,H}}$ = 7.2, 4.4 Hz, 1H, *H*-5'b), 4.11 (dd, $^2J_{\text{H,H}}$ = 11.0 Hz, $^3J_{\text{H,H}}$ = 4.4 Hz, 1H, *H*-2'b).

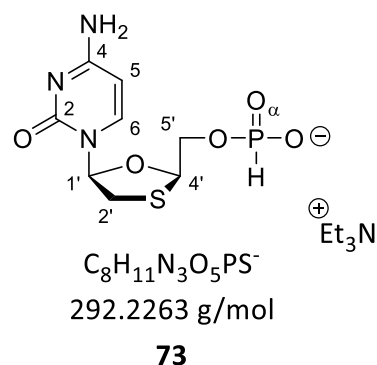
$^{13}\text{C-NMR}$ (151 MHz, Water-*d*2): δ [ppm] = 162.4 (*C*_q-4), 153.5 (*C*_q-2), 144.7 (*C*-6), 96.0 (*C*-5), 86.0 (d, $^3J_{\text{C,P}}$ = 8.7 Hz, *C*-4'), 77.1 (*C*-2'), 65.6 (d, $^2J_{\text{C,P}}$ = 5.2 Hz, *C*-5'), 64.2 (*C*-1').

$^{31}\text{P-NMR}$ (243 MHz, Water-*d*2): δ [ppm] = -10.72 (d, $^2J_{\text{P,P}}$ = 19.4 Hz, *P*- α), -11.52 (d, $^2J_{\text{P,P}}$ = 19.2 Hz, *P*- γ), -23.06 (t, $^2J_{\text{P,P}}$ = 19.2 Hz, *P*- β).

MALDI-MS⁺ (m/z): C₈H₁₄N₃O₁₂P₃SNa [M+Na]⁺ theo: 491.940, found: 491.738.

(-)-2'-Deoxy-3'-thiocytidine-*H*-phosphonate **73**

The reaction was performed according to the literature²⁴² with modifications: Under stirring, 3TC **25** (300 mg, 1.31 mmol) in pyridine (5.00 mL) was added to DPP (786 μ L, 3.93 mmol) at rt. The reaction process was monitored by TLC. After 30 min a solution of water and pyridine (1.00 mL; 1:1; v/v) was added and the mixture was stirred for additional 15 min. The solvent was removed under reduced pressure and the crude product was purified on silica gel with automated flash chromatography (ethyl acetate: methanol; 1:0 to 7:3 + 1% triethylamine; 15 min; v/v) to afford 3TC phosphonate **73** (488 mg, 1.24 mmol, 93 %) as a colourless foam.



¹H-NMR (600 MHz, Water-*d*2): δ [ppm] = 8.05 (d, ³*J*_{H,H} = 7.6 Hz, 1H, *H*-6), 6.80 (d, ¹*J*_{H,P} = 642.5 Hz, 1H, *PH*), 6.34 (dd, ³*J*_{H,H} = 5.3, 4.6 Hz, 1H, *H*-1'), 6.07 (d, ³*J*_{H,H} = 7.6 Hz, 1H, *H*-5), 5.45 (t, ³*J*_{H,H} = 3.7 Hz, 1H, *H*-4'), 4.29 (ddd, ²*J*_{H,H} = 11.3 Hz, ³*J*_{H,H} = 8.1, 3.0 Hz, 1H, *H*-5'a), 4.16 (ddd, ²*J*_{H,H} = 12.3 Hz, ³*J*_{H,H} = 8.3, 4.3 Hz, 1H, *H*-5'b), 3.56 (dd, ²*J*_{H,H} = 12.3 Hz, ³*J*_{H,H} = 5.5 Hz, 1H, *H*-2'a), 3.24 (dd, ²*J*_{H,H} = 12.3 Hz, ³*J*_{H,H} = 4.4 Hz, 1H, *H*-2'b), 3.20 (q, ³*J*_{H,H} = 7.3 Hz, Et₃N), 1.28 (t, ³*J*_{H,H} = 7.3 Hz, Et₃N).

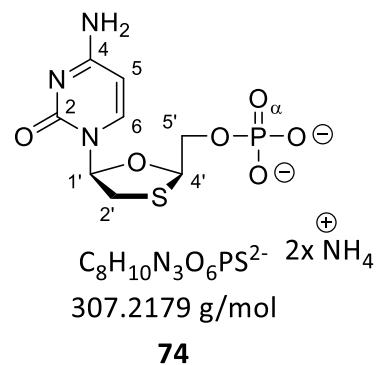
¹³C-NMR (151 MHz, Water-*d*2): δ [ppm] = 165.6 (*C*_q-4), 156.5 (*C*_q-2), 141.9 (*C*-6), 95.8 (*C*-5), 87.4 (*C*-1'), 84.3 (d, ³*J*_{C,P} = 7.2 Hz, *C*-4'), 64.1 (d, ²*J*_{C,P} = 4.3 Hz, *C*-5'), 46.6 (Et₃N), 36.7 (*C*-2'), 8.2 (Et₃N).

³¹P-NMR (243 MHz, Water-*d*2): δ [ppm] = 6.46 (s).

HRMS-ESI⁺ (m/z): C₈H₁₂N₃O₅PSNa [M+Na]⁺: theo.: 316.0128, found: 316.0119.

(-)-2'-Deoxy-3'-thiocytidine monophosphate **74**

The reaction was performed according to the literature²⁴⁷ with modifications: 3TC phosphonate **73** (469 mg, 1.19 mmol) was suspended in DMF (2.00 mL) and afterwards bis(trimethylsilyl)acetamide (1.45 mL, 2.38 mmol) was added followed by stirring for 10 min at rt. DCSO **72b** (710 mg, 2.38 mmol) was added and the reaction was stirred for additional 10 min at rt, then a mixture of methanol and DBU (2.20 mL, 97:3; v/v) was added followed by stirring for 10 min. The reaction mixture was poured into a mixture of water and pyridine (22.0 mL; 1:1; v/v) and washed with CH₂Cl₂ (3x 20 mL). The solvent of the aqueous phase was removed under reduced pressure and the crude product was purified by ion exchange chromatography on



Experimental Procedure

sephadex (water:5 M NH_4HCO_3 ; 100:0 to 0:100; v/v) to afford 3TC monophosphate **74** (375 mg, 1.09 mmol, 92 %) as a colourless solid. **HPLC (Method A)**: $t_R = 7.57$ min.

$^1\text{H-NMR}$ (400 MHz, Water-*d*2): δ [ppm] = 8.17 (d, $^3J_{\text{H,H}} = 7.7$ Hz, 1H, *H*-6), 6.34 (dd, $^3J_{\text{H,H}} = 5.4$, 4.0 Hz, 1H, *H*-1'), 6.11 (d, $^3J_{\text{H,H}} = 7.7$ Hz, 1H, *H*-5), 5.42 – 5.38 (m, 1H, *H*-4'), 4.30 (ddd, $^2J_{\text{H,H}} = 11.8$ Hz, $^3J_{\text{H,H}} = 6.0$, 3.1 Hz, 1H, *H*-5'a), 4.16 (ddd, $^2J_{\text{H,H}} = 11.8$ Hz, $^3J_{\text{H,H}} = 6.3$, 4.3 Hz, 1H, *H*-5'b), 3.58 (dd, $^2J_{\text{H,H}} = 12.4$ Hz, $^3J_{\text{H,H}} = 3.9$ Hz, 1H, *H*-2'a), 3.28 (dd, $^2J_{\text{H,H}} = 12.4$ Hz, $^3J_{\text{H,H}} = 3.9$ Hz, 1H, *H*-2'b).

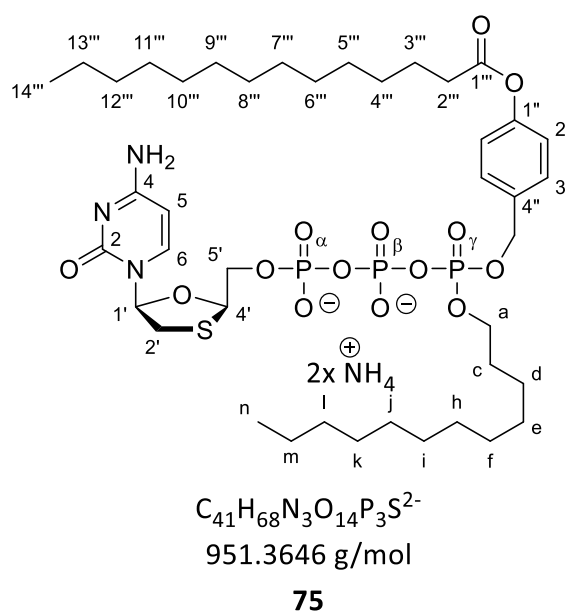
$^{13}\text{C-NMR}$ (151 MHz, Water-*d*2): δ [ppm] = 163.9 ($C_{\text{q-4}}$), 154.3 ($C_{\text{q-2}}$), 142.8 ($C_{\text{-6}}$), 95.4 ($C_{\text{-5}}$), 67.4 ($C_{\text{-1'}}$), 85.0 (d, $^3J_{\text{C,P}} = 8.7$ Hz, $C_{\text{-4'}}$), 65.2 (d, $^2J_{\text{C,P}} = 4.8$ Hz, $C_{\text{-5'}}$), 37.0 ($C_{\text{-2'}}$).

$^{31}\text{P-NMR}$ (243 MHz, Water-*d*2): δ [ppm] = 0.10 (s).

HRMS-ESI⁺ (m/z): $\text{C}_8\text{H}_{13}\text{N}_3\text{O}_6\text{PS}$ [$\text{M}+\text{H}$]⁺: theo.: 310.0257, found: 310.0254.

(-)-2'-Deoxy-3'-thiocytidine (4-tetradecanoyloxybenzyl)- γ -dodecyl triphosphate **75**

The synthesis of the pyrophosphate was carried out according to general procedure 4: Synthesis of pyrophosphate. With *H*-phosphonate **18c** (141.6 mg, 250 μmol), NCS (69.0 mg, 0.50 mmol) and 0.4 M TBA phosphate monobasic (1.56 mL, 0.63 mmol) in CH_3CN (3.0 mL). After purification the obtained pyrophosphate was used in the synthesis for triphosphate **75** according to general procedure 4: Preparation of γ -AB-triphosphates. With pyrophosphate **19c** (184 mg, 211 μmol , $n\text{Bu}_4\text{N}^+$), TFAA (141 μL , 1.00 mmol) and Et_3N (223 μL , 1.60 mmol) in CH_3CN (3.0 mL). The second step was carried out with Et_3N (101 μL , 1.00 μmol), 1-methylimidazole (39.9 μL , 500 μmol), 3TCMP **74** (34.3 mg, 100 μmol , H_4N^+) and the activated pyrophosphate **19c** in CH_3CN (3.0 mL). After evaporation of all volatiles the crude product was purified on RP_{18} -silica gel with automated flash chromatography ($\text{H}_2\text{O}:\text{CH}_3\text{CN}$, 100:0 to 0:100, v/v) followed by ion exchange chromatography (NH_4^+). Subsequent purification on RP_{18} -silica gel with automated flash chromatography ($\text{H}_2\text{O}:\text{CH}_3\text{CN}$, 100:0 to 0:100, v/v) afforded the γ -modified triphosphate **75** (24.7 mg, 25.3 μmol , 25 %) as a colourless solid. **HPLC (Method A)**: $t_R = 17.60$ min.



Experimental Procedure

¹H-NMR (400 MHz, Methanol-*d*4): δ [ppm] = 8.23 – 8.19 (m, 1H, *H*-6), 7.52 (d, $^3J_{\text{H,H}} = 8.6$ Hz, 2H, *H*-2''), 7.08 (d, $^3J_{\text{H,H}} = 8.6$ Hz, 2H, *H*-3''), 6.24 (t, $^3J_{\text{H,H}} = 4.8$ Hz, 1H, *H*-1'), 6.06 – 6.00 (m, 1H, *H*-5), 5.46 – 5.41 (m, 1H, *H*-4'), 5.27 (d, $^3J_{\text{H,H}} = 8.1$ Hz, 2H, *CH*₂Ph), 4.53 – 4.45 (m, 1H, *H*-5'a), 4.42 – 4.35 (m, 1H, *H*-5'b), 4.20 – 4.12 (m, 2H, *CH*₂-alkyl), 3.47 (dd, $^2J_{\text{H,H}} = 12.1$ Hz, $^3J_{\text{H,H}} = 5.2$ Hz, 1H, *H*-2'a), 3.29 – 3.20 (m, *CH*₂-NBu₄), 3.17 (dd, $^2J_{\text{H,H}} = 12.1$ Hz, $^3J_{\text{H,H}} = 4.5$ Hz, 1H, *H*-2'b), 2.58 (t, $^3J_{\text{H,H}} = 7.4$ Hz, 2H, *CH*₂-alkyl), 1.79 – 1.59 (m, *CH*₂-NBu₄, *CH*₂-alkyl), 1.49 – 1.37 (m, *CH*₂-NBu₄, *CH*₂-alkyl), 1.37 – 1.23 (m, 34H, *CH*₂-alkyl), 1.04 (t, $^3J_{\text{H,H}} = 7.3$ Hz, *CH*₃-NBu₄), 0.95 – 0.87 (m, 6H, *CH*₃-alkyl).

¹³C-NMR (126 MHz, Methanol-*d*4): δ [ppm] = 174.1 (*C*_q-1'''), 162.6 (*C*_q-4), 152.5 (*C*_q-1''), 150.5 (*C*_q-2), 146.0 (*C*-5), 135.7 (*C*_q-4''), 130.4 (*C*-2''), 122.8 (*C*-3''), 95.0 (*C*-6), 89.1 (*C*-1'), 86.9 (*C*-4'), 70.3 (*CH*₂Ph), 69.9 (*CH*₂-alkyl), 67.2 (*C*-5'), 59.5 (*CH*₂-NBu₄), 39.0 (*C*-2'), 35.0 (*CH*₂-alkyl), 33.1 – 20.7 (*CH*₂-alkyl, *CH*₂-NBu₄), 14.4 (*CH*₃-alkyl), 13.9 (*CH*₃-NBu₄).

³¹P-NMR (243 MHz, Methanol-*d*4): δ [ppm] = -12.05 (d, $^2J_{\text{P,P}} = 19.8$ Hz, *P*- α), -13.12 (dd, $^2J_{\text{P,P}} = 17.1$, 6.0 Hz, *P*- γ), -23.90 (t, $^2J_{\text{P,P}} = 18.9$ Hz, *P*- β).

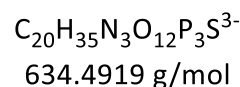
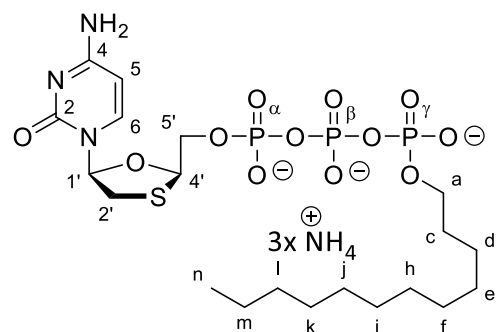
HRMS-ESI⁺ (*m/z*): C₄₁H₇₁N₃O₁₄P₃S [M+H]⁺: theo.: 954.3864, found: 954.3852.

(-)-2'-Deoxy-3'-thiocytidine - γ -dodecyl triphosphate **76**

The synthesis of the pyrophosphate was carried out according to general procedure 4: Synthesis of pyrophosphate. With *H*-phosphonate **38a** (118 mg, 390 μ mol), NCS (130 mg, 625 μ mol) and 0.4 M TBA phosphate monobasic (2.93 mL, 1.17 mmol) in CH₃CN (3.0 mL). After purification the obtained pyrophosphate was used in the synthesis of triphosphate **75** according to general procedure 4: Preparation of γ -alkyl-triphosphates.

With pyrophosphate **39a** (114 mg, 177 μ mol, *n*Bu₄N⁺), TFAA (141 μ L, 1.00 mmol) and Et₃N (223 μ L, 1.60 mmol) in

DMF (3.0 mL). The second step was carried out with Et₃N (101 μ L, 1.00 mmol), 1-methylimidazole (40.0 μ L, 500 μ mol), 3TCMP **74** (54.9 mg, 100 μ mol, *n*Bu₄N⁺) and the activated pyrophosphate **39a** in CH₃CN (3.0 mL). Removal of the cyanoethyl protecting group was performed with 10.0 eq. TBA hydroxide overnight. After evaporation of all volatiles the crude product was purified on RP₁₈-silica gel with automated flash chromatography (H₂O:CH₃CN, 100:0 to 0:100, v/v) followed by ion exchange chromatography (NH₄⁺). Subsequent purification on RP₁₈-silica gel with automated flash chromatography (H₂O:CH₃CN, 100:0 to 0:100, v/v) afforded the γ -modified triphosphate **76** (29.7 mg, 43.2 μ mol, 43 %) as a colourless solid. **HPLC (Method A):** *t*_R = 12.40 min.



76

Experimental Procedure

¹H-NMR (600 MHz, Methanol-*d*4): δ [ppm] = 8.31 (d, $^3J_{H,H}$ = 7.8 Hz, 1H, *H*-6), 6.26 (dd, $^3J_{H,H}$ = 5.2, 4.0 Hz, 1H, *H*-1'), 6.13 (d, $^3J_{H,H}$ = 7.8 Hz, 1H, *H*-5), 5.46 (t, $^3J_{H,H}$ = 3.7 Hz, 1H, *H*-4'), 4.49 – 4.44 (m, 1H, *H*-5'a), 4.36 - 4.30 (m, 1H, *H*-5'b), 4.24 – 4.17 (m, 2H, *CH*₂-alkyl), 3.53 (dd, $^2J_{H,H}$ = 12.2 Hz, $^3J_{H,H}$ = 5.3 Hz, 1H, *H*-2'a), 3.29 – 3.24 (m, 1H, *H*-2'b), 1.75 - 1.69 (m, 2H, *CH*₂-alkyl), 1.44 - 1.37 (m, 2H, *CH*₂-alkyl), 1.36 - 1.26 (m, 18H, *CH*₂-alkyl), 0.90 (t, $^3J_{H,H}$ = 7.0 Hz, 3H, *CH*₃-alkyl).

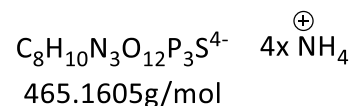
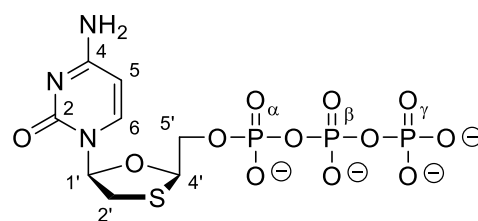
¹³C-NMR (151 MHz, Methanol-*d*4): δ [ppm] = 163.2 (*C*_q-4), 151.7 (*C*_q-2), 145.3 (*C*-5), 95.4 (*C*-6), 89.1 (*C*-1'), 86.9 (*C*-4'), 70.2 (d, $^2J_{C,P}$ = 6.2 Hz, *CH*₂-alkyl), 67.5 (d, $^2J_{C,P}$ = 5.3 Hz, *C*-5'), 38.6 (*C*-2'), 33.1 - 23.7 (*CH*₂-alkyl), 14.5 (*CH*₃-alkyl).

³¹P-NMR (162 MHz, Methanol-*d*4): δ [ppm] = -11.93 (d, $^2J_{P,P}$ = 19.2 Hz, *P*- α), -13.64 (d, $^2J_{P,P}$ = 16.7 Hz, *P*- γ), -23.74 (dd, $^2J_{P,P}$ = 19.3, 16.9 Hz, *P*- β).

MALDI-MS⁺ (m/z): C₂₀H₃₈N₃O₁₂P₃SK [M+K]⁺ theo: 676.102, found: 676.082.

(-)-2'-Deoxy-3'-thiocytidine triphosphate **77**

The reaction was performed according to general procedure 5: Nucleoside Triphosphates: With 3TCMP **74** (45.2 mg, 100 μ mol, *n*Bu₄N⁺), TFAA (141 μ L, 1.00 mmol) and Et₃N (223 μ L, 1.60 mmol) in CH₃CN (3.00 mL). After the first activation step the triphosphate was synthesised with Et₃N (101 μ L, 100 μ mol), 1-methylimidazole (47.8 μ L, 600 μ mol) and pyrophosphate (271 mg, 300 μ mol, *n*Bu₄N⁺) in CH₃CN (8.00 mL). The reaction was washed with CHCl₃



77

(3x 10 mL) the solvent was removed under reduced pressure and the crude product was purified on RP₁₈ silica gel with automated flash chromatography (H₂O:CH₃CN, 100:0 to 0:100, v/v) followed by an ion exchange chromatography (NH₄⁺) as well as purification on RP₁₈ silica gel with automated flash chromatography (H₂O:CH₃CN, 100:0 to 0:100, v/v) to afford the triphosphate **77** (35.6 mg, 66.3 μ mol, 66 %) as a colourless solid. **HPLC (Method A):** *t*_R = 9.93 min.

¹H-NMR (600 MHz, Water-*d*2): δ [ppm] = 8.19 (d, $^3J_{H,H}$ = 7.8 Hz, 1H, *H*-6), 6.33 (dd, $^3J_{H,H}$ = 5.4, 3.9 Hz, 1H, *H*-1'), 6.18 (d, $^3J_{H,H}$ = 7.8 Hz, 1H, *H*-5), 5.51 – 5.48 (m, 1H, *H*-4'), 4.44 (ddd, $^3J_{H,P}$ = 12.0 Hz, $^3J_{H,H}$ = 6.6, 2.9 Hz, 1H, *H*-5'a), 4.29 (ddd, $^3J_{H,P}$ = 11.7 Hz, $^3J_{H,H}$ = 6.9, 4.4 Hz, 1H, *H*-5'b), 3.58 (dd, $^2J_{H,H}$ = 12.5 Hz, $^3J_{H,H}$ = 5.4 Hz, 1H, *H*-2'a), 3.29 (dd, $^2J_{H,H}$ = 12.5 Hz, $^3J_{H,H}$ = 3.9 Hz, 1H, *H*-2'b).

Experimental Procedure

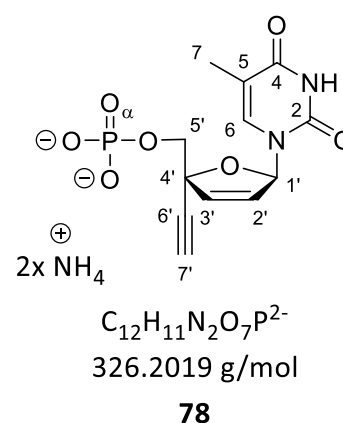
^{13}C -NMR (151 MHz, Water-*d*2): δ [ppm] = 162.7 (C_q -4), 152.7 (C_q -2), 143.3 (C -6), 95.3 (C -5), 87.4 (C -1'), 84.9 (C -4'), 66.1 (C -5'), 38.1 (C -2').

^{31}P -NMR (243 MHz, Water-*d*2): δ [ppm] = -10.65 (d, $^2J_{\text{P,P}} = 18.2$ Hz, P - α), -11.52 (d, $^2J_{\text{P,P}} = 19.3$ Hz, P - γ), -22.98 (t, $^2J_{\text{P,P}} = 19.4$ Hz, P - β).

MALDI-MS⁺ (m/z): $\text{C}_8\text{H}_{15}\text{N}_3\text{O}_{12}\text{P}_3\text{S}$ [M+H]⁺ theo: 469.958, found: 469.929.

2',3'-Didehydro-3'-deoxy-4'-ethynylthymidine monophosphate **78**

Method A (SOWA and OUCHI): The reaction was carried out according to the literature¹⁷⁷ with modifications: POCl_3 (96.7 μL , 1.06 mmol) was dissolved in CH_3CN (229 μL , 4.36 mmol) and cooled to 0 °C. Pyridine (93.3 mL, 1.16 mmol) and H_2O (12.2 μL , 675 μmol) were subsequently added dropwise to the solution and stirred at 0 °C for 10 min. The appropriate nucleoside (59.8 mg, 241 μmol) was added and the mixture was stirred for 2.5 h at 0 °C. The reaction was poured into ice-cold water and stirred for 30 min at 0 °C. The pH value was adjusted to 8 with solid NH_4HCO_3 . The solvent was removed by freeze drying



and the crude product was purified on RP_{18} silica gel with automated flash chromatography ($\text{H}_2\text{O}:\text{CH}_3\text{CN}$, 100:0 to 0:100, v/v), afterwards 10 % aq. TBA hydroxide (2.0 eq.) was added and all volatiles were evaporated. The residue was purified on RP_{18} silica gel with automated flash chromatography ($\text{H}_2\text{O}:\text{CH}_3\text{CN}$, 100:0 to 0:100, v/v) to afford 4'-Ed4T monophosphate **78** (55.5 mg, 152 μmol , 63 %) as a colourless resin.

Method B (YOSHIKAWA): The reaction was performed according to the literature¹⁷⁸ with modifications: 4'-Ed4T **24** (228 mg, 919 μmol) and 1,8-bis(dimethylamino)naphthalene (394 mg, 1.84 mmol) were suspended in trimethyl phosphate (0.84 mL). Then, POCl_3 (336 μL , 3.68 mmol) was added and the mixture was stirred at 0 °C for 3 h. The reaction progress was monitored by TLC. Ice-cold water (10 mL) was added to the reaction mixture, which was then adjusted to a pH value of 8 by adding solid NH_4HCO_3 . The reaction mixture was washed with CH_2Cl_2 (3x 10 mL), the solvent was removed under reduced pressure and the crude product was purified on RP_{18} -silica gel with automated flash chromatography ($\text{H}_2\text{O}:\text{CH}_3\text{CN}$, 100:0 to 0:100, v/v). After ion Exchange to Et_3N^+ , the product was purified on RP_{18} -silica gel with automated flash chromatography ($\text{H}_2\text{O}:\text{CH}_3\text{CN}$, 100:0 to 0:100, v/v) to afford 4'-Ed4T monophosphate **78** (418 mg, 582 μmol , 78 %, Et_3N^+). **HPLC (Method A):** $t_R = 8.44$ min.

Experimental Procedure

¹H-NMR (500 MHz, Methanol-*d*4): δ [ppm] = 7.77 – 7.74 (m, 1H, *H*-6), 7.06 – 7.03 (m, 1H, *H*-1'), 6.42 (dd, ³*J*_{H,H} = 5.8 Hz, ⁴*J*_{H,H} = 2.1 Hz, 1H, *H*-2'), 5.99 (dd, ³*J*_{H,H} = 5.8 Hz, ⁴*J*_{H,H} = 1.4 Hz, 1H, *H*-3'), 4.18 (dd, ²*J*_{H,H} = 11.2 Hz, ³*J*_{H,P} = 5.7 Hz, 1H, *H*-5'a), 4.04 (dd, ²*J*_{H,H} = 11.2 Hz, ³*J*_{H,P} = 4.2 Hz, 1H, *H*-5'b), 3.16 (s, 1H, *H*-7'), 3.13 (q, ³*J*_{H,H} = 7.3 Hz, 6H, CH₂-NEt₃), 1.92 (d, ⁴*J*_{H,H} = 1.3 Hz, 3H, *H*-7), 1.27 (t, ³*J*_{H,H} = 7.3 Hz, 9H, CH₃-NEt₃).

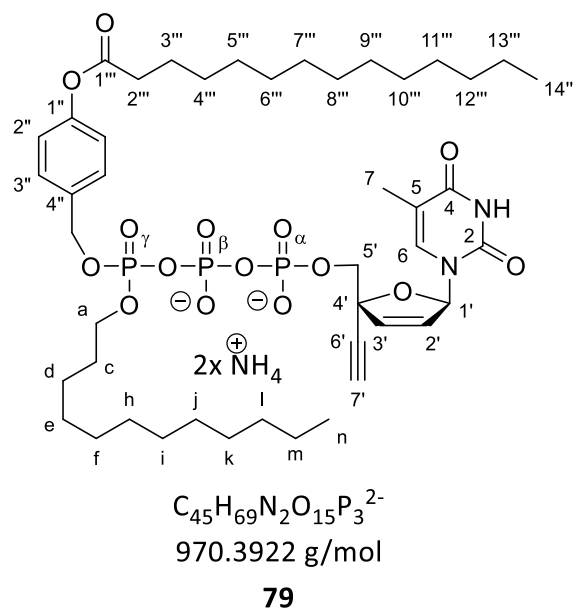
¹³C-NMR (126 MHz, Methanol-*d*4): δ [ppm] = 166.5 (C_q-4), 152.7 (C_q-2), 138.8 (C-6), 136.9 (C-2'), 128.0 (C-3'), 112.2 (C_q-5), 90.6 (C-1'), 87.1 (d, ³*J*_{C,P} = 10.5 Hz, C-4'), 80.9 (C_q-6'), 76.7 (C-7'), 69.5 (d, ²*J*_{C,P} = 4.5 Hz, C-5'), 47.2 (CH₂-NEt₃), 12.5 (C-7), 9.2 (CH₃-NEt₃).

³¹P-NMR (202 MHz, Methanol-*d*4): δ [ppm] = 1.97 (s).

HRMS-ESI⁻ (m/z): C₁₂H₁₂N₂O₇P [M-H]⁻: theo.: 327.0387, found: 327.0392.

2',3'-Didehydro-3'-deoxy-4'-ethynylthymidine (4-tetradecanoyloxybenzyl)- γ -dodecyl triphosphate **79**

The synthesis of the pyrophosphate was carried out according to general procedure 2: Synthesis of pyrophosphate. With *H*-phosphonate **18c** (283 mg, 250 μ mol), NCS (83.4 mg, 625 μ mol) and 0.4 M TBA phosphate monobasic (1.88 mL, 750 μ mol) in CH₃CN (3.0 mL). After purification the obtained pyrophosphate was used in the synthesis of triphosphate **79** according to general procedure 7: Preparation of γ -AB-triphosphates. With pyrophosphate **19c** (151 mg, 225 μ mol, *n*Bu₄N⁺), TFAA (141 μ L, 1.00 mmol) and Et₃N (223 μ L, 1.60 mmol) in CH₃CN (3.0 mL). The second step was carried out with Et₃N (101 μ L, 1.00 μ mol), 1-methylimidazole (39.9 μ L, 500 μ mol), 4'-Ed4TMP **78** (59.2 mg, 100 μ mol, Et₃N⁺) and the activated pyrophosphate **19c** in CH₃CN (3.0 mL). After evaporation of all volatiles the crude product was purified on RP₁₈-silica gel with automated flash chromatography (H₂O:CH₃CN, 100:0 to 0:100, v/v) followed by ion exchange chromatography (NH₄⁺). Subsequent purification on RP₁₈-silica gel with automated flash chromatography (H₂O:CH₃CN, 100:0 to 0:100, v/v) afforded the γ -modified triphosphate **79** (46.1 mg, 45.8 μ mol, 46 %) as a colourless solid. **HPLC (Method A):** *t*_R = 17.80 min.



Experimental Procedure

¹H-NMR (600 MHz, Methanol-*d*4): δ [ppm] = 7.78 – 7.75 (m, 1H, *H*-6), 7.50 – 7.46 (m, 2H, *H*-2''), 7.08 (dd, ³*J*_{H,H} = 8.5 Hz, ⁴*J*_{H,H} = 1.9 Hz, 2H, *H*-3''), 7.07 – 7.03 (m, 1H, *H*-1'), 6.50 – 6.47 (m, 1H, *H*-2'), 5.94 – 5.91 (m, 1H, *H*-3'), 5.25 - 5.16 (m, 2H, CH₂-Ph), 4.49 – 4.42 (m, 1H, *H*-5'a), 4.22 (dd, ²*J*_{H,H} = 11.5, ²*J*_{H,P} = 5.2 Hz, 1H, *H*-5'b), 4.15 - 4.06 (m, 2H, OCH₂), 3.12 – 3.07 (m, 1H, *H*-7'), 2.58 (t, ³*J*_{H,H} = 7.4, 2H, O=CCH₂), 1.94 – 1.90 (m, 3H, *H*-7), 1.77 - 1.70 (m, 2H, CH₂-alkyl), 1.61 (qu, ³*J*_{H,H} = 6.7 Hz, 2H, CH₂-alkyl), 1.48 – 1.40 (m, 2H, CH₂-alkyl), 1.37 - 1.25 (m, 36H, CH₂-alkyl), 0.94 – 0.89 (m, 6H, CH₃-alkyl).

¹³C-NMR (151 MHz, Methanol-*d*4): δ [ppm] = 173.8 (O=C_q-alkyl), 166.6 (C_q-4), 152.8 (C_q-2), 152.4 (C_q-1''), 138.9 (C-6), 136.8 (C-2'), 135.2 (C_q-4''), 130.5 (C-2''), 128.2 (C-3'), 122.9 (C-3''), 112.3 (C_q-5), 90.5 (C-1'), 86.9 (C_q-4'), 81.0 (C_q-6'), 76.8 (C-7'), 70.3 (d, ²*J*_{C,P} = 5.5 Hz, C-5'), 69.9 (CH₂-Ph), 69.8 (OCH₂), 35.0 (O=CCH₂), 33.1 - 23.7 (CH₂-alkyl), 14.5 (CH₃-alkyl), 14.5 (CH₃-alkyl), 12.5 (C-7).

³¹P-NMR (243 MHz, Methanol-*d*4): δ [ppm] = -12.53 (d, ²*J*_{P,P} = 19.4 Hz, *P*- α), -12.89 (dd, ²*J*_{P,P} = 16.7, 7.5 Hz, *P*- γ), -23.46 - -23.94 (m, *P*- β).

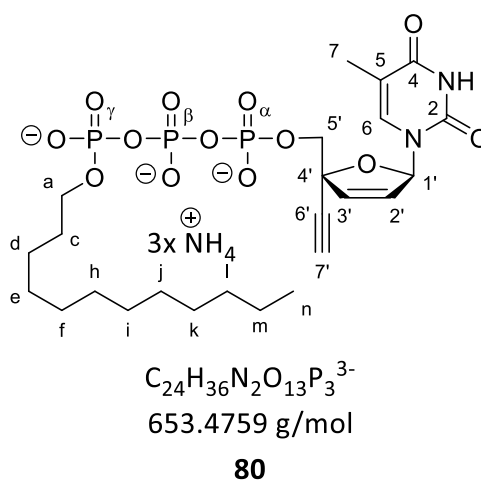
HRMS-ESI⁺ (m/z): C₄₅H₇₂N₂O₁₅P₃ [M+H]⁺: theo.: 973.4139, found: 973.4137.

2',3'-Didehydro-3'-deoxy-4'-ethynylthymidine γ -dodecyl triphosphate **80**

The synthesis of pyrophosphate was carried out according to general procedure 4: Synthesis of pyrophosphate. With *H*-phosphonate **38a** (94.7 mg, 312 μ mol), NCS (104 mg, 780 μ mol) and 0.4 M TBA phosphate monobasic (2.34 mL, 1.17 mmol) in CH₃CN (3.0 mL). After purification the obtained pyrophosphate was used in the synthesis of triphosphate **80** according to general procedure 4:

Preparation of γ -alkyl-triphosphates. With pyrophosphate **39a** (111 mg, 224 μ mol, *n*Bu₄N⁺), TFAA (154 μ L, 1.09 mmol) and Et₃N (243 μ L, 1.74 mmol) in DMF (3.0 mL).

The second step was carried out with Et₃N (152 μ L, 1.09 mmol), 1-methylimidazole (43.0 μ L, 545 μ mol), 4'-Ed4T monophosphate **78** (47.7 mg, 109 μ mol, Et₃N⁺) and the activated pyrophosphate **39a** in CH₃CN (3.0 mL). Removal of the cyanoethyl protecting group was performed with 10.0 eq. TBA hydroxide overnight. After evaporation of all volatiles the crude product was purified on RP₁₈-silica gel with automated flash chromatography (H₂O:CH₃CN, 100:0 to 0:100, v/v) followed by ion exchange chromatography (NH₄⁺). Subsequent purification on RP₁₈-silica gel with automated flash chromatography (H₂O:CH₃CN, 100:0 to 0: 100, v/v) afforded the γ -modified triphosphate **80** (31.2 mg, 44.2 μ mol, 40 %) as a colourless solid. **HPLC (Method A):** *t*_R = 13.19 min.



Experimental Procedure

¹H-NMR (600 MHz, Methanol-*d*4): δ [ppm] = 7.76 - 7.75 (m, 1H, *H*-6), 7.06 - 7.05 (m, 1H, *H*-1'), 6.51 - 6.47 (m, 1H, *H*-2'), 5.98 (dd, ³*J*_{H,H} = 5.9 Hz, ⁴*J*_{H,H} = 1.3 Hz, 1H, *H*-3'), 4.44 - 4.39 (m, 1H, *H*-5'a), 4.39 - 4.33 (m, 2H, *CH*₂-alkyl), 4.25 - 4.14 (m, 1H, *H*-5'b), 3.13 (s, 1H, *H*-7'), 1.93 (d, ⁴*J*_{H,H} = 1.2 Hz, 3H, *H*-7), 1.76 - 1.67 (m, 2H, *CH*₂-alkyl), 1.43 - 1.37 (m, 2H, *CH*₂-alkyl), 1.36 - 1.25 (m, 16H, *CH*₂-alkyl), 0.90 (t, ³*J*_{H,H} = 7.0 Hz, 3H, *CH*₃-alkyl).

¹³C-NMR (151 MHz, Methanol-*d*4): δ [ppm] = 166.6 (*C*_q-4), 152.8 (*C*_q-2), 152.4 (*C*_q-1''), 138.9 (*C*-6), 136.8 (*C*-2'), 128.2 (*C*-3'), 112.3 (*C*_q-5), 90.6 (*C*-1'), 86.9 (d, ³*J*_{C,P} = 10.1 Hz, *C*_q-4'), 81.0 (*C*_q-6'), 76.8 (*C*-7'), 70.3 - 70.1 (m, *C*-5'), 64.3 (OCH₂), 31.3 - 20.0 (*CH*₂-alkyl), 14.4 (*CH*₃-alkyl), 12.5 (*C*-7).

³¹P-NMR (243 MHz, Methanol-*d*4): δ [ppm] = -12.23 - -12.73 (m, *P*- α), -13.25 - -13.88 (m, *P*- γ), -23.38 - -23.88 (m, *P*- β).

MALDI-MS⁺ (*m/z*): C₂₄H₃₉N₂O₁₃P₃Na [M+Na]⁺ theo: 679.155, found: 679.135.

2',3'-Didehydro-3'-deoxy-4'-ethynylthymidine triphosphate **81**

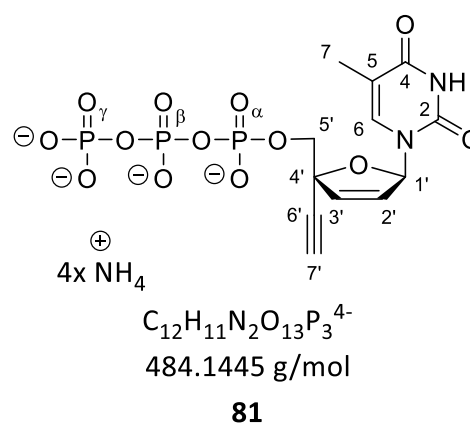
The reaction was performed according to general procedure

5: Nucleoside Triphosphates: With 4'-Ed4T monophosphate

78 (59.1 mg, 100 μ mol, *n*Bu₄N⁺), TFAA (141 μ L, 1.00 mmol) and Et₃N (223 μ L, 1.60 mmol) in CH₃CN (3.00 mL). After the first activation step the triphosphate was synthesised with Et₃N (101 μ L, 100 μ mol), 1-methylimidazole (47.8 μ L, 600 μ mol) and pyrophosphate (271 mg, 300 μ mol, *n*Bu₄N⁺) in CH₃CN (8.00 mL). The reaction was washed with CHCl₃ (3x

10 mL) the solvent was removed under removed pressure

and the crude product was purified on RP₁₈-silica gel with automated flash chromatography (H₂O:CH₃CN, 100:0 to 0:100, v/v) followed by an ion exchange chromatography (NH₄⁺) and purification on RP₁₈-silica gel with automated flash chromatography (H₂O: CH₃CN, 100:0 to 0:100, v/v) to afford triphosphate **81** (40.6 mg, 72.9 μ mol, 73 %) as a colourless solid. **HPLC (Method A):** *t*_R = 10.93 min.



Experimental Procedure

¹H-NMR (600 MHz, Water-d₂): δ [ppm] = 7.60 – 7.57 (m, 1H, H-6), 7.09 (dd, ³J_{H,H} = 2.1 Hz, ⁴J_{H,H} = 1.4 Hz, 1H, H-1'), 6.53 (dd, ³J_{H,H} = 6.0, 2.1 Hz, 1H, H-2'), 6.09 (dd, ³J_{H,H} = 6.0 Hz, ⁴J_{H,H} = 1.4 Hz, 1H, H-3'), 4.35 (dd, ²J_{H,H} = 11.6, ²J_{H,P} = 7.0 Hz, 1H, H-5'a), 4.15 (dd, ²J_{H,H} = 11.6 Hz, ²J_{H,P} = 5.9 Hz, 1H, H-5'b), 3.16 (s, 1H, H-7'), 1.89 (d, ⁴J_{H,H} = 1.3 Hz, 3H, H-7).

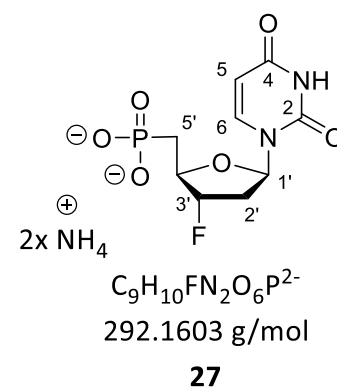
¹³C-NMR (151 MHz, Water-d₂): δ [ppm] = 166.8 (C_q-4), 152.2 (C_q-2), 138.1 (C-6), 135.1 (C-2'), 126.5 (C-3'), 111.6 (C_q-5), 90.0 (C-1'), 85.6 (C_q-4'), 79.1 (C_q-6'), 77.0 (C-7'), 68.7 (C-5'), 11.5 (C-7).

³¹P-NMR (243 MHz, Water-d₂): δ [ppm] = -10.68 (d, ²J_{P,P} = 19.2 Hz), -12.19 (d, ²J_{P,P} = 19.4 Hz), -23.10 (t, ²J_{P,P} = 19.3 Hz).

MALDI-MS⁺ (m/z): C₁₂H₁₆N₂O₁₃P₃ [M+H]⁺ theo: 488.986, found: 488.963.

3'-Deoxy-3'-fluorouridine phosphonate **27**

The reaction was performed according to the literature²⁶⁵ with modifications: Diethyl phosphonate **83** (170 mg, 900 μ mol) was dissolved in CH₃CN (15 mL) and afterwards TMSBr (409 μ L, 3.15 mmol) was added in one portion. The reaction was stirred for 72 h at rt, then quenched with water (10 mL) and washed with CH₂Cl₂ (3x 10 mL). The solvent of the aqueous layer was removed under reduced pressure and the crude product was purified on RP₁₈-silica gel with automated flash chromatography (H₂O:CH₃CN, 100:0 to 0:100, v/v) to afford uridine phosphonate **27** (236 mg, 718 μ mol, 79 %, NH₄⁺) as a colourless foam. **HPLC (Method A):** t_R = 8.52 min.



¹H-NMR (600 MHz, Water-d₂): δ [ppm] = 7.86 (d, ³J_{H,H} = 8.0 Hz, 1H, H-6), 6.25 (dd, ³J_{H,H} = 9.0, 5.6 Hz, 1H, H-1'), 5.90 (d, ³J_{H,H} = 8.1 Hz, 1H, H-5), 5.45 - 5.32 (m, 1H, H-3'), 4.60 (dq, ³J_{H,F} = 25.1 Hz, ³J_{H,H} = 7.6 Hz, 1H, H-4'), 2.77 - 2.66 (m, 1H, H-2'a), 2.44 - 2.34 (m, 1H, H-2'b), 2.11 - 1.88 (m, 2H, H-5').

Experimental Procedure

^{13}C -NMR (151 MHz, Water-*d*2): δ [ppm] = 166.2 (C_q -4), 151.5 (C_q -2), 141.88 (C -6), 102.2 (C -5), 96.6 (dd, $^1J_{\text{C,F}}$ = 176.0 Hz, C -3'), 86.0 (C -1'), 82.0 (d, $^2J_{\text{C,F}}$ = 25.7 Hz, C -4'), 36.2 (d, $^2J_{\text{C,F}}$ = 20.9 Hz, C -2'), 32.28 (dd, $^1J_{\text{C,P}}$ = 130.2 Hz, $^3J_{\text{C,F}}$ = 8.9 Hz, C -5').

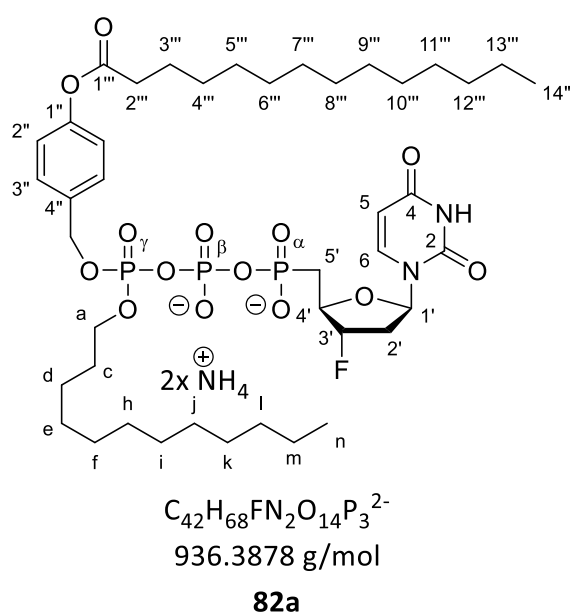
^{19}F -NMR (565 MHz, Water-*d*2): δ [ppm] = -173.63 (dddd, J = 52.8, 39.6, 25.2, 20.4 Hz).

^{31}P -NMR (243 MHz, Water-*d*2): δ [ppm] = 17.76 (s).

ESI-MS (m/z): $\text{C}_9\text{H}_{11}\text{FN}_2\text{O}_6\text{P}$ [M-H] $^-$: theo.: 293.0344, found: 293.0292.

3'-Deoxy-3'-fluorouridine (4-tetradecanoyloxybenzyl)- γ -dodecyl triphosphate **82a**

The synthesis of the pyrophosphate was carried out according to general procedure 4: Synthesis of pyrophosphate. With *H*-phosphonate **18c** (141.7 mg, 250 μmol), NCS (83.0 mg, 625 μmol) and 0.4 M TBA phosphate monobasic (1.88 mL, 750 μmol) in CH_3CN (3 mL). After purification the obtained pyrophosphate was used in the synthesis of triphosphate **82a** according to general procedure 4: Preparation of γ -AB-triphosphates. With pyrophosphate **19c** (202 mg, 224 μmol , $n\text{Bu}_4\text{N}^+$), TFAA (141 μL , 1.00 mmol) and Et_3N (223 μL , 1.60 mmol) in CH_3CN (3 mL). The second step was carried out with Et_3N (101 μL , 1.00 mmol), 1-methylimidazole (39.9 μL , 500 μmol), FLU phosphonate **27** (56.4 mg, 93 μmol , $n\text{Bu}_4\text{N}^+$) and the activated pyrophosphate **19c** in CH_3CN (3 mL). After evaporation of all volatiles the crude product was purified on RP_{18} -silica gel with automated flash chromatography ($\text{H}_2\text{O}:\text{CH}_3\text{CN}$, 100:0 to 0:100, v/v) followed by ion exchange chromatography (NH_4^+). Subsequent purification on RP_{18} -silica gel with automated flash chromatography ($\text{H}_2\text{O}:\text{CH}_3\text{CN}$, 100:0 to 0:100, v/v) afforded the γ -modified triphosphate **82a** (25.3 mg, 26.4 μmol , 28 %) as a colourless solid. **HPLC (Method A):** t_{R} = 18.35 min.



Experimental Procedure

¹H-NMR (600 MHz, Methanol-*d*4): δ [ppm] = 7.95 – 7.92 (m, 1H, *H*-6), 7.53 - 7.49 (m, 2H, *H*-2''), 7.09 (d, ³*J*_{H,H} = 8.5 Hz, 2H, *H*-3''), 6.19 (dd, ³*J*_{H,H} = 9.2, 5.2 Hz, 1H, *H*-1'), 5.77 – 5.73 (m, 1H, *H*-5), 5.51 (dd, ¹*J*_{H,F} = 52.7 Hz, ³*J*_{H,H} = 4.2 Hz, 1H, *H*-3'), 5.23 (d, ³*J*_{H,P} = 8.2 Hz, 2H, CH₂Ph), 4.74 - 4.65 (m, 1H, *H*-4'), 4.16 – 4.08 (m, 2H, CH₂-alkyl), 2.58 (t, ³*J*_{H,H} = 7.4 Hz, 2H, CH₂-alkyl), 2.39 - 2.18 (m, 4H, *H*-2', *H*-5'), 1.74 (qu, ³*J*_{H,H} = 7.4 Hz, 2H, CH₂-alkyl), 1.63 - 1.58 (m, 2H, CH₂-alkyl), 1.38 - 1.23 (m, 38H, CH₂-alkyl), 0.91 (t, ³*J*_{H,H} = 7.0 Hz, 6H, CH₃-alkyl).

¹³C-NMR (151 MHz, Methanol-*d*4): δ [ppm] = 174.0 (C_q-1'''), 166.3 (C_q-4), 152.6 (C_q-1''), 152.4 (C_q-2), 142.6 (C-6), 135.5 (C_q-4''), 130.6 (C-3''), 123.8 (C-2''), 103.1 (C-5), 97.4 (C-3'), 87.2 (C-1'), 83.3 (C-4'), 70.3 (CH₂Ph), 70.0 (CH₂-alkyl), 35.0 - 23.7 (CH₂-alkyl), 20.7 (C-5'), 13.9 (CH₃-alkyl).

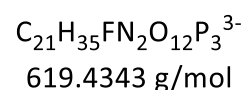
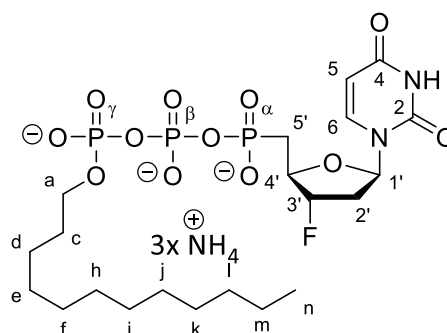
¹⁹F-NMR (565 MHz, Methanol-*d*4): δ [ppm] = -174.56 – -174.88 (m).

³¹P-NMR (243 MHz, Methanol-*d*4): δ [ppm] = 9.52 (d, ²*J*_{P,P} = 23.7 Hz, *P*- α), -12.85 (d, ²*J*_{P,P} = 16.8 Hz, *P*- γ), -23.40 - -23.70 (m, *P*- β).

MALDI-MS⁺ (m/z): C₄₂H₇₀FN₂O₁₄P₃K [M+K]⁺ theo: 977.365, found: 977.395.

3'-Deoxy-3'-fluorouridine γ -dodecyl triphosphate **82b**

The synthesis of the pyrophosphate was carried out according to general procedure 4: Synthesis of pyrophosphate. With H-phosphonate **38a** (75.9 mg, 250 μ mol), NCS (86.6 mg, 625 μ mol) and 0.4 M TBA phosphate monobasic (1.87 mL, 750 μ mol) in CH₃CN (3 mL). After purification the obtained pyrophosphate was used in the synthesis of triphosphate **82b** according to general procedure 4: Preparation of γ -alkyl-triphosphates. With pyrophosphate **39a** (114 mg, 225 μ mol, *n*Bu₄N⁺), TFAA (141 μ L, 1.00 mmol) and Et₃N (223 μ L, 1.60 mmol) in DMF (3 mL). The second step was carried out



82b

with Et₃N (101 μ L, 1.00 mmol), 1-methylimidazole (40.0 μ L, 500 μ mol), FLU phosphonate **27** (45.2 mg, 100 μ mol, *n*Bu₄N⁺) and the activated pyrophosphate **39a** in CH₃CN (3 mL). Removal of the cyanoethyl protecting group was performed with 10.0 eq. TBA hydroxide overnight. After evaporation of all volatiles the crude product was purified on RP₁₈-silica gel with automated flash chromatography (H₂O:CH₃CN, 100:0 to 0:100, v/v) followed by ion exchange chromatography (NH₄⁺). Subsequent purification on RP₁₈-silica gel with automated flash chromatography (H₂O:CH₃CN, 100:0 to 0:100, v/v) afforded the γ -modified triphosphate **82b** (8.49 mg, 12.6 μ mol, 13 %) as a colourless solid. **HPLC (Method A):** *t*_R = 13.53 min.

Experimental Procedure

¹H-NMR (600 MHz, Methanol-*d*4): δ [ppm] = 7.95 – 7.93 (m, 1H, *H*-6), 6.20 (dd, $^3J_{H,H} = 9.3, 5.2$ Hz, 1H, *H*-1'), 5.76 (d, $^3J_{H,H} = 8.1$ Hz, 1H, *H*-5), 5.47 (dd, $^2J_{H,F} = 52.8, ^3J_{H,H} = 4.4$ Hz, 1H, *H*-3'), 4.66 (dtd, $^3J_{H,F} = 24.7$ Hz, $^3J_{H,H} = 9.1, 5.6$ Hz, 1H, *H*-4'), 4.22 – 4.17 (m, 2H, *CH*₂-alkyl), 2.63 – 2.55 (m, 1H, *H*-2'a), 2.42 – 2.16 (m, 3H, *H*-2'b, *H*-5'), 1.76 – 1.69 (m, 2H, *CH*₂-alkyl), 1.45 – 1.37 (m, 2H, *CH*₂-alkyl), 1.37 – 1.25 (m, 16H, *CH*₂-alkyl), 0.90 (t, $^3J_{H,H} = 7.0$ Hz, 3H, *CH*₃-alkyl).

¹³C-NMR (151 MHz, Methanol-*d*4): δ [ppm] = 166.2 (*C*_q-4), 152.2 (*C*_q-2), 142.4 (*C*-6), 103.0 (*C*-5), 97.5 (dd, $^1J_{C,F} = 176.8$ Hz, $^3J_{C,P} = 6.4$ Hz, *C*-3'), 87.0 (*C*-1'), 83.3 (d, $^2J_{C,F} = 26.0$ Hz, *C*-4'), 70.1 (d, $^2J_{C,P} = 6.4$ Hz, *CH*₂-alkyl), 38.1 (d, $^1J_{C,P} = 21.0$ Hz, *C*-5'), 34.7 – 33.5 (m, *C*-2'), 30.8 – 20.0 (*CH*₂-alkyl), 14.4 (*CH*₃-alkyl).

¹⁹F-NMR (565 MHz, Methanol-*d*4): δ [ppm] = -174.46 – -174.88 (m).

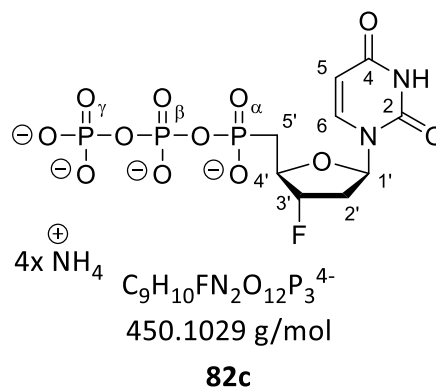
³¹P-NMR (243 MHz, Methanol-*d*4): δ [ppm] = 9.78 (d, $^2J_{P,P} = 24.3$ Hz, *P*- α), -13.56 (d, $^2J_{P,P} = 17.1$ Hz, *P*- γ), -23.70 (dd, $^2J_{P,P} = 24.5, 17.1$ Hz, *P*- β).

MALDI-MS⁺ (m/z): C₂₁H₃₈FN₂O₁₂P₃K [M+K]⁺ theo: 661.125, found: 661.094.

3'-Deoxy-3'-fluorouridine triphosphate **82c**

The reaction was performed according to general procedure 5:

Nucleoside Triphosphates: With FLU phosphonate **27** (60.6 mg, 100 μ mol, *n*Bu₄N⁺), TFAA (141 μ L, 1.00 mmol) and Et₃N (223 μ L, 1.60 mmol) in CH₃CN (3.00 mL). After the first activation step the triphosphate was synthesised with Et₃N (101 μ L, 100 μ mol), 1-methylimidazole (47.8 μ L, 600 μ mol) and pyrophosphate (271 mg, 300 μ mol, *n*Bu₄N⁺) in CH₃CN (8.00 mL). The reaction was washed with CHCl₃ (3x 10 mL) the



solvent was removed under reduced pressure and the crude product was purified on RP₁₈-silica gel with automated flash chromatography (H₂O:CH₃CN, 100:0 to 0:100, v/v) followed by an ion exchange chromatography (NH₄⁺) and purification on RP₁₈-silica gel with automated flash chromatography (H₂O:CH₃CN, 100:0 to 0:100, v/v) to afford the triphosphate **82c** (28.4 mg, 54.4 μ mol, 54 %) as a colourless solid. **HPLC (Method A):** $t_R = 10.04$ min.

¹H-NMR (600 MHz, Water-*d*2): δ [ppm] = 7.94 – 7.88 (m, 1H, *H*-6), 6.27 (dd, $^3J_{H,H} = 9.1, 5.6$ Hz, 1H, *H*-1'), 5.92 (d, $^3J_{H,H} = 8.1$ Hz, 1H, *H*-5), 5.50 – 5.35 (m, 1H, *H*-3'), 4.67 (dq, $^3J_{H,F} = 24.2$ Hz, $^3J_{H,H} = 7.9$ Hz, 1H, *H*-4'), 2.81 – 2.64 (m, 1H, *H*-2'a), 2.42 (dddd, $^3J_{H,F} = 40.2$ Hz, $^2J_{H,H} = 14.3$ Hz, $^3J_{H,H} = 9.0, 4.5$ Hz, 1H, *H*-2'b), 2.33 – 2.19 (m, 2H, *H*-5').

Experimental Procedure

¹³C-NMR (151 MHz, Water-*d*2): δ [ppm] = 166.3 (C_q-4), 151.6 (C_q-2), 141.9 (C-6), 102.2 (C-5), 96.5 (d, ¹J_{C,F} = 184.1 Hz, C-3'), 85.9 (C-1'), 81.5 (d, ²J_{C,F} = 26.5 Hz, C-4'), 36.3 (d, ²J_{C,F} = 20.7 Hz, C-2'), 32.5 - 31.7 (m, C-5').

³¹P-NMR (243 MHz, Water-*d*2): δ [ppm] = 11.31 (d, ²J_{P,P} = 25.6 Hz, P- α), -10.68 (d, ²J_{P,P} = 19.7 Hz, P- γ), -23.04 - -23.53 (m, P- β).

¹⁹F-NMR (565 MHz, Water-*d*2): δ [ppm] = -173.58 (dddd, *J* = 52.7, 40.5, 25.3, 20.4 Hz).

MALDI-MS⁺ (m/z): C₉H₁₅FN₂O₁₂P₃ [M+H]⁺ theo: 454.981, found: 454.982.

7. References

- (1) Gottlieb, M. S. AIDS: The Discovery. *New Engl. J. Med.* **1981**, *305*, 1425.
- (2) Broder, S. The development of Antiretroviral Therapy and its Impact on the HIV-1/AIDS Pandemic. *Antiviral Res.* **2010**, *85*, 1–18.
- (3) Barré-Sinoussi, F., Chermann, J. C., Rey, F., Chamaret, S., Gruest, J., Dauguet, C., Axler-Blin, C., Vezinet-Brun, F., Rouzioux, C., Rozenbaum, W., Montagnier, L. Isolation of a T-lymphotropic Retrovirus from a Patient at Risk for Acquired Immune Deficiency syndrome (AIDS). *Science* **1983**, *220*, 868–871.
- (4) Wain-Hobson, S., Sonigo, P., Danos, O., Cole, S., Alizon, M. Nucleotide Sequence of the AIDS Virus, LAV. *Cell* **1985**, *40*, 9–17.
- (5) *FDA-Approved HIV Medicines | NIH*, 2022. <https://hivinfo.nih.gov/understanding-hiv/fact-sheets/fda-approved-hiv-medicines>. Accessed 9 August 2022.
- (6) *HIV*, 2022. <https://www.who.int/news-room/fact-sheets/detail/hiv-aids>. Accessed 4 October 2022.
- (7) UNAIDS. Fact sheet -: Latest Global and Regional Statistics on the Status of the AIDS Epidemic. **2022**.
- (8) Dalakas, M. C., Illa, I., Pezeshkpour, G. H., Laukaitis, J. P., Cohen, B., Griffin, J. L. Mitochondrial Myopathy Caused by Long-Term Zidovudine Therapy. *N. Engl. J. Med.* **1990**, *322*, 1098–1105.
- (9) Kong, X.-B., Zhu, Q.-Y., Vidal, P. M., Watanabe, K. A., Polsky, B., Armstrong, D., Ostrander, M., Lang, S. A., JR., Muchmore, E., Chou, T.-C. Comparisons of Anti-Human Immunodeficiency Virus Activities, Cellular Transport, and Plasma and Intracellular Pharmacokinetics of 3'-Fluoro-3'-Deoxythymidine and 3'-Azido-3'-Deoxythymidine. *Antimicrob. Agents Chemother.* **1992**, *36*, 808–818.
- (10) Graziewicz, M. A., Longley, M. J., Copeland, W. C. DNA Polymerase Gamma in Mitochondrial DNA Replication and Repair. *Chem. Rev.* **2006**, *106*, 383–405.
- (11) Frankel, A. D., Young, J. A. T. HIV-1: Fifteen Proteins and an RNA. *Annu. Rev. Biochem.* **1998**, *67*, 1–25.
- (12) Coffin, J. M., Fan, H. The Discovery of Reverse Transcriptase. *Annu. Rev. Virol.* **2016**, *3*, 29–51.
- (13) Clercq, E. de. Three Decades of Antiviral Drugs. *Nat. Rev. Drug Discov.* **2007**, *6*, 941.
- (14) Maeda, K., Das, D., Kobayakawa, T., Tamamura, H., Takeuchi, H. Discovery and Development of Anti-HIV Therapeutic Agents: Progress Towards Improved HIV Medication. *Curr. Top. Med. Chem.* **2019**, *19*, 1621–1649.
- (15) Redshaw, S., Roberts, N. A., Thomas, G. J. The Road to Fortovase.: A History of Saquinavir, the First Human Immunodeficiency Virus Protease Inhibitor **2000**, *140*, 3–21.

Experimental Procedure

- (16) Jacob-Molina, A., Ding, J., Nanni, Clark, A. D., JR., Lu, X., Tantillo, C., Williams, R. L., Kamer, G., Ferris, A. L., Clark, P., Hizi, Amnon, Hughes, Stephen H., Arnold, E. Crystal Structure of Human Immunodeficiency Virus Type 1 Reversetranscriptase Complexed with Double-stranded DNA at 3.0 Å Resolution Shows Bent DNA. *Proc. Natl. Acad. Sci.* **1993**, *90*, 6320–6324.
- (17) Merluzzi, V. J., Hargrave, K. D., Labadia, M., Grozinger, K., Skoog, M., Wu, J. C., Shih, C.-K., Eckner, K., Hattox, S., Adams, J., Rosenthal, A. S., Faanes, R., Eckner, R. J., Koup, R. A., Sullivan, J. L. Inhibition of HIV-1 Replication by a Nonnucleoside Reverse Transcriptase Inhibitor. *Science* **1990**, *250*, 1411–1413.
- (18) Fesen, M. R., Kohn, K. W., Leteurtre, F., Pommier, Y. Inhibitors of Human Immunodeficiency Virus Integrase. *Proc. Natl. Acad. Sci.* **1993**, *90*, 2399–2403.
- (19) Métifiot, M., Marchand, C., Pommier, Y. HIV integrase inhibitors: 20-year landmark and challenges. *Adv. Pharmacol.* **2013**, *67*, 75–105.
- (20) Vella, S., Schwartländer, B., Sow, S. P., Eholie, S. P., Murphy, R. L. The History of Antiretroviral Therapy and of its Implementation in Resource-Limited Areas of the World. *AIDS* **2012**, *26*, 1231–1241.
- (21) Schader, S. M., Wainberg, M. A. Insights into HIV-1 Pathogenesis Through Drug Discovery: 30 Years of Basic Research and Concerns for the Future. *HIV AIDS Rev.* **2011**, *10*, 91–98.
- (22) Delaney, M. History of HAART –: The True Story of how Effective Multi-Drug Therapy was Developed for Treatment of HIV Disease. *Retrovirology* **2006**, *3*, 6.
- (23) Badri, M., Bekker, L.-G., Orrel, C., Pitt, J., Cilliers, F., Wood, R. Initiating Highly Active Antiretroviral Therapy in Sub-Saharan Africa: An Assessment of the Revised World Health Organization Scaling-Up Guidelines. *AIDS* **2004**, *18*, 1159–1168.
- (24) Natrass, N. South Africa’s “Rollout” of Highly Active Antiretroviral Therapy: A Critical Assessment. *J. Acquir. Immune. Defic. Syndr.* **2006**, *43*, 618–623.
- (25) Freed, E. O. HIV-1 Assembly, Release and Maturation. *Nat. Rev. Microbiol.* **2015**, *13*, 484–496.
- (26) Sogaard, O. S., Graversen, M. E., Leth, S., Olesen, R., Brinkmann, C. R., Nissen, S. K., Kjaer, A. S., Schleimann, M. H., Denton, P. W., Hey-Cunningham, W. J., Koelsch, K. K., Pantaleo, G., Krogsgaard, K., Sommerfelt, M., Fromentin, R., Chomont, N., Rasmussen, T. A., Østergaard, L., Tolstrup, M. The Depsipeptide Romidepsin Reverses HIV-1 Latency In Vivo. *PLoS Pathog.* **2015**, *11*, e1005142.
- (27) Barré-Sinoussi, F., Ross, A. L., Delfraissy, J.-F. Past, Present and Future: 30 Years of HIV Research. *Nat. Rev. Microbiol.* **2013**, *11*, 877–883.
- (28) Roser, M., Ritchie, H. HIV / AIDS. *Our World in Data* **2018**.
- (29) *National Institute of Allergy and Infectious Diseases* **2020**, 02 Mar. <https://www.niaid.nih.gov/news-events/experimental-hiv-vaccine-regimen-ineffective-preventing-hiv>. Accessed 7 October 2022.

Experimental Procedure

- (30) Archin, N. M., Sung, J. M., Garrido, C., Soriano-Sarabia, N., Margolis, D. M. Eradicating HIV-1 Infection: Seeking to Clear a Persistent Pathogen. *Nat. Rev. Microbiol.* **2014**, *12*, 750–764.
- (31) Wymant, C., Bezemer, D., Blanquart, F., Ferretti, L., Gall, A., Hall, M., Golubchik, T., Bakker, M., Ong, S. H., Zhao, L., Bonsall, D., Cesare, M. de, MacIntyre-Cockett, G., Abeler-Dörner, L., Albert, J., Bannert, N., Fellay, J., Grabowski, M. K., Gunsenheimer-Bartmeyer, B., Günthard, H. F., Kivelä, P., Kouyos, R. D., Laeyendecker, O., Meyer, L., Porter, K., Ristola, M., van Sighem, A., Berkhout, B., Kellam, P., Cornelissen, M., Reiss, P., Fraser, C. A Highly Virulent Variant of HIV-1 Circulating in the Netherlands. *Science* **2022**, *375*, 540–545.
- (32) Zinnen, S., Hsieh, J.-C., Modrich, P. Misincorporation and Mispaiied Primer Extension by Human Immunodeficiency Virus Reverse Transcriptase. *J. Biol. Chem.* **1994**, *269*, 24195–24202.
- (33) Collins, S. HIV Pipeline 2020: Targets in the HIV Lifecycle. *HIV Pipeline* **2020**, *21*.
- (34) Sarafianos, S. G., Marchand, B., Das, K., Himmel, D. M., Parniak, M. A., Hughes, S. H., Arnold, E. Structure and Function of HIV-1 Reverse Transcriptase: Molecular Mechanisms of Polymerization and Inhibition. *J. Mol. Biol.* **2009**, *385*, 693–713.
- (35) Flexner, C. HIV Drug Development: The Next 25 Years. *Nat. Rev. Drug Discov.* **2007**, *6*, 959.
- (36) Jordheim, L. P., Durantel, D., Zoulim, F., Dumontet, C. Advances in the Development of Nucleoside and Nucleotide Analogues for Cancer and Viral Diseases. *Nat. Rev. Drug Discov.* **2013**, *12*, 447–464.
- (37) Balzarini, J. Metabolism and Mechanism of Antiretroviral Action of Purine and Pyrimidine Derivatives. *J. Pharm. World Sci.* **1994**, *16*, 113.
- (38) Johns, D. G., Broder, S. Inhibition of Human Immunodeficiency Virus (HIV-1/HTLV-III_{Ba-L}) Replication in Fresh and Cultured Human Peripheral Blood Monocytes/Macrophages by Azidothymidine and Related 2',3'-Dideoxynucleosides. *J. Exp. Med.* **1988**, *168*, 1111–1125.
- (39) Balzarini, J., Herdewijn, P., Clercq, E. de. Differential Patterns of Intracellular Metabolism of 2',3'-Didehydro-2',3'-dideoxythymidine and 3'-Azido-2',3'-dideoxythymidine, Two Potent Anti-human Immunodeficiency Virus Compounds. *J. Biol. Chem.* **1989**, *264*, 6127–6133.
- (40) McGuigan, C. Certain Phosphoramidate Derivatives of Dideoxy Uridine (ddU) are Active Against HIV and Successfully By-pass Thymidine Kinase. *FEBS Lett.* **1994**, *351*, 11–14.
- (41) McGuigan, C. Aryl Phosphoramidate Derivatives of d4T Have Improved Anti-HIV Efficacy in Tissue Culture and May Act by the Generation of a Novel Intracellular Metabolite. *J. Med. Chem.* **1996**, *39*, 1748–1753.
- (42) Meier, C. cycloSal Phosphates as Chemical Trojan Horses for Intracellular Nucleotide and Glycosylmonophosphate Delivery —: Chemistry Meets Biology. *Eur. J. Org. Chem.* **2006**, *2006*, 1081–1102.

Experimental Procedure

- (43) Robbins, B. L., Srinivas, R. V., Kim, C., Bischofberger, N., Fridland, A. Anti-Human Immunodeficiency Virus Activity and Cellular Metabolism of a Potential Prodrug of the Acyclic Nucleoside Phosphonate 9-R-(2-Phosphonomethoxypropyl)adenine (PMPA), Bis(isopropylloxymethylcarbonyl)PMPA. *Antimicrob. Agents Chemother.* **1998**, *42*, 612–617.
- (44) Chapman, H., Kernan, M., Prisbe, E., Rohloff, J., Sparacino, M., Terhorst, T., Yu, R. Practical Synthesis, Separation, and Stereochemical Assignment of the PMPA Pro-Drug GS-7340. *Nucleosides Nucleotides Nucleic Acids* **2001**, *20*, 621–628.
- (45) Schulz, T., Balzarini, J., Meier, C. The DiPPro Approach: Synthesis, Hydrolysis, and Antiviral Activity of Lipophilic d4T Diphosphate Prodrugs. *ChemMedChem* **2014**, *9*, 762–775.
- (46) Weinschenk, L., Schols, D., Balzarini, J., Meier, C. Nucleoside Diphosphate Prodrugs: Nonsymmetric DiPPro-Nucleotides. *J. Med. Chem.* **2015**, *58*, 6114–6130.
- (47) Meier, C., Jessen, H. J., Schulz, T., Weinschenk, L., Pertenbreiter, F., Balzarini, J. Rational Development of Nucleoside Diphosphate Prodrugs: DiPPro-Compounds. *Curr. Med. Chem.* **2015**, *22*, 3933–3950.
- (48) Gollnest, T., Oliveira, T. D. de, Schols, D., Balzarini, J., Meier, C. Lipophilic Prodrugs of Nucleoside Triphosphates as Biochemical Probes and Potential Antivirals. *Nat. Commun.* **2015**, *6*, 8716.
- (49) Gollnest, T., Oliveira, T. D. de, Rath, A., Hauber, I., Schols, D., Balzarini, J., Meier, C. Membrane-Permeable Triphosphate Prodrugs of Nucleoside Analogues. *Angew. Chem. Int. Ed.* **2016**, *55*, 5255–5258.
- (50) Nack, T., Dinis de Oliveira, T., Weber, S., Schols, D., Balzarini, J., Meier, C. γ -Ketobenzyl-Modified Nucleoside Triphosphate Prodrugs as Potential Antivirals. *Journal of medicinal chemistry* **2020**, *63*, 13745–13761.
- (51) Jia, X., Weber, S., Schols, D., Meier, C. Membrane Permeable, Bioreversibly Modified Prodrugs of Nucleoside Diphosphate- γ -Phosphonates. *J. Med. Chem.* **2020**, *63*, 11990–12007.
- (52) Zhao, C., Weber, S., Schols, D., Balzarini, J., Meier, C. Prodrugs of γ -Alkyl-Modified Nucleoside Triphosphates: Improved Inhibition of HIV Reverse Transcriptase. *Angew. Chem. Int. Ed.* **2020**, *132*, 22247–22255.
- (53) Gumina, G., Chong, Y., Choo, H., Song, G.-Y., Chu, C. K. L-Nucleosides: Antiviral Activity and Molecular Mechanism. *Curr. Top. Med. Chem.* **2002**, *2*, 1065–1086.
- (54) Mathé, C., Gosselin, G. L-Nucleoside Enantiomers as Antiviral Drugs: A Mini-Review. *Antivir. Res.* **2006**, *71*, 276–281.
- (55) Vyas, R., Reed, A. J., Raper, A. T., Zahurancik, W. J., Wallenmeyer, P. C., Suo, Z. Structural basis for the D-stereoselectivity of human DNA polymerase β . *Nucleic Acids Res.* **2017**, *45*, 6228–6237.
- (56) Hahn, B. H., Shaw, G. M., Arya, S. K., Popovic, M., Gallo, R. C., Wong-Staal, F. Molecular Cloning and Characterization of the HTLV-III Virus Associated with AIDS. *Nature* **1984**, *312*, 166–169.

Experimental Procedure

- (57) Keele, B. F., van Heuverswyn, F., Li, Y., Bailes, E., Takehisa, J., Santiago, M. L., Bibollet-Ruche, F., Chen, Y., Wain, L. V., Liegeois, F., Loul, S., Ngole, E. M., Bienvenue, Y., Delaporte, E., Brookfield, J. F. Y., Sharp, P. M., Shaw, G. M., Peeters, M., Hahn, B. H. Chimpanzee Reservoirs of Pandemic and Nonpandemic HIV-1. *Science* **2006**, *313*, 523–526.
- (58) Clavel, F., Guétard, D., Brun-Vézinet, F., Chamaret, S., Rey, M.-A., Santos-Ferreira, M. O., Laurent, A. G., Dauguet, C., Katalama, C., Rouzioux, C., Klatzmann, D., Champalimaud, J. L., Montagnier, L. Isolation of a New Human Retrovirus from West African Patients with AIDS. *Science* **1986**, *233*, 343–346.
- (59) Chen, Z. Genetic Characterization of New West African Simian Immunodeficiency Virus SIVsm: Geographic Clustering of Household-Derived SIV Strains with Human Immunodeficiency Virus Type 2 Subtypes and Genetically Diverse Viruses from a Single Feral Sooty Mangabey Troop. *J. Virol.* **1996**, *70*, 3617.
- (60) Faria, N. R., Rambaut, A., Suchard, M. A., Baele, G., Bedford, T., Ward, M. J., Tatem, A. J., Sousa, J. D., Arinaminpathy, N., Pépin, J., Posada, D., Peeters, M., Pybus, O. G., Lemey, P. The Early Spread and Epidemic Ignition of HIV-1 in Human Populations. *Science* **2014**, *346*, 56–61.
- (61) Sharp, P. M., Hahn, B. H. Origins of HIV and the AIDS Pandemic. *Cold Spring Harb. Perspect. Med.* **2011**, *1*, a006841.
- (62) Lemey, P., Pybus, O. G., Wang, B., Saksena, N. K., Salemy, M., Vandamme, A.-M. Tracing the Origin and History of the HIV-2 Epidemic. *Proc. Natl. Acad. Sci.* **2003**, *100*, 6588–6592.
- (63) Hirsch, V. M., Olmsted, R. A., Murphey-Corb, M., Purcell, R. H., Johnson, P. R. An African Primate lentivirus (SIVsm) Closely Related to HIV-2. *Nature* **1989**, *339*, 389.
- (64) Garnier, L., Ratner, L., Rovinski, B., Cao, S.-X., Wills, J. W. Particle Size Determinants in the Human Immunodeficiency Virus Type 1 Gag Protein. *J. Virol.* **1998**, *72*, 4667–4677.
- (65) Campbell, E. M., Hope, T. J. HIV-1 Capsid: The Multifaceted Key Player in HIV-1 Infection. *Nat. Rev. Microbiol.* **2015**, *13*, 471–483.
- (66) Gu, W.-G., Zhang, X., Yuan, J.-F. Anti-HIV Drug Development Through Computational Methods. *AAPS J.* **2014**, *16*, 674–680.
- (67) Ghanam, R. H., Samal, Alexandra, Alexandra B., Fernandez, T. F., Saad, J. S. Role of the HIV-1 Matrix Protein in Gag Intracellular Trafficking and Targeting to the Plasma Membrane for Virus Assembly. *Front. Microbiol.* **2012**, *3*, 1–15.
- (68) Rossi, E., Meuser, M. E., Cunanan, C. J., Cocklin, S. Structure, Function, and Interactions of the HIV-1 Capsid Protein. *Life* **2021**, *11*.
- (69) Li, L., Li, H. S., Pauza, C. D., Bukrinsky, M., Zhao, R. Y. Roles of HIV-1 Auxiliary Proteins in Viral Pathogenesis and Host-Pathogen Interactions. *Cell Res.* **2005**, *15*, 923–934.

Experimental Procedure

- (70) RCSB: PDB-101. *PDB101: Learn: Flyers, Posters, & Calendars: Posters: The Structural Biology of HIV (Poster)*, 2022. <https://pdb101.rcsb.org/learn/flyers-posters-and-calendars/poster/the-structural-biology-of-hiv-poster>. Accessed 27 October 2022.
- (71) Berman, H. M., Westbrook, J., Feng, Z., Gilliland, G., Bhat, T. N., Weissig, H., Shindyalov, I. N., Bourne, P. E. The Protein Data Bank. *Nucleic Acids Res.* **2000**, *28*, 235–242.
- (72) Fackler, O. T., Murooka, T. T., Imle, A., Mempel, T. R. Adding New Dimensions: Towards an Integrative Understanding of HIV-1 Spread. *Nat. Rev. Microbiol.* **2014**, *12*, 563–574.
- (73) Deeks, S. G., Overbaugh, J., Phillips, A., Buchbinder, S. HIV Infection. *Nat. Rev.* **2015**, *1*, 1.
- (74) Doitsh, G., Greene, W. C. Dissecting How CD4 T Cells Are Lost During HIV Infection. *Cell Host Microbe.* **2016**, *19*, 280–291.
- (75) Whitney, J. B., Hill, A. L., Sanisetty, S., Penaloza-MacMaster, P., Liu, J., Shetty, M., Parenteau, L., Cabral, C., Shields, J., Blackmore, S., Smith, J. Y., Brinkman, A. L., Peter, L. E., Mathew, S. I., Smith, K. M., Borducchi, E. N., Rosenbloom, D. I. S., Lewis, M. G., Hattersley, J., Li, B., Hesselgesser, J., Geleziunas, R., Robb, M. L., Kim, J. H., Michael, N. L., Barouch, D. H. Rapid Seeding of the Viral Reservoir Prior to SIV Viraemia in Rhesus Monkeys. *Nature* **2014**, *512*, 74–77.
- (76) Nyamweya, S., Hegedus, A., Jaye, A., Rowland-Jones, S., Flanagan, K. L., Macallan, D. C. Comparing HIV-1 and HIV-2 Infection: Lessons for Viral Immunopathogenesis. *Rev. Med. Virol.* **2013**, *23*, 221–240.
- (77) Rumbwere Dube, B. N., Marshall, T. P., Ryan, R. P., Omonijo, M. Predictors of human immunodeficiency virus (HIV) infection in primary care among adults living in developed countries: a systematic review. *Syst. Rev.* **2018**, *7*, 82.
- (78) Leth, S., Schleimann, M. H., Nissen, S. K., Højen, J. F., Olesen, R., Graversen, M. E., Jørgensen, S., Kjær, A. S., Denton, P. W., Mørk, A., Sommerfelt, M. A., Krogsgaard, K., Østergaard, L., Rasmussen, T. A., Tolstrup, M., Søgaard, O. S. Combined Effect of Vacc-4x, Recombinant Human Granulocyte Macrophage Colony-Stimulating Factor Vaccination, and Romidepsin on the HIV-1 Reservoir (REDUC): A Single-Arm, Phase 1B/2A Trial. *Lancet HIV* **2016**, *3*, e463-e472.
- (79) Wilen, C. B., Tilton, J. C., Doms, R. W. HIV: Cell Binding and Entry. *Cold Spring Harb. Perspect. Med.* **2012**, *2*.
- (80) *Life Cycle – Science of HIV*, 2022. <https://scienceofhiv.org/wp/life-cycle/>. Accessed 5 August 2022.
- (81) Müller, T. G., Zila, V., Peters, K., Schifferdecker, S., Stanic, M., Lucic, B., Laketa, V., Lusic, M., Müller, B., Kräusslich, H.-G. HIV-1 Uncoating by Release of Viral cDNA from Capsid-Like Structures in the Nucleus of Infected Cells. *eLife* **2021**, *10*.
- (82) Francis, A. C., Melikyan, G. B. Single HIV-1 Imaging Reveals Progression of Infection through CA-Dependent Steps of Docking at the Nuclear Pore, Uncoating, and Nuclear Transport. *Cell host & microbe* **2018**, *23*, 536-548.e6.

Experimental Procedure

- (83) Hu, W.-S., Hughes, S. H. HIV-1 Reverse Transcription. *Cold Spring Harb. Perspect. Med.* **2012**, *2*.
- (84) Aiken, C., Rousso, I. The HIV-1 Capsid and Reverse Transcription. *Retrovirology* **2021**, *18*, 29.
- (85) Delelis, O., Carayon, K., Saïb, A., Deprez, E., Mouscadet, J.-F. Integrase and Integration: Biochemical Activities of HIV-1 Integrase. *Retrovirology* **2008**, *5*.
- (86) Craigie, R. The Molecular Biology of HIV Integrase. *Future virology* **2012**, *7*, 679–686.
- (87) Chiu, T. K., Davies, D. R. Structure and Function of HIV-1 Integrase. *Curr. Top. Med. Chem.* **2004**, *4*, 965–977.
- (88) Olson, A., Basukala, B., Wong, W. W., Henderson, A. J. Targeting HIV-1 Proviral Transcription. *Curr. Opin. Virol.* **2019**, *38*, 89–96.
- (89) Blissenbach, M., Grewe, B., Hoffmann, B., Brandt, S., Uberla, K. Nuclear RNA Export and Packaging Functions of HIV-1 Rev Revisited. *J. Virol.* **2010**, *84*, 6598–6604.
- (90) Göttliger, H. G., Dorfman, T., Sodroski, J. G., Haseltine, W. A. Effect of Mutations Affecting the p6 gag Protein on Human Immunodeficiency Virus Particle Release. *Proc. Natl. Acad. Sci.* **1991**, *88*, 3195–3199.
- (91) Pettit, S. C., Everitt, L. E., Choudhury, S., Dunn, B. M., Kaplan, A. H. Initial Cleavage of the Human Immunodeficiency Virus Type 1 GagPol Precursor by its Activated Protease Occurs by an Intramolecular Mechanism. *J. Virol.* **2004**, *78*, 8477–8485.
- (92) Amblard, F., Patel, D., Michailidis, E., Coats, S. J., Kasthuri, M., Biteau, N., Tber, Z., Ehteshami, M., Schinazi, R. F. HIV Nucleoside Reverse Transcriptase Inhibitors. *Eur. J. Med. Chem.* **2022**, *240*, 114554.
- (93) Richman Douglas D., Fischl Margaret A., Grieco Michael H., Gottlieb Michael S., Volberding Paul A., Laskin Oscar L., Leedom John M., Groopman Jerome E., Mildvan Donna, Hirsch Martin S., Jackson George G., Durack David T., Nusinoff-Lehrman Sandra. The Toxicity of Azidothymidine (AZT) in the Treatment of Patients with AIDS and AIDS-Related Complex. *N. Engl. J. Med.* **1987**, *317*, 192–197.
- (94) Hopkinson, D., Scheiner, P., Barile, F. A. In Vitro Cytotoxicity Testing of Potentially Active Anti-HIV Drugs with Cultured Cells. *Altern Lab Anim* **1996**, *24*, 413–418.
- (95) Margolis, A. M., Heverling, H., Pham, P. A., Stolbach, A. A Review of the Toxicity of HIV Medications. *J. Med. Toxicol.* **2014**, *10*, 26–39.
- (96) Li, G., Wang, Y., Clercq, E. de. Approved HIV Reverse Transcriptase Inhibitors in the Past Decade. *Acta Pharm. Sin. B* **2022**, *12*, 1567–1590.
- (97) Carr, A. Toxicity of Antiretroviral Therapy and Implications for Drug Development. *Nat. Rev. Drug Discov.* **2003**, *2*, 624–634.
- (98) Portsmouth, S. D., Scott, C. J. The Renaissance of Fixed Dose Combinations: Combivir. *Ther. Clin. Risk. Manag.* **2007**, *3*, 579–583.

Experimental Procedure

- (99) Sluis-Cremer, N., Temiz, N. A., Bahar, I. Conformational Changes in HIV-1 Reverse Transcriptase Induced by Nonnucleoside Reverse Transcriptase Inhibitor Binding. *Curr. HIV Res.* **2004**, *2*, 323–332.
- (100) Clercq, E. de. Anti-HIV Drugs: 25 Compounds Approved within 25 Years After the Discovery of HIV. *Int. J. Antimicrob. Agents* **2009**, *33*, 307–320.
- (101) Ghosh, A. K., Osswald, H. L., Prato, G. Recent Progress in the Development of HIV-1 Protease Inhibitors for the Treatment of HIV/AIDS. *J. Med. Chem.* **2016**, *59*, 5172–5208.
- (102) Laskey, S. B., Siliciano, R. F. A Mechanistic Theory to Explain the Efficacy of Antiretroviral Therapy. *Nat. Rev. Microbiol.* **2014**, *12*, 772–780.
- (103) Wang, Y., Gu, S.-X., He, Q., Fan, R. Advances in the Development of HIV Integrase Strand Transfer Inhibitors. *Eur. J. Med. Chem.* **2021**, *225*, 113787.
- (104) Smith, P. F., Robbins, G. K., Shafer, R. W., Wu, H., Yu, S., Hirsch, M. S., Merigan, T. C., Park, J.-G., Forrest, A., Fischl, M. A., Morse, G. D. Pharmacokinetics of Nelfinavir and Efavirenz in Antiretroviral-Naive, Human Immunodeficiency Virus-Infected Subjects When Administered Alone or in Combination with Nucleoside Analog Reverse Transcriptase Inhibitors. *Antimicrob. Agents Chemother.* **2005**, *49*, 3558–3561.
- (105) Wonganan, P., Limpanasithikul, W., Jianmongkol, S., Kerr, S. J., Ruxrungtham, K. Pharmacokinetics of Nucleoside/Nucleotide Reverse Transcriptase Inhibitors for the Treatment and Prevention of HIV Infection. *Expert Opin. Drug Metab. Toxicol.* **2020**, *16*, 551–564.
- (106) Casazza, J. P., Cale, E. M., Narpala, S., Yamshchikov, G. V., Coates, E. E., Hendel, C. S., Novik, L., Holman, L. A., Widge, A. T., Apte, P., Gordon, I., Gaudinski, M. R., Conan-Cibotti, M., Lin, B. C., Nason, M. C., Trofymenko, O., Telscher, S., Plummer, S. H., Wycuff, D., Adams, W. C., Pandey, J. P., McDermott, A., Roederer, M., Sukienik, A. N., O'Dell, S., Gall, J. G., Flach, B., Terry, T. L., Choe, M., Shi, W., Chen, X., Kaltovich, F., Saunders, K. O., Stein, J. A., Doria-Rose, N. A., Schwartz, R. M., Balazs, A. B., Baltimore, D., Nabel, G. J., Koup, R. A., Graham, B. S., Ledgerwood, J. E., Mascola, J. R. Safety and Tolerability of AAV8 Delivery of a Broadly Neutralizing Antibody in Adults Living with HIV: A Phase 1, Dose-Escalation Trial. *Nat. Med.* **2022**, *28*, 1022–1030.
- (107) IAVI. *40 Years of AIDS Vaccine Research - IAVI*, 2022. <https://www.iavi.org/iavi-report/vol-25-no-2-2021/40years-of-aids-vaccine-research>. Accessed 14 September 2022.
- (108) Schneider, S. E., Bray, B. L., Mader, C. J., Friedrich, P. E., Anderson, M. W., Taylor, T. S., Boshernitzan, N., Niemi, T. E., Fulcher, B. C., Whight, S. R., White, J., Jonathan M, Greene, R. J., Stoltenberg, L. E., Lichty, M. Development of HIV Fusion Inhibitors. *J. Peptide Sci.* **2005**, *11*, 744–753.
- (109) Feng, J. Y. Addressing the Selectivity and Toxicity of Antiviral Nucleosides. *Antivir. Chem. Chemother.* **2018**, *26*, 2040206618758524.

Experimental Procedure

- (110) Crane, H. M., Grunfeld, C., Willig, J. H., Mugavero, M. J., van Rompaey, S., Moore, R., Rodriguez, B., Feldman, B. J., Lederman, M. M., Saag, M. S., Kitahata, M. M. Impact of NRTIs on Lipid Levels Among a Large HIV-Infected Cohort Initiating Antiretroviral Therapy in Clinical Care. *AIDS* **2011**, *25*, 185–195.
- (111) Kohler, J. J., Lewis, W. A Brief Overview of Mechanisms of Mitochondrial Toxicity from NRTIs. *Environ. Mol. Mutagen.* **2007**, *48*, 166–172.
- (112) Legradi, J., Dahlberg, A.-K., Cenijn, P., Marsh, G., Asplund, L., Bergman, Å., Legler, J. Disruption of Oxidative Phosphorylation (OXPHOS) by Hydroxylated Polybrominated Diphenyl Ethers (OH-PBDEs) Present in the marine environment. *Environ. Sci. Technol.* **2014**, *48*, 14703–14711.
- (113) Maagaard, A., Kvale, D. Mitochondrial Toxicity in HIV-Infected Patients Both Off and On Antiretroviral Treatment: A Continuum or Distinct Underlying Mechanisms? *J. Antimicrob. Chemother.* **2009**, *64*, 901–909.
- (114) Lewis, W., Day, B. J., Copeland, W. C. Mitochondrial Toxicity of NRTI Antiviral Drugs: An Integrated Cellular Perspective. *Nat. Rev. Drug Discov.* **2003**, *2*, 812–822.
- (115) Yamanaka, H., Gatanaga, H., Kosalaraksa, P., Matsuoka-Aizawa, S., Takahashi, T., Kimura, S., Oka, S. Novel Mutation of Human DNA Polymerase Gamma Associated with Mitochondrial Toxicity Induced by Anti-HIV Treatment. *J. Infect. Dis.* **2007**, *195*, 1419–1425.
- (116) Urata, Y., Painsil, E., Cheng, Y.-C., Matsuda, T., Sevinsky, H., Hawthorne, D., Bertz, R., Hanna, G. J., Grasela, D., Hwang, C. Randomized, Placebo-Controlled Single-Ascending-Dose Study to Evaluate the Safety, Tolerability and Pharmacokinetics of the HIV Nucleoside Reverse Transcriptase Inhibitor, BMS-986001, in Healthy Subjects. *J. Clin. Pharmacol.* **2014**, *54*, 657–664.
- (117) Vivet-Boudou, V., Didierjean, J., Isel, C., Marquet, R. Nucleoside and Nucleotide Inhibitors of HIV-1 Replication. *Cell. Mol. Life Sci.* **2006**, *63*, 163–186.
- (118) Gupta, S., Fransen, S., Paxinos, E. E., Stawiski, E., Huang, W., Petropoulos, C. J. Combinations of Mutations in the Connection Domain of Human Immunodeficiency Virus Type 1 Reverse Transcriptase: Assessing the Impact on Nucleoside and Nonnucleoside Reverse Transcriptase Inhibitor Resistance. *Antimicrob. Agents Chemother.* **2010**, *54*, 1973–1980.
- (119) Meyer, P. R., Matsuura, S. E., So, A. G., Scott, W. A. Unblocking of Chain-Terminated Primer by HIV-1 Reverse Transcriptase Through a Nucleotide-Dependent Mechanism. *Proc. Natl. Acad. Sci.* **1998**, *95*, 13471–13476.
- (120) Sluis-Cremer, N., Arion, D., Parniak, M. A. Molecular Mechanisms of HIV-1 Resistance to Nucleoside Reverse Transcriptase Inhibitors (NRTIs). *Cell. Mol. Life Sci.* **2000**, *57*, 1408–1422.
- (121) Anderson, P. L., Kakuda, T. N., Lichtenstein, K. A. The Cellular Pharmacology of Nucleoside- and Nucleotide-Analogue Reverse-Transcriptase Inhibitors and Its Relationship to Clinical Toxicities. *Clin. Infect. Dis.* **2004**, *38*, 743–753.

Experimental Procedure

- (122) Becher, F., Pruvost, A., Schlemmer, D. D., Créminon, C. A., Goujard, C. M., Delfrassy, J. F., Benech, H. C., Grassi, J. J. Significant Levels of Intracellular Stavudine Triphosphate are Found in HIV-Infected Zidovudine-treated Patients. *AIDS* **2003**, *17*, 555.
- (123) Hurwitz, S. J., Schinazi, R. F. Practical Considerations for Developing Nucleoside Reverse Transcriptase Inhibitors. *Drug Discov. Today Technol.* **2012**, *9*, e183-e193.
- (124) Holec, A. D., Mandal, S., Prathipati, P. K., Destache, C. J. Nucleotide Reverse Transcriptase Inhibitors: A Thorough Review, Present Status and Future Perspective as HIV Therapeutics. *Curr. HIV Res.* **2017**, *15*, 411–421.
- (125) Törnevik, Y., Jacobsson, B., Britton, S., Eriksson, S. Intracellular Metabolism of 3'-Azidothymidine in Isolated Human Peripheral Blood Mononuclear Cells. *AIDS Res. Hum. Retroviruses* **1991**, *7*, 751.
- (126) Mehellou, Y., Balzarini, J., McGuigan, C. Aryloxy Phosphoramidate Triesters: A Technology for Delivering Monophosphorylated Nucleosides and Sugars Into Cells. *ChemMedChem* **2009**, *4*, 1779–1791.
- (127) Seley-Radtke, K. L., Yates, M. K. The Evolution of Nucleoside Analogue Antivirals: A Review for Chemists and Non-chemists. Part 1: Early Structural Modifications to the Nucleoside Scaffold. *Antivir. Res.* **2018**, *154*, 66–86.
- (128) Schutter, C., Ehteshami, M., Hammond, E. T., Amblard, F., Schinazi, R. F. Metabolism of Nucleosides and Nucleotides Prodrugs. *Curr. Pharm. Des.* **2017**, *23*, 6984–7002.
- (129) Zhao C. *Non-Symmetrically-Masked TriPPPro Prodrugs and γ -Modified Nucleoside Triphosphate Compounds as Potential Antivirals against HIV*. Dissertation: Hamburg, 2019.
- (130) Pruvost, A., Negrodo, E., Benech, H., Theodoro, F., Puig, J., Grau, E., García, E., Moltó, J., Grassi, J., Clotet, B. Measurement of Intracellular Didanosine and Tenofovir Phosphorylated Metabolites and Possible Interaction of the Two Drugs in Human Immunodeficiency Virus-Infected Patients. *Antimicrob. Agents Chemother.* **2005**, *49*, 1907–1914.
- (131) Ho, H.-T., Hitchcock, M. J. M. Cellular Pharmacology of 2',3'-Dideoxy-2',3'-Didehydrothymidine, a Nucleoside Analog Active against Human Immunodeficiency Virus. *Antimicrob. Agents Chemother.* **1989**, *33*, 844–849.
- (132) Montgomery, J. A., Thomas, H. J., Schaeffer, H. J. Synthesis of Potential Anticancer Agents. XXVIII. Simple Esters of 6-Mercaptopurine Ribonucleotide. *J. Org. Chem.* **1961**, *26*, 1929–1933.
- (133) Wagner, C. R., Iyer, V. V., McIntee, E. J. Pronucleotides: Toward the in Vivo Delivery of Antiviral and Anticancer Nucleotides. *Med. Res. Rev.* **2000**, *20*, 417.
- (134) McGuigan, C. Aryl Phosphate Derivatives of AZT Retain Activity Against HIV1 in Cell lines Which are Resistant to the Action of AZT. *Antiviral Res.* **1992**, *17*, 311–321.
- (135) Albert, A. Chemical Aspect of Selective Toxicity. *Nature* **1958**, *182*, 421–423.

Experimental Procedure

- (136) Heidel, K. M., Dowd, C. S. Phosphonate Prodrugs: An Overview and Recent Advances. *Future Med. Chem.* **2019**, *11*, 1625–1643.
- (137) Erion, M. D., van Poelje, P. D., Mackenna, D. A., Colby, T. J., Montag, A. C., Fujitaki, J. M., Linemeyer, D. L., Bullough, D. A. Liver-Targeted Drug Delivery Using HepDirect Prodrugs. *J. Pharmacol. Exp. Ther.* **2005**, *312*, 554–560.
- (138) Hecker, S. J., Erion, M. D. Prodrugs of Phosphates and Phosphonates. *J. Med. Chem.* **2008**, *51*, 2328–2345.
- (139) Rautio, J., Meanwell, N. A., Di, L., Hageman, M. J. The Expanding Role of Prodrugs in Contemporary Drug Design and Development. *Nat. Rev. Drug Discov.* **2018**, *17*, 559–587.
- (140) Pradere, U., Garnier-Amblard, E. C., Coats, S. J., Amblard, F., Schinazi, R. F. Synthesis of Nucleoside Phosphate and Phosphonate Prodrugs. *Chem. Rev.* **2014**, *114*, 9154–9218.
- (141) Rosowsky, A., Kim, S.-H., Ross, J., Wick, M. M. Lipophilic 5'-(Alkyl Phosphate) Esters of 1- β -D-Arabinofuranosylcytosine and its N4-Acyl and 2,2'-Anhydro-3'-O-Acyl Derivatives as Potential Prodrugs. *J. Med. Chem.* **1982**, *25*, 171–178.
- (142) Heußner, P., Willemze, R., Ganser, A., Hanauske, A., Amadori, S., Heil, G., Schleyer, E., Hiddemann, W., Selbach, J., Schüßler, M., Freund, M. YNK01, an Oral Cytosine Arabinoside Derivative in Acute Myeloid Leukemia and Chronic Myeloid Leukemia. In *Acute Leukemias VI*; Büchner, T., Schellong, G., Ritter, J., Creutzig, U., Hiddemann, W., Wörmann, B., Eds.; Springer Berlin Heidelberg: Berlin, Heidelberg, 1997; Vols. 38, pp. 882–885.
- (143) Abrahamsson K., Eriksson, B. O., Holme, E., Jodal, U., Lindstedt, S., Nordin, I. Impaired Ketogenesis in Carnitine Depletion Caused by Short-Term Administration of Pivalic Acid Prodrug. *Biochem. Med. Metab. Biol.* **1994**, *52*, 18–21.
- (144) Farquhar, D., Khan, S., Srivastva, D. N., Saunders, P. P. Synthesis and Antitumor Evaluation of Bis[(pivaloyloxy)methyl] 2'-Deoxy-5-fluorouridine 5'-Monophosphate (FdUMP): A Strategy To Introduce Nucleotides into Cells. *J. Med. Chem.* **1994**, *37*, 3902–3909.
- (145) Meier, C. Pro-Nucleotides -: Recent Advances in the Design of Efficient Tools for the Delivery of Biologically Active Nucleoside Monophosphates. *Synlett* **1998**, *3*, 233.
- (146) Devine, K. G., McGuigan, C., O'Connor, T. J., Nicholls, S. R., Kinchington, D. Novel Phosphate Derivatives of Zidovudine as Anti-HIV Compounds. *AIDS* **1990**, *4*, 371–373.
- (147) Česnek, M., Jansa, P., Šmídková, M., Mertlíková-Kaiserová, H., Dračínský, M., Brust, T. F., Pávek, P., Trejtnar, F., Watts, V. J., Janeba, Z. Bisamidate Prodrugs of 2-Substituted 9-2-(Phosphonomethoxy)ethyladenine (PMEA, adefovir) as Selective Inhibitors of Adenylate Cyclase Toxin from Bordetella Pertussis. *ChemMedChem* **2015**, *10*, 1351–1364.
- (148) Cahard, D., McGuigan, C., Balzarini, J. Aryloxy Phosphoramidate Triesters as Pro-Tides. *Mini-Rev. Med. Chem.* **2004**, *4*, 371–381.

Experimental Procedure

- (149) Slusarczyk, M., Serpi, M., Pertusati, F. Phosphoramidates and Phosphoramidates (ProTides) with Antiviral Activity. *Antivir. Chem. Chemother.* **2018**, *26*, 1-31.
- (150) Hung, A., Sinclair, M., Hemmersbach-Miller, M., Edmonston, D., Wyatt, C. Prescribing Rates and Characteristics of Recipients of Tenofovir-Containing Regimens Before and After Market Entry of Tenofovir Alafenamide. *J. Manag. Care Spec. Pharm.* **2020**, *26*, 1582–1588.
- (151) Cui, H., Ruiz-Pérez, L. M., Gonzáles-Pacanowska, D., Gilbert, I. H. Potential Application of Thymidylate Kinase in Nucleoside Analogue Activation in Plasmodium Falciparum. *Bioorg. Med. Chem.* **2010**, *18*, 7302–7309.
- (152) Dousson, C. B. Current and Future use of Nucleo(s)tide Prodrugs in the Treatment of Hepatitis C Virus Infection. *Antivir. Chem. Chemother.* **2018**, *26*, 2040206618756430.
- (153) Ju, J., Li, X., Kumar, S., Jockusch, S., Chien, M., Tao, C., Morozova, I., Kalachikov, S., Kirchdoerfer, R. N., Russo, J. J. Nucleotide analogues as inhibitors of SARS-CoV Polymerase. *Pharmacol. Res. Perspect.* **2020**, e00674.
- (154) Périgaud, C., Gosselin, G., Lefebvre, I., Giradet, J.-L., Benzaria, S., Barber, I., Imbach, J.-L. Rational Design for Cytosolic Delivery of Nucleoside Monophosphates: “SATE” and “DTE” as Enzyme-Labile Transient Phosphate Protecting Groups. *Bioorg. Med. Chem. Lett.* **1993**, *3*, 2521–2526.
- (155) Giradet, J.-L., Périgaud, C., Aubertin, A.-M., Gosselin, G., Kirn, A., Imbach, J.-L. Increase of the Anti-HIV Activity of d4T in Human T-Cell Culture by the Use of the Sate Pronucleotide Approach. *Bioorg. Med. Chem. Lett.* **1995**, *5*, 2981–2984.
- (156) Thomson, W., Nicholls, D., Irwin, W. J., Al-Mushadani, J. S., Freeman, S., Karpas, A., Petrik, J., Mahmood, N., Hay, A. J. Synthesis, Bioactivation and Anti-HIV Activity of the Bis(4-acyloxybenzyl) and Mono(4-acyloxybenzyl) Esters of the 5'-Monophosphate of AZT. *J. Chem. Soc. Perkin Trans. 1* **1993**, 1239.
- (157) Jessen, H. J., Schulz, T., Balzarini, J., Meier, C. Bioreversible Protection of Nucleoside Diphosphates. *Angew. Chem. Int. Ed.* **2008**, *47*, 8719–8722.
- (158) Meier, C. 2-Nucleos-5'-O-yl-4H-1,3,2-benzodioxaphosphinin-2-oxides-: A New Concept for Lipophilic, Potential Prodrugs of Biologically Active Nucleoside Monophosphates. *Angew. Chem. Int. Ed. Engl.* **1996**, *35*, 70–72.
- (159) Balzarini, J., Aquaro, S., Knispel, T., Rampazzo, C., Bianchi, V., Perno, C.-F., Clercq, E. de, Meier, C. Cyclosaligenyl-2',3'-didehydro-2',3'-dideoxythymidine Monophosphate: Efficient Intracellular Delivery of d4TMP. *Mol. Pharmacol.* **2000**, *58*, 928–935.
- (160) Meier, C., Balzarini, J. Application of the cycloSal-Prodrug Approach for Improving the Biological Potential of Phosphorylated Biomolecules. *Antivir. Res.* **2006**, *71*, 282–292.

Experimental Procedure

- (161) Gisch, N., Balzarini, J., Meier, C. Enzymatically Activated cycloSal-d4T-Monophosphates: The Third Generation of cycloSal-Pronucleotides. *J. Med. Chem.* **2007**, *50*, 1658–1667.
- (162) Hostetler, K. Y., Beadle, J. R., Kini, G. D., Gardner, M. F., Wright, K. N., Wu, T.-H., Korba Brent E. Enhanced Oral Absorption and Antiviral Activity of 1-O-Octadecyl-sn-glycero-3-phospho-acyclovir and Related Compounds in Hepatitis B Virus Infection, In Vitro. *Biochem. Pharmacol.* **1997**, *53*, 1815–1822.
- (163) Hostetler, K. Y., Aldern, K. A., Wan, W. B., Ciesla, S. L., Beadle, J. R. Alkoxyalkyl Esters of (S)-9-3-Hydroxy-2-(Phosphonomethoxy)Propyladenine are Potent Inhibitors of the Replication of Wild-Type and Drug-Resistant Human Immunodeficiency Virus Type 1 in Vitro. *Antimicrob. Agents Chemother.* **2006**, *50*, 2857–2859.
- (164) Erion, M. D., Reddy, K. R., Boyer, S. H., Matelich, M. C., Gomez-Galeno, J., Lemus, R. H., Ugarkar, B. G., Colby, T. J., Schanzer, J., van Poelje, P. D. Design, Synthesis, and Characterization of a Series of Cytochrome P(450) 3A-Activated Prodrugs (HepDirect Prodrugs) Useful for Targeting Phosph(on)ate-Based Drugs to the Liver. *J. Am. Chem. Soc.* **2004**, *126*, 5154–5163.
- (165) Bonnaffé, D., Dupraz, B., Ughetto-Monfrin, J., Namane, A., Huynh Dinh, T. Synthesis of Acyl Pyrophosphates. Application to the Synthesis of Nucleotide Lipophilic Prodrugs. *Tetrahedron Lett.* **1995**, *36*, 531–534.
- (166) Sommadossi, J.-P., Carlisle, R., Zhou, Z. Cellular Pharmacology of 3'-Azido-3'-Deoxythymidinewith Evidence of Incorporation Into DNA of Human Bone Marrow Cells. *Mol. Pharmacol.* **1989**, *36*, 9–14.
- (167) Harrington, J. A., Reardon, J. E., Spector, T. 3'-Azido-3'-Deoxythymidine (AZT) Monophosphate: An Inhibitor of Exonucleolytic Repair of AZT-Terminated DNA. *Antimicrob. Agents Chemother.* **1993**, *37*, 918–920.
- (168) Hostetler, K. Y., Stuhmiller, L. M., Lenting, H. B. M., van den Bosch, H. Synthesis and Antiretroviral Activity of Phospholipid Analogs of Azidothymidine and Other Antiviral Nucleosides. *J. Biol. Chem.* **1990**, *265*, 6112–6117.
- (169) Bonnaffé, D., Dupraz, B., Ughetto-Monfrin, J., Namane, A., Henin, Y., Huynh Dinh, T. Potential Lipophilic Nucleotide Prodrugs: Synthesis, Hydrolysis, and Antiretroviral Activity of AZT and d4T Acyl Nucleotides. *J. Org. Chem.* **1996**, *61*, 895–902.
- (170) van Wijk, G. M. T., Hostetler, K. Y., Kroneman, E., Richman, D. D., Sridhar, C. N., Kumar, R., van den Bosch, H. Synthesis and Antiviral activity of 3'-Azido-3'-Deoxythymidine Triphosphate Distearoylglycerol: A Novel Phospholipid Conjugate of the Anti-HIV Agent AZT. *Chem. Phys. Lipids* **1994**, *70*, 213–222.

Experimental Procedure

- (171) Rachwalak, M., Romanowska, J., Sobkowski, M., Stawinski, J. Nucleoside Di- and Triphosphates as a New Generation of Anti-HIV Pronucleotides. Chemical and Biological Aspects. *Appl. Sci.* **2021**, *11*, 2248.
- (172) Pertenbreiter, F., Balzarini, J., Meier, C. Nucleoside Mono- and Diphosphate Prodrugs of 2',3'-Dideoxyuridine and 2',3'-Dideoxy-2',3'-didehydrouridine. *ChemMedChem* **2015**, *10*, 94–106.
- (173) Warnecke, S., Meier, C. Synthesis of Nucleoside Di- and Triphosphates and Dinucleoside Polyphosphates with cycloSal-Nucleotides. *J. Org. Chem.* **2009**, *74*, 3024–3030.
- (174) Tan, X., Chu, C. K., Boudinot, F. D. Development and Optimization of Anti-HIV Nucleoside Analogs and Prodrugs: A Review of their Cellular Pharmacology, Structure-activity Relationships and Pharmacokinetics. *Adv. Drug Deliv. Rev.* **1999**, *39*, 117–151.
- (175) Sood, A., Kumar, S., Nampalli, S., Nelson, J. R., Macklin, J., Fuller, C. W. Terminal Phosphate-Labeled Nucleotides with Improved Substrate Properties for Homogeneous Nucleic Acid Assays. *J. Am. Chem. Soc.* **2005**, *127*, 2394–2395.
- (176) Kumar, S., Sood, A., Wegener, J., Finn, P. J., Nampalli, S., Nelson, J. R., Sekher, A., Mitsis, P., Macklin, J., Fuller, C. W. Terminal Phosphate Labeled Nucleotides: Synthesis, Applications, and Linker Effect on Incorporation by DNA Polymerases. *Nucleosides, nucleotides & nucleic acids* **2005**, *24*, 401–408.
- (177) Sowa, T., Ouchi, S. The Facile Synthesis of 5'-Nucleotides by the Selective Phosphorylation of a Primary Hydroxyl Group of Nucleosides with Phosphoryl Chloride. *Bull. Chem. Soc. Jpn.* **1975**, *48*, 2084–2090.
- (178) Yoshikawa, M., Kato, T., Takenishi, T. A Novel Method for Phosphorylation of Nucleosides to 5'-Nucleotides. *Tetrahedron Lett.* **1967**, *50*, 5065–5068.
- (179) Jia, X., Schols, D., Meier, C. Lipophilic Nucleoside Triphosphate Prodrugs of Anti-HIV Active Nucleoside Analogs as Potential Antiviral Compounds. *Adv. Sci.* **2023**, *10*, 2306021.
- (180) Jia, X., Schols, D., Meier, C. Pronucleotides of 2',3'-Dideoxy-2',3'-Didehydrothymidine as Potent Anti-HIV Compounds. *J. Med. Chem.* **2023**, *66*, 12163–12184.
- (181) Wang, W., Wu, E. Y., Hellinga, H. W., Beese, L. S. Structural Factors that Determine Selectivity of a High Fidelity DNA Polymerase for Deoxy-, Dideoxy-, and Ribonucleotides. *J. Biol. Chem.* **2012**, *287*, 28215–28226.
- (182) Coloma, J., Johnson, R. E., Prakash, L., Prakash, S., Aggarwal, A. K. Human DNA Polymerase α in Binary Complex with a DNA:DNA Template-Primer. *Sci. Rep.* **2016**, *6*, 23784.
- (183) Baranovskiy, A. G., Duong, V. N., Babayeva, N. D., Zhang, Y., Pavlov, Y. I., Anderson, K. S., Tahirov, T. H. Activity and Fidelity of Human DNA Polymerase α Depend on Primer Structure. *J. Biol. Chem.* **2018**, *293*, 6824–6843.

Experimental Procedure

- (184) Reijns, M. A. M., Kemp, H., Ding, J., Procé, S. M. de, Jackson, A. P., Taylor, M. S. Lagging-Strand Replication Shapes the Mutational Landscape of the Genome. *Nature* **2015**, *518*, 502–506.
- (185) Nakamura, J., La, D. K., Swenberg, J. A. 5'-Nicked Apurinic/Apyrimidinic Sites are Resistant to Beta-Elimination by Beta-Polymerase and are Persistent in Human Cultured Cells After Oxidative Stress. *J. Biol. Chem.* **2000**, *275*, 5323–5328.
- (186) Young, M. J. Off-Target Effects of Drugs that Disrupt Human Mitochondrial DNA Maintenance. *Front. Mol. Biosci.* **2017**, *4*, 74.
- (187) Beard, W. A., Wilson, S. H. Structure and Mechanism of DNA Polymerase β . *Biochemistry* **2014**, *53*, 2768–2780.
- (188) Kaufman, B. A., van Houten, B. POLB: A New Role of DNA Polymerase Beta in Mitochondrial Base Excision Repair. *DNA repair* **2017**, *60*, A1-A5.
- (189) Hudson, G., Chinnery, P. F. Mitochondrial DNA Polymerase-Gamma and Human Disease. *Hum. Mol. Genet.* **2006**, *15*, R244-R252.
- (190) Johnson, A. A., Ray, A. S., Hanes, J., Suo, Z., Colacino, Anderson, K. S., Johnson, K. A. Toxicity of Antiviral Nucleoside Analogs and the Human Mitochondrial DNA Polymerase. *J. Biol. Chem.* **2001**, *276*, 40847–40857.
- (191) Sohl, C. D., Szymanski, M. R., Mislak, A. C., Shumate, C. K., Amiralaei, S., Schinazi, R. F., Anderson, K. S., Yin, Y. W. Probing the Structural and Molecular Basis of Nucleotide Selectivity by Human Mitochondrial DNA Polymerase γ . *Proc. Natl. Acad. Sci.* **2015**, *112*, 8596–8601.
- (192) Triezenberg, S. J. Primer Extension. *Curr. Protoc. Mol. Biol.* **1992**, *20*, 3.18.1-10.3.12.
- (193) Wit, F. de, Pillalamarri, S. R., Sebastián-Martín, A., Venkatesham, A., van Aerschot, A., Debyser, Z. Design of Reverse Transcriptase-Specific Nucleosides to Visualize Early Steps of HIV-1 Replication by Click Labeling. *J. Biol. Chem.* **2019**, *294*, 11863–11875.
- (194) Jones H. *Plant Gene Transfer and Expression Protocols*; Humana Press: Totowa N.J., 1995.
- (195) Weising, S., Weber, S., Schols, D., Meier, C. Triphosphate Prodrugs of the Anti-HIV-Active Compound 3'-Deoxy-3'-fluorothymidine (FLT). *J. Med. Chem.* **2022**, *65*, 12163–12175.
- (196) Sohl, C. D., Kasiviswanathan, R., Kim, J., Pradere, U., Schinazi, R. F., Copeland, W. C., Mitsuya, H., Baba, M., Anderson, K. S. Balancing Antiviral Potency and Host Toxicity: Identifying a Nucleotide Inhibitor with an Optimal Kinetic Phenotype for HIV-1 Reverse Transcriptase. *Mol. Pharmacol.* **2012**, *82*, 125–133.
- (197) *Completed phase II study with MIV-310 does not justify further development by Boehringer Ingelheim*, 2023. <https://news.cision.com/medivir/r/completed-phase-ii-study-with-miv-310-does-not-justify-further-development-by-boehringer-ingelheim,c140889>. Accessed 25 May 2023.

- (198) *OBP-601 (Censavudine) - Pipeline | Oncolys BioPharma Inc*, 2022.
<https://www.oncolys.com/en/pipeline/obp-601.html>. Accessed 13 September 2022.
- (199) Gaffney, M. M., Belliveau, P. P., Spooner, L. M. Apricitabine: A Nucleoside Reverse Transcriptase Inhibitor for HIV Infection. *Ann. Pharmacother.* **2009**, *43*, 1676–1683.
- (200) Rajwanshi, V. K., Prhavic, M., Fagan, P., Brooks, J. L., Hurd, T., Cook, P. D., Wang, G. Synthesis of 5'-Triphosphate Mimics (P3Ms) of 3'-Azido-3',5'-Dideoxythymidine and 3',5'-Dideoxy-5'-Difluoromethylenethymidine as HIV-1 Reverse Transcriptase Inhibitors. *Nucleosides Nucleotides Nucleic Acids* **2005**, *24*, 179–189.
- (201) Hakimelahi, G. H., Moosavi-Movahedi, A. A., Sadeghi, M. M., Tsay, S.-C., Hwu, J. R. Design, Synthesis, and Structure-Activity Relationship of Novel Dinucleotide Analogs as Agents against Herpes and Human Immunodeficiency Viruses. *J. Med. Chem.* **1995**, *38*, 4648–4659.
- (202) Jia, X., Schols, D., Meier, C. Lipophilic Triphosphate Prodrugs of Various Nucleoside Analogues. *J. Med. Chem.* **2020**, *63*, 6991–7007.
- (203) Dinis de Oliveira T. *Substrateigenschaften Antiviral Aktiver Nucleotidanaloga Gegenüber Polymerasen*. Dissertation: Hamburg, 2017.
- (204) Hartmann, H., Vogt, M. W., Durno, Hirsch, M. S., Hunsmann, G., Eckstein, F. Enhanced In Vitro Inhibition of HIV-1 Replication by 3'-Fluoro-3'-deoxythymidine Compared to Several Other Nucleoside Analogs. *AIDS Res. Hum. Retroviruses* **1988**, *4*, 457–466.
- (205) Gollnest T. *Das TriPPPPro-Konzept: Entwicklung und Charakterisierung von antiviralen Nucleosidtriphosphat-Prodrugs*. Dissertation: Hamburg, 2015.
- (206) Witt J. *Synthese fluoreszenzmarkierter TriPPPPro- Verbindungen für Zellaufnahmestudien und Synthese antitumoraler TriPPPPro-Prodrugs*: Hamburg, 2022.
- (207) Roßmeier M. *Synthese γ -alkylierter fluoreszierender TriPPPPro-Verbindungen für Zellaufnahmestudien und symmetrischer antitumoraktiver TriPPPPro-Verbindungen für Zellproliferationsassays*. Dissertation: Hamburg, 2023.
- (208) Einhorn, A., Hollandt, F. Ueber die Acylierung der Alkohole und Phenole in Pyridinlösung. *Ann. Chem.* **1898**, *301*, 95–115.
- (209) Kullik G. A. *Synthese von acyclischen Phosphonat-Diphosphat-Prodrugs*. Dissertation: Hamburg, 2023.
- (210) Stark, H., Purand, K., Hüls, A., Ligneau, X., Garbarg, M., Schwarz, J.-C., Schunack, W. [125I]Iodoproxyfan and Related Compounds: A Reversible Radioligand and Novel Classes of Antagonists with High Affinity and Selectivity for the Histamine H3 Receptor. *J. Med. Chem.* **1996**, *39*, 1220–1226.
- (211) Meier, C. Nucleoside Diphosphate and Triphosphate Prodrugs -: An Unsolvable Task? *Antivir. Chem. Chemother.* **2017**, *25*, 69–82.

Experimental Procedure

- (212) Kumar, V., Kaushik, M. P. tert-Butyl-N-chlorocyanamide: A Novel and Versatile Reagent in Organic Synthesis. *Synth. Commun.* **2007**, *19*, 2937–2951.
- (213) Letsinger, R. L., Ogilvie, K. K. Synthesis of Oligothymidylates via Phosphotriester Intermediates. *J. Am. Chem. Soc.* **1969**, *91*, 3350–3355.
- (214) Sundseth, R., Joyner, S. S., Moore, J. T., Dornsife, R. E., Dev, I. K. The Anti-Human Immunodeficiency Virus Agent 3'-Fluorothymidine Induces DNA Damage and Apoptosis in Human Lymphoblastoid Cells. *Antivir. Chem. Chemother.* **1996**, *40*, 331–335.
- (215) Ghosn, J., Quinson, A.-M., Sabo, N. D., Cotte, L., Piketty, C., Dorléacq, N., Bravo, M.-L., Mayers, D., Harmenberg, J., Mårdh, G., Valdez, H., Katalama, C. Antiviral Activity of Low-dose Alovudine in Antiretroviral-experienced patients: Results from a 4-Week Randomized, Double-blind, Placebo-controlled Dose-ranging Trial. *HIV Med.* **2007**, *8*, 142–147.
- (216) Agarwal, H. K., Chhikara, B. S., Ye, G., Bhavaraju, S., Dixit, A., Kumar, A., Doncel, G. F., Parang, K. Synthesis and Biological Evaluation of 5'-O-Fatty Acyl Ester Derivatives of 3'-Fluoro-2',3'-dideoxythymidine as Potential Anti-HIV Microbicides. *Molecules* **2022**, *27*.
- (217) Srivastav, N. C., Shakya, N., Mak, M., Agrawal, B., Tyrrell, D. L., Kumar, R. Antiviral Activity of Various 1-(2'-Deoxy- β -D-lyxofuranosyl), 1-(2'-Fluoro- β -D-xylofuranosyl), 1-(3'-Fluoro- β -D-arabinofuranosyl), and 2'-Fluoro-2',3'-didehydro-2',3'-dideoxyribose Pyrimidine Nucleoside Analogues Against Duck Hepatitis B Virus (DHBV) and Human Hepatitis B Virus (HBV) Replication. *J. Med. Chem.* **2010**, *53*, 7156–7166.
- (218) Srivastav, N. C., Shakya, N., Bhavanam, S., Agrawal, A., Tse, C., Desroches, N., Kunimoto, D. Y., Kumar, R. Antimycobacterial Activities of 5-Alkyl (or Halo)-3'-Substituted Pyrimidine Nucleoside Analogs. *Bioorg. Med. Chem.* **2012**, *22*, 1091–1094.
- (219) Kortylewicz, Z. P., Kimura, Y., Inoue, K., Mack, E., Baranowska-Kortylewicz, J. Radiolabeled Cyclosaligenyl Monophosphates of 5-Iodo-2'-deoxyuridine, 5-Iodo-3'-fluoro-2',3'-dideoxyuridine, and 3'-Fluorothymidine for Molecular Radiotherapy of Cancer: Synthesis and Biological Evaluation. *J. Med. Chem.* **2012**, *55*, 2649–2671.
- (220) Marcuccio, S. M., Epa, R., White, J. M., Deadman, J. J. A New Process for Synthesis of Apricitabine, 2-(R)-Hydroxymethyl-4-(R)-(cytosin-1'-yl)-1,3-oxathiolane, an Anti-HIV NRTI. *Org. Process Res. Dev.* **2011**, *15*, 763–773.
- (221) Baar, M. P. de, Rooij, E. R. de, Smolders, K. G. M., van Schijndel, H. B., Timmermans, E. C., Bethell, R. Effects of Apricitabine and other Nucleoside Reverse Transcriptase Inhibitors on Replication of Mitochondrial DNA in HepG2 Cells. *Antiviral Res.* **2007**, *76*, 68–74.
- (222) National Center for Advancing Translational Science. <https://drugs.ncats.io/drug/K1YX059ML1>. Accessed 5 June 2023.

Experimental Procedure

- (223) Dutschman, G. E., Grill, S. P., Gullen, E. A., Haraguchi, K., Takeda, H., Baba, M., Cheng, Y.-C. Novel 4'-Substituted Stavudine Analog with Improved Anti-Human Immunodeficiency Virus Activity and Decreased Cytotoxicity. *Antimicrob. Agents Chemother.* **2004**, *48*, 1640–1646.
- (224) Haraguchi, K., Sumino, M., Tanaka, H. Nucleophilic Substitution at the 4'-Position of Nucleosides: New Access to a Promising Anti-HIV Agent 2',3'-Didehydro-3'-deoxy-4'-ethynylthymidine. *J. Org. Chem.* **2006**, *71*, 4433–4438.
- (225) Ortiz, A., Benkovics, T., Beutner, G. L., Shi, Z., Bultman, M., Nye, J., Sfougataki, C., Kronenthal, D. R. Scalable Synthesis of the Potent HIV Inhibitor BMS-986001 by Non-Enzymatic Dynamic Kinetic Asymmetric Transformation (DYKAT). *Angew. Chem. Int. Ed.* **2015**, *127*, 7291–7294.
- (226) Haraguchi, K., Shimada, H., Tanaka, H., Hamasaki, T., Baba, M., Gullen, E. A., Dutschman, G. E., Cheng, Y.-C. Synthesis and Anti-HIV Activity of 4'-Substituted 4'-Thiothymidines: A New Entry Based on Nucleophilic Substitution of the 4'-Acetoxy Group. *J. Med. Chem.* **2008**, *51*, 1885–1893.
- (227) Boyd, M. A., Cooper, D. A. Novel Antiretroviral Agents and Universal Access to HIV Care. *The Lancet HIV* **2016**, *3*, e2-3.
- (228) *TPN-101 | ALZFORUM*, 2022. <https://www.alzforum.org/therapeutics/tpn-101>. Accessed 13 September 2022.
- (229) Benkovics, T., Ortiz, A., Guo, Z., Goswami, A., Deshpande, P. Enantioselective Preparation of (S)-5-Oxo-5,6-dihydro-2H-pyran-2-yl Benzoate. *Org. Synth.* **2014**, *91*, 293–306.
- (230) Haraguchi, K., Takeda, S., Kubota, Y., Kumamoto, H., Tanaka, H., Hamasaki, T., Baba, M., Painsil, E., Cheng, Y.-C. From the Chemistry of Epoxy-Sugar Nucleosides to the Discovery of Anti-HIV Agent 4'-Ethynylstavudine-Festinavir. *Curr. Pharm. Des.* **2013**, *19*, 1880–1997.
- (231) Fu, L., Sui, X., Crolais, A. E., Gutekunst, W. R. Modular Approach to Degradable Acetal Polymers Using Cascade Enyne Metathesis Polymerization. *Angew. Chem. Int. Ed.* **2019**, *131*, 15873–15877.
- (232) Wang, H.-Y., Yang, K., Yin, D., Liu, C., Glazier, D. A., Tang, W. Chiral Catalyst-Directed Dynamic Kinetic Diastereoselective Acylation of Lactols for De Novo Synthesis of Carbohydrate. *Org. Lett.* **2015**, *17*, 5272–5275.
- (233) Arenas A. R. *DYKAT and Desymmetrization Strategies for the Synthesis of Axially Chiral Heterobiaryls*: Sevilla, 2019.
- (234) Steinreiber, J., Faber, K., Griengl, H. De-Racemization of Enantiomers Versus De-Epimerization of Diastereomers: Classification of Dynamic Kinetic Asymmetric Transformations (DYKAT). *Chemistry* **2008**, *14*, 8060–8072.
- (235) Zhao, G., Ullah, F., Deiana, L., Lin, S., Zhang, Q., Sun, J., Ibrahim, I., Dziedzic, P., Córdova, A. Dynamic Kinetic Asymmetric Transformation (DYKAT) by Combined Amine- and Transition-Metal-Catalyzed Enantioselective Cycloisomerization. *Chem. Eur. J.* **2010**, *16*, 1585–1591.

Experimental Procedure

- (236) Birman, V. B., Li, X. Benzotetramisole: a remarkably enantioselective acyl transfer catalyst. *Org. Lett.* **2006**, *8*, 1351–1354.
- (237) King, J. A., McMillan, F. H. The Decarboxylative Acylation of Arylacetic Acids. *J. Am. Chem. Soc.* **1951**, *73*, 4911–4915.
- (238) Steinreiber, J., Faber, K., Griengl, H. De-racemization of Enantiomers versus De-epimerization of Diastereomers—Classification of Dynamic Kinetic Asymmetric Transformations (DYKAT). *Chem. Eur. J.* **2008**, *14*, 8060–8072.
- (239) Vorbrüggen, H., Ruh-Pohlenz, C. Synthesis of Nucleosides. *Org. React.* **2000**, *55*, 1.
- (240) Marzinzik, A. L., Sharpless, K. B. A simple method for the preparation of N-sulfonylsulfilimines from sulfides. *J. Org. Chem.* **2001**, *66*, 594–596.
- (241) Mohamady, S., Jakeman, D. L. An Improved Method for the Synthesis of Nucleoside Triphosphate Analogues. *J. Org. Chem.* **2005**, *70*, 10588–10591.
- (242) Roy, B., Lefebvre, I., Puy, J.-Y., Périgaud, C. A facile and effective synthesis of lamivudine 5'-diphosphate. *Tetrahedron Lett.* **2011**, *52*, 1250–1252.
- (243) Weising S. *Stereoselective synthesis of carbocyclic nucleoside analogues and their triphosphate prodrugs. Synthesis of γ -alkyl-modified nucleoside triphosphates.* Dissertation: Hamburg, 2018.
- (244) Jia X. *Membrane-Permeable Nucleoside Triphosphate Prodrugs of Anti-HIV Active Nucleoside Analogues: γ -(Phosphate or Phosphonate)-Modified Nucleotide Analogues.* Dissertation: Hamburg, 2020.
- (245) Camarasa, M.-J. Prodrugs of Nucleoside Triphosphates as a Sound and Challenging Approach: A Pioneering Work That Opens a New Era in the Direct Intracellular Delivery of Nucleoside Triphosphates. *ChemMedChem* **2018**, *13*, 1885–1889.
- (246) Boyer, P. L., Clark, P. K., Hughes, S. H. HIV-1 and HIV-2 Reverse Transcriptases: Different Mechanisms of Resistance to Nucleoside Reverse Transcriptase Inhibitors. *J. Virol.* **2012**, *86*, 5885–5894.
- (247) Wada, T., Mochizuki, A., Sato, Y., Sekine, M. A Convenient Method for Phosphorylation Involving a Facile Oxidation of H-Phosphonate Monoesters via Bis(trimethylsilyl) Phosphites. *Tetrahedron Lett.* **1998**, *39*, 7123–7126.
- (248) Davis, F. A., Vishwakarma, L. C., Billmers, J. G., Finn, J. Synthesis of α -Hydroxycarbonyl Compounds (Acylons): Direct Oxidation of Enolates Using 2-Sulfonyloxaziridines. *J. Org. Chem.* **1984**, *49*, 3241–3243.
- (249) Sun, J., Gong, S. S., Sun, Q. Efficient Synthesis of Pyrimidine-Nucleoside Monophosphates from H-Phosphonates. *Adv. Mater. Res.* **2014**, *1023*, 87–90.

Experimental Procedure

- (250) Wainberg, M. A., Cahn, P., Bethell, R. C., Sawyer, J., Cox, S. Apricitabine: A Novel Deoxycytidine Analogue Nucleoside Reverse Transcriptase Inhibitor for the Treatment of Nucleoside-Resistant HIV Infection. *Antivir. Chem. Chemother.* **2007**, *18*, 61–70.
- (251) Taylor, D. L., Ahmed, P. S., Tyms, A, Stanley, Wood, L. J., Kelly, L. A., Chambers, P., Clarke, J., Bedard, J., Bowlin, T. L., Rando, R. F. Drug Resistance and Drug Combination Features of the Human Immunodeficiency Virus Inhibitor, BCH-10652 [(±)-2'-Deoxy-3'-Oxa-4'-Thiocytidine, dOTC]. *Antivir. Chem. Chemother.* **2000**, *11*, 291–301.
- (252) Singh, I. R., Gorzynski, J. E., Drobysheva, D., Bassit, L., Schinazi, R. F. Raltegravir Is a Potent Inhibitor of XMRV, a Virus Implicated in Prostate Cancer and Chronic Fatigue Syndrome. *PLoS one* **2010**, *5*, e9948.
- (253) Nies, A. T., Schaeffeler, E., van der Kuip, H., Cascorbi, I., Bruhn, O., Kneba, M., Pott, C., Hofmann, U., Volk, C., Hu, S., Baker, S. D., Sparreboom, A., Ruth, P., Koepsell, H., Schwab, M. Cellular Uptake of Imatinib Into Leukemic Cells is Independent of Human Organic Cation Transporter 1 (OCT1). *Clin. Cancer Res.* **2014**, *20*, 985–994.
- (254) García-Trejo, J. J., Ortega, R., Zarco-Zavala, M. Putative Repurposing of Lamivudine, a Nucleoside/Nucleotide Analogue and Antiretroviral to Improve the Outcome of Cancer and COVID-19 Patients. *Front. Oncol.* **2021**, *11*, 664794.
- (255) Kearney, B. P., Flaherty, J. F., Shah, J. Tenofovir Disoproxil Fumarate: Clinical Pharmacology and Pharmacokinetics. *Clin. Pharmacokinet.* **2004**, *43*, 595–612.
- (256) Ma, X., Xu, Q., Li, H., Su, C., Yu, L., Zhang, X., Cao, H., Han, L.-B. Alcohol-based Michaelis–Arbuzov reaction: An Efficient and Environmentally-benign Method for C-P(O) Bond Formation. *Green Chem.* **2018**, *20*, 3408–3413.
- (257) Chen, L., Zhu, Y., Chen, T., Liu, L., Zhang, J.-S., Han, L.-B. Direct C-OH/P(O)-H dehydration coupling forming phosphine oxides. *Organic & biomolecular chemistry* **2018**, *16*, 5090–5093.
- (258) Batesky, D. C., Goldfogel, M. J., Weix, D. J. Removal of Triphenylphosphine Oxide by Precipitation with Zinc Chloride in Polar Solvents. *J. Org. Chem.* **2017**, *82*, 9931–9936.
- (259) Mohamady, S., Taylor, S. D. General Procedure for the Synthesis of Dinucleoside Polyphosphates. *J. Org. Chem.* **2011**, *76*, 6344–6349.
- (260) Tanaka, H., Yoshimura, Y., Jørgensen, M. R., Cuesta-Seijo, J. A., Hindsgaul, O. A simple Synthesis of Sugar Nucleoside Diphosphates by Chemical Coupling in Water. *Angew. Chem. Int. Ed.* **2012**, *51*, 11531–11534.
- (261) Srivastva, D. N., Farquhar, D. Bioreversible Phosphate Protective Groups: Synthesis and Stability of Model Acyloxymethyl Phosphates. *Bioorg. Chem.* **1984**, *12*, 118–129.
- (262) Kraus, J.-L., Attardo, G. Synthesis of New 2,5-Substituted 1,3-Oxothiolanes. Intermediates in Nucleoside Chemistry. *Synthesis* **1991**, *11*, 1046–1048.

Experimental Procedure

- (263) Bartlett, M. J., Turner, C. A., Harvey, J. E. Pd-Catalyzed Allylic Alkylation Cascade with Dihydropyrans: Regioselective Synthesis of Furo[3,2-c]pyrans. *Org. Lett.* **2013**, *15*, 2430–2433.
- (264) Tsuji, T., Takenaka, K. Facile 5'-Halogenation of Unprotected Nucleosides. *Nucleosides Nucleotides Nucleic Acids* **1987**, *6*, 575–580.
- (265) Sander, M. Herstellung von Polyphosphinsäure-Estern durch Michaelis-Arbusow-Reaktion. *Macromol. Chem. Phys* **1962**, *55*, 191.

8. Appendix

8.1. Hazard and Precaution Statements

The hazard and precautionary statements used are listed below.



Compounds	Pictogram	Hazard statements	Precautionary statements
Acetic acid		226, 314	210, 280, 301 + 330 + 331, 303 + 361 + 353, 305 + 351 + 338 + 310
Acetic anhydride		226, 302, 314, 330	210, 233, 240, 241, 242, 243, 260, 264, 270, 271, 280, 284, 301 + 312 + 330, 301 + 330 + 331, 303 + 361 + 353, 304 + 340 + 310, 305 + 351 + 338 + 310, 363, 370 + 378, 403 + 233, 403 + 235, 405, 501
Acetic anhydride		226, 302, 314, 330	210, 233, 240, 241, 242, 243, 260, 264, 270, 271, 280, 284, 301 + 312 + 330, 301 + 330 + 331, P303 + 361 + 353, 304 + 340 + 310, 305 + 351 + P338 + 310, 370 + 378, 403 + 233, 403 + 235, 405, 501
Acetone		225, 319, 336	210, 233, 240, 241, 242, 243, 261, 264, 271, 280, 303 + 361 + 353, 304 + 340 + 312, 305 + 351 + 338, 337 + 313, 370 + 378 403 + 233, 403 + 235, 405, 501

Experimental Procedure

Acetonitrile		225, 302 + 312 + 332, 319	210, 233, 240, 241, 242, 243, 261, 264, 270, 280, 301 + 312 + 330, 303 + 361 + 353, 304 + 340 + 312, 305 + 351 + 338, 337 + 313, 363, 370 + 378, 403 + 235, 501
Acrylamide: Bisacrylamide (40% aqueous solution, 19:1)		302 + H332, 315, 317, 319, 340, 350, 361, 372, 402	201, 202, 260, 264, 270, 271, 272, 773, 280, 301 + 312 + 330, 302 + 352, 304 + 340 + P312, 305 + 351 + 338, 08 + 313, 333 + 313, 337 + P313, 362, 405, 501
Ammonium acetate			Not a hazardous substance or mixture according to Regulation (EC) No. 1272/2008
Ammonium bicarbonate		302, 402	264, 270, 273, 301 + 312 + 330, 501
Ammonium chloride		302, 319	264, 270, 280, 312 + 330, 305 + 351 + 338, 337 + 313; 501
25% Ammonium hydroxide solution	 	314, 335, 400, 411	261, 264, 271, 273, 280, 301 + 330 + 331, 304 + 340 + 310, 305 + 351 + 338 + 310, 363, 391, 403 + 233, 405, 501
Ammonium persulfate	 	272, 302, 315, 317, 319, 334, 335, 402	210, 220, 221, 264, 271, 272, 273, 280, 285, 301 + 312 + 330, 304 + 340 + 312, 305 + 351 + 338, 333 + 313, 337 + 313, 342 + 311, 362, 370 + 378, 403 + 233, 405, 501
Benzoic acid		315, 318, 372, 402	260, 264, 270, 273, 280, 302 + 352, 305 + 351 + 338 + 310, 314, 332 + 313, 362, 501
Benzoic anhydride		315, 318, 372, 402	260, 264, 270, 273, 280, 302 + 352, 305 + 351 + 338 + 310, 314, 332 + 313, 362, 501

Experimental Procedure

Benzoyl chloride		227, 302 + 201, 202, 210, 261, 264, 270, 312, 314, 317, 271, 272, 273, 280, 301 + 312 + 331, 350, 402 330, 301 + 330 + 331, 303 + 361 + 353, 304 + 340 + 310, 305 + 351 + 338 + 310, 308 + 313, 333 + 313, 363, 370 + 378, 403 + 233, 403 + 235, 405, 501
<i>N</i> ⁴ -Benzoylcytosine		312 + 332, 261, 270, 271, 280, 301 + 312 + 315, 319, 335 330, 302 + 352, 304 + 340 + 312, 305 + 351 + 338, 332 + 313, 337 + 313, 362, 403 + 233, 405, 501
N,O-Bis(trimethylsilyl)- acetamide		226, 302, 314 210, 233, 240, 241, 242, 243, 264, 270, 280, 301 + 312 + 330, 301 + 330 + 331, 303 + 361 + 353, 304 + 340 + 310, 305 + 351 + 338 + 310, 363, 370 + 378, 403 + 235, 405, 501
<i>Tert</i> -Butanol		225, 319, 332, 210, 233, 240, 241, 242, 243, 336 261, 264, 271, 280, 303 + 361 + 353, 304 + 340 + 312, 305 + 351 + 338, 337 + 313, 370 + 378, 403 + 233, 403 + 235, 405, 501
<i>n</i> -Butyllithium solution 2.5 M in hexane		225, 260, 304, 201, 202, 210, 223, 231 + 232, 314, 336, 361, 233, 240, 241, 242, 243, 261, 411 264, 271, 273, 280, 301 + 310, 301 + 330 + 331, 303 + 361 + 353, 304 + 340 + 310, 305 + 351 + 338 + 310, 308 + 313, 335 + 334, 363, 370 + 378, 391, 402 + 404, 403 + 233, 403 + 235, 405, 501
<i>tert</i> -Butyl methyl ether		225, 315 210, 233, 240, 241, 242, 243, 264, 280, 303 + 361 + 353, 332 + 313, 362, 370 + 378, 403 + 235, 501

Experimental Procedure

Butyryl chloride		225, 290, 302, 318, 331	210, 233, 234, 240, 241, 242, 243, 261, 264, 270, 271, 280, 301, + 312 + 330, 303 + 361 + 353, 304 + 340 + 311, 305 + 351 + 338 + 310, 370 + 378, 390, 403 + 233, 403 + 235, 405, 406, 501
(1S)-(+)-(10-Camphorsulfonyl)oxaziridine	Not a hazardous substance or mixture according to Regulation (EC) No. 1272/2008		
Celite®		372	260, 264, 270, 314, 501
Chloramine-T hydrate		302, 314, 334, 411	260, 264, 270, 273, 280, 285, 301 + 312 + 330, 301 + 330 + 331, 303 + 361 + 353, 304 + 340 + 310, 305 + 351 + 338 + P310, 342 + 311, 363, 391, 405, 501
Chloroform		302, 315, 319, 331, 336, 351, 361, 372, 412	201, 202, 260, 264, 270, 271, 273, 280, 301 + 312 + 330, 302 + 352, 304 + 340 + 311, 305 + 351 + 338, 308 + 313, 332 + 313, 337 + 313, 362, 403 + 233, 405, 501
3-Chloroperbenzoic acid		242, 315, 317, 319, 335	210, 220, 234, 261, 264, 271, 272, 280, 302 + 352, 304 + 340 + 312, 305 + 351 + 338, 333 + 313, 337 + 313, 362, 403 + 233, 403 + 235, 405, P410, 420, 501
N-Chlorosuccinimide		290, 302, 314, 335, 410	234, 260, 264, 270, 271, 273, 280, 301 + 312 + 330, 301 + 330 + 331, 303 + 361 + 353, 304 + 340 + 310, 305 + 351 + 338 + 310, 363, 390, 391, 403 + 233, 405, 406, 501
Copper(II) chloride		302 + 312, 315, 318, 400, 411	264, 270, P273, 280, 301 + 312 + 330, 302, + 352, + 312, 305 + 351 + 338 + 310, 332 + 313, 362, 391, 501

Experimental Procedure

Deuterium oxide- <i>d</i> 2			Not a hazardous substance or mixture according to Regulation (EC) No. 1272/2008
1,8-Diazabicyclo- [5.4.0]undec-7-ene		290, 301, 314, 412	234, 264, 270, 273, 280, 301 + 310 + 330, 301 + 330 + 331, 303 + 361 + 353, 304 + 340 + 310, 305 + 351 + 338 + 310, 363, 390, 405, 406, 501
(+)-(8,8-Dichloro- camphorylsulfonyl)oxaziridine			Not a hazardous substance or mixture according to Regulation (EC) No. 1272/2008
2,3-Dichloro-5,6-dicyano- <i>p</i> - benzoquinone		301	264, 270, 301 + 310 + 330, 405, 501
Dichloromethane		315, 319, 336, 351	201, 202, 261, 264, 271, 280, 302 + 352, 304 + 340 + 312, 305 + 351 + 338, 308 + 313, 332 + 313, 337 + 313, 362, 403 + 233, 405, P501
2',3'-Didehydro-3'- deoxythymidine			Not a hazardous substance or mixture according to Regulation (EC) No. 1272/2008
2',3'-Dideoxy-3'-fluorouridine		341	201, 202, 281, 308 + 313, 405, 501
Diethyl ether		224, 302, 336,	210, 233, 240, 241, 242, 243, 261, 264, 270, 271, 280, 301 + 312 + 330, 303 + 361 + 353, 304 + 340 + 312, 370 + 378, 403 + 233, 403 + 235, 405, 501
4,4'- Dimethoxytriphenylmethyl chloride		314, 317, 335, 411	260, 264, 271, 272, 273, 280, 301 + 330 + 331, 303 + 361 + 353, 304 + 340 + 310, 305 + 351 + 338 + 310, 333 + 313, 363, 391, 403 + 233, 405, 501
5'-O-(4,4'- Dimethoxytrityl)thymidine		none	401, 413
			273, 501

Experimental Procedure

(Diethylamino)sulfur trifluoride (DAST®)	 	H226, 242, 314	210, 220, 233, 234, 240, 241, 242, P243, 264, 280, 301 + 330 + 331, 303 + 361 + 353, 304 + 340 + 310, 305 + 351 + 338 +310, 363, 370 + 378, 403 + 235, 420, 501
4-(dimethylamino)-pyridine	   	301 + 331, 310, 315, 318, 370, 411	260, 262, 264, 270, 271, 273, 280, 301 + 310 + 330, 302 + 350 + 310, 302 + 352, 304 + 340 + 311, 305 + 351 + 338 + 310, 307 + 311, 332 + 313, 362, 403 + 233, 405, 501
Dimethylformamide	  	226, 312 + 332, 319, 350, 360	201, 202, 210, 233, 240, 241, 242, 243, 261, 264, 271, 280, 303 + 361 + 353, 304 + 340 + 312, 305 + 351 + 338, 308 + 313, 337 + 313, 363, 370 + 378, 403 + 235, 405, 501
Diphenyl phosphite	 	302, 315, 318, 335	261, 264, 270, 271, 280, 301 + 312 + 330, 302 + 352, 304 + 340 + 312, 305 + 351 + 338 + 310, 332 + 313, 362, 403 + 233, 405, 501
1-Dodecanol	 	319, 410	264, 273, 280, 305 + 351 + 338, 337 + 313, 391, 501
Dodecanoyl chloride		314, 318	264, 280, 301 + 330 + 331, 303 + 361 + 353, 304 + 340 + 310, 305 + 351 + 338 + 310, 363, 405, 501
Dowex® 50WX8 hydrogen form		319	264, 280, 305 + 351 + 338, 337 + 313
Ethanol	 	225, 319	P210, 233, 240, 241, 242, 243, 264, 280, 303 + 361 + 353, 305 + 351 + 338, 337 + 313, 370 + 378, 403 + 235, 501

Experimental Procedure

Ethyl acetate		225, 319, 336	210, 233, 240, 241, 242, 243, 261, 264, 271, 280, 303 + 361 + 353, 304 + 340 + 312, 305 + 351 + 338, 337 + 313, 370 + 378, 403 + 233, 403 + 235, 405, 501
Ethylnyltrimethylsilane		225, 315, 319	210, 233, 240, 241, 242, 243, 264, 280, 303 + 361 + 353, 305 + 351 + 338, 332 + 313, 337 + 313, 362, 370 + 378, 403 + 235, 501
Furfuryl alcohol		227, 302 + 312, 319, 331, 335, 351, 373	201, 202, 210, 260, 264, 270, 271, 280, 301 + 312 + 330, 302 + 352 + 312, 304 + 340 + 311, 305 + 351 + 338, 308 + 313, 337 + 313, 363, 370 + 378, 403 + 233, 403 + 235, 405, 501
<i>n</i> -Heptane		225, 304, 315, 336, 361, 410	225, 304, 315, 336, 410, 210, 233, 240, 241, 242, 243, 261, 264, 271, 273, 280, 301 + 310, 303 + 361 + 353, 304 + 340 + 312, 331, 332 + 313, 362, 370 + 378, 391, 403 + 233, 403 + 235, 405, 501
1-Hexadecanol	Not a hazardous substance or mixture according to Regulation (EC) No. 1272/2008		
Hexamethyldisilazane		225, 302 + 332, 311, 412	210, 233, 240, 241, 242, 243, 261, 264, 270, 271, 273, 280, 301 + 312 + 330, 303 + 361 + 353, 304 + 340 + 312, 362, 370 + 378, 403 + 235, 405, 501
<i>n</i> -Hexane		225, 304, 315, 336, 361, 373, 411	201, 202, 210, 233, 240, 241, 242, 243, 260, 264, 271, 273, 280, 301 + 310, 303 + 361 + 353, 304 + 340 + 312, 308 + 313, 331, 332 + 313, 362, 370 + 378, 391, 403 + 233, 403 + 235, 405, 501

Experimental Procedure

1 M Hydrochloric acid		290	234, 390, 406
Hydrogen peroxide solution 30%		318, 401, 412	261, 264, 270, 271, 273, 280, 301 + 312 + 330, 302 + 352, 304 + 340 + 312, 305 + 351 + 338 + 310, 332 + 313, 362, 403 + 233, 405, 501
4-Hydroxybenzyl alcohol		319, 412	273, 280, 305 + 351 + 338 + 310, 501
3-Hydroxypropionitrile	Not a hazardous substance or mixture according to Regulation (EC) No. 1272/2008		
Iodine	  	302 + 312 + 332, 315, 319, 335, 372, 400	260, 264, 270, 271, 273, 280, 301 + 312 + 330, 302 + 352 + 312, 304 + 340 + 312, 305 + 351 + 338, 314, 332 + 313, 337 + 313 362, 391, 403 + 233, 405, 501
Iodotrimethylsilane	 	225, 314, 318	210, 233, 240, 241, 242, 243, 264, 280, 301 + 330 + 331, 303 + 361 + 353, 304 + 340 + 310, 305 + 351 + 338 + 310, 363, 370 + 378, 403 + 235, 405, 501,
Isobutyric anhydride	 	227, 301 + 311, 314, 318	210, 264, 270, 280, 301 + 310 + 330, 301 + 330 + 331, 303 + 361 + 353, 304 + 340 + 310, 305 + 351 + 338 + 310, 363, 370 + 378, 403 + 235, 405, 501
Lamivudine		361	201, 202, 280, 308 + 313, 405, 501
Levamisol hydrochloride		301	264, 270, 301 + 310 + 330, 405, 501

Experimental Procedure

Lithium aluminium hydride 1 M in THF		225, 302, 315, 318, 335, 336, 351	201, 202, 210, 233, 240, 241, 242, 243, 261, 264, 270, 271, 280, 301 + 312 + 330, 303 + 361 + 353, 304 + 340 + 312, 305 + 351 + 338 + 310, 308 + 313, 332 + 313, 362, 370 + 378, 403 + 233, 403 + 235, 405, 501
4-Methylbenzenethiol		319	264, P280, 305 + 351 + 338, 337 + 313
Methanesulfonyl chloride		290, 301 + 311, 314, 317, 330, 335, 402	234, 260, 264, 270, 271, 272, 273, 280, 284, 301 + 310 + 330, 301 + 330 + 331, 303 + 361 + 353, 304 + 340 + 310, 305 + 351 + 338 + 310, 333 + 313, 362, 390, 403 + 233, 405, 406, 501
Methanol		225, 301 + 311 + 331, 370	210, 233, 240, 241, 242, 243, 260, 264, 270, 271, 280, 301 + 310 + 330, 303 + 361 + 353, 304 + 340 + 311, 307 + 311, 362, 370 + 378, 403 + 233, 403 + 235, 405, 501
Methanol- <i>d</i> 4		225, 301 + 311 + 331, 370	210, 233, 240, 241, 242, 243, 260, 264, 270, 271, 280, 301 + 310 + 330, 303 + 361 + 353, 304 + 340 + 311, 307 + 311, 362, 370 + 378, 403 + 233, 403 + 235, 405, 501
1-Methylimidazol		227, 302, 311, 314,	210, 264, 270, 280, 301 + 312 + 330, 301 + 330 + 331, 303 + 361 + 353, 304 + 340 + 310, 305 + 351 + 338 + 310, 362, 370 + 378, 403 + 235, 405, 501
1-Pentadecanol			Not a hazardous substance or mixture according to Regulation (EC) No. 1272/2008

Experimental Procedure

Pentane		225, 304, 336, 411	210, 233, 240, 241, 242, 243, 261, 271, 273, 280, 301 + 310, 303 + 361 + 353, 304 + 340 + 312, 331, 370 + 378, 391, 403 + 233, 403 + 235, 405, 501
Petroleum ether		224, 304, 315, 336, 411	210, 233, 240, 241, 242, 243, 261, 264, 271, 273, 280, 301 + 310, 303 + 361 + 353, 304 + 340 + 312, 331, 332 + 313, 362 370 + 378, 391, 403 + 233, 403 + 235, 405, 501
Phenylacetyl chloride		314, 335	261, 264, 271, 280, 301 + 330 + 331, 303 + 361 + 353, 304 + 340 + 310, 305 + 351 + 338 + 310, 363, 403 + 233, 405, 501
Phosphorous acid		290, 302, 314	234, 260, 264, 270, 280, 301 + 312 + 330, 301 + 330 + 331, 303 + 361 + 353, 304 + 340 + 310, 305 + 351 + 338 + 310, 363, 390, 405, 406, 501
Phosphorous oxychloride		302, 314, 330, 372	260, 264, 270, 271, 280, 284, 301 + 312 + 330, 301 + 330 + 331, 303 + 361 + 353, 304 + 340 + 310, 305 + 351 + 338 + 310, 314, 363, 403 + 233, 405, 501
Potassium phosphate monobasic	Not a hazardous substance or mixture according to Regulation (EC) No. 1272/2008		
<i>iso</i> -Propanol		225, 319, 336	210, 233, 240, 241, 242, 243, 261, 264, 271, 280, 303 + 361 + 353, 304 + 340 + 312, 305 + 351 + 338, 337 + 313, 370 + 378, 403 + 233, 403 + 235, 405, 501

Experimental Procedure

Proton-sponge®		315, 319, 335	261, 264, 271, 280, 302 + 352, 304 + 340 + 312, 305 + 351 + 338, 332 + 313, 337 + 313, 362, 403 + 233, 405, 501
Pyridine		225, 302 + 312 + 332, 315, 319, 402	210, 233, 240, 241, 242, 243, 261, 264, 270, 271, 273, 280, 301 + 312 + 330, 303 + 361 + 353, 304 + 340 + 312, 305 + 351 + 338, 332 + 313, 337 + 313, 362, 370 + 378, 403 + 235, 501
Sephadex®		Not a hazardous substance or mixture according to Regulation (EC) No. 1272/2008	
Silica gel		Not a hazardous substance or mixture according to Regulation (EC) No. 1272/2008	
Sodium bicarbonate		Not a hazardous substance or mixture according to Regulation (EC) No. 1272/2008	
Sodium hydroxide		290, 314, 402	234, 260, 264, 273, 280, 301 + 330 + 331, 303 + 361 + 353, 304 + 340 + 310, 305 + 351 + 338 +310, 363, 390, 405, 406, 501
Sodium phenylacetate		318	280, 305 + 351 + 338, 310
Sodium sulfate		Not a hazardous substance or mixture according to Regulation (EC) No. 1272/2008	
Sodium thiosulfate		Not a hazardous substance or mixture according to Regulation (EC) No. 1272/2008	
Sulfuric acid		290, 314	234, 264, 280, 301 + 330 + 331, 303 + 361 + 353, 304 + 340 + 310, 305 + 351 + 338 + 310, 363, 390, 405, 406, 501
Tetrabromomethane		302, 315, 318, 335,	261, 264, 270, 271, 280, 301 + 312 + 330, 302 + 352, 304 + 340 + 312, 305 + 351 + 338 + 310, 332 + 313, 362, 403 + 233, 405, 501

Experimental Procedure

Tetrabutylammonium hydroxide 10% in water		314	280, 301 + 330 + 331, 303 + 361 + 353, 304 + 340, 305 + 351 + 338, 501
Tetrabutylammonium iodide		302	264, 270, 301 + 312 + 330, 501
Tetrabutylammonium phosphate monobasic 0.4 M in acetonitrile		225, 302 + 312 + 332, 319,	210, 233, 240, 241, 242, 243, 261, 264, 270, 271, 280, 301 + 312 + 330, 303 + 361 + 353, 304 + P340 + 312, 305 + 351 + 338, 337 + 313, 363, 370 + 378, 403 + 235, 501
Tetrabutylammonium bisulfate		302, 314, 412	260, 264, 270, 273, 280, 301 + 312 + 330, 301 + 330 + 331, 303 + 361 + 353, 304 + 340 + 310, 305 + P351 + 338 + 310, 363, 405, 501
1-Tetradecanol		319, 401, 410	264, 273, 280, 305 + 351 + 338, 337 + 313, 391, 501
Tetrahydrofuran	 	225, 302, 319, 335, 336, 351	201, 202, 210, 233, 240, 241, 242, 243, 261, 264, 270, 271, 280, 301 + 312 + 330, 303 + 361 + 353, 304 + 340 + 312, 305 + 351 + 338, 308 + 313, 337 + 313, 370 + 378, 403 + 233, 403 + 235, 405, 501
<i>N,N,N',N'</i> -Tetramethyl ethylenediamine	 	225, 301 + 331, 314, 402	210, 233, 240, 241, 242, 243, 261, 264, 270, 271, 273, 280, 301 + 310 + 330, 301 + 330 + 331, 303 + 361 + 353, 304 + 340 + 310, 305 + 351 + 338 + 310, 370 + 378, 403 + 233, 403 + 235, 501
Thymine	Not a hazardous substance or mixture according to Regulation (EC) No. 1272/2008		

Experimental Procedure

Thymidine		Not a hazardous substance or mixture according to Regulation (EC) No. 1272/2008	
Toluene		225, 304, 315, 336, 361, 373, 401, 412	201, 202, 210, 233, 240, 241, 242, 243, 260, 264, 271, 273, 280, 301 + 310, 303 + 361 + 353, 304 + 340 + 312, 308 + 313, 331, 332 + 313, 362, 370 + 378, 403 + 233, 403 + 235, 405, 501
Tridecanoyl chloride		Not a hazardous substance or mixture according to Regulation (EC) No. 1272/2008	
Triethylamine		225, 302, 311 + 331, 314, 335, 401	210, 233, 240, 241, 242, 243, 261, 264, 270, 271, 273, 280, 301 + 312 + 330, 301 + 330 + 331, 303 + 361 + 353, 304 + 340 + 310, 305 + 351 + 338 + 310, 362, 370 + 378, 403 + 233, 403 + 235, 405, 501
Triethyl phosphate		302, 319	264, 270, 280, 301 + 312 + 330, 305 + 351 + 338, 337 + 313, 501
Triethyl phosphite		226, 302, 317, 412	210, 233, 240, 241, 242, 243, 261, 264, 270, 272, 273, 280, 301 + 312 + 330, 303 + 361 + 353, 333 + 313, 363, 370 + 378, 403 + 235, 501
Trifluoroacetic anhydride		314, 332, 412	261, 264, 271, 273, 280, 301 + 330 + 331, 303 + 361 + 353, 304 + 340 + 310, 305 + 351 + 338 + 310, 363, 405, 501
Trimethyl phosphate		302, 315, 319, 340, 351	201, 202, 264, 270, 280, 281, 301 + 312 + 330, 302 + 352, 305 + 351 + 338, 308 + 313, 332 + 313, 337 + 313, 362, 405, 501

Experimental Procedure

Trimethylsilyl trifluoromethanesulfonate		226, 314	210, 233, 240, 241, 242, 243, 264 280, 301 + 330 + 331, 303 + 361 + 353, 304 + 340 + 310, 305 + 351 + 338 + 310, 363, 370 + 378, 403 + 235, 405, 501
Triphenylphosphine		302, 317, 318, 372	260, 270, 272, 280, 301 + 312 + 330, 302 + 352, 305 + 351 + 338 + 310, 314, 333 + 313, 363, 501
Valeroyl chloride		226, 290, 314, 331, 412	210, 233, 234, 240, 241, 242, 243, 261, 271, 273, 280, 301 + 330 + 331, 303 + 361 + 353, 304 + 340 + 310, 305 + 351 + 338 + 310, 363, 370 + 378, 390, 403 + 233, 403 + 235, 405, 406, 501
Vanilin		319, 402	264, 273, 280, 305 + 351 + 338, 337 + 313, 501

8.2. Acknowledgements

Mein Dank gilt...

Herrn Prof. Dr. Chris Meier für die freundliche Aufnahme in seinen Arbeitskreis und das Vertrauen, mir dieses interessante und herausfordernde Thema zu überlassen. Sowohl die Freiheit, diesem Thema mit eigenen Ideen nachgehen zu können, als auch die wegweisende Unterstützung führten zum Erfolg dieser Arbeit.

Herrn Prof. Dr. Ralph Holl für die freundliche Übernahme des Zweitgutachtens sowie Herrn Prof. Dr. Wolfgang Maison und Herrn Dr. Thomas Hackel für die Teilnahme am Disputationskolloquium.

Herrn Dr. Thomas Hackel und Frau Dr. Jennifer Menzel und ihren jeweiligen Abteilungen für die Anfertigung unzähliger Spektren und die aufschlussreiche Beratung bei besonderen Problemstellungen.

Dr. Simon Weising, der mir stets mit viel Geduld und unvergleichlicher Expertise zu Seite stand. Ohne ihn und seine Korrekturen wäre diese Arbeit eine andere.

Dr. Vincente Sterrenberg, Dr. Moritz Münzmay, Dr. Patrick Dekiert, Dr. Eric Ruf und Nils Walter für die Korrekturen dieser Arbeit.

Meinen PraktikantInnen Michelle, Amrei, Berk und ganz besonders Iven, die mir wertvolle Ergebnisse geliefert haben und am Erfolg dieser Arbeit beteiligt waren.

Den Arbeitskreismitgliedern des AK Meier, ehemaligen wie aktuellen, die meine Zeit im Labor unvergesslich gemacht haben.

Mein ganz besonderer Dank gilt...

Meinen Freunden, Desiree, Vanessa, Benedikt, mit euch vergeht die Zeit wie im Flug.

Vincente, einen besseren und strengeren Laborpartner hätte ich mir nicht wünschen können. Schön, dass du es mit mir ausgehalten hast.

Ebenfalls meinen Nicht-Chemiker-Freunden, die mich immer in die Realität zurückholen konnten.

Meiner Familie und insbesondere meiner Mutter Ellen. Ohne eure Unterstützung wäre ich nie so weit gekommen.

Meiner Freundin Katja. Du hast mir zu jedem Zeitpunkt zur Seite gestanden, egal was war. Dank dir hatte ich immer das Gefühl: Das schaffe ich schon.

Danke!

8.3. Eidesstattliche Erklärung

Hiermit versichere ich an Eides statt, die vorliegende Dissertation selbst verfasst und keine anderen als die angegebenen Hilfsmittel benutzt zu haben. Die eingereichte schriftliche Fassung entspricht der auf dem elektronischen Speichermedium. Ich versichere, dass diese Dissertation nicht in einem früheren Promotionsverfahren eingereicht wurde.

Hamburg den 22.03.2024

Ort, Datum

Stefan Weber, M.Sc.